2020

Novel Lipase(s): Application in Biodiesel production from Wastewater Grown Microalgae

Priyanka Anilkumar
Technological University Dublin

Novel Lipase(s): Application in Biodiesel production from Wastewater Grown Microalgae

Priyanka Anilkumar, B.Tech, M.Tech, MBA

A thesis submitted to Technological University Dublin in fulfilment of requirement for the degree of

DOCTOR OF PHILOSOPHY

School of Food Science and Environmental Health,

College of Sciences and Health,

Technological University, Dublin, Ireland

February 2020

Supervisor: Dr. Barry Ryan

Advisory Supervisors: Dr. Gemma Kinsella, Prof. Gary Henehan

Abstract

Lipase-based catalysis in organic solvents offer several advantages and, therefore, have been widely researched and applied. Nature provides a vast microbial enzyme pool that can be easily bio-discovered through the targeted exploration of existing extremophiles. Among the large number of bacterial lipases, those from species like *Geotrichum, Bacillus, Pseudomonas, Burkholderi and Streptomyces* have shown adequate stability for biosynthetic application. In this study, several bacterial strains isolated from soils in the Dublin and Laois regions of Ireland were screened for presence of solvent stable lipases. Five bacterial strains producing most solvent stable lipase(s) were identified as *Pseudomonas sp.* BIM B-86, *Sphingomonas* sp., *Listeria monocytogenes*, *Pseudomonas reinekei* and *Pseudomonas brenneri* via 16S rRNA sequencing. Amonst these five strains, new lipolytic enzymes from only two strains of *Pseudomonas* sp. i.e. *P. reinekei* and *P. brenneri* were explored in the present work. Production of lipase(s) from *P. reinekei* (termed H1) and *P. brenneri* (termed H3) was enhanced by changing the nitrogen source in culture medium to 1% (w/v) *L*-Lysine and 1% (w/v) peptone respectively. Characterisation of these purified lipases revealed their stability towards broad pH range (5.0-9.0) and activation in the presence of organic solvents with log P≥ 2.0. T_{50} (half-life) of lipase from *P. brenneri* (H3) and *P. reinekei* (H1) was found to be 189mins at 60°C and 89mins at 45°C respectively. These purified lipase were used in industrially relevant applications, specifically biodiesel synthesis.

This study also explored development of an alternative and sustainable lipids source for biodiesel production. Microalgae were selected as cheap, alternate source as they can grow in wide range of environmental conditions and can utilise nutrients from wastewater for their growth. In this study, two microalgae strains i.e. *Chlorella emersonii* and *Pseudokirchneriella subcapitata* were examined as potential lipids source for biodiesel production. Both strains were grown in simulated wastewater and under nitrogen deficient conditions generated neutral lipid content of 0.61±0.017mg/mg and 0.31±0.006mg/mg biomass respectively. *In-situ* transesterification of neutral lipids generated from these two microalgae strains using lipases from H1 (*P. reinekei*), H3 (*P. brenneri*) and porcine pancreas (as a standard) generated FAMEs (Fatty Acid Methyl Esters) with a high proportion of unsaturated fatty acids esters. Blending these FAMEs

with other FAME sources can produce biodiesel comparable to existing biofuels. This study is a good illustration for generation/production of energy rich molecules from waste byproducts exploiting enzymes obtained from extremophiles and wastewater grown microalgae.

Declaration

I certify that this thesis which I now submit for examination for the award of Doctor of Philosophy (PhD), is entirely my own work and has not been taken from the work of others, save and to the extent that such work has been cited and acknowledged within the text of my work.

This report is prepared according to the regulations for postgraduate study by research of the Technological University Dublin and has not been submitted in whole or in part for another award in any other third level institution.

The work reported on in this thesis confirms to the principles and requirements of the Technological University Dublin Guidelines for Ethics in Research.

Signature Date

Acknowledgement

I wish to express my deepest respect, profound gratitude, and great appreciation to my supervisors Dr. Barry Ryan, Dr. Gemma Kinsella and Prof. Gary Henehan for their continuous support, valuable guidance, patience and encouragement during this PhD journey. Besides my advisors, I would also like to express many thanks to all the laboratory technicians in Technological University Dublin, especially Mr. Tony Hutchinson, Mr. Plunkett Clarke, Mr. Noel Grace and Ms. Jyothi Iyer for their constant assistance all these years. I would like to acknowledge Dr. Paul Dowling, from Maynooth University for the excellent help rendered with MS analysis during my work. I am also thankful to Technological University Dublin for affording me this opportunity for postgraduate research and funding my research work through *Fiosraigh* research scholarship. It has truly been a life changing journey and I hope to always measure up to the confidence reposed in me by my mentors at Technological University Dublin.

I would also like to thank my friends and lab mates Ms. Yeqi Tan, Ms. Harshitha Venkataratnam, Ms. Tobiloba Sojinrin and Mr. Albert Ngoga for their friendship, support, encouragement and for all the fun we have had in the last four years. Last but not least, I would like to thank my husband Mr. Anilkumar KJ, my son Pranil and my parents for their encouragement and unfailing support throughout my years of PhD. All this would not have been possible without them.

Abbreviations

°C	Degree Celsius
µg/mL	Micrograms/milliliter
µL	Microliter
16S rRNA	16S ribosomal RNA
AuNPs	Gold Nanoparticles
CFU	Colony Forming Units
cm	Centimeter
EDC	1-ethyl-3-(3-di- methylaminopropyl) carbodiimide hydrochloride
EDTA	Ethylenediaminetetraacetic acid
FA	Fatty Acids
FFA	Free Fatty Acids
FAME	Fatty Acid Methyl Ester
FAEE	Fatty Acid Ethyl Ester
FID	Flame Ionisation Detector
g	Gravitational force for centrifugation
GC	Gas Chromatography
gm	Grams
GSH	Glutathione
h	Hour(s)
HIC	Hydrophobic Interaction Chromatography
ID	Internal Diameter
IU	International Units
IU/ml	International Units/milliliter
kDa	Kilo Daltons
kPa	Kilopascal
L	Liter
LB	Luria-Bertani Broth
Log P	Partition Coefficient (octanol: water)
ml/min	Milliliter per minute
mM	Millimolar

MUF	4-Methylumbelliferone
MW	Molecular weight
nBLAST	Nucleotide Basic Local Alignment Search Tool
NHS	N-hydroxysuccinimide
nm	Nanometer
O.D.	Optical Density
PAGE	Polyacrylamide Gel Electrophoresis
PBS	Phosphate Buffer Saline
PEG	Polyethylene Glycol
pI	Isoelectric point
p-NP	*p*-Nitrophenol
p-NPP	*p*-Nitrophenol Palmitate
PPL	Porcine Pancreas Lipase
R^2	Regression coefficient
Rf	Relative Mobility
rpm	Revolutions per minute
RT	Retention Time
SDS	Sodium Dodecyl Sulphate
SEM	Scanning Electron Microscope
TAG(s)	Triacylglycerol(s)
TEMED	N, N, N′, N′-Tetramethylethylenediamine
UV	Ultra-Violet
v/v	Volume/volume
w/v	Weight/volume

Table of Contents

List of Tables

List of Figures

Chapter 1: General introduction

Energy plays a central role in the global economy but current supplies are unsustainable for the economic and environmental development of the world (Owusu and Asumadu-Sarkodie, 2016). Transportation, residential, commercial and industrial are the four major sectors utilizing energy. Of these, transportation is the largest oil consuming sector utilizing approximately 60% of oil worldwide (Members, 2018). Consumption of petroleum and other liquid fuels increased from 98.49 in 2017 to 99.93 (million barrels per day) by the end of 2018 and is estimated to reach 102.40 by the end of 2020. The Energy Information Administration expects global petroleum, and other liquid fuel consumption to increase by 1.7 million barrels per day in 2019. The extensive use of fuel in transportation has caused high carbon dioxide (CO_2) emissions; 65% of the greenhouse gases are contributed by fossil fuel and industrial processes (Olivier, Schure and Peters, 2017). The transport sector is a major contributor to CO_2 global emissions, which, by 2030 is estimated to increase to 2 billion vehicles (Balat and Balat, 2010). Dwindling reserves of crude oil, increasing crude oil prices (because of increasing demands for energy) have led to demand for alternative fuels (Brennan and Owende, 2010). Concerns regarding environmental hazards coupled with high energy demand have directed attention towards the production of clean biofuels as an alternative source of energy (Milano *et al.*, 2016).

Biofuels are a source of energy that may provide a solution to the current unsustainable demand on fossil fuels, the insecurity of energy supply and climate change mitigation. Biofuels produced from biological oils can be used directly in existing engines with little or no modifications (Scott *et al.*, 2010). First generation biofuels (circa 2009) were produced from the processing of expensive feedstock, generally sugars, grains or seeds. More than 85% of biodiesel was produced using edible crop oils via first generation processes in 2013 (Rawat *et al.*, 2013). The amount of fossil energy consumed during feedstock production (cultivation and crop harvesting), transport, and fertilizer/pesticide manufacture and/or in the biofuel production plant itself contributed to greenhouse gas load (Ashfaq *et al.*, 2015); thus making first generation biofuels inappropriate in terms of economic feasibility and environmental safety. Although second generation biofuels

(circa 2010) produced from non-edible lignocellulose biomass (non-edible residues of food crop/whole plant biomass) do not affect food security, they suffer from high processing costs and underdeveloped technologies (Mohr and Raman, 2013). The removal of biomass from fields accelerates top soil erosion and require greater nitrate supplementation thus expanding N_2O (nitrous oxide) production as well as nitrate over-burdening (Agency, 2010). Moreover, the removal of dead/dying biomass from forests prompts lower carbon sequestration in forests thereby affecting biodiversity (Balan, 2014). Growing perennial crops for bioenergy over millions of hectares puts pressure on both the land and biological communities. The environmental and economic concerns associated with first and second-generation biofuels required *third* generation biofuels to fulfil energy demands in an eco-friendly and efficient manner. Such technology will be driven by enhanced biocatalysis using alternative sources of raw biofuel substrates. One area of growing interest is the use of microorganisms such as microalgae for oil production. This approach avoids the loss of food crops, avoids the difficulties with valorisation of biofuels and provides for higher oil yields. The key step in conversion of a biological lipid into biodiesel involves a transesterification reaction. The process involves the reaction of triglyceride molecules, present in oils/fats, with an alcohol to produce esters and glycerol in the presence of a catalyst. This transformation can be accomplished using a biocatalyst such as a lipase enzyme.

1.1. LIPASES AS BIOCATALYSTS

Lipases (triacylglycerol acylhydrolases, E.C. 3.1.1.3) are ubiquitous carboxylic ester hydrolases (carboxylesterases) that can catalyse both hydrolysis and synthesis of long chain acylglycerols. Due to their diverse substrate specificities, stereoselectivity, and stability in extreme conditions (e.g. heat, pH, organic solvents), lipases have long been used as catalysts in biodiesel production (Jaegera and Reetzb, 1998). Bacterial and fungal lipases contribute 45% and 21% respectively to industrial biocatalytic applications (Patil, Chopda and Mahajan, 2011). Lipase-based biocatalysis can, however, be constrained by the presence of organic solvents that are employed for biodiesel synthesis. There is a therefore, need for lipases with greater solvent tolerance and higher thermal stability.
Microorganisms belonging to *Bacillus*, *Pseudomonas*, *Rhodococcus*, *Staphylococcus* and *Arthrobacter* species produce organic solvent tolerant lipases

(Kumar *et al.*, 2016), and hence can be used for transesterification reactions in an organic reaction medium. These lipases that can catalyse in anhydrous organic solvents can favour synthesis by shifting the thermodynamic equilibrium and can, therefore, be used with hydrophobic substrates. Lipase mediated transesterification reactions can be performed at relatively low temperatures (25–50°C) and do not produce soap, making biodiesel-glycerol separation/purification easier and more economically feasible. Production of environmentally friendly biodiesel not only requires a natural catalyst but also requires a natural oil source. Microalgae, explored in this thesis, provide an excellent source of oil production for biodiesel synthesis since their carbon is directly acquired via photosynthesis.

1.2. MICROALGAE

Microalgae are the fastest growing photosynthesizing organisms and can complete an entire growth cycle in a few days if adequate sunlight, water, CO_2 and nutrients are available. Their high growth rates help in rapid accumulation of a significant amounts of lipids (Mairet *et al.*, 2011). The average oil content in microalgae is 25-200 times higher than crop-based biofuels, making microalgae a highly productive feedstock (Lee *et al.*, 2014). Low harvesting and transport costs make the process more economical. Cultivation of microalgae for biodiesel production requires roughly 2% of the land required to produce the same amount of biodiesel from oil bearing crops (Ahmad *et al.*, 2011a). Furthermore, microalgae are readily adaptable to their environment, do not require fertile land, and therefore, can be grown almost anywhere; even on sewage, saltwater or wastewater.

Wastewater from municipal sources, dairy/poultry industry and other agricultural practices is a highly concentrated stream of waste-based nutrients. It is unsuitable feed for terrestrial crops as leached nutrients from soil will cause serious eutrophication of surface waters. In contrast, these wastewater nutrients can be utilized by microalgae. Hence, culturing of microalgae in wastewater not only provides an inexpensive alternative method of wastewater treatment, but also substantially reduces the need for chemical fertilizers and their associated life cycle burden (Lam and Lee, 2012). Sustainable use of underutilized resources by microalgae culture will provide benefits in both economic and environmental sectors.

Research Motivation

Considering the demand for environmentally friendly fuel, the aim of this thesis was to isolate and utilise environmentally friendly and sustainable components (lipases and microalgal triacylglycerols) for fuel (biodiesel) production. To achieve the aim of the thesis following objectives were identified:

1.3. RESEARCH OBJECTIVES

- To develop synthesized knowledge around solvent stable lipases, microalgae and their implementation in biodiesel synthesis (Chapter 2)
- To screen bacterial strains producing solvent stable lipases (Chapter 4)
- To optimise lipase production conditions for selected strains, to purify and characterise solvent stable lipases of interest (Chapter 5)
- To immobilize/entrap purified lipases for the specific application of biofuel synthesis (Chapter 6)
- To optimise growth conditions of the microalgae, *Chlorella emersonii* and *Pseudokirchneriella subcapitata* in simulated secondary-treated municipal wastewater for neutral lipids production (Chapter 7)
- To perform *in-situ* transesterification reactions using microalgal neutral lipids/triacylglycerol(s) using free or immobilized/entrapped lipases and compare synthesised crude biodiesel with commercially available product (Chapter 8).

CHAPTER 2: LITERATURE REVIEW

2.1. INTRODUCTION

Catalysts are the workhorses of biochemical transformations. Catalysts accelerate reactions in thermodynamically favourable regimes, requiring milder processing conditions such as temperature and pressure. This reduces both the investment and operational cost of biochemical processes. Catalysts provide alternative chemical reaction pathways which are energetically favourable (Champe, Harvey and Ferrier, 2005).

2.2. CHEMICAL VS. ENZYME CATALYSIS

From a commercial and environmental point of view, many chemical transformation processes have inherent drawbacks. The high temperature/pressure needed to drive chemically catalysed reactions leads to high energy costs and requires large volumes of cooling water. They are also associated with nonspecific reactions resulting in poor product yields (Gurung *et al.*, 2013). These processes need high capital investment and specially designed equipment. High energy consumption and unwanted by-products can have a negative impact on the environment. Since biological catalysts (i.e. enzymes) are biodegradable and can work at moderate reaction conditions; they are considered environmental friendly (Anastas *et al.*, 2000). Enzymes provide high selectivity and specificity towards substrates, resulting in little to no side reactions, with no unwanted by-products, further eliminating the need for extensive downstream processing. This decreases overall cost and energy consumption (Singh *et al.*, 2016). Moreover, through immobilization, enzymes can be reused; saving time and energy, (Salihu & Alam 2015, Villeneuve et al. 2000). These advantages of enzymes over chemical catalysts are responsible for them occupying 75% of industrial applications (Andualema and Gessesse, 2012). In 2014, the global market for industrial enzymes was estimated about $4.2 billion and by 2020 is expected to reach nearly $6.2 billion (Singh *et al.*, 2016).

2.3. LIPASES

Lipases, also known as serine hydrolases, are ubiquitous enzymes which belong to the family of triacylglycerol ester hydrolases (E.C. 3.1.1.3; (Aravindan, Anbumathi and Viruthagiri, 2007). Lipases are also termed carboxyl-esterases, since they catalyse the hydrolysis (and synthesis) of long-chain triglycerides. They were first discovered by Claude Bernard from pancreatic juice in 1856 (Romo, 1989). Later in 1901, their presence was observed in the *Bacillus* genus (*B. prodigiosus*, *B.pyocyaneus* and *B. flyorescens;* (Jaeger *et al.*, 1994). To date a large number of lipase producing microbes have been identified. Amongst them *Candida, Geotrichum, Rhizopus* and *Bacillus, Pseudomonas, Burkholderi, Streptomyces* are the most studied (Bose and Keharia, 2013). Lipases possess a unique characteristic among enzymes; the ability to catalyse reactions at the interface of aqueous and non-aqueous solutions. Due to their characteristics, performance and applications, lipases have long been subjected to intensive research and study (Andualema and Gessesse, 2012). Lipases can be isolated from many sources (plant, animal or microbe); however, lipases isolated from microbes contribute a greater portion of industrial applications (Borrelli and Trono, 2015). Advantages of microbial lipases over higher organism lipases are detailed in Table 2.1.

Table 2.1: The advantages offered by using microbes as lipase source.

Factor	Advantage	Reference
Stability	Thermostable, higher catalytic activities, optimum catalytic pH in neutral-alkaline range	(Salihu and Alam, 2015)
Availability	Low production cost due to rapid growth in inexpensive media	(Andualema and Gessesse, 2012)
	High yields due to short growth stages	(Salihu and Alam, 2015)
	Easy lipase production control by changing the inducer (oil/fatty acid)	(Aravindan, Anbumathi and Viruthagiri, 2007).
	Mostly extracellular, easy economical and efficient purification	(Andualema and Gessesse, 2012)
Modifications	Easy due to availability of genetic data, short life cycles	(Salihu and Alam, 2015)

2.3.1 Lipase structure and catalysis

Lipases are classified as serine hydrolases (Andualema and Gessesse, 2012), with an α/β hydrolase fold (comprising α-helices and β-strands).The core of a typical lipase contains eight different β sheets (β1- β8) that are connected to six α helices (A-F). All eight β sheets are parallel, except the second anti-parallel β sheet. This second β sheet has left-handed super-helical twist, covering about half a cylinder and making an angle of 90° with the last strands (Figure 2.1). Lipases differ in the curvature of the β sheet and on the spatial positions of α helices. Lipases also differ from each other in length and in the architecture of the binding domain of the α/β-hydrolase fold; resulting in their wide substrate diversity (Andualema and Gessesse, 2012).

Many lipases contain a helical segment termed the 'lid' (Aravindan, Anbumathi and Viruthagiri, 2007). The lid is amphipathic in nature; in the "closed" conformation the hydrophilic side of lid faces the solvent; however, in the "open" conformation (e.g. at the oil-water interface), the hydrophobic face is exposed, thereby contributing to substrate binding (Khan, Dutta and Ganesan, 2017). In the presence of lipid aggregates the enzyme undergoes interfacial activation whereby the lid opens up, increasing enzyme activity (Andualema and Gessesse, 2012).

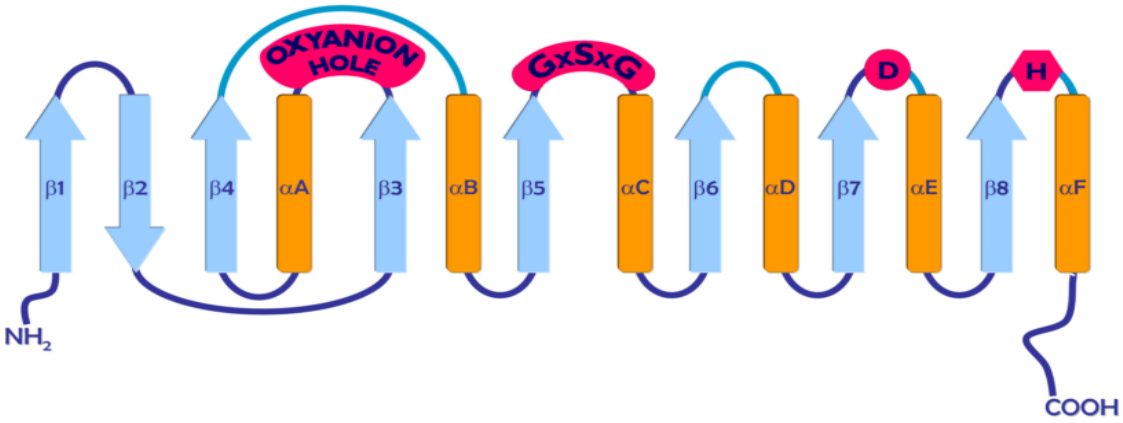

(a)

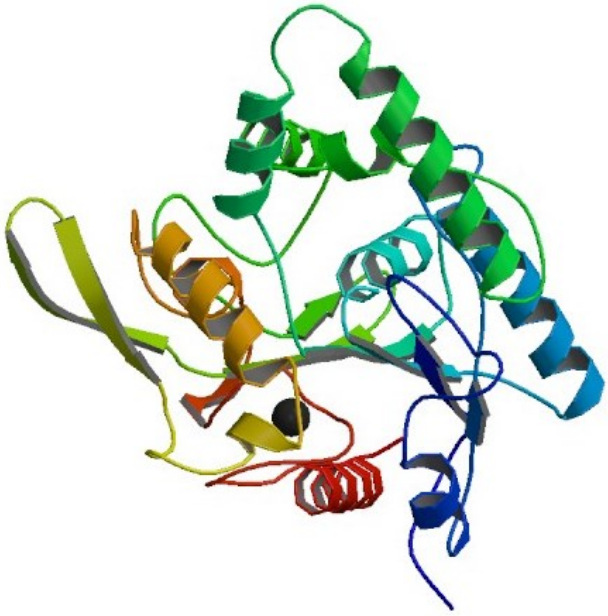

(b)

Figure 2.1: (a) Canonical fold of the α/β-hydrolase, arrows are β strands while cylinders are α helices. Motifs in pink: oxyanion hole, which stabilizes negatively charged intermediate generated during ester-bond hydrolysis; GXSXG, is the 'nucleophilic elbow' of lipase consisting of the catalytic serine; D, H are aspartate and histidine residues respectively, that are involved in catalytic site formation (Borrelli and Trono, 2015). (b) open conformation of *Pseudomonas cepacia* lipase (3LIP) adapted from Protein Data Bank. The black dot represents Ca^{2+} ion.

The active site of an α/β-hydrolase lipase is typically composed of three catalytic residues: a nucleophilic residue (serine, cysteine or aspartate), a catalytic acid residue (aspartate or glutamate) and a histidine residue. This amino acid sequence is unique for every lipase and is different from any other enzyme that contains a catalytic triad (e.g. hydrolase and transferase enzymes). The nucleophilic residue is located at the C-terminal end of strand β5 in a highly conserved pentapeptide GxSxG (Andualema and Gessesse, 2012); G-x1-S-x2-G is the catalytic moiety (see Figure 2.1 a), where G-glycine, S-serine, x1-histidine and x2-glutamic or aspartic acid (Aravindan, Anbumathi and Viruthagiri, 2007).

Hydrolysis of the substrate (e.g. oil/triglyceride) by a lipase begins with a nucleophilic attack by the catalytic-Serine/Cysteine/Aspartate on the carbonyl carbon atom of the substrates' ester bond (see Figure 2.2a). This results in the formation of a tetrahedral intermediate (Figure 2.2b), which is stabilized by hydrogen bonding with the nitrogen atoms of main chain –NH groups of two amino acid residues from the 'oxyanion hole'

(see Figure 2.2c). This acyl-lipase complex releases an alcohol, which is hydrolysed, producing fatty acid and enzyme regeneration (Figure 2.2d).

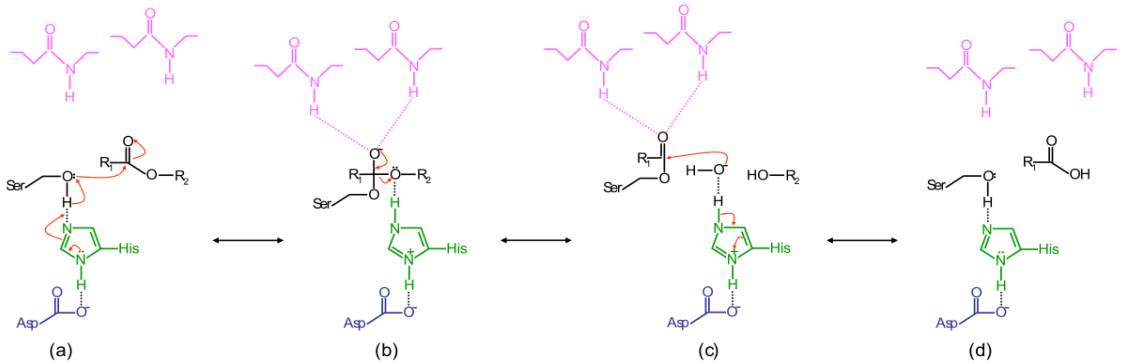

Figure 2.2: Lipase based hydrolysis of an ester bond (a): nucleophilic attack of a serine hydroxyl on the triglyceride ester bond - facilitated by proton transfer to an active site histidine, (b): formation of a tetrahedral intermediate, (c): an alcohol is released followed by a water molecule nucleophilic attack on the acyl enzyme (d): the acyl product is released and free enzyme is regenerated (Borrelli and Trono, 2015).

Since lipases work at the interface of water and oil, their kinetics cannot be described by the Michaelis-Menten model, which is valid when both the enzyme and substrate are present in a homogeneous phase (Rajendran, Palanisamy and Thangavelu, 2009). Lipolysis involves two successive equilibria; the first involves the penetration of the water-soluble enzyme into an interface (E ⇌ E*; see *Lipase** in Figure 2.3). The second equilibrium involves binding of this enzyme to a single substrate molecule forming the enzyme substrate complex (E*S; see Figure 2.3). All the products generated diffuse away, inducing no change over time in the physiochemical properties of the interface (Verger and de Haas, 1976).

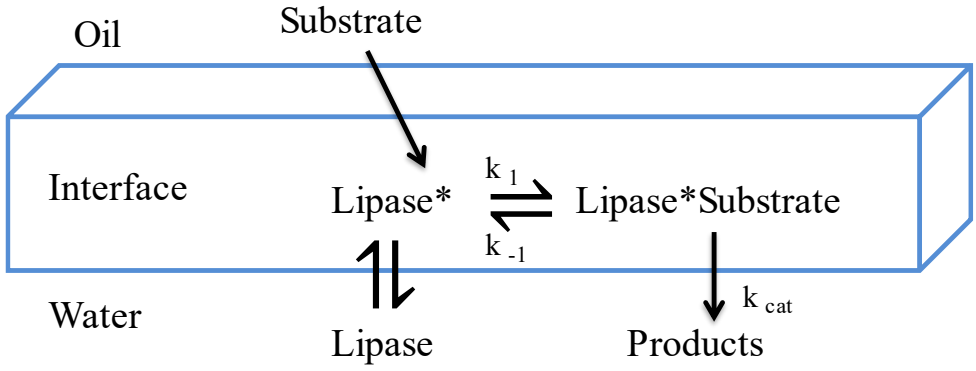

Figure 2.3: Schematic of lipolysis at an oil-water interface. Lipase* represents the transition phase of lipase when the enzyme is in its open conformation. k_{cat}, k_{-1}, k_1 represents the rate constants for individual steps. k_{cat}: describes the turnover rate of enzyme-substrate complex to form product and regenerate free enzyme; k_1 details the forward constant rate (product formation), k_{-1}: is the reverse constant rate (enzyme availability after reaction).

The hydrolysis of fats or oils is theoretically a reversible reaction and the direction of the reaction can be changed by the reaction conditions. The water content of the reaction mixture controls the equilibrium between forward and reverse reactions. *In vivo,* where water concentrations are high, the reaction is essentially irreversible. However, in non-aqueous environments, lipases can catalyze ester synthesis (esterification, transesterification or interesterification); while in an aqueous environment, lipases catalyse a hydrolysis reaction. The esterification reaction involves ester synthesis from alcohols and carboxylic acids. In transesterification, in place of the acid, the acyl donor may be an ester. The transesterification can be further divided into glycerolysis and alcoholysis, involving transfer of acyl group from a triglyceride to either glycerol or an alcohol. In interesterification, the acyl group is exchanged between a glyceride and either a fatty acid (acidolysis) or a fatty acid ester (Malcata *et al.*, 2000) Figure 2.4)

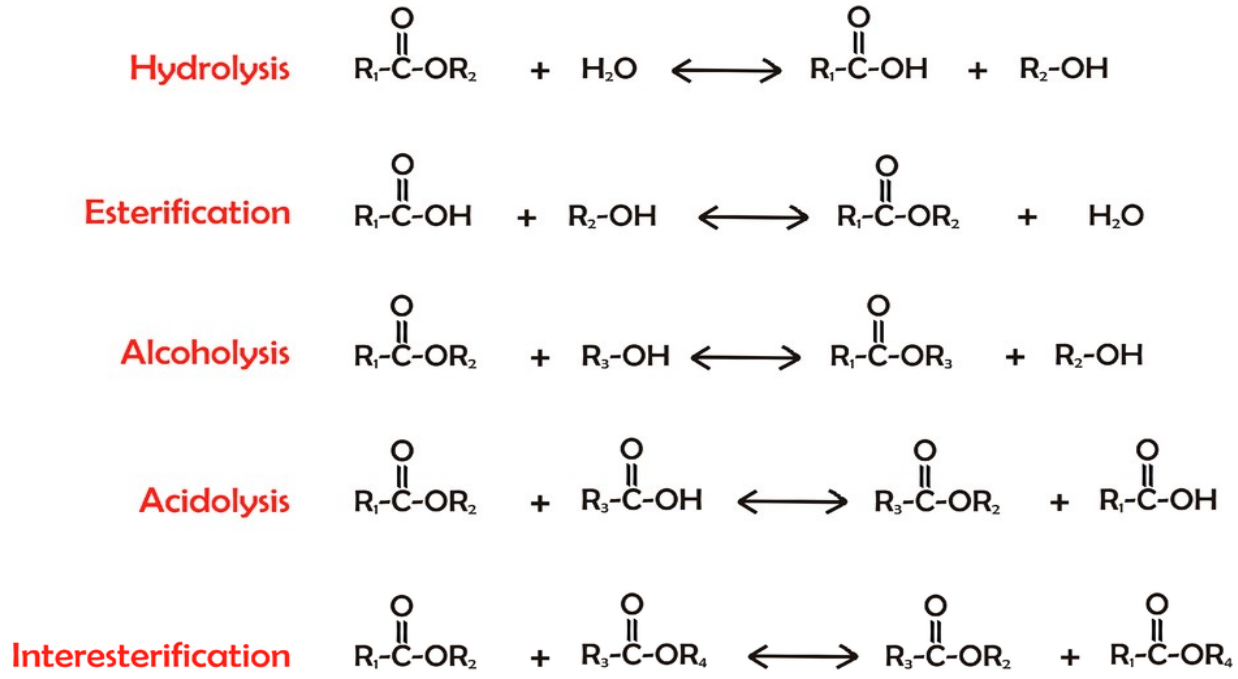

Figure 2.4: Summary of some possible lipase catalyzed reactions: Hydrolysis is cleavage of carboxyl ester bonds in the presence of water. In the presence of a carboxylic acid and an alcohol the lipase catalyses esterification while an ester and an alcohol give rise to alcoholysis. In presence of organic acid acidolysis occurs. A reaction between two esters is known as as inter-esterification (Borrelli and Trono, 2015).

Since lipases act on a variety of substrates and, have complex kinetics and varied applications, a variety of assay methods have been developed for their qualitative and quantitative estimation.

2.4. LIPASE ACTIVITY DETECTION METHODS

Lipolytic activity is difficult to determine since lipases catalyse hydrolysis at oil-water interfaces. For this reason, factors such as substrate concentration at the interface or the use of different detergents must be considered. Several assay methods are described in the literature which take these factors into account and have been used for quantifying the activity of lipases.

2.4.1. Agar Plate Assay

Non-quantitative methods, such as the Agar Plate Assay (APA) are used to detect the presence of lipase in a solution. Lipase activity is detected by the appearance of degradation haloes on culture media supplemented with emulsions of substrates like tween, tributyrin, triolein or even olive oil (Samad *et al.*, 1989). The release of FAs (Fatty Acids) from these substrates can be detected by either pH indicators, such as neutral red/crystal violet - whose colour changes in response to the acidification produced upon liberation of free FAs (Bornscheuer, Altenbuchner and Meyer, 1999) - or by adding fluorophores such as Rhodamine B, which forms a complex with FAs producing an orange-pink fluorescence under UV irradiation (Bornscheuer, Altenbuchner and Meyer, 1999).

2.4.2. Spectrophotometric assay

Quantitative assays, such as spectrophotometric assays are widely used because of their fast and simple estimation of lipase activity. Lipase activity is determined by employing synthetic substrates that, after hydrolysis, release products that can be detected spectrophotometrically. The most common artificial substrates for these assays are *p*-nitrophenyl and napthyl esters/thioesters of long chain fatty acids. Lipolysis of *p*-nitophenyl esters (palmitate, butyrate *etc*), for example, releases *p*-nitrophenol which is yellow in colour and its absorbance can be measured between 405-410nm (Charles and Jack, 1947). This method is highly pH dependent and does not work at acidic pH where it can generate false positive results due to non-enzymatic hydrolysis of *p*-nitrophenol esters (Martin, Golubow and Frazier, 1958). Upon lipolysis, naphthyl esters (naphthylcaprylate, napthylacetate, napththylpropionate) release naphthol which forms a

red coloured complex with diaxonuim salts giving strong absorbance at 560nm (Martin, Golubow and Frazier, 1958).

Since spectrophotometric assays involve synthetic lipase substrates and their analogues; they suffer from low specificity, and therefore, true lipase concentrations can be underestimated. Other methods for spectrophotometric quantification include the quantification of glycerol released upon triacylglycerols lipolysis. One such assay for glycerol quantification was developed by Sigma whereby glycerol formation is coupled with a series of intermediates, ultimately reducing a quinoneimine dye which can be monitored at 545nm (Isobe, Akiba and Yamaguchi, 1988).

2.4.3. Spectrofluorimetric methods

Fluorometry is a sensitive analytical technique that can be used for continuous monitoring of enzyme activity. A fluorimetric method for lipase activity can be carried out using substrates that, upon hydrolysis, release chromogenic products. Furthermore, fluorophore substrates, which generate fluorescence upon hydrolysis, can be employed. A variety of fatty acid esters derived from parinaric acid and coumarin (umbelliferone) are chromogenic. Parinaric acid is a naturally occurring chromophore, which fluoresces at 432nm when excited at a wavelength of 320nm (Andualema and Gessesse, 2012). However, this assay is limited due to oxidation of parinaric acid by atmospheric oxygen.

Other chromogenic products like Rhodamine B have been widely used for lipase activity determination. Rhodamine B emits fluorescence at 535nm when excited at a wavelength of 485nm (Kouker and Jaeger, 1987), (Jarvis and Thiele, 1997). Fluorophores from sansyl, resorufin or 4-methylumlelliferone (MUF) groups are also used for lipase detection via fluorometry (Hospital, Creu and Pau, 1999).

2.4.4. Titrimetric/volumetric methods

Although titrimetric methods have low sensitivity, they have been used as a reference method for the determination of lipase activity. Free fatty acids released from lipase-mediated hydrolysis of triacylglycerols (emulsion of natural/synthetic triacylglycerols i.e. TAGs) are measured titrimetically. The titration can be carried out manually with

standardized NaOH to achieve an end point alkalinity, or with a pH-instrument (Peled and Krenz, 1981).

2.4.5. Radiometric methods

Radioactive assays for lipase determination require triacylglycerols that are radioactively tagged (at the acyl chains). Commonly used radioactive substrates are oleoyl-glycerols (labelled with 14C or 3H) or iodine-131-labeled triglyceride analogues. The assay is very sensitive and can detect to 1 milliunit (1mμmoles of released fatty acids per minute; (Kaplan, 1970). However, special substrates are required, and this method cannot be used for continuous enzyme activity monitoring. Moreover, the assay requires expensive radioactive substrates, which are harmful, and the assay is time-consuming (Stoytcheva *et al.*, 2012).

2.4.6. Tensiometric methods

Lipolysis often involves interfacial activation where the lipase undergoes adsorption at the interface of an oil-water matrix to initiate catalysis. The nature of the interfacial layer around lipid droplets determines the rate of lipid hydrolysis (Reis *et al.*, 2008). Since the lipid layer is formed between air/water interfaces, lipolysis releases fatty acids, which change the surface pressure. This surface pressure can be monitored using a barostat. The assay is very useful to determine the kinetic parameters of a lipase, however, the entire set up is expensive and cumbersome (Stoytcheva *et al.*, 2012).

2.4.7. FTIR spectrophotometry

FTIR can be used for a direct monitoring of enzymatic reactions. During enzyme catalysis, the molecular structure of compounds is modified (the loss of an ester bond signal), thereby altering the infrared spectrum. This change can be monitored in order to follow the progress of the lipase reaction (Martin, Golubow and Frazier, 1958). Lipase catalysed hydrolysis can be quantified by the presence of isosbestic points in the FTIR spectrum. The C=O band formed by fatty acids at 1715cm^{-1} can provide an estimation of fatty acids released during lipolysis (Walde and Luisi, 1989).

2.4.8. Turbidimetry

Detachment of triacylglycerides after lipolysis produces a soap-like substance and also creates a micelle capable of electrostatic interaction. These two phenomena influence interfacial tension (Burlina and Galzigna, 1973). Lipase activity can therefore be quantified by measuring the change in intensity of an incident beam at 546nm. In a variation of this principle, Tween 20 or 80 can be used to estimate lipase activity. Hydrolysis of Tween in a liquid media containing calcium chloride yields a fine, evenly suspended precipitate of calcium salts of fatty acids (Stelmaschuk and Tigerstrom, 1988). An increase in the turbidity of the solution, due to precipitation of lipolysis products as calcium salts, is proportional to lipase activity. This method is more sensitive than the spectrophotometric assay with *p*-nitrophenol palmitate and thirty-six times more sensitive than the titrimetric assay with Tween 20. Unfortunately, Tweens are not broadly applicable lipase substrates (Gupta *et al.*, 2010).

2.4.9. Chromatography

Free fatty acids released from a substrate after lipase catalyzed lipolysis can be measured by; silicic acid columns, thin layer chromatography, gas chromatography of FA methyl esters and high-performance liquid chromatography. Estimation and detection of lipase activity is usually performed by detecting β-naphthol, *p*-nitrophenol or products of FA ester derivatives after lipolysis. Although chromatography is a very sensitive method for lipase determination, it is expensive and time consuming. Moreover, experienced personnel and sophisticated laboratory equipment are required (Stoytcheva et al. 2012).

With the development of lipase dectection assays the identification of lipases has increased. Enzymologists have sourced lipases from wide-ranging sources, especially from extremophiles. The combined detection assays and improved isolation approaches have supported the identification and use of solvent compatible, tolerant and stable lipases with an expanded application spectrum of these adaptable enzymes resulting.

2.5. POTENTIAL SOURCES OF BIOTECHNOLOGICALLY USEFUL LIPASES

Organic solvents are commonly used as non-aqueous media for biocatalysis (Wang *et al.*, 2016). However, many enzymes are either inactivated or denatured in organic solvents,

which limits their use as catalysts in non-aqueous environments (Kumar *et al.*, 2016). Despite these challenges, the use of solvents in biosynthetic applications has not been eliminated completely and many industrial processes (biodiesel, biopolymers, cosmetics, pharmaceuticals) still employ non-aqueous environments (Section 2.5.2). The benefits of non-aqueous biocatalysis have encouraged researchers to discover, or engineer, enzymes that are stable in non-aqueous environments (see Figure 2.5). From a processing and economic viewpoint, aqueous biotransformation reactions results in expensive purification due to the low vapour pressure and the high boiling point of water (Qayed *et al.*, 2015). Similarly, water-based transformations can result in unwanted side reactions such as hydrolysis, racemization, polymerization and decomposition; thus, limiting the reaction of interest. The product yield often depends directly on the solubility of substrates/products. Since non-aqueous reactions offer higher solubility for non-polar compounds (substrate/product); they are often more favourable as a catalytic environment (Kumar *et al.*, 2016).

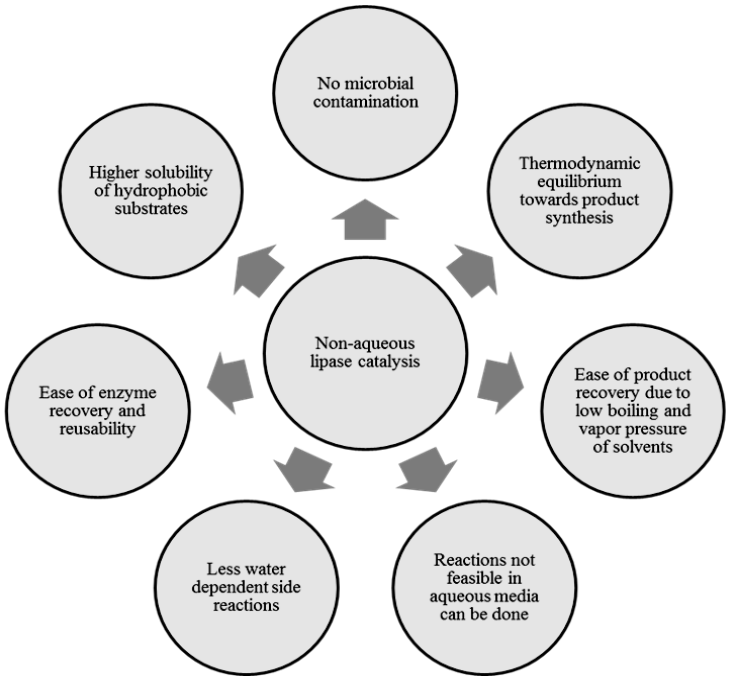

Figure 2.5: Schematic overview of the advantages offered by non-aqueous catalysis compared to aqueous catalysis for applications where synthesis is required.

Though various enzymes; proteases for example (Ogino *et al.*, 1999), are known to possess impressive solvent stability; solvent stable lipases are one of the leading biocatalysts in non-aqueous environment due to their unique property of catalyzing reactions at the water solvent interface (Figure 2.4; (Sharma and Kanwar, 2014); however, sourcing novel, stable, lipases can be challenging.

2.5.1. Extremophiles

Industrial enzyme-based biocatalysis has evolved from catalysis in an aqueous medium, to reactions of molecular synthesis in non-conventional (non-aqueous) media. Since non-aqueous biocatalysis is superior in many processes, significant research effort in recent decades has been devoted to establishing platforms for the enhancement of non-aqueous biocatalysis (Illanes, 2016). Physical (immobilisation), chemical (protein engineering) and genetic methods (*de novo* pathway engineering) have been employed to tailor lipases in order to increase their activity, stability and selectivity in non-aqueous environments (Villeneuve *et al.*, 2000). However, nature provides a vast natural microbial enzyme pool; which can be easily bio-discovered by exploring the diversity of microbes in the biosphere (Adrio and Demain, 2014).

Evolution developed mechanisms by which microorganisms adapted to extreme environments. The presence of potential novel genes, new bioproducts, enzymes or metabolites in these extremophiles has already been revealed by metagenomic studies (Dalmaso, Ferreira and Vermelho, 2015). Enzymes, which remain catalytically active under extreme conditions can display poly-extremophilicity (i.e., stability and activity in more than one extreme condition) making them interesting for a variety of industrial applications (Rampelotto, 2013). Since enzymes from these extremophiles are already adapted to extreme conditions the possibility of isolating thermostable or salt tolerant enzymes from a thermophile or halophile microorganism, is higher (Salameh and Juergen, 2007). Studies have demonstrated that this theory extends to extracellular enzymes secreted by solvent-tolerant microorganisms (Mahanta, Gupta and Khare, 2008; Dandavate *et al.*, 2009). This interconnection between the habitat of micro-organism and their enzymes helps in the determination of an enzyme's properties (Ahmed et al. 2010). Microorganisms producing lipase(s) have been isolated from diverse and extreme habitats such as industrial waste, oil processing factories, oil contaminated soil etc. (Sharma, Yusuf and Uttam Chand, 2001). Lipases isolated from these sources are quite diverse and vary in terms of physical, chemical and biological properties, as well as have varying optimum catalytic conditions (pH, temperature, tolerance to emulsification and surfactants; (Ugo *et al.*, 2017). Lipases obtained from conventional sources typically have an optimal temperature working range from 30°C-60°C (Andualema and Gessesse,

2012). Conversely, lipases from thermostable microbes, e.g. *Bacillus thermocatenulatu, Geobacillus thermodenitrificans* possess maximum activity over 70°C (Christopher *et al.*, 2015; Bakir and Metin, 2016). Furthermore, lipases isolated from solvent stable *Staphylococcus aureus, Pseudomonas stutzeri* possess solvent stability (Cao *et al.*, 2012; Ben Bacha, Moubayed and Al-Assaf, 2016).

2.5.1.1.Solvent stable microbes

Organic solvents are generally extremely harsh to living cells (Kumar *et al.*, 2016). They can accumulate in the cell membrane increasing its permeability resulting in ions/metabolites being released from the cell thereby triggering cell death (due to change in intracellular pH and membrane electrical potential of the cell; (Henderson and Block, 2014)). Microbial cells have been observed to undergo oxidative damage due to failure of the native cellular transport system, resulting in the production of peroxide and other reactive oxygen species (Segura *et al.*, 2012). Despite all these effects, solvent tolerant bacteria are capable of thriving in presence of these toxic chemicals; which make them an interesting system for understanding the mechanisms behind their survival and proliferation (see Figure 2.6).

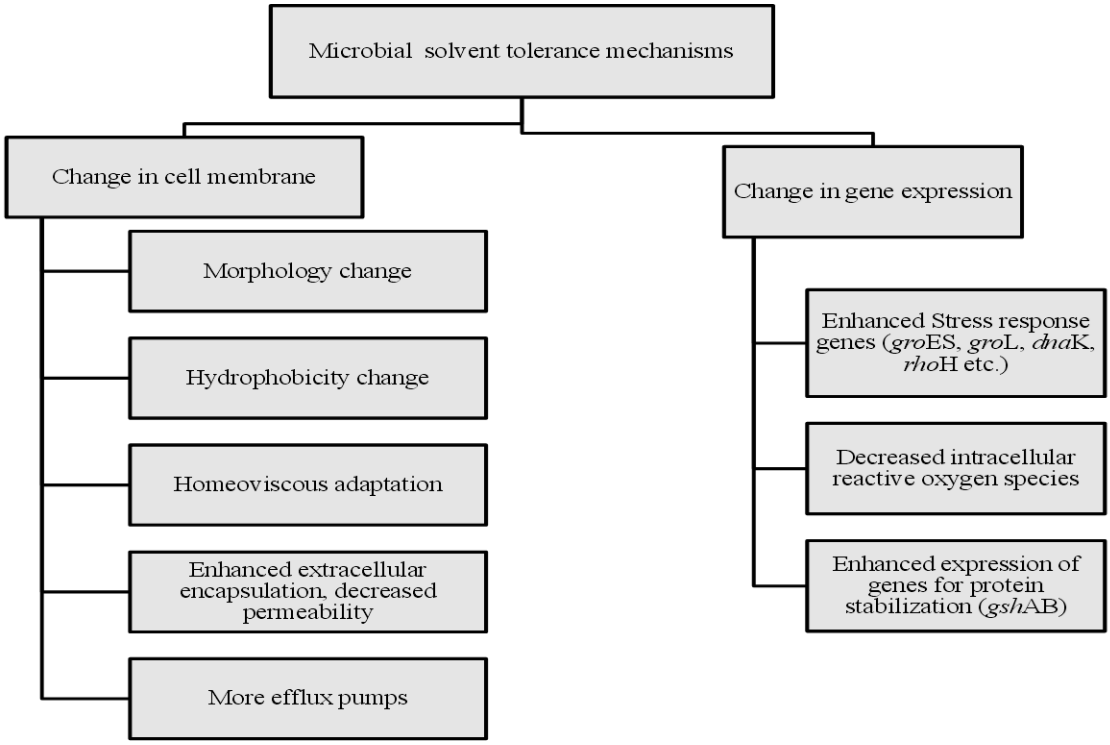

Figure 2.6: The common solvent tolerance mechanisms observed in Gram-negative and Gram-positive bacteria can provide insights into the biological pathways responsible for survival and proliferation of solvent stable microbes. Single, or a combination of, factors can contribute in generation of diverse metabolic profile(s), diverse building blocks and enzymes. The mechanisms were summarized from various literature references mentioned in section 2.5.1.1.

Solvent stability adaptive mechanisms have been observed in both Gram negative and positive bacterial strains (see Table 2.2), which help them to survive and proliferate in the presence of organic solvents. However, there is no single mechanism that solely confers microbial adaptation to organic solvents but instead a complex and coordinated group of adaptive mechanisms are involved in microbial cell survival in non-aqueous environments.

Table 2.2: A summary of the mechanisms of adaptation to organic solvents by microorganisms. Microbes adopt different survival mechanisms when exposed to organic solvents, either *in vivo* or *in vitro*. Changes in the cell membrane, for example, its composition, fluidity and number of efflux pumps help in the removal of solvents from the cell membrane while production of various secondary metabolites reduces cellular oxidative stress**.**

Gram stain	**Microorganism**	**Stability mechanisms**	**Reference**
Gram Negative	*Escherichia coli*	Up-regulating efflux pumps (acrRAB genes; AcrAB-TolC)	(Lee, Cho and Kim, 2014)
		Up-regulation of gadAB, downregulation of aspA, tnaA, malE, mglB, cstA and lamb	(Geng and Jiang, 2015)
		Up-regulation of gadABCE, hdeABD (acid resistance), Down-regulation of proVWX, manXYZ (transporters)	(Chong *et al.*, 2014)
		Disturbance in nuo and cyo operons (respiration); sodA, sodC, yqhD (oxidative stress); malE and opp operons (biosynthesis/metabolic transport)	(Rutherford *et al.*, 2010)
	Shewanella putrefaciens	Change in cell permeability and hydrophobicity; Production of secondary metabolites (carotenoids and biosurfactants); Biofilm formation; Changes in expression of catabolic (alkB1 and alkM1) and transporter gene (HAE1)	(Stancu, 2015)
	Pseudomonas putida	Enhanced impermeabilisation; Activation of stress response system; Enhanced energy generation; Induction of efflux pumps	(Ramos *et al.*, 2015)
Gram Positive	*Enterococcus faecalis*	Change in membrane fluidity by enhanced formation of long chain fatty acids, saturated and cyclopropane fatty acids (CFA's)	(Kanno *et al.*, 2013)
	Clostridium acetobutylicum	Over expression of glutathione gshAB cluster for protein stabilization	(Zhu *et al.*, 2011)

Other mechanisms have been observed for microbial solvent tolerance; for example, *cis-trans* isomerase is activated in *Pseudomonas oleovorans* GP012, catalyzing isomerization of *cis*- to *trans*-unsaturated fatty acids (Pedrotta and Witholt, 1999). In Gram-negative bacteria, the most effective method for solvent tolerance is the expression of efflux pumps of the RND family. For example, *P. putida* DOT-TIE has twenty efflux pumps which support its survival in the presence of toluene (Segura *et al.*, 2012).

Although changes in cell membrane composition or expression of various efflux pumps help many microbes to show tolerance towards solvents; for their proliferation and growth they also require solvent tolerant enzymes/proteins.

2.6. SOLVENT STABLE LIPASES

Solvents generally have an adverse effect on the stability and activity of an enzyme. The extent of solvent toxicity for an enzyme is determined by the log P value of the solvent (Pogorevc, Stecher and Faber, 2002). The log P value for a compound is the logarithm (base 10) of the partition coefficient (P), which is defined as the ratio of the compounds organic (oil)-to-aqueous phase partition concentration

$$Partition\ coefficient\ (P) = \frac{(conc.of\ compound\ in\ organic\ phase)}{(conc.of\ compound\ in\ aqueous\ phase)}$$

Log P of a solvent is directly proportional to its hydrophobicity; i.e. a lower log P value means lower hydrophobicity, the higher water solubility and, hence, the higher the toxicity. Therefore, solvents with log P< 2 are highly toxic to most enzymes (Segura *et al.*, 2012). Due to higher toxicity of solvents with log P<2 and reduced stability of enzymes in these solvents; solvents with a higher log P (>2) are preferably used in enzyme-catalysed reactions (Salihu and Alam, 2015).

2.6.1. Interaction between organic solvent and lipases

The stability of an enzyme in a solution depends on the interaction between the enzyme and surrounding solvent. Changes in the activity and stability of a lipase within an organic solvent is often correlated with solvent hydrophobicity (log P) value (Yang *et al.*, 2012). Polar organic solvents have a high degree of partitioning and they cause enzyme deactivation by hydrogen bond disruption and hydrophobic interactions depriving the enzyme of a water hydration shell. Lipases are generally more unstable in polar, water miscible-solvents (log P<2) than in water-immiscible solvents (log P>2(Kumar *et al.*, 2016). However, a few lipases, for example that from *Bacillus sphaericus* MTCC 7542, are stable in both polar as well as non-polar organic solvents with a residual activity of 80-95%, even after 12 hours of incubation (Tamilarasan and Kumar, 2012). Conversely, some lipases are stable only in non-polar organic solvents (log P≥2) even after 7 days of incubation (e.g, *Stenotrophomonas maltophilia* CGMCC 4254 lipase; Salihu & Alam,

2015). *Acinetobacter radioresistens* CMC-1 and *Acinetobacter* EH 28 lipase have higher activity in 30% v/v *n*-Hexane, dimethyl sulfoxide and acetone than 15% v/v of *n*-Hexane, dimethyl sulfoxide and acetone (Ahmed, Raghavendra and Madamwar, 2010b). A lipase from *Burkholderia ambifaria* YCJ01 was stable for 60 days in most hydrophilic and hydrophobic solvents (25% v/v) and had 100% stability in 25% v/v ethanol and 80% stability in 25% v/v acetonitrile respectively, even after 30 days (Yao *et al.*, 2013).

Lipases that were found to be stable in organic solvents remain fixed in the native conformation due to restricted conformational flexibility (Kumar *et al.*, 2016) and the interfacial activation characteristic of lipase. Here the flexible 'lid' exposes the active site of the lipase only after interaction with a hydrophobic phase (Adlercreutz, 2013). Lipase stability is not just based on the logP value of the solvent, but on a cumulative effect of other parameters like hydrogen bonding and dielectric constant. The network of hydrogen bonds, electrostatic and hydrophobic interactions determines the conformation of any enzyme in a solvent system, directly determining activity and stability (Khmelnitsky *et al.*, 1988; Zaks, 1996). Despite all these adverse effects of organic solvents; lipases have been reported to be stable in several organic solvents (see Table 2.3).

Table 2.3: An overview of lipases stability in various solvents, catagorised based on log P value. Lipases are known to be stable in various organic solvents ranging from log P>2 and log P<2. Lipases stable in log P<2 are of more interest in the production of biofuels.

Log P	Lipase Source	% (v/v) solvent	Solvent used	Residual activity	Reference
Log P<2	*Pseudomonas* sp. DMVR46	10%	Acetone (Log P= -0.04), ethanol (Log P=0.25), iso-propanol (Log P=0.54)	>30% residual activity, 37°C for 4 hours	(Patel et al. 2014)
	Aureobasidium melanogenum	10%	Acetonitrile (Log P=-0.19), methanol (Log P=-1.26), ethanol (Log P=0.25) and chloroform (Log P=1.97)	>80% relative activity, 30 min at 37°C followed by 24 hours at 4°C	(Wongwatanapaiboon *et al.*, 2016)
	Aneurinibacillus thermoaerophilus	25%	DMSO (Log P=-1.40) and methanol (Log P=-1.26)	>100% relative activity, 30mins of incubation	(Masomian *et al.*, 2013)
	Staphylococcus epidermidis AT2	25%	DMSO (Log P=-1.40), Diethyl ether (Log P=1.35)	>120% residual activity, 30mins of incubation	(Kamarudin *et al.*, 2014)
	Bacillus sp.	25%	Acetone (Log P=-0.04), t-butanol (Log P=0.58), methanol (Log P=-1.26) and ethanol (Log P=0.25)	>80% relative activity, 30 min at 37°C	(Sivaramakrishnan and Incharoensakdi, 2016)
	Streptomyces sp. OC119-7	50%	Methanol (Log P=-1.26), ethanol (Log P=0.25), acetone (Log P=-0.04)	>70% residual activity, 30°C for 24 hours	(Ayaz, Ugur and Boran, 2014)
	Penicillum corylophilum	50%	Ethanol (Log P=0.25), acetone (Log P=-0.04), methanol (Log P=-1.26), butanol (Log P=0.68) and hexanol (Log P=1.86)	>50% residual activity, 37°C after 1 hour	(Romero *et al.*, 2014)
	Pseudoalteromonas lipolytica SCSIO 04301	50%	Ethanol (Log P=0.25), Acetone (Log P=-0.04), DMSO (Log P=-1.40), *t*-butanol (Log P=0.68), acetonitrile	>50% residual activity3 and 12 hours at room temperature	(Su, Mai and Zhang, 2016)
	Haloarcula sp. IG41	50%	Chloroform (Log P=1.97)	>60% residual activity after 2 days at 30°C	(Li and Yu, 2014)
	Staphylococcus aureus ALA1	25%	Acetone (Log P=-0.04), ethanol (Log P=0.25), methanol (Log P=-1.26), 2-propanol (Log P=0.54)	>90% residual activity after 30 min at 37°C	(Ben Bacha, Moubayed and Al-Assaf, 2016)
	Staphylococcus epidermidis AT2	25%	Acetone (Log P=-0.04)	~100% residual activity, 30 min at room temperature	(Kamarudin *et al.*, 2014)

	Burkholderia cepacia RQ3	25%	Isopropanol (Log P=0.05), ethanol (Log P=0.25), DMSO (Log P=-1.40)	Half-life >6 days at 40°C	(Xie *et al.*, 2016)
	Aneurinibacillus thermoaerophilus	25%	Propyl acetate (Log P=1.24), 1-propanol (Log P=0.54)	>60% relative activity, 30min of incubation	(Masomian *et al.*, 2013)
	Xanthomonas oryzae	20%	Methanol (Log P=-1.26)	Specific activity of >250 U/mg, 70°C for 24 hours	(Mo *et al.*, 2016)
Log P>2	*Idiomarina* sp. W33	50%	Toluene (Log P=3.07), cyclohexane (Log P=3.97), *n*-hexane (Log P=3.76), 1-decanol (Log P=4.57) and isooctane (Log P=4.37)	>70% residual activity, 30°C for 12 days	(X. Li *et al.*, 2014)
	Haloarcula sp. IG41	50%	Toluene (Log P=3.07), cyclohexane (Log P=3.97), *n*-hexane (Log P=3.76), 1-decanol (Log P=4.57) and isooctane (Log P=4.37)	>60% residual activity, 30°C after 5 days	(Li and Yu, 2014)
	Pseudoalteromonas lipolytica SCSIO 04301	50%	Toluene (Log P=3.07), *n*-hexane (Log P=4.66)	>50% residual activity, 3 and 12 hours at room temperature	(Su, Mai and Zhang, 2016)
	Staphylococcus aureus ALA1	25%	Benzene (Log P=2.13), toluene (Log P=3.07)	>90% residual activity, 30 min at 37°C	(Ben Bacha, Moubayed and Al-Assaf, 2016)
	Staphylococcus epidermidis AT2	25%	*n*-hexane (Log P=3.76), toluene (Log P=3.07)	~100% residual activity, 30 min at room temperature	(Kamarudin *et al.*, 2014)
	Burkholderia cepacia RQ3	25%	*n*-octane (Log P=4.78)	Half-life >10 days, 40°C	(Xie *et al.*, 2016)
	Aneurinibacillus thermoaerophilus	25%	p-xylene (Log P=3.15), toluene (Log P=3.07), benzene (Log P=2.13)	>60% relative activity, 30min of incubation	(Masomian *et al.*, 2013)
	Xanthomonas oryzae	20%	Heptane (Log P=4.27), *n*-hexane (Log P=4.66)	Specific activity of >250 U/mg, 70°C for 24 hours	(Mo *et al.*, 2016)
	Streptomyces sp. CS133	25%	*n*-Hexane (log P=3.76), octane (log P=4.9)	>100% relative activity, 30°C for 48 hours	(Mander *et al.*, 2012)
	Pseudomonas aeruginosa AAU2	75%	Iso-octane (log P=4.78), n-heptane (log P=4.27), *n*-hexane (log P=3.76), cyclohexane (log P=3.97), xylene (log P=3.15), toluene (log P=3.07), benzene (Log P=2.13)	>50% relative activity, 37°C 48 hours	(Bose & Keharia 2013)

Generally, organic solvents with a high log P are used in lipase-catalyzed reactions in non-aqueous medium because of their limited stripping of essential water from lipase molecules (Salihu and Alam, 2015). Since the catalytic process is strongly linked to any conformational changes in the lipase, it is important to understand how changes in lipase structure can result in organo-stability (Soares, Teixeira and Baptista, 2003); Figure 2.7). Hence, understanding the stability of lipases in organic solvents is important for their potential applications (Hwang *et al.*, 2014).

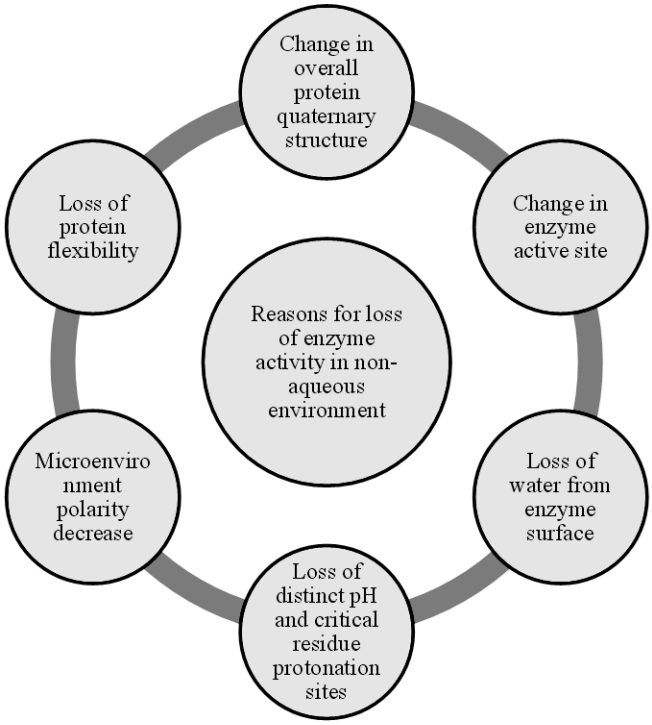

Figure 2.7: A schematic of the major factors known to effect lipase activity in non-aqueous environments. Understanding these factors can help in designing a non-aqueous environment compatible with a specific lipase catalysied reaction that will have a reduced impact on lipase activity/stability.

2.6.1.1.Essential water

Stripping of water molecules from the protein surface by solvent molecules is an important factor responsible for denaturation of enzymes in a non-aqueous environment. Since water molecules around the enzyme in an aqueous environment contribute to all the major factors that stabilize enzyme conformation, including Van der Waals interactions, hydrogen bonds, and salt bridges; conventional wisdom dictates that water is essential for enzyme stability

(Zaks, 1996). Water protects the enzyme from direct contact with other solvent molecules (Díaz-García & Valencia-González 1995; Halling 1997). Hence, complete removal of water drastically distorts enzyme conformation and can lead to enzyme inactivation. Although this reasoning is appropriate, the real question is not whether water is required, but instead how much water is crucial to retain functional enzyme activity. The water dependency of enzyme activity often follows a bell shaped curve proposed by Affleck and colleagues (Affleck *et al.*, 1992). The activity of an enzyme will increase as the percentage of water in the solvent system increases and drop after a critical level (Micaêlo and Soares, 2007). As long as this water is present surrounding the enzyme molecule, the rest (bluk phase) of water can be replaced with an organic solvent without adversely affecting the performance of the enzyme. Lipases from *Candida rugosa* and *Rhizopus arrhizus* display a bell-shaped activity response curve in the presence of solvents, however; some lipases e.g. *Pseudomonas* sp. lipase display a linear increasing response for enzyme activity in water-based solutions (Wehtje and Adlercreutz, 1997).

2.6.1.2. Nature of organic solvent

The extent of lipase activity and stability in non-aqueous environments is also determined by the polarity of the environment. Non-aqueous solutions with low polarity, cause dispersion of enzymatic hydrophobic domains resulting in enzyme inactivation (Ogino and Ishikawa, 2001). Non-polar solvents tend to have a stabilizing effect compared to their polar counterparts (Salihu and Alam, 2015). Organic solvents with functional groups located on internal carbon atoms have a larger steric effect on enzyme activity than organic solvents with functional groups on terminal carbon atoms; hence the former exhibit reduced interactions with enzyme, resulting in reduced enzyme activity inhibition (Wang *et al.*, 2016). For instance, *Pseudomonas cepacia* lipase has more activity in the presence of isooctane than *n*-butanol despite both organic solvents have a log P=0.8, but have different functional group locations (Liu *et al.*, 2010).

The association of alcohols with hydrophobic groups of an enzyme directly results in enzyme denaturation. Lipases have hydrophobic active sites, hence are more prone to alcohol

denaturation (Kumar *et al.*, 2016). Although, lipase specificity and activity can alter with a change in the surrounding organic solvent, a few lipases display different activities even in the same log P organic solvents. For example, *Candida rugosa* lipase is more active in *iso*octane than octane (log P for both solvents=4.5; (Wang *et al.*, 2016). Based on the activity and stability, it can be concluded that organic solvents modify the oil-water interface, making the substrate easily accessible to the lipase or the solvent disaggregates the lipase effecting structural changes and thus enhancing enzymatic activity (Ahmed, Raghavendra and Madamwar, 2010b).

2.6.1.3. Enzyme surface charge distribution

The polarity of the solvent and the nature of an enzyme's active site are interconnected; together they determine the activity and stability of the enzyme (Kamal *et al.*, 2013). Enhanced lipase stability in organic solvent is correlated with the presence of more negatively charged amino acids in comparison to basic amino acids on the enzyme surface. The surface charge distribution can be used to explain the stability of lipases in organic solvents with differing polarity (Chakravorty et al. 2012). The presence of negatively charged amino acids on the lipase surface maintains the stability of lipases in organic solvents, either by forming a hydrated ion network or by preventing protein aggregation because of the repulsive charges at the enzyme surface (Jain & Mishra 2015). The repulsive force created between the negative charges of the enzyme surface and the organic solvent eliminates the organic solvent effect, thus maintaining the hydration shell of essential water molecules around the lipase. The reverse is true for a lipase having greater surface-exposed positive charges which make them stable in organic solvents having log P≥2. Lipases exhibiting equivalent distribution of positive and negative charges show stability in varied organic solvents (Chakravorty et al. 2012).

2.6.1.4. Amino acids within the enzyme active site and on the enzyme surface

Lipases are known to be stable in organic solvents due to their conformation being more rigid in the presence of organic solvents (Sharma and Kanwar, 2014). Changing the rigidity of a lipase to improve it's stability has been an important target for protein engineering (Reetz, Carballeira and Vogel, 2006). Conformational changes associated with hydrophobic amino acid interactions present on the enzyme lid (covering the active site) with the surrounding solvent can maintain the enzyme in an open active conformation, enhancing its activity. For example, the lipase from *P. aeruginosa* AAU2 shows higher activity (102%) in the presence of a higher concentration of *iso*-octane (Salihu and Alam, 2015). Similarly, DMSO interacts very well with Trp, Leu and Ala present on the surface of lipases, while the interaction is not favoured by neutral polar glycine molecules (Nagao *et al.*, 2002). At higher DMSO concentrations, neutral polar glycine interacts with DMSO, enhancing the stability of the unfolded enzyme by decreasing the enzyme's free energy. Lipases which are stable in DMSO have more Gly and less Trp, Ala and Leu residues at their surfaces (Arakawa, Kita and Timasheff, 2007). The presence of small or long non-polar amino acid residues on the surface of lipases determines their activity and stability in polar and non-polar solvents. Lipases with small non-polar amino acid residues at their surface are unstable in small chain alcohols while lipases with long non-polar amino acid residues at their surface are unstable in acetonitrile (Gekko *et al.*, 1998). The interaction of organic solvents with catalytically important amino acid residues in active sites by either hydrophobic, electrostatic or hydrogen bonding can be the most important reason for lipase instability (Chakravorty *et al.*, 2012). Solvents with aromatic rings (e.g. benzene) can cause lipase instability by breaking internal and substrate cation-π interactions with aromatic amino acid residues present in the active site. These solvents form stronger bonds with the groups holding the enzyme conformational shape causing lipase denaturation. Hence, lipases with aromatic residues on their active site surfaces are unstable in benzene as strong cation-π interaction among aromatic residues and benzene can remove essential water (Gromiha, Santhosh and Ahmad, 2004). Conversely, neutral residues on the enzyme surface form stronger hydrogen bonds than charged residues,

enhancing overall enzyme stability and hence are often seen on the surface of organic solvent-stable lipases (Gromiha, Santhosh and Ahmad, 2004).

2.7. APPLICATION OF SOLVENT STABLE LIPASES

Due to the benefits of non-aqueous biocatalysis, solvent stable enzymes have been broadly used in the food, biopharmaceutical and environmental industries (Ahmed, Raghavendra and Madamwar, 2010b).

2.7.1. Food industry

The flavour and fragrance world market was USD$ 22 billion in 2011 and has been increasing at a rate of 5.6% annually (Badgujar, Pai and Bhanage, 2016). The isolation and extraction of flavour esters from natural sources is expensive and consumers prefer products with a 'natural' label (Ahmed, Raghavendra and Madamwar, 2010b). Therefore, alternatives to the chemical synthesis of flavour esters including alternative production technologies, like esterification (see Figure 2.4) by solvent stable lipases (see Table 2.4), have gained attention (Matte *et al.*, 2016).

Solvent stable lipases have also been used in the hydrolysis of various oils, especially for the production and enrichment of Monounsaturated Fatty Acids (MUFAs; Patel et al. 2014). Apart from hydrolysis of fats, lipases from species like *M.miehei* have also been used, for example, as catalysts for the inter-esterification of vegetable oils, to produce *omega*-3-polyunsaturated fatty acids from vegetable oils (Hasan, Shah and Hameed, 2006). The limited supply, high price and inter-batch quality variation of food additives like natural cocoa, provides opportunities for alternative lipase catalysed reactions. For example, acidolysis reactions of palm olein oil and palmitic-stearic fatty acid by lipase from *Mucor miehei* in presence of *n*-hexane has successfully produced a viable cocoa butter equivalent (Mohamed, 2012).

Table 2.4: Examples applications of solvent stable lipases in the food industry flavour, aromas and supplements production. Lipases have been widely used in non-aqueous environment for flavours and aromas production via esterification-based reactions.

Application	Source	Component synthesized	Solvent system	Reference
Flavour	*Aspergillus oryzae*	*Cis*-3-hexen-1-yl-acetate	acetic acid and cis-3-hexen-1-ol	(Kirdi *et al.*, 2017)
	Pseudomonas cepacia	*Cinnamyl Propionate (spicy floral flavor)*	*n*-hexane and toluene (non-polar solvents)	(Badgujar, Pai and Bhanage, 2016)
			acetone, dioxane (hydrophobic solvents	
	Thermomyces lanuginosus	Butyl butyrate (pineapple flavor)	butanol: butyric acid	(Matte *et al.*, 2016)
	Candida rugosa	Ethyl caprylate (flavor ester)	ethanol and cyclo-octane	(Patel *et al.*, 2015)
		Aroma ester methyl acetate	*n*-hexane and methanol	(Trbojevic et al. 2016)
	Bacillus aerius	Isoamyl acetate (pear/banana flavor)	acetic acid and isoamyl alcohol	(Narwal *et al.*, 2016)
	Bacillus licheniformis	Ethyl lactate (fruity odour and fruity flavor)	ethyl alcohol and lactic acid	(Jain and Mishra, 2015)
		Isobutyl acetate (pineapple flavor)	isobutyl alcohol and acetic acid	
	Pseudomonas sp. DMVR46	Ethyl butyrate	ethanol and *n*-heptane	(Vrutika and Datta, 2015)
Aroma		Pentyl valerate (fruity aroma)	pentanol and valeric acid	(Patel, Nambiar and Madamwar, 2014)
	Bacillus safensis	Ethyl laurate (waxy odour and flavor)	lauric acid and ethanol	(Kumar et al. 2014)
Supplements	*Candida rugosa*	Vitamin E succinate	DMSO	(Jiang et al. 2013)

2.7.2. Pharmaceutical and Agriculture Industry

Sugar esters are widely used in the production of detergents, pharmaceutical and oral care products (see Table 2.5). Due to the poor solubility of sugars in organic solvents and poor regio-selectivity of chemical catalysis, the conventional esterification production of sugar esters is challenging. Such esterification can be achieved using solvent tolerant lipases which are stable in DMSO (the polar DMSO enhances sugar solubility in organic solvents). Lipase B from *Candida Antarctica* (Novozyme® 435) has been used for the production of xylose caproate esters in DMSO and acetone 1:10 (v/v; (Abdulmalek, Hamidon and Abdul Rahman, 2016).

The properties of esterification, inter-esterification and regio-selectivity have enhanced the application of lipases in the manufacturing of various precursor molecules required for the synthesis of pharmaceutical and agrochemical products (see Table 2.5).

2.7.3. Environmental

2.7.3.1. Biodegradable polymers

The increased use of polymers in biomedical research, food packaging and agricultural industries has increased environmental concerns over their disposal (Banerjee, Chatterjee and Madras, 2014). Therefore, significant research has focused on the development of biodegradable polymers (polyesters). Solvent stable lipases have been widely used as catalysts for the synthesis of biodegradable polymers (Barrera-rivera, Flores-carreón and Martinez-Richa, 2012); Table 2.6). The lipase from *Candida antarctica* (lipase B) is the most commonly used catalyst for polyester synthesis (Chen *et al.*, 2008). Although, the production of biodegradable polyesters plays a significant role in a green environment approaches; recycling is equally important from an environmental perspective. Chemical recycling often requires high-energy (temperature and pressure) and raises concerns over environmental safety. Conversely, enzymatic degradation is environmentally safe, cost effective and requires lower energy and milder conditions (Table 2.6). As lipase catalyzed degradation generates oligomers with lower molecular weight (Banerjee, Chatterjee and Madras, 2014), they can be used for a '*one-pot degradation-polymerisation*' reaction, for recycling of polyesters (Kobayashi, Uyama and Takamoto, 2000).

Table 2.5: Lipases have been used for the synthesis as well as separation of various pharmaceutical and cosmetic products via esterification, racemic resolution and regio-selectivity. Pharmaceutical products synthesized by lipases in the presence of various solvent systems are widely available.

Lipase	Solvent system	Application	Reference
Candida antarctica	methyl *tert*-butyl ether	Resolution of racemic alcohols and kinetic resolution of racemic flurbiprofen	(Xun *et al.*, 2013)
	Toluene and diisopropyl ether	Precursor of drugs (Sertraline, Indinavir, Irindalone, Rasagiline mesilate)	(De Souza *et al.*, 2016)
	Toluene	Inhibition of Age-related macular degeneration (AMD); For high acuity vision; decrease UV-induced damage on skin	(R. Wang *et al.*, 2015)
	Acetone and n-hexane	Food, Pharmaceuticals, cosmetic, insecticidal, antimicrobial, oral care	(Jia *et al.*, 2010)
Candida antarctica Sp-435	Dimethylformamide		(Gumel *et al.*, 2011)
Porcine pancreatic lipase IIII	Hexane		
Thermomyces lanuginosus and *Pseudomonas fluorescens*	*tert*-butyl alcohol		(Vescovi *et al.*, 2017)
Candida rugosa	*n*-Hexane	Cholesterol reduction, anti-viral and anti-inflammatory	(Jiang et al. 2013)
Pseudomonas stutzeri		Cosmetics and the pharmaceutical industry	(Cao *et al.*, 2012)
Burkholderia ambifaria	Di-isopropyl ether	Intermediates for pharmaceutical industry	(Yao *et al.*, 2013)
Geobacillus stearothermophilus	Ethanol and DMSO	Solvent for preparation of steroids; plasticizer	(Kumar *et al.*, 2015)
Ophiostoma piceae	Isooctane	Decreasing cholesterol absorption	(Molina-Gutiérrez *et al.*, 2016)
Porcine Pancreas	Halo propionic acids; butanol and hexane	Herbicide (phenoxypropionate)	(Hasan, Shah and Hameed, 2006).

Table 2.6: The production and degradation of polymers in the presence of lipases is a key factor for environmental applications. Lipases provide an alternative eco-friendly solution for the production and regeneration of biopolymers. Lipases from different sources have been used for the synthesis and degradation of polymers in the presence of different solvent systems.

Action	Lipase Source	Substrate	Solvent system	Reference
Polyester synthesis	*Yarrowia lipolytica*	Ɛ-caprolactone	Heptane	(Barrera-rivera, Flores-carreón and Martinez-Richa, 2012)
	Candida antarctica		Toluene	(Duskunkorur et al. 2014)
		Ɛ-caprolactone and Ɛ-thiocaprolactone		(Duchiron *et al.*, 2017)
Polymer degradation		Poly(Ɛ-caprolactone)		(Aris, Annuar and Ling, 2016)
	Lactobacillus plantarum		Chloroform	(Khan, Ray Dutta and Ganesan, 2017)
	Bacillus subtilis	Polyhydroxyalkanoates (PHAs)		(Kanmani *et al.*, 2016)

2.7.3.2. Fuel additives

The cold flow property of a fuel is the lowest temperature at which the fuel will provide trouble-free operation (Dunn, 2009). The cloud properties of a fuel are determined by measuring the cloud and pour points of a fuel. The cloud point (CP) is the temperature at which a cloud of hydrocarbons available in the fuel forms crystals and becomes visible. The pour point (PP) is the lowest temperature at which a fuel retains its flowing properties before freezing. In the case of biodiesel, these properties depend on biodiesel fatty acid composition (Wang et al. 2015). Biodiesel produced from oils with higher saturated fatty acid content (e.g. Jatropha oil, cooking oil or waste grease) have higher cloud points and pour points (Knothe 2005), making them unsuitable for use in cold environments. The cold flow properties of a fuel can be changed by blending or by addition of additives, such as branched chain esters (Dunn, Ngo and Haas, 2015). The addition of branched chain esters can change the molecular and crystalline structure of biodiesel, producing hydroxyl esters which do not freeze, even at 0°C (Wang et al. 2015). Esters like 1-butyl oleate produced by the direct esterification of butanol and oleic acid via *Rhizopus oryzae* lipase in a *n*-hexane environment, have been used to enhance the cold flow properties of biodiesel (Ghamgui, Karra-chaˆ and Gargouri, 2004). Similarly, branched chain α-hydroxy esters produced by the direct

esterification of alkyl oleates are known to reduce the CP and PP of biodiesel by 3°C (Dunn, Ngo and Haas, 2015).

2.7.3.3. Automotive lubricants

Petroleum derived automotive lubricants typically contain toxic aromatic hydrocarbons and are not completely biodegradable (Santos Corrêa et al. 2016). Conversely, esters such as dioctyl sebacate, are biodegradable, thermally stable, have low toxicity and provide excellent lubricity (Gryglewicz, et al. 2013; Santos Corrêa, et al. 2016). The lipase, Novozyme 435, in the presence of sebacic acid and octane has been used for the synthesis of biodegradable lubricants (Santos Corrêa et al. 2016).

2.8. BIOFUELS AND LIPASES

2.8.1. Biofuel requirement

The emission of total anthropogenic greenhouse gases is projected to increase by 23% by 2030 (Ullah *et al.*, 2015). Although policies to curb CO_2 continue to tighten, global CO_2 emissions from energy use continue to grow by 1.1% per annum (Members, 2018). Currently fossil fuels such as petrol, coal, and natural gas contribute 88% of global energy consumption. Being non-renewable, these fossil fuels will deplete over time. To limit the use of fossil fuels, renewable energy sources such as biomass and waste have been successfully developed (Mustafa and Gunhan, 2005). Energy produced from combustible renewables and waste have the highest potential among renewable sources (International Energy Agency, 2018). Dwindling reserves of crude oil, rising energy demands and crude oil prices, and detrimental effects of global warming due to greenhouse gas emission demand alternative fuels (Jassinnee *et al.*, 2016). Therefore, more promising new strategies are required for energy security as well as to mitigate CO_2 emission (Hanaki and Portugal-Pereira, 2018). Biofuels offer an alternate source of energy that can tackle both fuel demand and climate change mitigation. Biological lipids can be converted to biodiesel by chemically catalysed transesterification (acid or alkali) or by enzyme catalysed transesterification. Biofuels are produced from biological oil sources like vegetable oil, animal fats or non-edible plant feed stocks (Stuart *et al.*, 2010). Three generations of biofuels have been studied to date. The first-generation biofuels (circa 2009) increase the cost of food crops, impacting food security and, make biodiesel production more expensive. The second-generation biofuels (circa 2010) suffer from high processing costs and

inadequate technologies. Also, large-scale production of second-generation biofuel requires a constant supply of large amounts of biomass (wood, grasses, and plant waste). With the concerns of first and second-generation biofuels, a third-generation biofuel utilizing microalgae as oil source has been widely sought.

2.8.2. Third generation biofuels using microalgae as a lipid source

Microalgae are photosynthesizing, fast growing organisms capable of completing an entire growth cycle in a few days if sunlight, water, CO_2 and nutrients are available. Due to the rapid growth rate and the short harvesting cycle, microalgae allow rapid accumulation of significant amount of lipids with continuous harvesting. The lipid content in microalgae varies from 20-40%; however, lipid content as high as 85% has also been reported in certain microalgal strains (Mairet *et al.*, 2011). The average oil content in microalgae is 25-200 times more than crop-based biofuels. This, combined with the low harvesting and transport costs make microalgae a more economical source for biofuel production (Keesoo *et al.*, 2014). Cultivation of microalgae for biodiesel production requires approximately 2% of the land required to produce the same amount of biodiesel from oil bearing crops (Ahmad *et al.*, 2011b). Plants, via photosynthesis, fix approximately 77 Giga tons of CO_2, leading to production of 100 Giga tons of biomass annually (lignocellulose materials; (Gupta and Tuohy, 2013). Microalgae, conversely, have a higher photosynthetic efficiency, utilizing approximately 183 Gtons of CO_2 to produce 100 Giga tons of biomass (Najafi, Ghobadian and Yusaf, 2011). For every 1kg of dry biomass produced by microalgal growth, 1.83kg of CO_2 is utilized, sequestering CO_2 and subsidising CO_2 induced global warming (Chisti, 2007). Marine algae species, like *Chlorococcum littorale*, have even an exceptional tolerance to high CO_2 (up to 40%). Species like *Scenedesmus obliquus* and *Spirulina* sp. also have good capacities for CO_2 fixation (Trivedi *et al.*, 2015). Flue gases from industry usually contain more than 15% (v/v) of CO_2 and therefore, could be a useful source of carbon for microalgae cultivation (Kumar *et al.*, 2010).
Microalgae are highly adaptable and do not require fertile land and can be grown almost anywhere, even on sewage or saltwater. Since microalgae require CO_2 to grow and can efficiently remove phosphates and nitrates from wastewater, they offer a good alternative source for bioremediation and biofixation (Lam and Lee, 2012). One of the key benefits of using microalgae in wastewater treatment is that microalgae produce O_2 during photosynthesis which promotes aerobic bacterial

degradation of the other organic components. Bacterial degradation in turn, produces CO_2, which promotes photosynthesis and the algal uptake of inorganic nutrients (Juan *et al.*, 2016). Significant pollution control can be achieved where the waste stream from one process is used to generate alternative renewable bioenergies to mitigate the current energy crisis (Owusu and Asumadu-Sarkodie, 2016).

If the environmental conditions are not suited to cell growth (i.e. biomass generation), many microalgae tend to accumulate neutral lipids to form lipid droplets decentralized in the cytoplasm as energy storage. Lipid accumulation occurs through two different pathways: *de novo* synthesis and *ex novo* accumulation (Huang *et al.*, 2017). The first pathway is a synthesis process from non-fatty acid precursors such as carbohydrates, amino acids or short-chain organic acids; then they produce acetyl Co-A, which is a precursor for this pathway. The second pathway involves the uptake of fatty acids, oils and TAG from the culture medium and their accumulation in an unchanged or modified form within the cell (Harwati, 2013). The main fatty acids in storage lipids are saturated fatty acids (e.g., palmitic acid, C16:0; stearic acid, C18:0) and unsaturated fatty acids (e.g., oleic acid C18:1; linoleic acid, C18:2; linolenic acid C18:3). However, polyunsaturated fatty acids with 20 and 22 carbon atoms are also found; which are either with triacylglycerols or phospholipids (Breuer *et al.*, 2013). Transesterification in the presence of organic solvents is required to convert these fatty acids/lipids to biofuel/biodiesel.

2.8.3. Transesterification

Converting a biological lipid into biodiesel is usually achieved by a chemically catalysed transesterification process (alcoholysis; see Figure 2.4, Figure 2.8). The process involves reaction of triglyceride molecules present in oils/fats with an alcohol to produce esters and glycerol in the presence of a catalyst (either acid, base or enzyme).

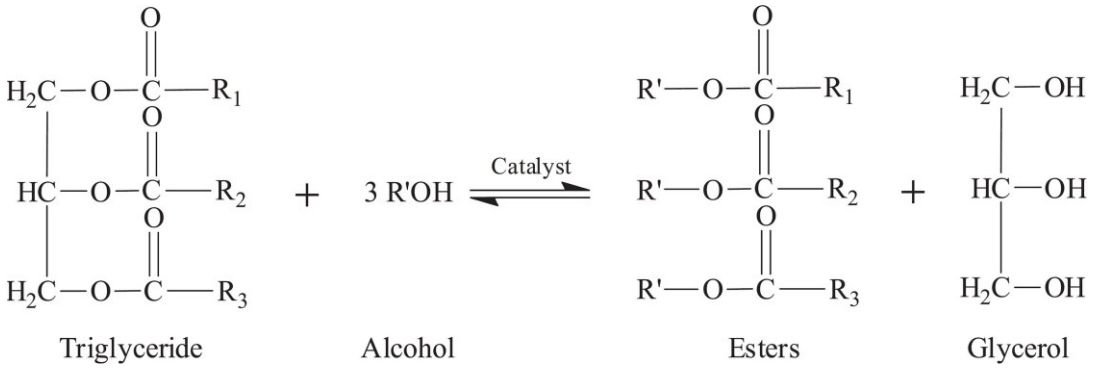

Figure 2. 8: Transesterification of oil (triglyceride) catalyzed by a catalyst (acid/base/enzyme) in presence of alcohol resulting in generation of biodiesel (esters) and glycerol (Patel and Shah, 2015).

2.8.3.1.Acid catalysed transesterification:

These chemical transesterification reactions use acid (H_2SO_4, HCl, BF_3, H_3PO_4 and organic sulfonic acid) as catalyst. Acid catalysed transesterifications have high yields of alkyl esters but reaction rates are very slow and require high temperatures, sometimes above 100°C (Swarnali, 2015). The volume of acid used determines the efficiency of the transesterification reaction; excess use of acid makes the process more efficient by providing better conversion of the triglyceride. Acid catalysed transesterification is often insensitive to the quality of triglycerides and the water content in the oil, hence, cheap/low quality feedstock can be used (Melero, Iglesias and Morales, 2009). The main advantage of acid catalysed ester formation is the simultaneous esterification and transesterification step, allowing direct production of biodiesel from low-cost lipid feedstocks, generally associated with high free fatty acid (FFA) concentrations. Though the method gives high yields and does not suffer from soap formation, one main challenge associated with this process is metal corrosion due to the use of acids. Separation of catalyst from product is another challenge which limits the usage of these catalysts for transesterification (Talha and Sulaiman, 2016).

2.8.3.2.Alkali catalysed transesterification:

Alkaline catalysts such as NaOH, KOH, CH_3ONa, and CH_3OK are often used in the production of biodiesel. Since they are soluble in methanol, they generate sodium methoxide and potassium methoxide, which lead to the completion of the reaction. CH_3ONa is the most active alkali catalyst

and has been shown to give a 98 wt% biodiesel yield in a 30min reaction time (Helwani *et al.*, 2009). Most alkali catalysed transesterification reactions are executed at 60°C, but based on the oil source and catalyst, temperatures ranging from 25 to 120°C can generate different degrees of conversion (Bharathiraja *et al.*, 2014**).** Though alkali/base catalysed transesterification has convenient standard reaction conditions they need high purity feedstocks (level of FFAs should not exceed 3wt%, beyond which the reaction will not occur). Also, undesirable saponification reactions interrupt the transesterification reaction if the triglycerides and/or alcohol are not anhydrous (Sharma, Singh and Korstad, 2011). When the catalyst is consumed due to soap formation, decreasing ester yields are observed. Moreover, the soap formed during the reaction hinders biodiesel-glycerol separation (Kondamudi, Mohapatra and Misra, 2011). Biodiesel produced through alkali catalysed transesterification contains K/Na traces, which require washing and purification steps further adding to the overall production cost. Furthermore, the high quantities of water used in the washing and purification steps generates significant volumes of wastewater. The subsequent treatment of this effluent waste water further adds to the overall process cost (Semwal *et al.*, 2011).

2.8.3.3.Enzyme catalyzed transesterification

Lipases can catalyse both hydrolysis and the synthesis of long-chain acylglycerols and, importantly, can catalyse biodiesel production (Jaeger and Reetzb, 1998). Due to the easy solubility of non-polar compounds, the majority of industrial scale transesterification reactions are carried out in organic solvents. Since most lipases are easily denatured in organic solvents and therefore lose their catalytic activities, solvent stable lipases (see Section 2.6) are required for transesterification reactions. Lipase from the filamentous fungus *Rhizopus oryzae* is widely used and has provided a yield of 80% and 90% by esterification of jatropha oil (Tamalampudi *et al.*, 2008) and soybean oil (Hama *et al.*, 2007) respectively.

Lipase catalysed transesterification is superior to acid or alkali catalysed transesterification as it requires moderate conditions such as temperature. This is in contrast with acid and alkali catalysed transesterifications where sometimes temperature can be above 100°C (Tiwari, Kumar and Garg, 2006). Furthermore, the overall cost and energy consumption, due to the moderate reaction conditions is low as compared to acid/alkali catalysed transesterification. Lipases have a broad

substrate range (FFA content, water content) due to their ability to esterify both glyceride-linked and non-esterified fatty acids in one step, they can be used on oils with variable chemical compositions (Andualema and Gessesse, 2012). This offers a great advantage when waste oils and fats are used for the synthesis of a cost-effective biodiesel. Lipase catalysed reactions are environmentally friendly due to enzyme biodegradability, giving an opportunity to produce a green fuel with a green technology. Lipase catalysed transesterification allows easy removal of glycerol maintaining equilibrium in the positive domain (alkyl ester formation;(Leao *et al.*, 2016). Finally, after immobilization, lipases can be reused, decreasing the overall production cost of biofuels. Table 2.7 provides some examples where FAMEs and FAEEs have been successfully synthesised via lipase catalysed transesterification reactions.

Table 2.7: Lipases used for FAMEs and FAEEs production with different oil sources. FAME and FAEE provide an alternate source of fuel for the automobile industry. Use of lipases in FAME and FAEE production is an eco-friendly approach where lipases convert oil to fuel via transesterification reaction.

Product	**Lipase source**	**Substrate**	**Reference**
Fatty Acid Methyl Esters (FAME's)	*Bacillus licheniformis*	Waste vegetable oil	(Jain and Mishra, 2015)
		Palm Oil	
		Cotton oil	
	Pseudomonas aeruginosa	Jatropha oil	(Bose and Keharia, 2013)
	Pseudomonas fluorescens	*Scenedesmus obliquus* lipids	(Guldhe *et al.*, 2015)
	Rhodotorula mucilagenosa P11	Palm oil	(Salihu and Alam, 2015)
Fatty Acid Ethyl Esters (FAEE's)	*Rhizomucor miehei*	*Chlorella vulgaris* lipids	(Huang *et al.*, 2015)

2.8.3.3.1. Challenges associated with enzyme catalysed transesterification

Transesterification reactions require the addition of polar/non-polar solvents to drive the equilibrium towards ester formation. Polar and non-polar solvents have effects on the stability, and therefore activity, of each lipase (see Section 2.6.1). Although, lipases of microbial origin are more stable than plant and animal lipases; factors like carbon, nitrogen source; pH, temperature, dissolved oxygen also affect the stability and expression of lipases from microbial origin

(Christopher, Hemanathan Kumar and Zambare, 2014). The structural properties of lipases from different sources are different and this also effects the catalytic activity on different oil substrates (Prakash *et al.*, 2010). Based on substrate specificity, lipases can be 1,3-specific; fatty acid-specific; or non-specific. The 1,3-specific lipases hydrolyze ester bonds in the position 1 and 3 of triacylglycerols (TAGs). The fatty acid-specific lipases are known to hydrolyse esters of long chain fatty acids with double bonds in a *cis*-position at C9, whereas the non-specific lipases randomly cleave the acylglycerols in FFAs (Ribeiro *et al.*, 2011). Non-stereospecific lipases are optimal for biodiesel production as they can convert all three forms of glycerides (mono-, di-, and triglycerides) to biodiesel. There are many process related challenges which limit the use of lipases as transesterification catalysts. Firstly, the most commonly used acyl acceptors in transesterification reactions are either alcohols (primary, secondary, straight and branched chain) or esters. Since the degree of enzyme inactivation by an alcohol is inversely proportional to the number of carbon atoms present in the alcohol (see Section 2.6.1.2; Chen and Wu, 2003), use of methanol and ethanol over long aliphatic alcohols, causes enzyme denaturation. Secondly, organic solvents (like isooctane, *n*-heptane, petroleum ether, *n*-hexane and cyclohexane) used in transesterification reactions improve mutual solubility of hydrophobic triglycerides and hydrophilic alcohols while simultaneously preventing enzyme denaturation from alcohols. The presence of these solvents caused insolubility of by-product glycerol which can adsorb to the immobilized lipase. Conversely, the strong interaction of hydrophilic organic solvents with the essential water layer of the enzyme makes the use of hydrophilic organic solvents less obligatory (Gog *et al.*, 2012). However, a few hydrophilic organic solvents like 1,4-dioxane and *tert*-butanol have ensured high transesterification yields due to their moderate polarity, solving the negative effects of both glycerol and methanol (short chain alcohols; Jeong and Park, 2008b). While enzyme catalysed transesterification reactions can be performed at lower temperatures; enzyme activity varies with temperature. For example, the rate of transesterification by a lipase from *P. fluorescens* increased with temperature till 60°C (Iso *et al.*, 2001), whereas the lipase from *R. oryzae* lost its activity above 40°C (Chen, Ying and Li, 2006). The catalytic activity and stability of a lipase is also affected by the presence of water in the reaction system. The availability of water at the oil-water interface causes conformational changes to the lipase permitting enzyme activation (see Section 2.6.1.1). The size of the interfacial area determines transesterification yield. The addition of excess water can increase the interfacial area;

however, excess water shifts the reaction equilibrium to hydrolase activity, and therefore, decreases transesterification yields (Ghaly *et al.*, 2010).

Apart from these challenges, reuse of extracellular bacterial lipases requires enzyme immobilization which is often expensive and/or sophisticated. While using immobilized lipases for transesterification reactions, the by-product glycerol could bind to the supports, effecting the operational stability and activity of lipase. Besides, soluble lipases can be produced and sold at a 30–50 times lower price than immobilized ones, making the reusable lipase process sustainable and competitive (W. Yang *et al.*, 2016). The presence of glycerol and unused methanol affects the enzymatic reaction rate (Gog *et al.*, 2012). Due to the limited solubility of methanol/ethanol in oil, performing methanolysis/ethanolysis in solvent-free systems sometimes leaves non-solubilized methanol/ethanol, which causes lipase deactivation. However, stepwise addition of methanol, with *t*-butanol as the solvent, can eliminate this challenge (Li *et al.*, 2008), but this approach adds additional process steps.

2.8.4. Transesterification of microalgae neutral lipids

Microalgae lipid extraction usually follows two steps: cell disruption and solvent extraction. Due to the large variations in algal cell shape, size, cell wall structure and characteristics of algal lipids, the diverse lipid extraction methods work differently on the various algae species (Shen *et al.*, 2009). During oil extraction, microalgal internal oils are excreted to the outside medium by cell wall disruption and are partitioned into hydrophobic solvents, such as hexane and diethyl ether. Disruption of the microalgal cell wall for the extraction of oil in an extraction solvent increases the energy requirement and cost due to the additional steps of dewatering and drying of microalgal cells (Ronald, Micheal and Paul, 2012). Furthermore, cell disruption of oil-rich eukaryotic microalgal cells is a tedious process due to the thick and tough microalgal cell walls. Several mechanical, chemical or combinational cell (ultrasound, high-pressure homogenization, bead-beating, osmotic shocks) methods have been suggested to facilitate oil extraction from algal cells (Halim *et al.*, 2012; Ronald, Micheal and Paul, 2012). However, due to higher processing costs and time, other transesterification methods are required.

2.8.4.1. *In-Situ* Transesterification

The combination of oil extraction and biodiesel conversion, called direct (or *in-situ*) transesterification involves direct contact of oil/lipid-bearing biomass (with the omission of the extraction step) with solvent in the presence of the catalyst (Hidalgo *et al.*, 2013). The solvent plays two significant roles in this process: (i) to extract the oil/lipid from biomass and (ii) as a reactant in the transesterification reaction. *In-situ* transesterification offers several advantages over the conventional biodiesel production method, such as minimizing the solvent separation step, reducing the processing time and consequently, cutting down the overall biodiesel production costs. This approach simplifies the production process and improves the biodiesel yield in comparison to the conventional extraction process because of the elimination of an oil extraction step that sustains oil loss (Griffiths, Hille and Harrison, 2010). The reactions are simple and comprise the addition of alcohols, catalysts, and biomass and sometimes co-solvents (Baumgartner *et al.*, 2013). The use of a co-solvent, such as hexane or chloroform, facilitates the easy extraction of oils from microalgal cells and enhances the transesterification reaction (Cao *et al.*, 2013).

Though direct transesterification eliminates the oil extraction process difficulties, it suffers from water inhibition (Sathish, Smith and Sims, 2013, Brian and Sims, 2013). The formation of fatty acid methyl ester (FAME) is a reversible reaction and water can hydrolyse the biodiesel back to methanol and free fatty acids. Also, water contained within the biomass can shield oils from the extracted solvent and can prevent reaction. These challenges have been addressed by excess methanol (solvent) and catalyst. Solvents such as pentane and diethyl ether have also been used to reduce the volume of methanol required and enhance reaction yield. These solvents assist microalgal oils extraction in conjugation with methanol by improving the diffusion of the microalgal oils across the cell walls (Park et al. 2015).

The most important issue in microalgal biodiesel production is the utilization of wet biomass. While a wet extraction process eliminates the amount of energy and costs required for drying of the microalgal biomass, this process still requires a large amount of energy that is associated with the thermal input required for heating and cooling of the reactor. Therefore, the extraction or direct conversion process needs to be further developed for operational efficiency at lower temperatures and pressure through usage of optimised and enhanced enzymes as catalysts. Though wet/direct transesterification reaction is in line with the efforts to find a solution for low harvesting cost of

microalgal biomass, further research is required to examine wet extraction methods since it has been frequently reported that the oil extraction yield of dry microalgal cells is relatively higher than that of wet microalgal cells (Guldhe *et al.*, 2014).

2.9. CONCLUSION

The research outlined in this thesis is focused on the implementation of environmental friendly catalysts and feedstock for the generation of environmental friendly biofuels. The research involves isolation, characterisation, and overproduction of lipases from novel bacterial strains; with potential in various biotechnological applications. Secondly, for the generation of clean biofuels; microalgae grown in simulated wastewater will provide lipids as feedstock for an enzyme catalysed transesterification reaction. For biodiesel synthesis a combination of natural enzyme catalysts and lipids from wastewater grown microalgae in the presence of organic solvents could offer an alternative energy source in the current and future energy crisis. Using microalgae grown on simulated wastewater as transesterification feedstock can provide an alternate to expensive feedstocks, wastewater treatment and CO_2 mitigation.

Chapter 3: Materials and methods

3.1. GENERAL

3.1.1. Commercial sources of common reagents

All reagents and chemicals used for the study were of analytical grade or higher.

A-B

Acetic acid: Sigma-Aldrich

Acetone: Sigma-Aldrich

Acetonitrile: Sigma-Aldrich

Acrylamide-Bisacrylamide: Sigma-Aldrich

Ammonium molybdate tetrahydrate: Sigma-Aldrich

Ammonium persulfate: Sigma-Aldrich

Ammonium Sulphate: Thermo-Fisher

Bacteriological agar: Fluka

Bacteriological Peptone: Lab M

Biotin: Sigma-Aldrich

Boric acid: Sigma-Aldrich

Bovine Serum Albumin (BSA): Sigma Aldrich

Bradford Reagent: Sigma-Aldrich

Bromophenol Blue: BDH limited

C-E

Calcium chloride Dihydrate: Sigma-Aldrich

Calcium Chloride: Sigma-Adrich

Calcium Nitrate Tetrahydrate: Sigma-Aldrich

Cobaltous chloride hexahydrate: Sigma-Aldrich

Coomassie Brilliant Blue G-250: Sigma-Aldrich

Cyanocobalamin: Sigma-Aldrich

M-P

Magnesium Chloride: Merck

Magnesium sulfate heptahydrate: Sigma-Aldrich

Manganese (II) chloride tetrahydrate: Sigma-Aldrich

Meat Extract: Sigma-Aldrich

Methanol: Merck

Monopotassium phosphate

MUF-butyrate: Fluka

n-Heptane: Merck

n-Hexane: Sigma

N-Hydroxysuccinimide (NHS): Sigma-Aldrich

Nile red: Sigma-Aldrich

Olive oil: Sigma

Polysorbate 80: Scharlau

Potassium phosphate dibasic: Sigma

Potassium phosphate monobasic: Thermo-fisher

Q-S

Q Sepharose HP: Sigma

Rhodamine B: VWR

Sodium Acetate: Sigma-Aldrich

Sodium Alginate: Sigma-Aldrich

Sodium bicarbonate: Sigma-Aldrich

Cyclohexane: Sigma

Diethyl ether: Sigma

Dipotassium hydrogen phosphate trihydrate: Sigma-Aldrich

Disodium ethylenediaminetetraacetate dihydrate: Sigma-Aldrich

DMSO: Sigma-Aldrich

D-sorbitol: Sigma

EDTA ferric sodium salt: Sigma-Aldrich

EDTA: Scharlau

Ethanoic phosphomolybdic acid: Sigma- Aldrich

Ethanol: Merck

Ethyl(dimethylaminopropyl) carbodiimide (EDC): Sigma-Aldrich

F-L

Ferric chloride hexahydrate: Sigma-Aldrich

Glucose: Sigma-Aldrich

Glutathione: Sigma-Aldrich

Glycerol: Sigma-Aldrich

Glycine: Sigma

Gold (III) Chloride trihydrate: Sigma-Aldrich

Isopropanol: Acros

L-Arginine: Sigma-Aldrich

LB Agar: Sigma-Aldrich

LB Broth: Sigma-Aldrich

Lipase from Porcine pancreas: Sigma

L-Lysine: Sigma-Aldrich

Sodium Chloride: Thermo-Fisher

Sodium citrate: Sigma-Aldrich

Sodium Dihydrogen Phosphate Dodecahydrate

Sodium Dodecyl Sulphate: Sigma-Aldrich

Sodium Hydroxide: Sigma-Aldrich

Sodium molybdate dihydrate: Sigma-Aldrich

Sodium Nitrate: Sigma-Aldrich

Sodium Phosphate dibasic: Sigma-Aldrich

T-Z

t-butanol: Sigma-Aldrich

TEMED: Sigma-Aldrich

Thiamine HCl: Sigma-Aldrich

Toluene: Sigma-Aldrich

Triolein: Sigma-Aldrich

Triton X-100: Sigma-Aldrich

Trizma Base: Sigma-Aldrich

Tryptone: Sigma-Aldrich

Urea: Sigma-Aldrich

Vitamin B1: Sigma-Aldrich

Vitamin B12: Sigma-Aldrich

Yeast Extract: Scharlau

Zinc Chloride: Sigma-Aldrich

2-Mercaptoethanol: BDH laboratory

4-nitrophenol palmitate: Sigma

4-nitrophenol: Sigma-Aldrich

3.1.2. Instruments

Instrument	Manufacturer	Model
-80°C deep freezer	Thermo-Scientific	Revco Elite Plus
4°C refrigerator	Liebherr Medline & Bosch	-
Autoclave	Tomy	SX-500E High Pressure Sterilizer
Camera	Computer	H6Z0812 8-48mm 1:1.2
Centrifuge	Rotanta	460R Hettich Zentrifugen & ALC multispeed centrifuge
Columns	BioRad (multiple sizes used)	-
Fluorescence Spectrophotometer	Perkin Elmer Lambda	900 UV/VIS/NIR Spectrometer
Freeze Dryer	Labconco	Freezone 6
Gas Chromatography	Scion	456-GC
Hotplate & Stirrer	-	AGB1000
Incubator	Binder	-
Microcentrifuge	Thermo-Scientific	Heraeus PICO 21 centrifuge
Peristaltic pump	Bio-rad	-
SDS apparatus	Bio-rad	-
Sonicator	QSonica	Q55
Shaker incubator	Stuart Orbital incubator	SI 500 & Innova 40
Shaker water bath	Grant	OLS 200
Spectrophotometer	Biotek Powerwave & Biotek Synergy	Pharmacia LKB Ultraspec III
UV illuminator	UVP laboratory products	-
Vortex	Fisherbrand™ Wizard™	Infrared Vortex mixer
Water bath	Clifton	GD100
Weighing Balance	Sartorius	BPZIOS
Zeta-sizer	Malvern Nanoseries	-

3.2. METHODS

3.2.1. Microbiological methods

3.2.1.1. Different media

3.2.1.1.1. Sterilization

All the culture media (solid/liquid) used for isolation, growth and maintenance of microorganisms were prepared in double distilled water at a final pH of 7.0±0.2 (unless mentioned otherwise). Glass, autoclave compatible plastic and culture media were sterilized by wet heat and 15psi (1.03bar)

pressure by autoclaving at 121°C for 15mins. Thermolabile solutions, such as Rhodamine B, were sterilized by sterile filtration using Millipore sterile nitrocellulose filters (0.22µm) under laminar flow.

3.2.1.1.2. Rhodamine B agar plates

Rhodamine B agar plates were prepared by using the Kouker and Jaeger (Kouker and Jaeger, 1987) method and were used for the detection of lipolytic activity from microbial strains. These plates were supplemented with lipid substrate (olive oil) and with a chromogenic dye (Rhodamine B). The agar solution containing the nitrogen source (yeast extract and peptone) was prepared separately (Solution A, Table 3.1). The lipid substrate (carbon source) was emulsified with a detergent (polysorbate 80 at 250µL/L), by vigorous hand mixing, in order to obtain a homogeneous mixture (Solution B, Table 3.1) of the oil in the final agar plate. Rhodamine B was prepared at a concentration of 1mg/ml (0.1% w/v) in double distilled water (Solution C, Table 3.1). Using a 0.22µm sterile filter (Cruinn Diagnostics), Solution C was filter sterilized and stored at -20°C. Emulsified olive oil (Solution B) was autoclaved (Section 3.2.1.1) separately before addition to the autoclaved (Solution A) agar containing nitrogenous components. The autoclaved olive oil and agar solution were cooled for 15mins to room temperature, after which an appropriate volume of sterile filtered Rhodamine B solution was added to achieve a final concentration of 0.001% (v/v). The mixture was vigorously mixed by hand to ensure homogeneity before aseptically pouring to the petri plates.

Table 3.1: Composition of Rhodamine B agar plates. Solution A and B were prepared and autoclaved separately while solution C was filter sterilized (0.22µm). All solutions were mixed together to a final Rhodamine B concentration of 0.001% (v/v). After pouring, agar plates were allowed to set for 30mins in laminar flow before usage.

Solution A		**Solution B**	
Peptone Yeast Extract Agar	9g/L 2.5g/L 20g/L	Olive oil Tween 80	1.5% (w/v) 250µL/L
		Solution C	
		Rhodamine B	10µg/mL

3.2.1.1.3. Soil Enrichment medium

Soil enrichment medium was prepared by providing oil as a sole carbon source for the growth of microbes (Mo *et al.*, 2016)**.** The media was autoclaved as per Section 3.2.1.1.

Table 3.2: Composition of soil enrichment medium.

Component	**g/L**
Olive oil	10
Ammonium sulfate	10
Di-sodium hydrogen Phosphate	3
Magnesium sulfate	1
pH	7.0±0.2

3.2.1.1.4. Basal Lipase producing medium

Basal lipase producing medium was prepared as per Baharum et al. (2003), with one minor adjustment (1% (w/v) olive oil, instead of 10% (w/v) olive oil). The medium was autoclaved as per section 3.2.1.1.

Table 3.3: Composition of basal lipase producing medium

Component	**g/L**
Bacteriological peptone	50
Sodium chloride	2
Magnesium sulfate	0.4
Ammonium sulfate	0.5
Di-potassium hydrogen phosphate	0.3
Potassium hydrogen phosphate	0.03
Olive oil	10
pH	7.0±0.2

3.2.1.1.5. LB agar and LB Broth

LB broth and LB agar were prepared as per Sigma-Aldrich instructions. For 1L of LB broth, 20g of LB powder was dissolved in 1L of double distilled water. Similarly, for 1L of LB agar, 35g of LB agar powder was dissolved in 1L of double distilled water. Both were autoclaved as per Section 3.2.1.1.

3.2.1.2. Soil sample collection

Nine different soil samples were purposefully collected from locations in Co. Laois (A-C) and Co. Dublin (D-I), Ireland. 20-30g of all soil samples were collected from a depth of 5-10 cm from surface via digging with a small sterile spatula; sample I being an exception (Figure 3.1), where soil was scraped from the floor surface. All the samples were collected in a sterile 50ml falcon tubes and were brought directly to the laboratory, where they were immediately processed. As part of the soil sample processing, large debris such as stones and roots were removed by gloved hand, and the samples were stored at 4°C until processed for culturing. The location for the collection of soil samples are mentioned in Figure 3.1

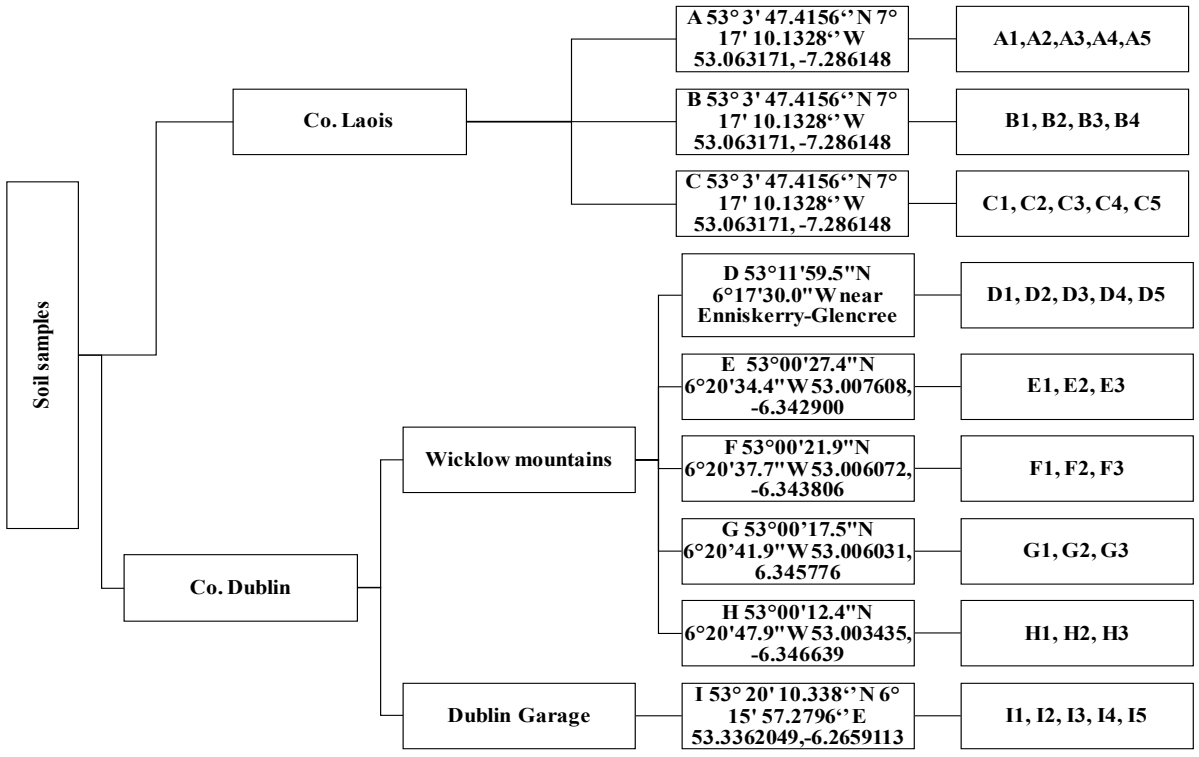

Figure 3.1: Location and nomenclature of soil samples collected from various locations around Co. Laois and Co. Dublin. Soil samples collected from Co. Laois were labeled as A-C respectively. While from the Wicklow Mountains as D- H and from a Dublin Garage as sample I.

3.2.1.3. Isolation of lipase producing microorganisms/soil enrichment

The soil samples were stored at 4°C and were protected from direct sun light until they were processed for the isolation of lipase producing micro-organisms. Microorganisms from all soil samples were isolated by suspending 0.1g of each soil sample in 50ml of soil enrichment medium

(Mo *et al.*, 2016) and cultured for 72h, 200rpm at 28°C. After enrichment, samples were left undisturbed for 30mins to allow heavy soil settlement. The supernatant from the enriched sample was used for the isolation of microbes by means of serial dilution (10^{-1} to 10^{-11}) in autoclaved distilled water. 100µL of each diluted sample was spread on Rhodamine B plates (Section 2.3.1.3) and the plates were statically incubated at 28°C and 37°C for 2-3 days until microbial colonies were observed (Figure 3.2). Lipase producing colonies were observed by irradiating the Rhodamine B plates under UV (365nm).

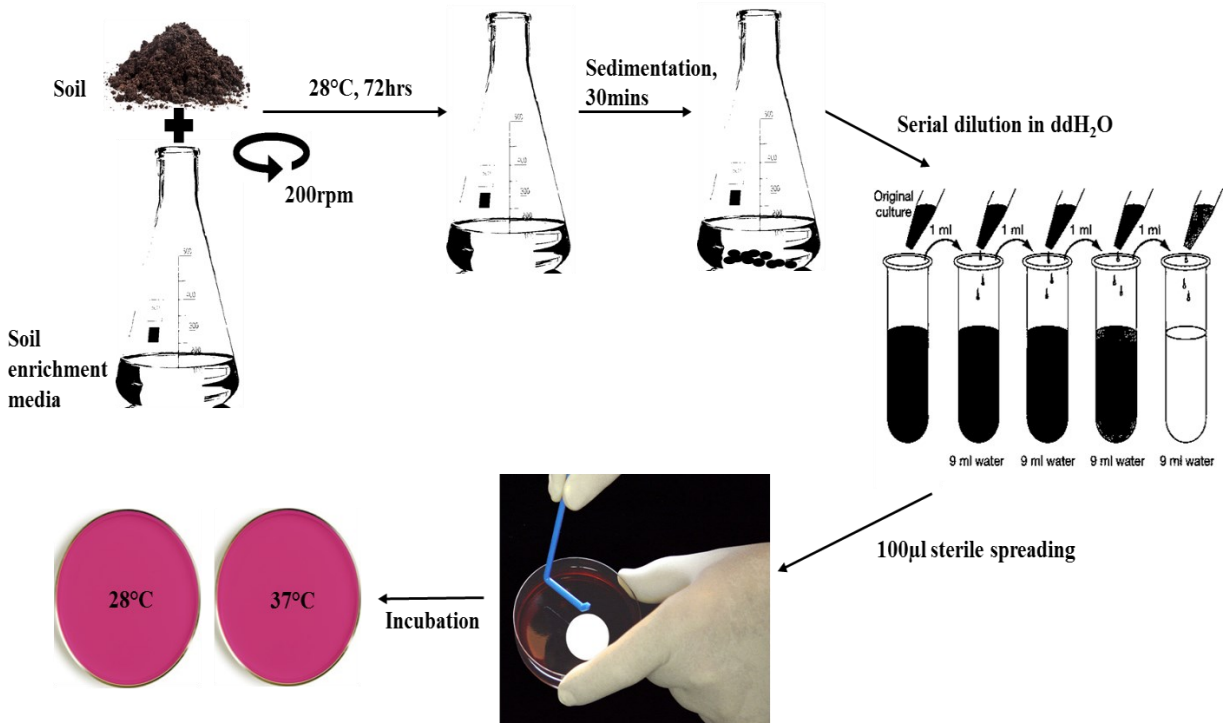

Figure 3.2: The process for the isolation of lipase producing strains from soil. In brief, 0.1g of soil was enriched in lipase producing media for 72h, 28°C, 200rpm. The media was allowed to settle under gravity; the upper, liquid phase was later diluted (10^{-1} to 10^{-11}) in sterile double distilled water. Dilutions were later plated on Rhodamine B plates and were incubated at 28°C and 37°C for 2-3 days until pink-orange fluorescent colonies were observed under UV illumination.

Individual lipase producing colonies were aseptically picked from the Rhodamine B plates and were sub-cultured 10 times on LB agar plates at 28°C until pure colonies were isolated. The pure colonies were grown in LB media overnight at 28°C, 200rpm and were re-screened for the presence of lipase by streaking on Rhodamine B plates and statically incubating the plates at 28°C overnight (16h).

3.2.1.4.Identification of solvent stable cultures

The solvent stability of lipase producing cultures was determined by the plate-overlay method (Patel, Nambiar and Madamwar, 2014). Pure cultures of lipase producing strains were grown overnight (16h) at 28°C, 200rpm. 20µL of this culture was spot inoculated onto LB agar plate and allowed to dry in sterile laminar flow for 30min. The plates were then overlaid with 10mL of different concentrations of organic solvents dissolved in autoclaved ddH_2O (Table 3.4), and were statically incubated at 28°C. After 6h of incubation, solvents were aspired with sterile tips and the plates were incubated overnight at 28°C to observe any growth in the spotted cultures.

Table 3.4: Organic solvents used in this study to characterise the solvent stability in lipase producing strains by plate-overlay method.

Solvent	**% (v/v) tested**
Diethyl ether	100%
Ethyl acetate	100%
Toluene	100%
Cyclohexane	100%
n-Hexane	100%
n-Heptane	100%
t-butanol	50%
Isopropanol	50%
Ethanol	10%, 20%, 30%
Methanol	10%, 20%, 30%

3.2.1.5.Identification of solvent stable lipases

Lipase producing strains stable in multiple organic solvents were grown in basal lipase producing media (see Table 3.3) for 96h at 28°C, 200rpm. Only extracellular lipases were investigated, and these were harvested by the removal of cells from the culture broth, via centrifugation at 5,000**g*, 4°C for 20min. The cell free supernatant was treated with 50% (v/v) of *n*-hexane, *n*-heptane and cyclohexane, and with 10% (v/v) of methanol and ethanol at 28°C under continuous stirring in a shaker water bath for 24h.

3.2.1.6.Identification of bacterial strains

Strains exhibiting maximum solvent stability were identified via 16S rRNA sequencing. Liquid broth cultures were grown overnight at 28°C in basal media at 220rpm and subsequently centrifuged at 5,000*g*, 4°C for 20min. The cell pellet was re-suspended in Tris-HCl pH 7.0 containing 2mg/mL lysozyme solution. Lysozyme treated samples were sent to Eurofins Operon, Germany for double strand sequencing. The generated 16S rRNA sequences with 27F (forward) and 1492R (reverse) primers were used to identify the strains using nBLAST in NCBI.

3.2.1.7. Maintenance of cultures

For short term storage (two weeks), pure cultures were streaked on LB agar plates. The plates were then incubated overnight (16h) at 28°C and later were sealed with parafilm. The sealed plates were then transferred to 4°C, in upside down position for short term storage.

For long term storage (years), first sterile 50% glycerol in 2ml cryovials was prepared by diluting glycerol with ddH_2O followed by autoclaving the glycerol containing cryovials. Later, pure cultures were grown overnight (16h) in LB media at 28°C. 500µl of this overnight LB grown culture was transferred to 500 µL of 50% glycerol in a 2 mL cryovial and was mixed gently by pipetting.

3.2.1.8. Fermentation optimization

For the identification of optimal fermentation time and inoculum percentage for maximum lipase production from basal lipase producing medium (section 3.2.1.1.4), bacterial cultures were grown overnight in LB medium (section 3.2.1.1.6). Once the bacterial culture reached $O.D_{600}$ of 0.85±0.03 (measured after diluting the inoculum by 1:3 with blank), different percentage (1-15% for H1 and 1-8% v/v for H3) of the culture was added to basal lipase producing medium. The inoculated basal lipase medium was then left for lipase production at 28°C, 200rpm. After every 24hr of fermentation, 1ml of culture was withdrawn, was processed (section 3.2.2.1) and was checked for lipase activity via spectrophotometer assay (section 3.2.3.3).

Once fermentation time and inoculum percentage were optimised, effect of different nitrogen sources on lipase and total protein production was checked by replacing peptone in basal lipase producing medium (section 3.2.1.1.4) with 1% (w/v) of different nitrogen sources (peptone, tryptone, yeast extract, ammonium sulphate, *L*-arginine, *L*-lysine, glutamic acid, glutamine,

asparagine, urea or their combinations). Fermentation was carried out at 28°C, 200rpm with respective optimised fermentation time and inoculum percentage.

Further fermentation optimisation conditions involving effect of different percentages of optimised nitrogen source and optimum fermentation pH for maximum lipase production were also done at 28°C, 200rpm.

In all cases after fermentation, 1ml of culture was withdrawn, was processed (section 3.2.2.1) to check for lipase activity (section 3.2.3.3) and for total protein concentration (section 3.2.2.3).

3.2.2. Protein techniques

3.2.2.1.Preparation of cell extracts and culture supernatants

After fermentation, crude culture supernatants of lipolytic strains were prepared by centrifuging at 5,000**g* for 20min at 4°C. The supernatants were recovered and stored at 4°C.

3.2.2.2.Protein Concentration

Protein rich clarified liquid broth cultured supernatant was concentrated by ultrafiltration using Centricon (Sartorius) at 1500**g*, 4°C and Microcon (Millipore) at 10,800**g* with a molecular weight exclusion size of 10kDa and 3kDa respectively. Microcon (Millipore) were used for concentrating protein samples which were <2mL volume.

3.2.2.3.Determination of protein concentration

The total protein concentration of the samples was determined using the Bradford protein microassay (Ernst and Zor, 2010). Bovine serum albumin (BSA) solutions, at concentrations from 10µg/mL to 200µg/mL, were used as standards (Appendix B). To 50µL of the protein sample 100µL of Bradford reagent was added (in triplicate) in a sterile flat bottom U-shaped 96-well plate. Absorbance was recorded at 595nm after 10min of incubation at ambient temperature after shaking the 96-well plate at medium speed for 2sec in spectrophotometer.

3.2.2.4.Protein purification

3.2.2.4.1. H1 Lipase from *P. reinekei*

Two purification steps were performed, both with Q-Sepharose High Performance (HP) chromatography resin. The first chromatography column (Column 1) was used as negative mode of chromatography; the flow through of column 1 was used as the load solution for the second chromatography (Column 2). Both column 1 and column 2 were packed with Q-Sepharose HP (Table 3.5).

Table 3.5: Parameters followed during purification of lipase from lipolytic strain

Column manufacturer	**Bio-rad**
Column Diameter	1.5cm
Resin	Q-Sepharose High Performance
Bed height	6cm
Column volume	10.5mL
Flow rate (volumetric)	4mL/min

Column 1 was equilibrated with 10mM Tris-HCl buffer at pH 9.0±0.1; while Column 2 was equilibrated with 10mM Tris-HCl buffer containing 250mM NaCl at pH 9.0±0.1. Between 3 and 6 column volumes of respective equilibration buffer were passed through the columns, until buffer at the column outlet attained pH 9.0±0.1.

The protein to be loaded was prepared from bacterial fermentation after 144h growth at 28°C, 200rpm, in basal lipase producing media containing 1% *L*-Lysine (w/v; instead of bacteriological peptone at pH 6.5±0.2, see Table 3.3). Bacterial cells were separated by centrifugation at 5000**g* for 20min at 4°C. The cell free supernatant was recovered and was pre-filtered with a 1.2µm filter (Cruinn Diagnostics), followed by sub-filtration through a sterile 0.45µm filter (Cruinn Diagnostics). Clarified culture supernatants were stored at 4°C while all purifications were performed at room temperature. The filtered cell free supernatant was dialyzed in a 14kDa cut off dialysis membrane (Sigma-Aldrich) at 1:20 ratio in 10mM Tris HCl, pH 9.3±0.2, for 4h at room temperature under continuous stirring using a magnetic stirrer. After 4h, the buffer was replaced with fresh buffer and dialysis was continued overnight (15h) at 4°C (Ahmed, Raghavendra and Madamwar, 2010b). The dialysate was later loaded onto equilibrated Column 1 after adjusting the

pH to 9.0±0.1 using 2M Tris solution or HCl; at a flow rate of 4ml/min. The flow through of Column 1 was collected separately and 250mM of NaCl was added to the flow through under continuous stirring. This protein solution (flow through of Column 1 and 250mM NaCl) was subsequently loaded onto an equilibrated Column 2 at a flow rate of 4mL/min.

After protein loading, Column 2 was washed with three column volumes of equilibration buffer (10mM Tris-HCl buffer containing 250mM NaCl, pH 9.0±0.1). Protein samples were eluted in three column volumes each at salt concentrations of 0.5M, 0.75M and 1M NaCl in 10mM Tris-HCl buffer at pH 9.0±0.1. The eluted samples were subsequently analysed for protein concentration via Bradford assay (Section 3.3.2.2) and for lipase activity via *p*-NPP spectrophotometry (Section 3.3.3.3). The eluted protein was later stored at 4°C in the presence of 5% (v/v) sorbitol.

For long term storage, the sample was initially dialysed (1:20) in Tris-HCl buffer pH 9.0±0.1, 5% (v/v) sorbitol overnight at 4°C. Following dialysis, the protein sample was transferred to an air-tight container and was stored in -80°C for 12h. The frozen sample was later freeze dried using the default parameters of the Labconco Freezone 6 Freeze Dryer.

3.2.2.4.2. H3 lipase from *P. brenneri*

A one step chromatographic purification was carried out with a Q-Sepharose High Performance (HP) chromatography resin (Table 3.5). The protein sample to be loaded was prepared from a bacterial fermentation of *P. brenneri* after 48h growth at 28°C, 200rpm, in basal lipase producing media containing 1% (w/v) bacteriological peptone at pH 6.8±0.2 (see Table 3.3). Bacterial cells were separated by centrifugation at 5000**g* for 20min at 4°C. The cell free supernatant was recovered and was pre-filtered with a 1.2µm filter (Cruinn Diagnostics), followed by sub-filtration through a sterile 0.45µm filter (Cruinn Diagnostics). Clarified culture supernatants were stored at 4°C while all purifications were performed at room temperature. The filtered cell free supernatant was dialyzed in a 14kDa cut-off dialysis membrane (Sigma-Aldrich) at 1:20 ratio in 10mM Tris HCl, pH 8.5±0.2, for 4h at room temperature under continuous stirring using a magnetic stirrer. After 4h, the buffer was replaced with fresh buffer and dialysis was continued overnight (15h) at 4°C (Ahmed, Raghavendra and Madamwar, 2010b). After dialysis, the crude extract was alkaline precipitated for 30mins in pH 9.0±0.2 at room temperature. After centrifugation at 5000**g* for 20

mins at 4°C and filtration through 0.45µm filter; the alkaline precipitated filtrate was loaded onto equilibrated anion exchange Q-Sepharose HP after adjusting the pH to 8.5±0.1 using 2M Tris solution or HCl; at a flow rate of 4ml/min. Protein samples were eluted in three column volumes each at salt concentrations of 0.25M, 0.5M, 0.75M and 1M NaCl in 10mM Tris-HCl buffer at pH 8.5±0.1. The eluted samples were subsequently analysed for protein concentration via Bradford assay (Section 3.3.2.2) and for lipase activity via *p*-NPP spectrophotometry (Section 3.3.3.3). The eluted protein was later stored at 4°C.

For long term storage, the sample was initially dialysed (1:20) in Tris-HCl buffer pH 8.5±0.1 overnight at 4°C. Following dialysis, the protein sample was transferred to an air-tight container and was stored in -80°C for 12h. The frozen sample was later freeze dried using the default parameters of the Labconco Freezone 6 Freeze Dryer.

3.2.2.5.Protein Electrophoresis

3.2.2.5.1. Reducing SDS-PAGE

The purity of a protein sample was analysed via polyacrylamide gels containing using SDS as a denaturing agent (Laemmli, 1970). The composition of the solutions and gels used are detailed in Table 3.6. The sample loading dye was added to the samples to get a final concentration of 1X, and the samples were boiled for 10min at 100°C in the case of a reducing SDS-PAGE (loading dye has β-mercaptaethanol); this step was eliminated for a non-reducing SDS-PAGE (and no β-mercaptaethanol was used in the loading dye). The Bio-Rad gel running tank was filled with 1X SDS-running buffer. 20µL of each prepared protein sample was loaded onto each lane of the SDS-PAGE gel. Electrophoresis was carried out at 75 volts through the stacking gel (approx. 15-20min) and at 150-180 volts through the resolving gel (approx. 40min), using Bio-Rad apparatus. Once the electrophoresis was completed, gels were stained for 20min in Comassie Brilliant Blue G250 dye solution. The gels were subsequently de-stained with de-staining solution until clear visualisation of protein bands was achieved. The molecular mass of the sample proteins was determined by comparison of their migration in SDS-PAGE with that of Pierce™ Unstained Protein marker (Appendix G). The molecular weights (kDa) of marker proteins were 116, 66.2, 45, 35, 25, 18.4, 14.4 kDa.

Table 3.6: Gel composition and solutions used for SDS-PAGE

<table>
<tr><td>30% (w/v) Acrylamide-Bisacrylamide mix</td><td>SDS Running buffer (10X)</td></tr>
<tr><td>Acrylamide: 29g
BisAcrylamide: 1g
Distilled water: 100mL</td><td rowspan="2">Tris: 30g
Glycine: 144g
SDS: 10g
Final volume: 1000mL
pH 8.3</td></tr>
<tr><td>Separating/Resolving gel composition (12%): 5mL-1gel</td></tr>
<tr><td>Double distilled water: 1.65mL
30% (w/v) acrylamide-bisacrylamide mix: 2mL
1.5M Tris, pH 8.8: 1.25mL
10% (w/v) SDS: 50µL
10% (w/v) Ammonium Persulfate: 50µL
TEMED: 8µL</td><td>Brilliant Blue G-250 (staining): 1X
Coomassie Brilliant Blue G-250: 0.5% (w/v)
Acetic Acid: 10% (v/v)
Ethanol: 45% (v/v)
Distilled water: 45% (v/v)</td></tr>
<tr><td>Stacking gel composition (2mL-1gel)</td><td>Destaining solution</td></tr>
<tr><td>Double distilled water: 1.4mL
30% (w/v) acrylamide-bisacrylamide mix: 0.33mL
0.5M Tris pH 6.8: 0.25mL
10% (v/v) SDS: 20µL
10% (w/v) Ammonium Persulfate: 20µL
TEMED: 8µL</td><td>Methanol: 30% (v/v)
Acetic Acid: 10% (v/v)
Distilled water: 60% (v/v)
Sample loading dye (5X)
Bromophenol Blue (0.02% w/v)
Glycerol (30% v/v)
SDS (10% w/v)
Tris-HCl (250mM pH 6.8)
β-mercaptoethanol (5% v/v)</td></tr>
<tr><td>Zymogram Wash Buffer</td><td rowspan="2"></td></tr>
<tr><td>Phosphate Buffer: 50mM
Triton X-100: 1.5% (w/v)
pH 7.0±0.2</td></tr>
</table>

3.2.2.5.2. Non-reducing SDS-PAGE

Non-reducing SDS-PAGE can be used to understand the enzymatic activity of lipase captured in the polyacrylamide gel via fluorimetry (termed the Zymogram Assay, Section 2.3.3.2). Reducing and non-reducing SDS-PAGE differ only in the presence and absence of β-mercaptaethanol in the protein loading dye; hence protein samples were not heated to 100°C for 5-10min for non-reducing SDS-PAGE.

3.2.2.6. MS analysis for Amino acid sequence identification

Purified lipase from H1 (*P. reinekei*) and H3 (*P. brenneri*) were sent for MS analysis to Maynooth University, Ireland. After receiving the data, the amino acid sequences generated were checked for similarities with available *Pseudomonas* lipase sequences in NCBI using BlastP.

3.2.3. Enzymatic assays

3.2.3.1.Plate assay using lipid substrates

The lipolytic activity of strains was detected by means of a direct test based on streaking or spotting these strains on Rhodamine B agar plates followed by subsequent incubation at 28°C for 2days (Section 3.2.1.3).

3.2.3.2.Zymogram analysis

Detection of lipolytic activity using fluorogenic substances (as a zymogram, Section 2.4.3) was performed using 4-methylumbelliferone (MUF) butyrate. MUF butyrate was prepared fresh each time for the detection of lipase in non-reducing SDS-PAGE at a final concentration of 100µM in 50mM phosphate buffered saline, pH 7.0±0.2. The lipolytic activity of proteins separated by non-reducing SDS-PAGE gel was detected before Coomassie Brilliant Blue staining. In brief, after electrophoresis non-reducing SDS-PAGE gels were incubated in the zymogram wash solution containing 50mM phosphate buffer saline with 1.5% (v/v) Triton X-100 at pH 7.0±0.2 for 30mins at room temperature under continuous shaking (Table 3.6). The gels were subsequently washed twice in 50mM phosphate buffer (pH 7.0±0.2; (Hospital, Creu and Pau, 1999) and then were treated with a solution of freshly prepared 100µM MUF-butyrate for 10-15mins under continuous shaking at 50rpm. After incubation, activity bands resulting from MUF liberation were visible under UV illumination to qualitatively confirm presence, or absence, of lipase.

3.2.3.3.Determination of lipase activity by spectrophotometry

p-NPP substrate was used for the estimation of lipase activity via spectrophotometry and was prepared as per Glogauer and colleagues (Glogauer *et al.*, 2011) with some modifications. A 20mM stock solution of *p*-NPP (Stock A) was prepared in a 1:4 ratio of Acetonitrile:Isopropanol. Stock B, containing Tris, $CaCl_2$ and Triton X-100 at pH 7.5, was used to prepare the substrate for the lipase assay (Table 3.7). The lipase substrate was prepared fresh each time directly before the assay by the addition of Stock A to a preheated (60°C) Stock B, under continuous stirring. 0.54mL of

Stock A was added to 9.46mL of stock B to achieve a final concentration of substrate as 50mM Tris-HCl, 1mM $CaCl_2$, 0.30% (v/v) Triton X-100, 1mM *p*-NPP.

Table 3.7: Substrate solution for *p*-NPP spectrophotometry assay. Solution A was added to 60°C of solution B under continuous mixing to get a final concentration of 50mM Tris, 1mM $CaCl_2$, 0.3% Triton X-100 and 1mM p-NPP.

Stock A		**Stock B**	
Total Volume	5mL	Total Volume	100mL
Acetonitrile	1mL	Tris	696.21mg
Isopropanol	4mL	Triton X-100	400mg
p-NPP	37.8mg	$CaCl_2$	575µL of 0.2M $CaCl_2$
		pH	7.5±0.2

In brief, 230µL of assay substrate was added to 20µL of lipase sample in triplicate in a sterile flat bottom U-shaped 96-well plate. Porcine pancreas lipase solution, at concentrations ranging from 6mg/mL to 30mg/mL, was used as standard. The mixture was incubated at 28°C for 30min. After incubation, the absorbance was measured at 410nm using Powerwave Microplate spectrophotometer. One International Unit (IU) of lipase activity was defined as the amount of enzyme needed to liberate 1µmol of *p*-NP per minute under the conditions described for each assay system (Appendix C).

3.2.4. Biochemical characterization of purified lipase

Lipase inhibition or (in)activation was estimated as a percentage of the residual activity detected after exposure to the external factor in question. Characterisation was performed by exposing the lipase solution to various external factors such as temperature, pH, organic solvents and quantifying their effect on lipase stability and activity. All samples of purified lipase were standardised to obtain same IU for characterisation (30IU/ml). Suitable positive and negative controls were used; 30IU/mL of porcine pancreas lipase (Sigma) was used as positive control for all the characterization experiments and the respective buffer was used as a negative control.

3.2.4.1.pH stability

To ascertain the effect of pH on the stability of the lipases, purified lipase solution was prepared in 50mM of buffer depending on the pH of incubation. 50mM of Glycine-HCl (pH 3, 4), 50mM of Tris-Acetate (pH 5, 6), 50mM of Tris-HCl (pH 7, 8, 9) and 50mM of Borate Buffer (pH 10) were

used to examine the effect of pH at 4°C and 28°C after 24h of incubation. Before the assay, all the samples were adjusted to pH 7.0 using 2M Tris/HCl and lipase activity was estimated via *p*-NPP end point spectrophotmetry (Section 3.2.3.3). Buffer blanks and positive/negative controls were implemented to negate dilution factors, to identify and validate assay interference.

3.2.4.2.Thermostability

Purified lipase solutions (30IU/ml) prepared in 50mM Tris-HCl buffer (pH 7.0) were incubated at 20, 30, 40, 50, 60, 70, 80°C for 24h. Samples were withdrawn after 30mins of incubation and were analysed to determine the effect of temperature on lipase activity via *p*-NPP end point spectrophotometry (Section 3.2.3.3). Buffer blanks and positive/negative controls were implemented to identify and validate assay interference.

3.2.4.3.Effect of metal ions and chemical reagents

The effect of various metal ions and chemical reagents on lipase activity was examined at 28°C and 40°C. A purified lipase solution prepared in 50mM Tris-HCl (pH 7.0) was independently incubated with 10mM of $CaCl_2$, $MgCl_2$, KCl, NaCl, EDTA, β-mercaptaethanol, SDS, Urea, Tween 20 and Triton X-100. The purified lipase sample was incubated for 24h. The effect of metal ions and surfactants on lipase activity was measured by end point *p*-NPP assay (Section 3.2.3.3). Buffer blanks and positive/negative controls were implemented to identify and validate assay interference.

3.2.4.4.Solvent stability

Purified lipase solutions prepared in 50mM Tris-HCl buffer (pH 7.0) were incubated in airtight vials with 10-50% (v/v) organic solvents at 28°C and 40°C for 24h under continuous stirring. Samples were withdrawn after 1h and 24h of incubation and were later analysed for stability of lipase in presence of organic solvents via *p*-NPP end point spectrophotometry (Section 3.2.3.3). Buffer and solvent blanks were used to check their interference on the assay.

3.2.5. Immobilization methods

3.2.5.1. Immobilization on Gold nanoparticles

3.2.5.1.1. Gold nanoparticles synthesis

Gold nanoparticles (AuNPs) were synthesized as per Khutale and Casey (Khutale and Casey, 2017). Briefly, 100ml of 1mM $HAuCl_4.3H_2O$ was brought to boil with vigorous stirring. To this boiling solution; 8 ml of 38.8mM sodium citrate was added instantly. The solution was left to boil for

another 10mins, after which the solution was removed from heat and was stirred for another 15mins at room temperature. The synthesized AuNPs were checked for size and charge by using a Malvern Nanoseries Zeta-sizer. The concentration of nanoparticles was determined by atomic absorption spectroscopy, using Au as the standard. 5-30mg/ml concentrations of Au standard were prepared in ddH_2O; and were used to generate a standard curve for estimation of unknown Au samples (Appendix H).

3.2.5.1.2. Glutathione reduction of AuNPs

Citrate reduced gold nanoparticles, synthesized as per Khutale and Casey (Khutale and Casey, 2017), were treated with reduced glutathione as per Akella and Mitra (Akella and Mitra, 2007) with no deviations. Briefly, to 10ml of AuNPs synthesized, 1ml of 25µM of GSH (Gluthatione) was added under continuous stirring. The addition of GSH turned the AuNPs solution from ruby red to ink blue followed by precipitation after 1-2h of incubation. The precipitate was collected by centrifugation at 8000**g* for 5mins and was washed twice with 5ml methanol. The precipitate was later dissolved in 10ml of 50mM phosphate buffer at pH 9.0±0.2. The solution was subsequently used for enzyme immobilization reactions.

3.2.5.1.3. Covalent and physical adsorption of lipase on AuNPs

Lipase immobilization trials were carried out using AuNPs with and without glutathione reduction. Glutathione forms a surface monolayer on AuNPs via sulfur bonds. The functional groups (-COOH) available on GSH can be used for physical, as well as covalent immobilization of compounds/enzymes (Akella and Mitra, 2007). Both physical adsorption and covalent binding modes of immobilization were attempted to immobilise H1 (*P. reinekei*) and the lipase standard (porcine pancreas lipase) on AuNPs. For adsorption, the lipase was added directly to AuNPs; however, for covalent binding, glutathione reduced AuNPs were treated with NHS-EDC (coupling agents for activation of GSH and enzyme functional group; N-hydroxysuccinimide; 1-ethyl-3-(3-di-methylaminopropyl)carbodiimide hydrochloride) as per Akella and Mitra (Akella and Mitra, 2007) followed by addition of the enzyme. A ratio of 1:1 (AuNPs: enzyme concentration) was employed for both the physical and covalent binding of lipase on AuNPs.

3.2.5.1.4. Estimation of immobilization efficiency

After immobilization, gold nanoparticles were centrifuged at 8000**g* for 5mins. The supernatant was collected, and subsequently the particles were washed twice with double distilled water with the supernatant being collected after each wash. The activity of lipase in each supernatant was verified via *p*-NPP assay spectrophotometry (Section 3.2.3.3).

3.2.5.1.5. Zeta sizer and SEM

Zeta sizer was used to check the size and charge on the AuNPs. Instrument was truned on 30mins before usage to stabilize the laser. After 30mins, Zetasizer software was started from the computer desktop. 1ml of AuNPs in solution were added to the cuvette, any air bubbles present were removed and the cuvette was placed in zeta sizer.

In the software, under *File* menu appropriate cuvette cell used for the sample was selected along with measurement type. New Measurement File was created in personal folder by following the path File-> New-> Measurement File.

In *Measure* menu, *Start SOP* or Manual was selected and the paramaters for the analysis were chosen. These parameters included *Measurement type* (size, zeta potential or molecular weight); *Sample* (label); *Material* (Gold); *Dispersant* (water/solvent used); *Temperature* (25°C); *Measurement* (number of runs per measurement). The SOP was later saved with the desired settings. After SOP was saved, in the measurement widow *Start* was pressed to begin the measurement. A beep sound confirmed completion of the measurement. The measurements were taken from the software using .xls files. After completion of sample analysis, cuvette was removed from the instrument and the sample was discarded in the nearby waste bin. The cuvette was cleaned and washed using deionized water.

AuNPs in solution form with known concentrations were sent in 2ml cryovials to Focas Research Institute for SEM analysis. The pictures from the microscopic analysis provided the size of the synthesized AuNPs and were also used to identify AuNPs shape.

3.2.5.2.Entrapment in calcium alginate beads

A 5% (w/v) solution of sodium alginate was prepared in double distilled water (ddH_2O) under continuous stirring. Lyophilized lipase (from both H1 and H3) and porcine pancreas lipase

(standard) were reconstituted separately in 10mM Tris-HCl buffer pH 7.0±0.2 to a final concentration of 1IU/ml (*p*-NPP, Section 3.2.3.3). Reconstituted lipase solutions were used to dilute stock sodium alginate solution (5% w/v) to achieve a final concentration of 2% (w/v) sodium alginate. Under continuous stirring, the alginate enzyme solution was mixed for another 10 minutes. Each alginate enzyme solution was later added dropwise to a beaker containing 0.2M $CaCl_2$.

Hard calcium alginate beads were formed after sodium alginate drops remained in the $CaCl_2$ solution for 60mins. After 60mins, the beads were separated from the $CaCl_2$ solution by using a 1.2µm filter and were washed twice in double distilled water following filtration after every wash. The beads were stored overnight (10h) at room temperature in a vacuum desiccator to remove any water present on the bead surface. The beads were then stored at 4°C in glass air-tight container until further use.

3.2.5.3. Characterization of lipase activity/stability in calcium alginate beads

3.2.5.3.1. Estimation of reaction time

Calcium alginate beads, with and without entrapped lipase, were checked for lipase activity as per *p*-NPP spectrophotometer assay (Section 3.2.3.3). The catalysis of *p*-NPP substrate was verified by measuring absorbance at 410nm every 15 mins, for 90mins, at 28°C (see *p*-NPP spectrophotometer assay, Section 3.2.3.3). The rate of hydrolysis of the free enzyme was also monitored under the same conditions. The amount of enzyme activity obtained with free and entrapped enzyme over a 90min incubation period was compared.

3.2.5.3.2. Activity and stability studies of lipase in entrapped alginate beads

The effect of pH, temperature, solvent and other additives on the stability and activity of calcium entrapped lipase from *P. reinekei* (H1), *P. brenneri* (H3) and lipase standard (porcine pancreas) was estimated using *p*-NPP spectrophotometry (see Section 3.2.3.3). Enzyme entrapped beads were incubated in different solutions based on the requirement of the experiment (as per Section 3.2.4). After incubation, the buffer (and additives) was removed and the beads were washed twice with Tris-HCl buffer at pH 7.0±0.2. The substrate, *p*-NPP, was added to the beads and incubated for 60mins. The *p*-NPP released by the action of the lipases was collected from the reaction mixture via pipette and was checked for absorbance at 410nm.

For all the free lipase vs. calcium alginate entrapped lipase trials; the ratio of enzyme and substrate (*p*-NPP) was maintained constant as per p-NPP spectrophotometer assay (see Section 3.2.3.1). Calcium alginate beads generated from one batch of entrapment were weighed and concentration of enzyme in beads was calculated by comparing with initial concentration of lipase used for beads generation. If X gm of beads were generated from Y gm of lipase, amount of lipase in 1 bead = X / Y. The volume of p-NPP (substrate) required for Y gm of beads was calculated by using the same enzyme: p-NPP ratio as that for free lipase.

3.2.5.3.3. Reusability and stability of alginate beads

To investigate the reusability of the enzyme entrapped calcium alginate beads, the beads were incubated in *p*-NPP as per *p*-NPP spectrophotometer assay (see Section 3.2.3.3) for 60mins. After 60mins of incubation, the product generated was removed and measured at 410nm as per standard *p*-NPP assay. The calcium alginate beads were later washed twice with Tris-HCl buffer at pH 7.5±0.2, before fresh *p*-NPP substrate was added to measure the remaining enzyme activity entrapped in calcium alginate beads. This washing process was repeated for 7 cycles to calculate the reusability of calcium alginate beads entrapping lipase.

To explore the stability of enzyme entrapped calcium alginate beads, the beads were stored at 4°C. A fixed weight of beads was removed at respective time-points and this was examined for lipase activity by incubation in *p*-NPP substrate for 60mins. The stability was compared against the activity of lipase obtained at day 0 (freshly entrapped lipase in calcium alginate beads).

3.2.6. Microalgae methods

3.2.6.1.Culturing Media

3.2.6.1.1. 3N-BBM+V

Bold basal medium, with 3-fold nitrogen and vitamins (3N-BBM+V modified), was prepared as per manufacturer's instructions (see Table 3.8). After mixing all the components, the medium was autoclaved according to standard autoclaving (121°C, 1.5 bar for 15mins).

Table 3.8: Composition of 3N-BBM+V microalgal medium as provided by CCAP (The Culture Collection of Algae and Protozoa).

Chemical	MW	Stock solution (g/L)	Volume (ml) required for 1L medium	Final conc. (g/L)
$NaNO_3$	84.99	25	30	0.750
$CaCl_2$. $2H_2O$	110.98	2.5	10	0.025
$MgSO_4.7H_2O$	246.47	7.5	10	0.075
$K_2HPO_4.3H_2O$	228.22	7.5	10	0.075
KH_2PO_4	136.09	17.5	10	0.175
NaCl	58.4	2.5	10	0.025
Trace element solution			6	
Vitamin B1			1	
Vitamin B12			1	

A Trace Element (TE) solution was prepared by adding the following chemicals in the same order detailed in Table 3.9 of which 6ml was added to prepare 1L of 3N-BBM+V medium.

Table 3.9: Composition of trace element stock solution as provided by CCAP.

Chemical	MW	mg/L
Na_2EDTA	372.24	750
$FeCl_3.6H_2O$	270.3	97
$MnCl_2.4H_2O$	197.91	41
$ZnCl_2$	136.286	5
$CoCl_2.6H_2O$	237.93	2
$Na_2MoO_4.2H_2O$	241.95	4

Stock solutions of Vitamin B1 (Thiaminhydrochloride) and Vitamin B12 (Cyanocobalamin) were prepared as follows; 0.12g of Vitamin B1 was dissolved in 100ml of ddH_2O. 1ml of this Vitamin B1 was further diluted into 99ml ddH_2O. For Vitamin B12 stock; 0.1g of Vitamin B12 was dissolved in 100ml of ddH_2O. Both working stocks of vitamin B1 and B12 were filter sterilised through a 0.2µm sterile filter and stored in -20°C until required for use.

3.2.6.1.2. Simulated wastewater

Synthetic secondary wastewater as per EU composition (DIN 38412-26) was prepared as per Table 3.10 and autoclaved under standard autoclave conditions (121°C, 1.5 bar for 15mins). Stock solutions were kept separate and were mixed to form their respective concentrations immediately prior to use.

Table 3.10: Composition of simulated wastewater as per EU (DIN 38412-26).

Stock No.	Stock solution	Conc. (g/L)	Vol (ml) Stock for 1L wastewater	Final conc. (mg/L) In wastewater
1	Peptone	8	20	160
	Meat Extract	5.5		110
	Urea	1.5		30
2	NaCl	0.35	20	7
	$CaCl_2.2H_2O$	0.2		4
	$MgSO_4.7H_2O$	0.1		2
3	K_2HPO_4	1.4	30	28

3.2.6.1.3. Nitrogen deficient wastewater

Simulated wastewater without nitrogen components (Stock 1, Table 3.10) were prepared by combining the respective concentrations of stock 2 and stock 3 only (see Table 3.10) in a sterile autoclaved conical flask. The final volume (see Table 3.10) of the culture media was made up by addition of autoclaved distilled water. As conical flask, stock 2, 3 and ddH_2O were already sterilised by autoclaved; media preparation was carried out in sterile environment.

3.2.6.1.4. Jaworski Medium

One litre of Jaworski medium was prepared by the addition of 1ml of the stock solution of each component (see Table 3.11) made up to the final volume of the solution using distilled water. The final solution was autoclaved as per standard autoclave conditions (121°C, 1.5 bar for 15mins).

Table 3.11: Composition of Jaworski medium (Yeh and Chen, 2006)

Component	Stock concentration (g/L)
$Ca(NO_3)_2.4H_2O$	20
KH_2PO_4	12.4
$MgSO_4.7H_2O$	50
$NaHCO_3$	15.9
$NaNO_3$	80
$Na_2HPO_4.12H_2O$	36
EDTA.Fe.Na	2.25
$EDTA.Na_2$	2.25
H_3BO_3	2.48
$MnCl_2.4H_2O$	1.39
$(NH_4)6Mo_7O_{24}.4H_2O$	1
Cyanocobalamin	0.04
Thiamine HCl	0.04
Biotin	0.04

3.2.6.2.Microalgae revival

Chlorella emersonii (CCAP 211/8C) was supplied by the CCAP (Culture Collection of Algae and Protozoa SAMS Limited, Scottish Marine Institute, Scotland, United Kingdom) as a liquid medium in two 10ml tubes. Immediately upon delivery, the culture was transferred to 3N-BBM+V media in 1:10 ratio (culture: media). *Pseudokirchneriella subcapitata*, was supplied by RESC ExoTox lab of the FOCAS Research Institute, TU Dublin. 1ml of the liquid culture present in Jaworski media (Section 3.2.6.1.4) was transferred to 10ml of 3N-BBM+V media (1:10 ratio). Both cultures were grown in an environmentally controlled shaker incubator (Innova 40 Shaker incubator; 18°C with a 16h:8h light: dark cycle and a constant mixing at 120rpm). After 10 days, fresh 3N-BBM+V media was added to both the microalgal strains (*Chlorella emersonii* and *Pseudokirchneriella subcapitata*) and were grown until significant growth was observed for storage and experimentation.

3.2.6.3.Microalgae maintenance

The microalgal culture was maintained by routine serial transfer. After 2-3weeks of growth, 1ml of culture was transferred to 250ml of fresh sterile autoclaved media (3N-BBM+V). The culture was grown at 18°C with a 16h:8h light: dark cycle and a constant mixing at 120rpm until further serial transfer.

3.2.6.4.Cryopreservation and post-cryopreservation recovery

10ml of 10% (v/v) DMSO (acting as a cryoprotectant) was prepared with 3N-BBM+V culture medium and was filter sterilized using a 0.2µm sterile syringe filter into a sterile universal tube. The microalgal culture was centrifuged (5,000**g*, 5mins) and the pellet was resuspended in 10ml of fresh autoclaved media (3N-BBM+V) to obtain a concentrated culture. To this concentrated culture, 10ml of sterilized cryoprotectant solution was added. The tube was sealed and inverted twice to ensure a homogenous solution. Aseptically, 1.5ml aliquots were pipetted into 2ml cryovials and were incubated at room temperature for 10min. A passive cooler (Mr Frosty™ Unit) was filled with isopropanol to a final volume of 250ml. The isopropanol was replaced after every fifth use. Cryovials were then transferred to the cooling chamber of the passive cooler. The passive cooler was placed in a -80°C freezer and was incubated for 1.5h. The freezer was closed over this period to avoid influencing the cooling rate. After 1.5h the passive cooler was removed and the cryovials were rapidly transferred to a small drawer containing liquid nitrogen using long forceps. The cryovials were not allowed to warm up prior to plunging into liquid nitrogen. The final storage

temperature was below -130°C. To recover cultures, the vials were thawed by placing them in a pre-heated water-bath (40°C) and with gentle agitation until the ice crystals melted. After thawing, cryovials were rapidly transferred to a laminar flow/biological safety cabinet. The outside of the cryovials was wiped with 70% (v/v) ethanol to remove residual viable bacterial and fungal spores from the liquid nitrogen storage that might contaminate recovered cultures. Using a disposable plastic pipette, 1.5ml of the thawed culture was transferred into a sterile 250ml, labelled conical flask containing 20ml of sterile autoclaved medium (3N-BBM+V). After an appropriate period (2-8 weeks, 16h: 8h Light: Dark, 18°C, 120rpm) a normal culture was obtained. This culture was maintained by routine serial transfer (Section 3.2.6.3) or was employed for experimental use (Section 3.2.6.5 and 3.2.6.6).

3.2.6.5.Biomass generation and neutral lipid(s)/Triacylglycerol(s) production

Revived microalgae cultures (Section 3.2.6.2) were grown in simulated wastewater media (Section 3.2.6.1.2) under three different conditions. The autotrophic condition had no other source of carbon than fixation via photosynthesis, the mixotrophic condition contained 1% (w/v) glucose as an additional carbon source to photosynthesis while heterotrophic culture had only 1% (w/v) glucose as carbon source. Growth curves of microalgal cultures for all three conditions were generated by monitoring absorbance at 590nm.

The culturing conditions resulting in highest biomass were used for the generation of microalgal biomass as the first step in neutral lipid(s) production. The microalgal biomass generated in growth media was harvested by centrifugation at 5,000**g* for 5 mins at 18°C and was washed twice with sterile autoclaved distilled water before further experimentation. The washed pellet was later transferred to simulated nitrogen deficient wastewater (Section 3.2.6.1.3) with, and without, 1% (w/v) glucose. The culture was mixed thoroughly by shaking the conical flask in rotatory motion for a uniform cell distribution and was cultured for neutral lipid(s) production at 18°C, 16h:8h (light: dark), 120 rpm. Every three days, 2ml of culture were withdrawn from the flask and was used for the estimation of neutral lipid(s) as per the Nile Red Assay (Section 3.2.6.6).

3.2.6.6.Nile Red assay development

A fixed number of cells (1O.D$_{@590nm}$=10^7 cells/ml) from the simulated wastewater growth media was transferred to nitrogen deficient media. After one week of incubation in nitrogen deficient wastewater at 18°C with 16h:8h (light: dark) cycle, 120rpm; 10ml of culture was removed

aseptically into a universal tube. The culture was centrifuged at 5,000**g* for 5mins and the culture media (supernatant) was discarded. The microalgal cell pellet was later mixed thoroughly in 10ml of double distilled water; 50µl of this was used for one assay value. Into a flat bottom, transparent 96-well microtiter plate; 100µl of double distilled water was added in quintuplet to which 50µl of microalgae culture prepared earlier was added. For the method optimisation (Section 3.2.6.1-3.2.6.6.4), 100µl of Nile Red dye, comprising various solvent (DMSO and acetone) and concentrations (1-50µg/ml) was added to this 150µl of solution generating a final volume of 250µl.

3.2.6.6.1. Solvent and solvent percentage

For the identification of appropriate solvent and concentration for the Nile Red assay; 10µg/ml of Nile Red solution was prepared over a concentration range (10-60% v/v) of the solvents examined (DMSO and acetone). To 150µl of the assay solution (Section 3.2.6.6), 100µl of this dye solution was added in quintuplet. The microalgal cells treated with the respective solvents, in respective concentrations, were incubated at room temperature in the dark for 30mins before monitoring the fluorescence intensity using a Perkin Elmer Lambda 900 UV/VIS/NIR Spectrometer at various excitation wavelengths (485nm-530nm) and emission wavelength of 580nm.

3.2.6.6.2. Dye conentration

To identify the concentration of Nile Red required to obtain the maximum fluorescence intensity; a concentration range between 1µg/ml and 50µg/ml Nile Red was prepared in 20% (v/v) DMSO. 100µl of this solution was added to 150µl of diluted microalgal culture (Section 3.2.6.6) in quintuplet. The assay plate was then statically incubated, at 40°C in the dark, for 60mins before recording the fluorescence intensity using a Perkin Elmer Lambda 900 UV/VIS/NIR Spectrometer at 530nm excitation and 580nm emission wavelength.

3.2.6.6.3. Incubation time

A 10µg/ml Nile Red solution was prepared in 20% (v/v) DMSO; 100µl of this solution was added to 150µl of diluted microalgal culture (see Section 3.2.6.6) in quintuplet. A kinetic study of the assay was performed by incubating the plate at 40°C in the dark and recording the fluorescence intensity using a Perkin Elmer Lambda 900 UV/VIS/NIR Spectrometer after every 5-15mins over a 90mins incubation period, with an excitation and emission wavelength of 530nm and 580nm respectively.

3.2.6.6.4. Effect of cell concentration

Different cell concentrations (0.05-0.9 at OD_{590nm}) of *Chlorella emersonii* and *Pseudokirchneriella subcapitata* were prepared in ddH_2O. 50µl of these microalgae cultures was added to each 96-well plate, in quadruplicate, to which a further 100µl of ddH_2O was added. 50µl of either a 10µg/ml or 5µg/ml of the Nile Red solution (20% v/v, DMSO) was added to this 150µl of *Chlorella emersonii* and *Pseudokirchneriella subcapitata* respectively (Section 3.2.6.6). The mixture was statically incubated, at 40°C, for 60mins and 40mins respectively before recording the fluorescence intensity using a Perkin Elmer Lambda 900 UV/VIS/NIR Spectrometer at 530nm excitation and 580nm emission.

3.2.6.6.5. Triolein standard curve

A working range of triolein standard (between 1µg/ml to 15µg/ml) was prepared in neat chloroform. In a 96-well plate, 100µl of ddH_2O, 100µl of 10µg/ml Nile Red (in 20% v/v DMSO) and 50µl of the respective triolein concentration was mixed in quintuplicate. The assay monitored fluorescence intensity at 530nm excitation and 580nm emission wavelength after 5mins incubation. The fluorescence intensity measured using a Perkin Elmer Lambda 900 UV/VIS/NIR Spectrometer for various concentrations of triolein was used for preparing a standard curve (Appendix J).

3.2.6.7. Fluorescence microscope

Microalgae biomass containing neutral lipids generated after nitrogen starvation (section 3.2.6.5) was harvested by centrifuging 1ml of culture at 5,000**g* for 5 mins. The pellet was washed twice with ddH_2O and after wash was mixed gently with 200µl of 5µg/ml of nile red dye dissolved in 20% (v/v) DMSO. The solution was left undisturbed for incubation at 40°C for 20mins. The microscope was switched on meanwhile along with the mercury lamp to get full brightness.

After 20mins, 20µl of the microalgae nile red solution was spotted in glass slide and was spread evenly using a cover slip. The micoalge cells were first observed under 400X magnification and later under oil emulsion lens at 1000X magnification. Once the image was clear, a pulse of laser was shot to the cells by pressing the mercury lamp button for 5sec. The filters were adjusted to green excitation zone and a red emission zone to check for the presence of neutral lipids in the microalgae

cells under focus. Using the camera attached on the microscope, pictures of the microalgae cells under focus were taken with and without fluorescence.

3.2.7. Transesterification methods

3.2.7.1. Transesterification

500IU of lipase/g of olive oil was used for all transesterification experiments. The reaction mixture was maintained at 40°C (unless otherwise noted) and 120rpm in a shaker water bath for each time point.

In-situ transesterification of microalgae biomass was executed as per Tran and co-workers' protocol (2012) with slight deviations. In brief, 0.5g of freeze-dried microalgae biomass was mixed with 20ml of neat methanol and sonicated at 70 amplitude, for 20mins using a QSonica Q55 sonicator. After sonication, the methanol was evaporated by placing the containers in fume hood for 60mins. The subsequent oil-containing slurry was mixed with 5ml of neat *n*-hexane by vortexing for 5mins using a Fisherbrand™ Wizard™ Infrared vortex mixer. 500IU of lipase/g of microalgae oil was subsequently added to the mixture along with 5ml of methanol for the transesterification reaction and incubated at 40°C for 72h. To overcome the issue of solvent evaporation; each reaction was carried out in a sealed glass container.

After transesterification, the sample was centrifuged at 5,000**g* for 10mins and the solvent layer (top layer) containing FAME was pipetted carefully to a clean sealed glass container. FAMEs generated were later analyzed by TLC (Section 3.2.7.2) and GC (Section 3.2.7.3).

3.2.7.2. Thin Layer Chromotography

Initial analysis for FAME detection post transesterification reaction was carried out using TLC, as per Kim G.V. and colleagues (2014) with no deviations. Pre-coated TLC sheets ALUGRAM® SIL G/UV254 (0.20mm silica gel 60 with fluorescent indicator UV_{254}) were purchased from Macherey-Nagel. Briefly, 1µl of the sample was spotted onto the designated position on the TLC plate. A 90:10 (v/v) *n*-hexane: diethyl ether solvent mix was used as the mobile phase and after full development of TLC plate, the FAME spots were visualized using a 10% (v/v) ethanoic phosphomolybdic acid spray, followed by drying at 105°C for 5mins. The developed TLC plate image was captured using a Canon digital camera.

Via TLC, estimation of FAME(s) produced after transesterification reaction was done by visual inspection of staining intensity. No software or other quantification methods were used for the analysis of TLC plates.

3.2.7.3. Fatty Acid Methyl Ester Gas Chromatography

The GC method (Table 3.12) published by Agilent (David, Sandra and Vickers, 2005) was used for the analysis of FAME mixture (Appendix L) and the FAMEs generated after transesterification of olive oil (Section 3.2.7.1) and microalgae neutral lipids (Section 3.2.7.1). A Scion-436GC machine, with FID detector and GC column BR-SWax 0.25mmID*30m (Internal Diameter*Length); 0.25µm particle size from Bruker® (Cat# BR89377; Serial#1235841) was used for FAME analysis. FAMEs generated by transesterification reaction of olive oil and microalgae neutral lipids were identified by comparing their RT (Retention time) with RT of FAME mix. The same volume of FAME mix was injected 5 times using the same analytical method to understand the method variability.

Table 3.12: GC parameters used for the analysis of fatty ester composition in biodiesel.

Parameter	Set at
Inlet temperature	250°C
Injection volume	1µl
Split ratio	1:50
Carrier gas	Hydrogen
Head pressure	53 kPa constant pressure (36 cm/s at 50°C)
Oven temperature	50°C for 1min 25°C/min to 200°C 3°C/min to 230°C, hold 18mins
Detector temperature	280°C
Detector gases	Hydrogen: 40ml/min Air: 450ml/min Helium make-up gas: 30ml/min

3.2.7.4. Biodiesel yield

The yield of biodiesel generated after transesterification reaction of olive oil using lipase(s) was calculated as (Dianursanti, Religia and Wijanarko, 2015):

$$Yield\ of\ biodiesel\ (\%) = Mass\ of\ biodisel\ obtained \div mass\ of\ oil\ used$$

3.2.8. Statistical analysis

Data were analysed using analysis of variance. In all these cases, the analyses were conducted general linear model (Tukey test) in .xls files. The level of tested significance was at $p \leq 0.05$.

Chapter 4: Biodiscovery, screening and characterization of crude solvent stable lipases

4.1. INTRODUCTION AND OBJECTIVES

Enzymes found in nature have been used since ancient times in the production of food products and in the manufacture of commodities. Enzyme-catalysed reactions are highly efficient, selective, non polluting, and often low cost (Andualema and Gessesse, 2012). Microbial enzymes are more widely used than plant and animal enzymes (Borrelli and Trono, 2015). Among these enzymes, lipases are extensively studied due to their numerous applications (see Section 2.7). Soil is an excellent source of novel enzyme-producing strains because of the nutrient rich environment which supports the proliferation of microorganisms. The diversity of these microorganisms depends on nutrient availability, physicochemical properties of climate and the composition of the soil including elements such as texture, pH, temperature, solar irradiation, aeration, water content, mineral composition, etc. (Vieira and Nahas, 2005).

This chapter is focused on the isolation and identification of microbial strains from soil, which possess native solvent stability and, therefore, produce solvent stable lipase(s). The aims were:

- To isolate lipase producing microorganisms from purposefully obtained soil samples from sampled regions in the Wicklow Mountains, Co. Dublin and Co. Laois
- To isolate pure cultures of bacterial strains capable of growing aerobically on olive oil-Rhodamine B agar and to store them at −80°C for further analysis
- To identify the microorganisms showing the highest extracellular lipolytic activity
- To determine the solvent stability of the highest activity lipolytic strains
- To screen the solvent stability of the crude lipase(s) from the cell free supernatant fraction from solvent stable strains
- To evaluate the combined effect of temperature (28°C and 40°C) and methanol (20% v/v and 30% v/v) on the stability of crude lipase(s) (in form of cell free supernatant)
- To identify and classify the best performing, solvent stable strains by 16S rRNA sequencing.

4.2. RESULTS

4.2.1. Isolation of lipase producing strains

There was an observable difference in lipolytic activity and relative number of lipase producing colonies based on the conditions of isolation. Soil enriched at 37°C resulted in no observable lipase producing colonies. Therefore, this temperature was not considered for further experiments for lipase-producing strain isolation. Conversely, soil enriched at 28°C generated large numbers of lipase-producing colonies with intense fluorescence on Rhodamine B agar plates (see Table 4.1). A total of 36 lipase-producing colonies were selected from the seven soil samples. The criterion for selection was based on the intensity of fluorescence produced by the colonies on Rhodamine B plates. The lipases producing colonies were named as X-Y where "X" was the soil sample name and "Y" was the number of the lipase producing colony e.g. A1 was the 1st colony picked from soil sample named A.

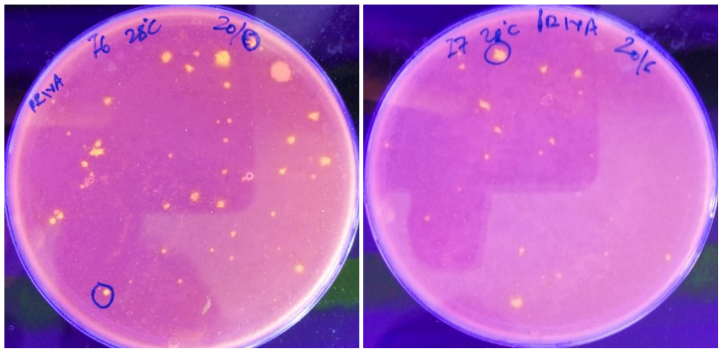

(a) (b)

Figure 4.1: UV illuminated olive oil-Rhodamine B agar plate with serially diluted 10^{-6} (a) and 10^{-7} (b) enriched soil media "I". Orange-pink fluorescence emitting colonies, confirming the presence of hydrolytic activity from these strains appeared after 2days of incubation at 28°C (Section 3.2.1.3).

Table 4.1: Location of soil sample and lipase producing colonies picked from the Rhodamine B agar plate after 2days of incubation at 28°C. Colonies were named based on the name of the soil sample.

Soil sample	Source of Isolation	Selected lipase producing colonies	Nomenclature
A	Co. Laois (Garage)	5	A1, A2, A3, A4, A5
B	Co. Laois (Garage)	4	B1, B2, B3, B4
C	Co. Laois (Garage)	5	C1, C2, C3, C4, C5
D	Wicklow Mountains	5	D1, D2, D3, D4, D5
E	Wicklow Mountains	3	E1, E2, E3
F	Wicklow Mountains	3	F1, F2, F3
G	Wicklow Mountains	3	G1, G2, G3
H	Wicklow Mountains	3	H1, H2, H3
I	Dublin City (Garage)	5	I1, I2, I3, I4, I5

These 36 lipase-producing colonies were sub-cultured on LB agar ten times to isolate pure-cultures (Figure 4.2). Pure cultures were later stored at -80°C in 40% (v/v) glycerol for long term storage.

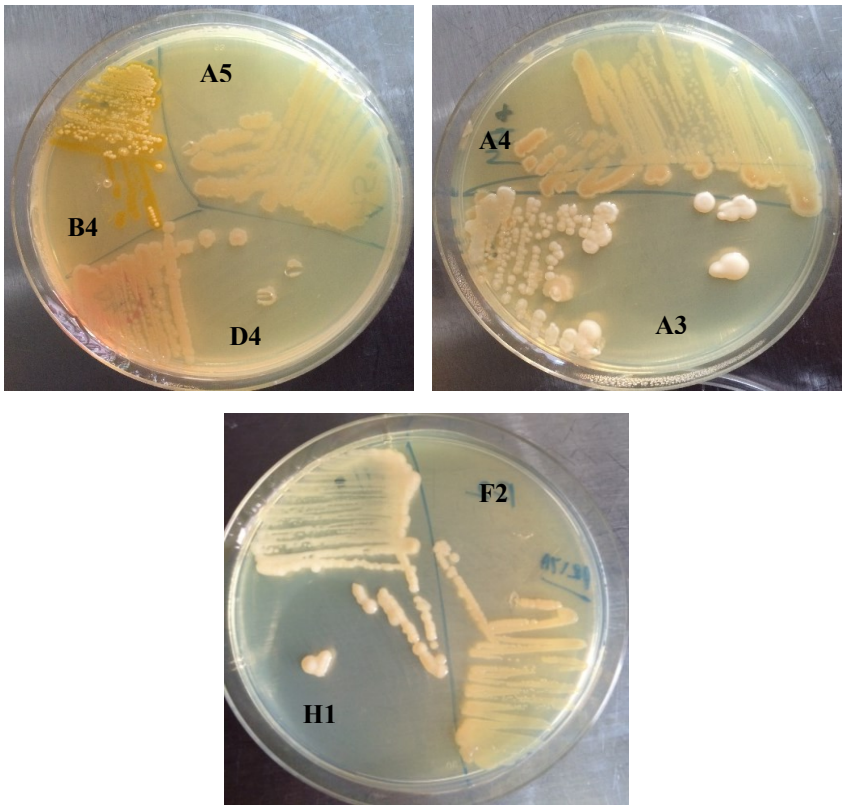

Figure 4.2: After the tenth sub-culture, pure cultures of lipase producing colonies were checked for their morphology on an LB agar. Pure cultures of B4, A5, D4, A4, A3, H1 and F2 strains with distinct morphologies are noted here.

4.2.2. Identification of superior lipolytic cultures

The lipolytic activity of the 36 isolated pure cultures was analysed in more detail. These isolates were grown in LB media overnight and the cell density was adjusted to an optical density of 0.6 at 600nm. 20µL of each culture was inoculated onto olive-oil Rhodamine B plates and was incubated overnight (16h) at 28°C. Strains producing fluorescence zones >1cm diameter were selected for further testing (see Figure 4.3).

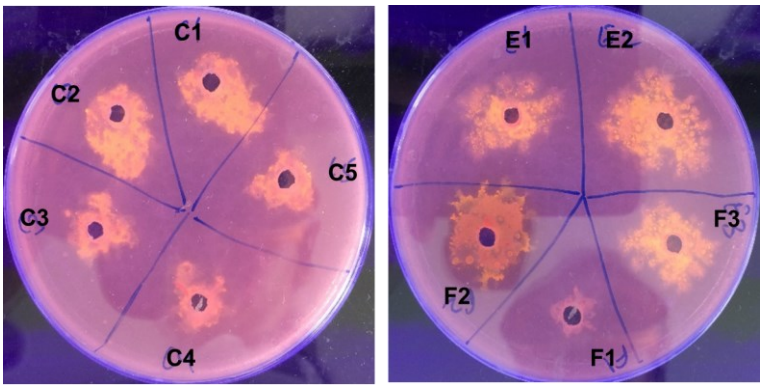

(a) (b)

Figure 4.3: UV-illuminated Rhodamine B plates containing overnight (16h) incubated cultures of different lipase producing strains. The difference in the size of fluorescence zones represents different amounts of lipase activity. As represented here strains C1 and C2 display a larger fluorescent zone compared to C3, C4 and C5 (a), indicating a higher lipase production. On plate (b) E2, E3, F2 showed higher lipase production when compared to F1.

Of the 36 lipase-producing strains, 25 cultures showed maximum fluorescence after UV-illumination (considered as >1cm fluorescence halo; Table 4.2). These 25 cultures were used for further investigation.

Table 4.2: Lipase producing colonies which displayed a >1cm diameter of fluorescence halo on Rhodamine B agar plate after 16h of incubation at 28°C.

Soil sample	Number of Lipase producing strains isolated	Significant lipase producing strains	Strains selected
A	5	4	A1, A2, A3, A4
B	4	2	B1, B2
C	5	3	C1, C2, C3
D	5	5	D1, D2, D3, D4, D5
E	3	2	E2, E3
F	3	2	F2, F3
G	3	1	G1
H	3	2	H1, H3
I	5	4	I2, I3, I4, I5

4.2.3. Solvent stable cultures

Isolates with the greatest lipase activity were tested for their stability in organic solvents by the plate overlay method (Section 3.2.1.10). Their organic solvent stability was tested against diethyl ether, ethyl acetate, toluene, cyclohexane, *n*-hexane, heptane, *t*-butanol, isopropanol, ethanol and methanol as described in Section 3.2.1.10. After overnight incubation, the plates were checked for the presence of any visible bacterial growth on the location in which they were inoculated. No colonies were observed in diethyl ether, ethyl acetate, toluene, *t*-butanol and isopropanol. However,

eight lipase-producing cultures were observed post-incubation in cyclohexane; 15 following incubation in neat *n*-hexane and heptane; 18 following incubation in 20% (v/v) methanol and 20% (v/v) ethanol (see Table 4.3). The presence of growth on solvent-treated LB agar plates was considered as a proxy for solvent stability of that culture against that organic solvent.

Table 4.3: A data set representing the solvent stable lipase producing colonies in respective percentage of solvent by plate overlay method, categorised by hydrophobicity.

Solvent nature	Solvent	Log P	% (v/v)	Isolates stable	Cultures
Non-polar/ Hydrophobic	Diethyl ether	0.85	100	0	-
	Ethyl acetate	0.68	100	0	-
	Toluene	2.5	100	0	-
	Cyclohexane	3.2	100	8	A1, A2, A3, D1, D5, H1, H3, I3
	n-Hexane	3.5	100	15	A1, A2, A3, C3, D1, D2, D3, D4, D5, E2, E3, F2, H1, H3, I3
	Heptane	4.0	100	15	A1, A2, A3, C3, D1, D2, D3, D4, D5, E2, E3, F2, H1, H3, I3
Polar/ hydrophilic	*t*-butanol	0.58	50	0	-
	Isopropanol	0.54	50	0	-
	Ethanol	-0.18	20	18	A1, A2, A3, A4, B1, B2, C3, D1, D2, D3, D4, D5, F2, F3, G1, H1, H3, I3
	Methanol	-0.81	20	18	A1, A2, A3, A4, B1, B2, C3, D1, D2, D3, D4, D5, F2, F3, G1, H1, H3, I3

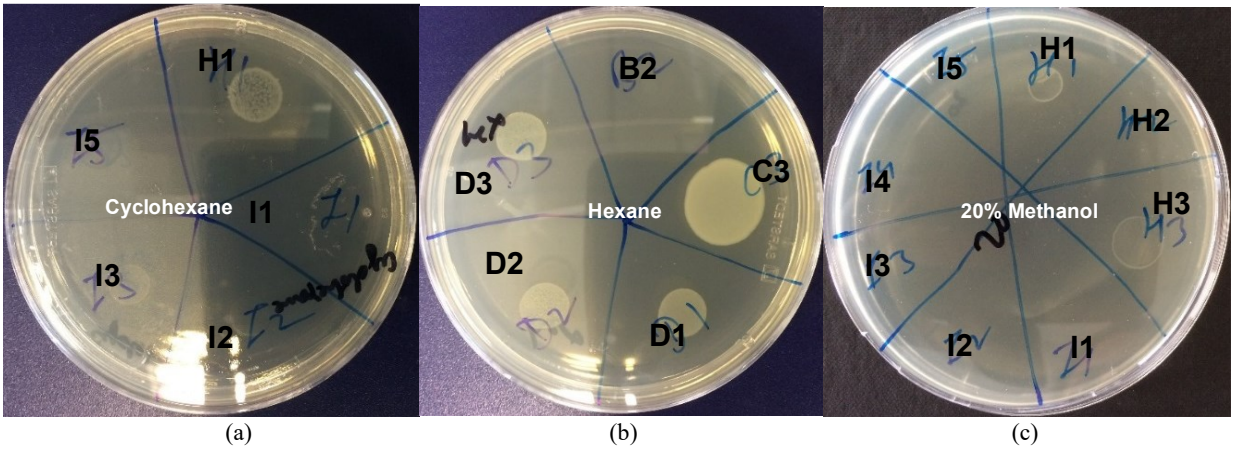

(a) (b) (c)

Figure 4.4: Lipase producing strains on LB agar plates treated with (a) 100% cyclohexane for 6h at 28°C, H1 and I3 showed stability towards cyclohexane as compared to I5, I2 and I1. (b) 100% *n*-hexane for 6h at 28°C, except B2; C3, D1, D2, D3 were stable. Plate (c) 20% (v/v) methanol for 6h at 28°C, only H1 and H3 showed stability amongst the other lipase producing strains incubated on the solvent- treated LB agar plate. The presence of growth indicated stability of the strain towards the organic solvent.

Of the 25 lipase-producing strains, 8 showed stability against multiple organic solvents i.e. against *n*-hexane, heptane, cyclohexane, methanol and ethanol. Since solvent stability of a bacterial culture is dependent on many parameters (Section 2.5.1.1), in this study it was important to identify whether the culture was stable in multiple organic solvents and that it produces lipases that are also stable in these organic solvents (explored in Section 4.2.4).

4.2.4. Presence of solvent stable lipases

Eight strains (A1, A2, A3, D1, D5, H1, H3, I3) that were stable in multiple organic solvents (cyclohexane, *n*-hexane, heptane, 20% v/v Ethanol and 20% v/v Methanol; Section 4.2.3) were investigated for the presence of extracellular, solvent stable, secreted lipases within a crude sample matrix. Cell free supernatants of cultures grown overnight in LB medium were spot inoculated onto olive-oil-Rhodamine B agar plates and were subsequently tested for their solvent stability by the plate-overlay assay method (Section 3.2.1.10). After overnight incubation, the plates were illuminated under a UV light source and the presence of solvent stable lipase was confirmed by the presence of pink-orange fluorescence.

The cell free supernatant of overnight grown cultures was also incubated with 50% (v/v) of organic solvents (*n*-hexane, heptane, cyclohexane, diethyl ether, isopropanol, toluene, ethyl acetate, ethanol and methanol) for 24h at 28°C under continuous shaking. Each treated crude sample was subsequently added to an olive-oil Rhodamine B plate and incubated at 28°C for 16h to check for the presence of any orange-pink fluorescence. Crude lipase/cell free supernatants of A1, A2, A3, D1, D5, H1, H3 were found to be stable in 50% (v/v) of *n*-hexane, cyclohexane and heptane (Table 4.4). No lipase activity was observed in 50% (v/v) methanol and ethanol.

Comparing the data for solvent stable cultures and solvent stable lipase(s) we found that cultures that were stable in cyclohexane, produced lipase(s) that were stable in cyclohexane. Similar observations were noted for n-hexane and heptane. No lipase producing culture was stable in diethyl ether, ethyl acetate, toluene, t-butanol, isopropanol; no cell free supernatant (crude lipase) was observed to be active in 50% (v/v) of these solvents.

Table 4.4: A data set representing the cell free supernatants found to be stable in various levels of solvent by plate overlay and incubation method, categorised by hydrophobicity.

Nature of Solvent	Solvent	% (v/v)	Isolates stable	Stable Cell free supernatant (crude lipase)
Non-Polar/ Hydrophobic	Diethyl ether	50	0	-
	Ethyl acetate	50	0	-
	Toluene	50	0	-
	Cyclohexane	50	8	A1, A2, A3, D1, D5, H1, H3, I3
	n-Hexane	50	15	A1, A2, A3, C3, D1, D2, D3, D4, D5, E2, E3, F2, H1, H3, I3
	Heptane	50	15	A1, A2, A3, C3, D1, D2, D3, D4, D5, E2, E3, F2, H1, H3, I3
Polar/ Hydrophilic	*t*-butanol	50	0	-
	Isopropanol	50	0	-
	Ethanol	50	0	-
	Methanol	50	0	-

For methanol and ethanol, 50% (v/v) concentration was investigated, though 18 cultures were stable in 20% (v/v) methanol and ethanol, no cell free supernatant was observed to be stable in 50% (v/v) methanol and ethanol. Porcine pancreas treated with and without 50% (v/v) of these organic solvents was used as a negative and positive control respectively. Figure 4.5 shows the lipase activity of cell free supernatants when treated with selected undiluted organic solvent (except 50% (v/v) methanol and ethanol) via plate overlay method for 24h at 28°C.

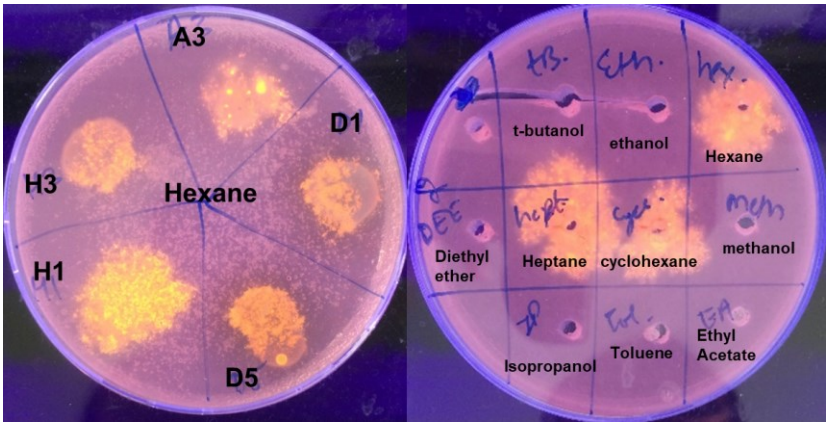

(a) (b)

Figure 4.5: UV-illumitaed Rhodamine B agar plates (a) cell free supernatant of cultures treated with *n*-hexane by plate over lay method; (b) cell free supernatants of cultures treated with 50% (v/v) organic solvents for 24h at 28°C. Presence of fluorescene in (a) and (b) indicates stability of crude lipases towards *n*-hexane, heptane and cyclohexane.

4.2.5. Effect of methanol on crude lipases

Cell free supernatant from cultures grown in basal lipase producing media at 28°C for 72h at 200rpm was used to investigate the effect of methanol on the activity of crude extracellular lipase(s). Eight strains which showed stability in multiple solvents were examined to characterise the effect of 20% (v/v) and 30% (v/v) methanol on lipolytic activity after 24h of incubation at 28°C via *p*-NPP spectrophometric assay (Figure 4.6).

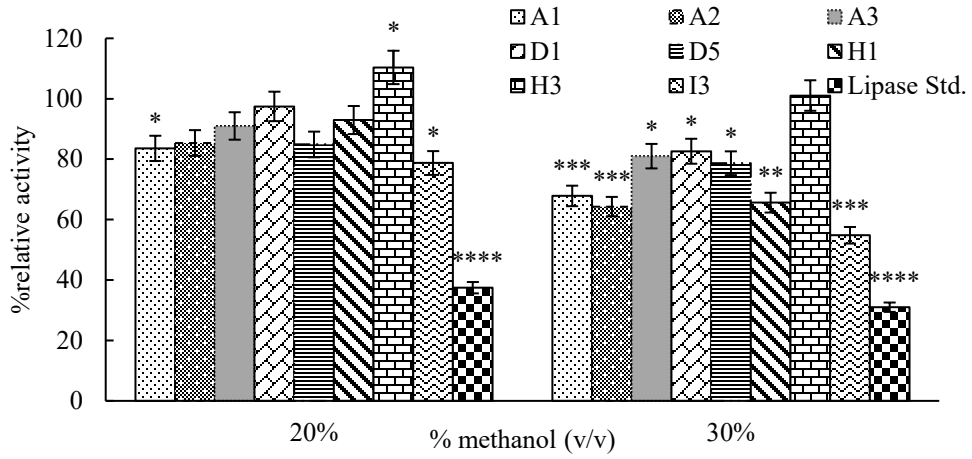

Figure 4.6: The relative activity of extracellular crude lipases when treated with 20%(v/v) and 30%(v/v) methanol for 24h at 28°C, as compared to the same samples in the absence of methanol. 30mg/mL of porcine pancreas lipase (Sigma) was used as a positive control (noted as Lipase Std. in the graph), while basal lipase producing media was used as a negative control. The assay was performed in triplicate using *p*-NPP as substrate and relative activity was calculated by comparing the activity of lipase in 20% (v/v) and 30% (v/v) methanol to crude sample with no methanol at 28°C. Data represented here are the mean of three independent experiments with error bars indicating standard deviation. (****, ***, **, * represents significant changes in activity where **** p< 0.0001; ***p = 0.0001 to 0.001; **p=0.001 to 0.01, *p=0.01 to 0.05 by t-test).

The greatest stability in 20% (v/v) and 30% (v/v) methanol was exhibited by H3. Conversely, I3 displayed the lowest stability in both 20% (v/v) and 30% (v/v) methanol. D1 and H1 showed comparable stability in 20% (v/v) methanol, H1 was less stable than D1 in 30% (v/v) methanol. Only A3, D1, D5, H1 and H3 showed >60% relative activity in the presence of 30% (v/v) methanol, and therefore, were chosen for further study (Section 3.3.6). Significant loss of activity ($p \leq 0.05$, t-test) was observed in A1, I3 and standard lipase (control) with 20% (v/v) methanol. H3, by contrast, showed a significant increase in activity ($p \leq 0.05$, t-test) in 20% (v/v) methanol. With 30% (v/v) methanol, all cell free supernatants, except H3 and standard lipase (control) showed a significant loss of lipolytic activity ($p \leq 0.05$, t-test).

4.2.6. Combined effect of methanol and temperature on crude lipases:

Cell free supernatants from selected cultures (A3, D1, D5, H1 and H3) grown in basal lipase producing media for 72h at 28°C were harvested. The harvested cell free supernatants were further incubated at 28°C and 40°C in the presence of 30% (v/v) methanol. The relative activity of extracellular crude lipase in the presence of methanol after 24h of incubation at both 28°C and 40°C was estimated (Figure 4.7) in comparison to crude lipase without methanol.

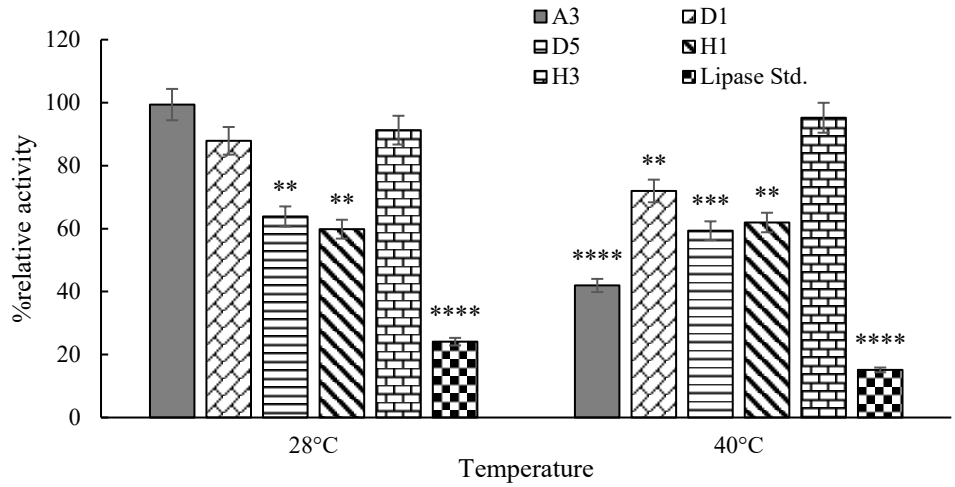

Figure 4.7: The relative activity of extracellular crude lipase when treated with 30% (v/v) methanol for 24h at 28°C and 40°C. 30mg/mL of porcine pancreas lipase (Sigma) was used as a positive control (noted as Lipase std. in the graph), while basal lipase producing media was used as a negative control. The assay (Section 3.2.3.3) was performed in triplicate using *p*-NPP as substrate and relative activity was measured by comparing the activity of lipase in 30% (v/v) methanol to crude sample with no methanol at 28°C and 40°C respectively. The average of relative value (n=3) and error bars are shown. (****, ***, **, * represents significant changes in activity when **** $p < 0.0001$; ***$p = 0.0001$ to 0.001; **$p=0.001$ to 0.01, *$p=0.01$ to 0.05 by t-test).

Significant loss of activity ($p \leq 0.05$, t-test) was observed for D5, H1 and standard lipase in 30%(v/v) methanol at both 28°C and 40°C. H3, however, showed no significant loss in activity at both incubation temperatures. A3 and D1 were stable at 28°C, however at 40°C a significant loss of activity was seen ($p \leq 0.05$, t-test).

4.2.7. 16S rRNA sequencing

Five solvent stable lipase-producing cultures (A3, D1, D5, H1 and H3) were sequenced by 16S rRNA sequencing by Eurofins Germany. The sequences (Appendix A) were compared to those in NCBI database by nBLAST. The sequencing data revealed A3 as a *Pseudomonas sp.* BIM B-86,

D1 as a *Sphingomonas* sp., D5 as *Listeria monocytogenes*, H1 as *Pseudomonas reinekei* and H3 as *Pseudomonas brenneri* (see Figure 4.8)

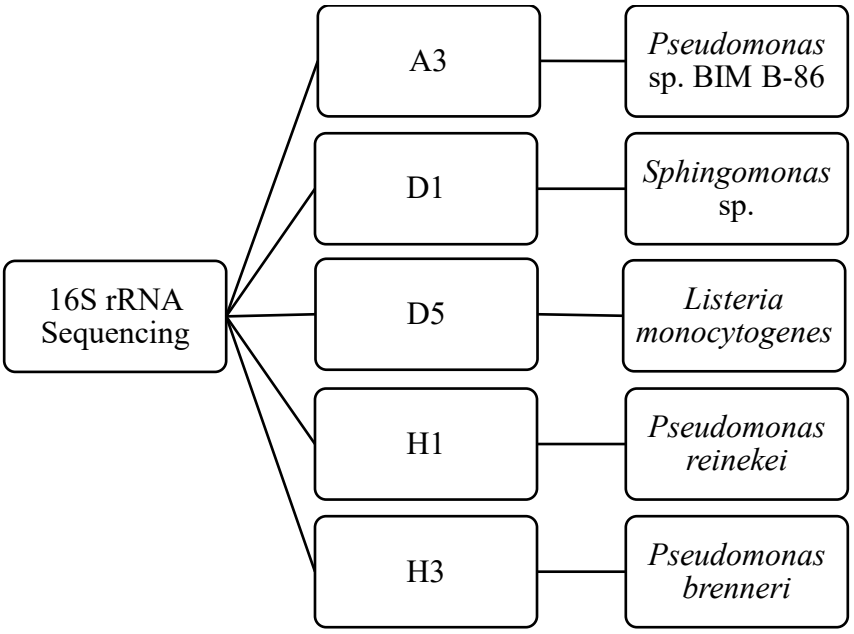

Figure 4.8: 16S rRNA sequencing obtained from Eurofins Germany revealed 99% homology of A3 with 16S rRNA of *Pseudomonas* sp. BIM B-86; 84% homology of D1 with *Sphingomonas* sp. PP-2; 99% homology of D5 with *Listeria monocytogenes* strain J1926; 99% homology of H1 with *P.reinekei* SN8; 98% homology of H3 with *P.brenneri*.

4.3.DISCUSSION

4.3.1. Biodiscovery of lipase producing strains

Soil contains phylogenetically diverse groups of bacteria that are globally distributed and abundant. With the help of selective and non-selective culture media, various soil microorganisms were isolated. The composition of the bacterial community isolated from a soil sample depends on the interaction between soil type, plant species and its rhizosphere localization (Davis *et al.*, 2005). In this research, a selective-media screening approach was used for the isolation and enrichment of lipase producing microbes from soil samples collected in the Leinster region of Ireland. Lipid substrates are necessary for production of lipase from microorganisms and the addition of a lipid as the sole carbon source can enhance the selective growth of lipase producing microorganisms in a selective media (Mo *et al.*, 2016).

In this research, soil samples from the Wicklow mountains, Dublin City and Co. Laois were cultured using soil enrichment media containing olive oil as the primary carbon source to aid the isolation of lipase producing microorganisms. Two different temperatures, 28°C and 37°C, were screened to achieve the maximum colony forming units (CFU) on olive-oil Rhodamine B agar plates (see section 3.2.1.3). The number of lipase producing CFUs depended on the soil type, time and temperature of incubation. Irrespective of the enrichment time, no lipase producing colonies were observed in soil samples enriched at 37°C. Since all the soil samples were collected from temperate environment, 37°C is probably too harsh for the lipase producing cultures. Soil based microbes are better adapted to temperatures in the regions where the soils were collected; the majority of soil microorganisms are mesophilic with maximal growth temperatures between 25-35°C (Davis *et al.*, 2005). 24h incubation was not sufficient for enrichment at 28°C; and resulted in fewer CFUs; however, a significant number of lipase producing colonies were observed in soil enriched for 72h at 28°C.

Soil organisms include spore-forming, Gram-negative bacteria, actinomycetes and fungi, but only a small percentage of these microbes are culturable (Hasan, Shah and Hameed, 2006). Many groups of soil microbes cannot be easily isolated due to their inability to grow in the laboratory. By extending the incubation periods, the number of colonies formed can be enhanced; increasing the chances of isolating microbes which are rarely studied (Davis *et al.*, 2005). This suggests that the number of lipase producing colonies in 72h enrichment should be higher than at 24h, which is what was observed in this study. In this research, only enriched soil samples from a 28°C, 72h incubation were used for the isolation of lipase producing colonies.

At lower dilutions, high number of CFUs were observed and at higher dilutions lower number of CFU's were seen. Typically, supernatants from soil samples resulted in $2\text{-}5\times10^{6}$ CFU at 10^{-1} to 10^{-7} dilutions; however, the number decreased to 10-20 CFU for 10^{-10} and 10^{-11} dilutions. The source of soil, sampling process and sample preparation can affect the results obtained. For example, soil sample "I" which was collected from the surface and cracks of oil tanks; resulted in lower CFU (5-10) at 10^{-1} to 10^{-7} dilutions. In contrast soil samples "A-H" which were collected by digging soil showed higher CFUs (section 3.2.1.8, 3.2.1.9). Therefore, olive oil-Rhodamine B plates with 10^{-10} and 10^{-11} dilutions were employed for soil samples "A-H"; whilst 10^{-1} to 10^{-7} dilutions were used for soil sample "I" during the isolation of lipase producing colonies. A total of 36 lipase producing

colonies were selected based on the observed intensity on olive oil-Rhodamine B agar plates (Table 4.1); higher intensity correlated with higher lipolytic activity (Rabbani *et al.*, 2013).

Several limitations should be taken in account with respect to the 36 lipase producing isolates obtained in this initial biodiscovery work-package. First, it is possible that some of isolates were duplicates because the same microorganisms could be present in the soil samples. A repeated sub-culturing of the isolated lipase producing colonies allows generation of pure cultures and in determination of morphological similarities, if any. Pure cultures of all the 36 lipase producing strains revealed different morphologies on LB agar plates (Figure 4.2). Though cellular and colonial morphologies of many microorganisms change at different stages of growth (Jones *et al.*, 1982), all the 36 lipase producing strains were considered different based on the morphology during 10^{th} subculture (Figure 4.2). For long-term storage, all the 36 lipolytic strains were stored in 40% (v/v) glycerol at -80°C.

4.3.2. Identification of superior lipolytic cultures

As the production cost of lipases is a major obstacle to widespread commercialization, this research focused on the isolation of microbes that produced lipases with enhanced lipolytic activity in basic growth media. All 36 isolated strains obtained as a pure culture were analysed in detail to select the most prolific lipolytic strains (i.e. producing high quantity of lipase). Microbial lipases are mostly extracellular, and it is known that lipids can modulate the expression of lipolytic genes in many microorganisms (Zarevúcka, 2012). Therefore, to execute a cost effective, positive screening approach, olive-oil Rhodamine B agar plates were used to reflect the lipolytic activity of the 36 isolated microbial strains. Lipases produced by any microbial strain on olive-oil Rhodamine B plate create an orange fluorescent halo (zone) upon UV irradiation (Kouker and Jaeger, 1987). The complex formed between Rhodamine B and partially hydrolysed olive oil (mono- and di-glycerides) is responsible for the generation of pink-orange halos (Kumar *et al.*, 2012). There is a direct relationship between the diameter of fluorescent halo and quantity of lipase secreted by a culture (Lomolino, Di Pierro and Lante, 2012), provided the culturing conditions are the same and the number of microbial cells remain reasonably constant for comparison. In this research the number of microbial cells for each lipase producing colony was constant (20µL of 0.6 O. D_{600}); and, therefore, larger halos correlate to higher lipolytic activity. The diameter of the orange

fluorescence halos generated on the Rhodamine B plates can be used as an index for lipolytic activity (Rabbani *et al.*, 2013). Twenty-five lipase producing colonies with fluorescent halos >1cm diameter were considered, qualitatively, as the most lipolytic colonies amongst the total of 36 lipase producing isolates. Using olive-oil Rhodamine B agar plates to estimate the lipolytic activity of a microbial strain is a convenient approach that has reduced susceptibility to compounds which can cause background interference (Gilham and Lehner, 2005). In this research, many colonies were screened simultaneously, and the method can be used as an alternative to other high-throughput methods (such as a microplate-based fluorescent lipase assay). Another advantage of the plate assay developed in this study included the determination of lipolytic activity even in the presence of insoluble compounds that produced turbidity or caused measurement interference for the UV-spectrophotometer and fluorimeter (Lomolino, Di Pierro and Lante, 2012).

4.3.3. Solvent stable cultures

The solvent stability of a microorganism can be tested by growing the microorganism in either liquid or solid media exposed to the solvent(s) of choice. The plate overlay method is a convenient approach commonly used for microbial solvent stability determination using solid media. The presence of microbial growth after incubation in organic solvent confirms the solvent stability of that microbe in the respective solvent. Since the log P of a solvent determines the toxicity of the solvent towards a microbe, solvents with lower log P will generally have greater detrimental effect (see Section 2.6; (Segura *et al.*, 2012). Therefore, 25 of the most lipolytic cultures (Section 4.3.2) were exposed to different solvents of varying log P values (ranging from -0.81 to 4.0) to determine their solvent stability. In this research, an incubation time of 6h in the respective solvent was considered sufficient to challenge the microbial colonies. This aligned with previous research detailed by Lazaroaire (2009) where 6h of solvent treatment was sufficient to identify solvent stability in *Pseudomonas aeruginosa* in the presence of *n*-hexane, *n*-heptane, styrene, xylene isomers and ethylbenzene (Lazaroaie, 2009). Diethyl ether, ethyl acetate, toluene, *n*-hexane, heptane and cyclohexane are hydrophobic solvents, hence were not diluted with water. However, *t*-butanol, isopropanol, methanol and ethanol are water soluble, and were used in lower concentrations (50% v/v and 20% v/v respectively) to check microbial solvent stability. No culture grew in undiluted diethyl ether, ethyl acetate, toluene, *t*-butanol and isopropanol. However, eight

were found to be stable in low % (v/v) methanol, ethanol, *n*-hexane, heptane and cyclohexane. Methanol and ethanol are considered harsher solvents based on their log P value (-0.81 and -0.18 respectively); the stability of 18 lipolytic colonies in these solvents could be due to lower (20% v/v) concentrations of methanol and ethanol. Solvents like cyclohexane and *n*-hexane have very similar log P, with 8 cultures displaying activity after incubation in these solvents. The toxicity of a given organic solvent depends not only on its physicochemical properties but also on the specific response of the cells (Segura *et al.*, 2008). Since microbes follow different modes of survival in presence of solvents (Section 3.5.1.1)**,** cellular response is not the same in all strains.

The solvents used for the current screening were selected based on the proposed application of lipase(s) in biodiesel production from waste-water culture algae. Biodiesel has been successfully synthesized by using different acyl acceptors; ethyl acetate (Mukesh *et al.*, 2007), methanol (L. Li *et al.*, 2014; Sahoo, Subudhi and Kumar, 2014; Dror *et al.*, 2015; Huang *et al.*, 2015; Lotti *et al.*, 2015; Cao *et al.*, 2017) and ethanol (Huang *et al.*, 2015). Other than biodiesel synthesis, these solvents have also been used in other applications. Flavouring and fragrance agents; such as geranyl acetate, have been produced in a *n*-hexane solvent system (Bartling *et al.*, 2001). Isopropanol has been used for the synthesis of fragrance fatty acid esters in the presence of *n*-hexane (Verma, Azmi and Kanwar, 2011). Resolution of (RS)-Phenylethylamine was executed in the presence of ethyl acetate (Pilissao, De and Da, 2010). Likewise *n*-heptane has been used for the kinetic resolution of lactic acid esters (Richard *et al.*, 2013). Transesterification of phospholipids for the production of structured lipids was successfully demonstrated in the presence of *n*-hexane, diethyl ether and methanol (Kim and Yoon, 2014). The eight lipolytic cultures (A1, A2, A3, D1, D5, H1, H3 and I3) which were stable in multiple solvents (methanol, ethanol, *n*-hexane, heptane and cyclohexane) suggested many potential applications for the corresponding solvent stable lipase(s) that might be stable in the same solvents.

4.3.4. Presence of solvent stable lipase(s)

It is hypothesized that extremophiles produce enzymes that are tolerant to extreme conditions (Ahmed, Raghavendra and Madamwar, 2010b). Based on this hypothesis, it was expected that the eight lipolytic cultures (A1, A2, A3, D1, D5, H1, H3 and I3) stable in *n*-hexane, cyclohexane, heptane, methanol and ethanol (see Section 3.3.3) should also produce solvent stable enzymes.

Microbial lipases are mostly extracellular; therefore, the cell free supernatant was utilised as a crude lipase containing source to investigate for the presence of solvent stable lipase in the 8 solvent stable cultures (Section 4.2.4). Most of solvent stable lipases isolated to date have originated from *Pseudomonas* and *Bacillus* sp. (Rahman *et al.*, 2010).

In this study, the cell free supernatants (crude lipase containing matrix) from the solvent stable cultures indicated the presence of solvent stable lipase(s). After 6h of incubation by the plate overlay method, all supernatants presented fluorescent orange-pink halos on olive-oil Rhodamine B plate, confirming the presence of solvent stable lipases. However, a 24h incubation of the cell free supernatants showed activity only in *n*-hexane, heptane and cyclohexane. The longer incubation played an important role in the loss of lipase activity for methanol and ethanol treated cell free supernatants. Also, the activity loss of crude lipase samples in methanol and ethanol treated samples may be below the detection limit of olive oil-Rhodamine B plates (Lomolino, Di Pierro and Lante, 2012), because of which no lipolytic activity was observed.

4.3.5. Effect of methanol

Enzyme catalysed transesterification reactions (e.g. biofuel production) require the presence of an acyl acceptor (i.e. methanol or ethanol); however, methanol is almost universally used due to its high reactivity and low cost. Therefore, a key element of this research was to characterise the methanol stability of the lipases from Section 4.2.4. Furthermore, methanol is a solvent with applications beyond lipid transesterification; it can be used in a variety of reactions including preparation of food emulsifiers, cosmetic products, flavour and pharmaceuticals (see Section 2.7).

In this study, methanol concentrations of 20%(v/v) and 30%(v/v) were used to estimate the loss of lipolytic activity in the cell free supernatant crude lipase containing matrix of the eight solvent stable cultures (A1, A2, A3, D1, D5, H1, H3, I3). Only A3, D1, D5 and H3 showed a relative activity of >80% in 30%(v/v) methanol; however, all cell free supernatants had >80% relative activity in 20%(v/v) methanol. Crude lipase from A2, A3, D1, D5 and H1 showed significant loss of activity ($p \leq 0.05$, t-test) when 30%(v/v) methanol was used instead of 20%(v/v). The significant loss in lipolytic activity of A2, A3, D1, D5 and H1 in 30%(v/v) makes the crude lipase(s) unsuitable for usage in 30%(v/v) methanol.

The effect of methanol on lipases varies, it can be responsible for loss of activity by competitive inhibition, by stripping of essential water molecules from the enzyme surface or by causing enzyme aggregation due to conformational changes (Lotti *et al.*, 2015). In lower concentrations, according to molecular dynamics simulations, methanol causes disruption of intra-protein hydrophobic interactions by adsorption of alcohol molecules on hydrophobic sites on protein surface. The formation of hydrogen bonds between methanol and the active site serine residue can also be responsible for the denaturation or loss of lipase activity (C. Li *et al.*, 2010). Significant loss of lipolytic activity ($p \leq 0.05$, t-test) in crude lipase of A1, I3 irrespective of the methanol concentration is likely to be due to one, or many of these reasons. Although, methanol can cause irreversible deactivation by unfolding and denaturing lipase(s); lipases from *Pseudomonas*/*Burkholderia* genera are considered to be highly tolerant to methanol (Lotti *et al.*, 2015). Of all the eight lipolytic cultures tested, H3 showed no significant loss in activity ($p > 0.05$, t-test) in either 20% or 30%(v/v). Since lipolytic activity loss for H3 crude lipase in methanol was minimal, it was possible that H3 belongs to either *Pseudomonas* or *Burkholderia* sp; which was later confirmed by 16S rRNA sequencing (section 4.2.7).

4.3.6. Combined effect of methanol and temperature

Lipase catalysed biofuel production involves the utilisation of solvents; hydrophilic, (primarily methanol), or a hydrophobic, to enhance oil solubility at temperatures less than or equal to 60°C (Heitz *et al.*, 2016). Transesterification reactions involve interaction of one mole of triacylglycerol with three moles of alcohol. But to achieve maximum biodiesel production, a higher molar ratio of alcohol is used (Musa, 2016). This molar ratio depends on the type of feedstock (oil), form of catalyst (free or immobilised), temperature, and reaction time (batch mode or continuous; (Taher *et al.*, 2011). Transesterification is rarely influenced by temperature fluctuations as long as it remains between 20-70°C with 30-40°C being most favourable (Ghaly *et al.*, 2010). Since a molar ratio of 1:4 for oil and methanol generates a near boiling point of 55°C (Kumari *et al.*, 2009), temperatures above 55°C with this molar ratio are not frequently used. The optimum temperature for transesterification reaction, therefore, depends on enzyme stability, molar ratio of alcohol and oil, and acyl acceptor (Antczak *et al.*, 2009). Since, A3, D1, D5, H1 and H3 produce methanol stable crude extracellular lipase(s) at 28°C, it was important to determine the combined effect of

temperature and methanol. Therefore, two different temperatures (28°C and 40°C) were combined with 30% (v/v) methanol treated crude lipase(s).

Temperature played a major role in lipolytic activity of the crude lipase(s) for A3, D1, D5 and H1. A significant loss in lipolytic activity ($p \leq 0.05$, t-test) was observed for these crude lipase(s) with a temperature increase from 28°C to 40°C. Conversely, crude lipase from H3 showed no significant loss in lipolytic activity ($p > 0.05$, t-test) with an increase in temperature to 40°C. Since the stability and activity of a lipase depends on the external environmental conditions (i.e. pH, presence of ions, detergents; (Zarinviarsagh, Ebrahimipour and Sadeghi, 2017); and in a crude lipase matrix the factors that could be responsible for maintaining or affecting the stability of lipase(s) cannot be identified. The presence of lipids/ions in the crude cell free supernatant matrix might have contributed to stability of the H3 crude lipase (Miller and Smith, 1973; Kordel *et al.*, 1991). The loss of activity at 40°C in 30% (v/v); for A3, D1, D5 and H1 crude lipase(s), could be due to temperature alone, the combined effect of temperature and methanol or due to degradation of compounds responsible for lipase stability. Since, no deviations were observed in the positive and negative controls; unidentified sample parameters (colour, turbidity, metal ions, presence of other compounds in crude lipase etc.) could be responsible for the loss, or gain, of lipolytic activity.

Though increased temperature can speed up enzyme catalysed reactions (Kumari *et al.*, 2009), a maximum optimum catalytic temperature should not be surpassed. Transesterification using *Candida antarctica* lipase in the presence of methanol showed an optimum temperature of 40°C; above this temperature an overall decrease in biodiesel yield was observed (Jeong and Park, 2008). Similarly, for *Rhizopus chinensis* lipase optimal temperature of 30°C was required for transesterification reaction in presence of methanol (Qin *et al.*, 2008). Transesterification using *Pseudomonas cepacia* lipase, with butanol as acyl acceptor, required an optimal temperature of 50°C for 1h which dropped to 40°C after 2h (Salis *et al.*, 2005). It is important to note that thermostability and solvent stability of a lipase can be increased by immobilization (Mateo *et al.*, 2007). As all five solvent stable cultures (A3, D1, D5, H1 and H3) showed positive results on solvent treated olive-oil Rhodamine B agar plates (Section 4.2.4) and had >60% lipolytic activity in 30% (v/v) methanol at 40°C (expect A3) (Figure 4.7); their thermo/solvent stability could be enhanced by immobilization; further enhancing their potential application as catalysts for biodiesel synthesis.

4.3.7. 16S rRNA sequencing

Traditional identification of microbes on the basis of their phenotypic characteristics is generally not as accurate as their identification by genotypic methods. In recent years, taxonomic classification on novel microbial strains has focussed on the use of 16S rRNA as it is present in in all bacteria; its function has not varied with time and the 16S rRNA gene (~1500 bp) is large enough for taxonomic studies (Patel, 2001). 23S rRNA on the other hand is excessively conserved and 5S rRNA is too small for research purposes (Novik, Savich and Kiseleva, 2015). Since the 16S rRNA gene sequence within a species is common; comparison of 16S rRNA gene sequence can better identify poorly described, rarely isolated, or phenotypically aberrant strains, leading to the recognition of non-cultured and novel bacterial strains. Despite its accuracy, 16S rRNA gene sequence analysis lacks widespread use because of technical and cost considerations (Clarridge and Alerts, 2004).

In this study, the 16S rRNA analysis performed on the five (A3, D1, D5, H1 and H3) solvent stable lipolytic strains classified them as members of *Pseudomonas* and *Listeria* genus. The genus *Pseudomonas* includes flagellated Gram negative, non-spore forming aerobic rods. As a result of their metabolic diversity, ease of culture and availability of genome sequences, the *Pseudomonads* attract attention for industrial and environmental biocatalysts (Kim and Gadd, 2008). The genomes of several members of the *Pseudomonads* have been sequenced (and are openly available.; e.g. www.genomesonline.org and www.pseudomonas.com), and studies have explained specific aspects of their genomes, physiology and behaviour under various stresses (e.g., www.psysmo.org, http://www.probactys.org, www.kluyvercentre.nl; (Puchałka *et al.*, 2008) and these have been used to categorise the isolates identified in this study. Conversely*, Listeria monocytogenes* is a Gram-positive bacterium and can grow at temperatures as low as 0°C. *Listeria monocytogenes* is an increasingly prevalent pathogen involved more frequently in severe illnesses and outbreaks of food-borne infections. It is interesting to observe that it is solvent stable and produces a solvent stable lipase. Lipases are an important virulence factors in *Listeria monocytogenes* and are responsible for listeriosis by pore formation and invasion (Alina Maria, 2014).

4.4.CONCLUSION

Five lipolytic organisms (A3, D1, D5, H1 and H3) were identified as potential strains for biodiesel production based on their multiple solvent stability characteristics (methanol, ethanol, *n*-hexane, heptane and cyclohexane). Of the five strains, three belong to the *Pseudomonas* genus, which is of great interest for many biotechnological applications (Silby *et al.*, 2011). H1 and H3 identified as *Pseudomonas reinekei* and *Pseudomonas brenneri* respectively, are novel bacterial strains in terms of lipases. Hence, isolation and characterisation of solvent stable lipase(s) from these strains was of significant interest in terms of novelty and potential industrial application.

Chapter 5: Lipase production, purification and characterization from *P. reinekei* (H1) and *P. brenneri* (H3)

5.1. INTRODUCTION AND OBJECTIVES

Pseudomonas is one of the most studied species of bacteria (Novik, Savich and Kiseleva, 2015). They are gram-negative, aerobic, motile, rod-shaped, polar-flagellated and non-spore forming bacteria; however, some *Pseudomonas* sp. (e.g. *P. stutzeri, P. mendocina*) have shorter lateral flagella (Lalucat *et al.*, 2006), whilst others form pili (Shen *et al.*, 2006). *Pseudomonas* sp. display remarkable metabolic and physiologic versatility, enabling them to colonize a wide variety of habitats (Palleroni, 1992). The diversity and adaptability of *Pseudomonas* sp. originates from the allelic differences of common regulatory and metabolic genes (Klockgether *et al.*, 2011). This diversity allows *Pseudomonas* sp. to adapt to challenging environments; this adaptation most likely evolved through genome arrangements resulting in strain and species specific activities (Kung, Ozer and Hauser, 2010). Due to a versatile metabolic capacity, genetic fluidity and a broad potential for adaptation to fluctuating environmental conditions, *Pseudomonas* sp. are of great interest in terms of biotechnological applications (Silby *et al.*, 2011).

Many members of the *Pseudomonas* genus are able to produce high value compounds and degrade toxic molecules; making them ideal for bulk chemical production and for bioremediation respectively (Desai and Banat, 1997). *Pseudomonas* sp. are known for their ability to degrade hydrocarbons, aromatic compounds, and their derivatives. *P. putida*, for example, has been extensively studied for its bioremediation capabilities in relation to toxic organic wastes, including aromatic hydrocarbon compounds degradation (Kai Chee Loh and Cao, 2008). Other *Pseudomonas* sp. identified with inherent bioremediation properties include *P. aeruginos* (Kulkarni and Kaliwal, 2015) and *P. stutzeri* (Halder and Basu, 2016). Due to the enormous biosynthetic capacity of *Pseudomonas* sp. they are involved in the production of a wide range of secondary metabolites and biopolymers (Novik, Savich and Kiseleva, 2015) including insecticides; for example *P. fluorescens* produces secondary metabolites against tobacco hornworm (Halder and Basu, 2016). The genus *Pseudomonas* is also frequently associated with plant-growth promotion by solubilization of

phosphorous present in organic compounds (such as phytate, phosphonates and phosphites (Lidbury *et al.*, 2016). *Pseudomonas stutzeri's* ability to fix nitrogen has been developed as a bioinoculant to stimulate plant growth (Pham *et al.*, 2017). Though all the members of the *Pseudomonas* genus are aerobic, in some cases they can carry out denitrification by using nitrate as an alternate electron acceptor, reducing nitrate to N_2O or N_2 (Lalucat *et al.*, 2006).

Pseudomonas sp. are an excellent source for the isolation of novel enzymes for various biochemical and biotechnological reactions (Novik, Savich and Kiseleva, 2015). For this reason, this Chapter explores

- production of novel lipases from *P. reinekei* (termed H1) and *P. brenneri* (termed H3), detailing effect of various fermentation parameters (upstream)
- purification (downstream) of novel lipases produced after optimised upstream conditions
- and stability of these purified lipases in various physio-chemical conditions (pH, temperature, effector molecules and selected solvents).

5.2. RESULTS

5.2.1. Upstream

5.2.1.1. Fermentation time and inoculum percentage

Following the fermentation optimisation process (section 3.2.1.8), cell free supernatant for H1, showed maximum lipase activity (0.05±0.008 IU/mL) with 15% (v/v) inoculum after 6 days of fermentation (Figure 5.1). However; for H3, the maximum lipase activity (0.92±0.08 IU/mL) was attained using 2.5% (v/v) inoculum after 2 days of fermentation (Figure 5.2).

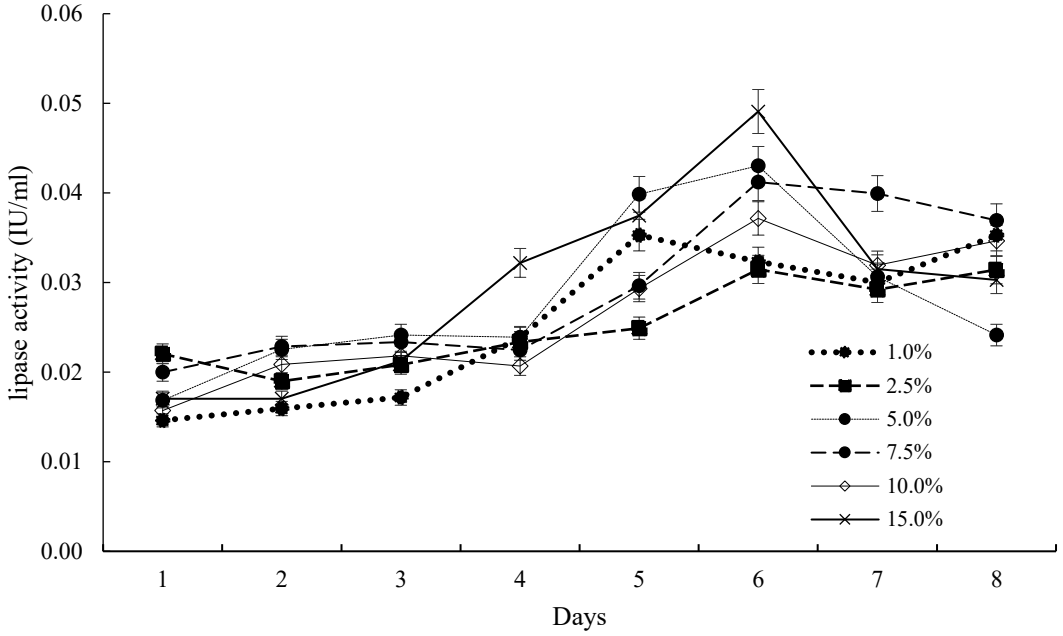

Figure 5.1: The effect of different percentage inocula (1-15% v/v) on lipase production from H1, as estimated via the *p*-NPP spectrophotometric assay (Section 3.2.3.3). This shake flask experiment was performed in basal lipase producing media at 28°C with 200rpm continuous shaking. Activity was measured every day over an 8-day period. Data represented here are the mean of three independent determinants, with error bars as standard deviation.

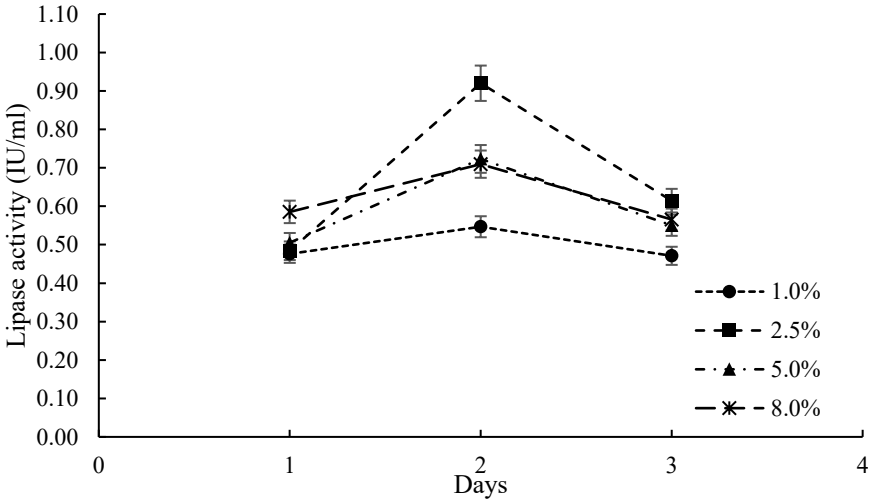

Figure 5.2: The effect of different percentage inocula (1-8% v/v) on lipase production from H3 as estimated via the *p*-NPP spectrophotometry assay (Section 3.2.3.3). This shake flask experiment was performed in basal lipase producing media at 28°C with 200rpm continuous shaking. Activity was measured every day over a 3-day period. Data represented here are the mean of three independent determinants with error bars as standard deviation.

5.2.1.2. Nitrogen source

Following fermentation optimisation process (section 3.2.1.8), different nitrogen sources were explored for their effect on lipase production. H1 lipase production was enhanced with 1% (w/v) *L*-Lysine (0.46±0.023IU/mL; Figure 5.3). Furthermore, the maximum protein concentration was noted with 1% (w/v) *L*-Arginine supplementation (131.59±4.58µg/mL), followed by 1% (w/v) yeast extract supplementation (104.16±4.22µg/mL). The lowest protein concentration and lipase activity was observed with 1% (w/v) ammonium sulphate supplemented media.

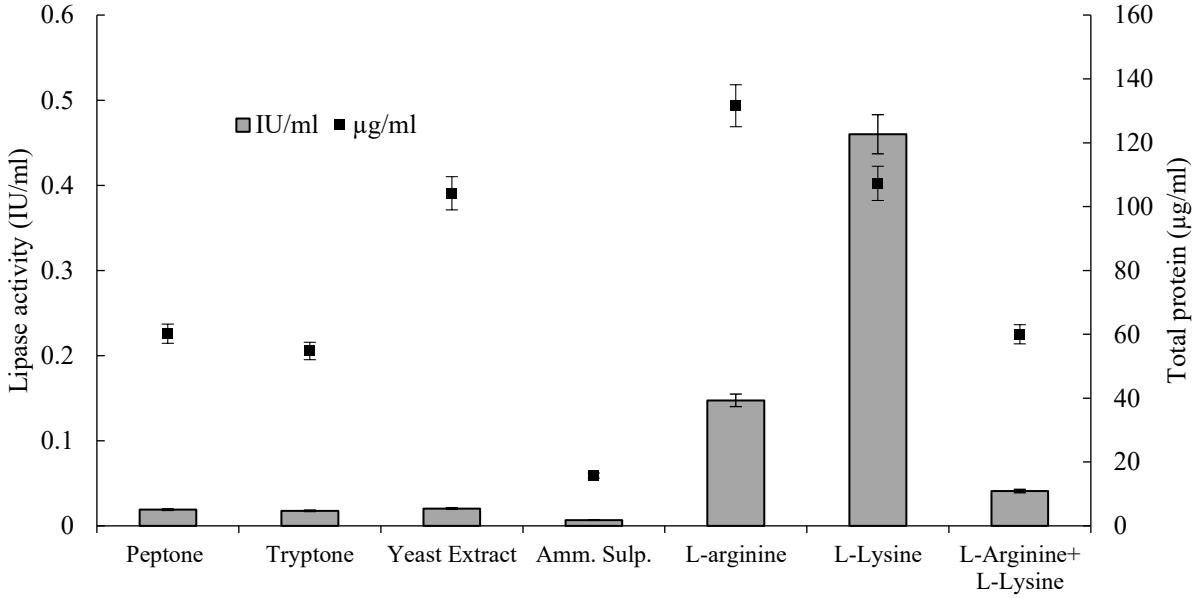

Figure 5.3: A small scale (250ml), shake flask, media supplementation optimization experiment for H1 was performed by replacing the nitrogen source in basal lipase producing media (without peptone) with 1% (w/v) of different nitrogen sources. 15% (v/v) of inoculum was used for lipase production at 28°C for 6 days under continuous shaking at 200rpm. Peptone represents the control (basal lipase producing media). Amm. sulp. represents 1% (w/v) of ammonium sulfate; while *L*-Arginine & *L*-Lysine represents lipase producing media containing 1% (w/v) of both *L*-Arginine and *L*-Lysine. Data represented here are the mean of three determinants with standard deviations as error bars.

For H3 a 1% (w/v) peptone supplement enhanced lipase production, as well as total protein production, (0.91±0.08 IU/mL & 229.03±µg/mL; Figure 5.4). The lowest lipase activity, and total protein concentration, were observed with 1% (w/v) ammonium sulphate, Urea, *L*-Lysine supplemented media.

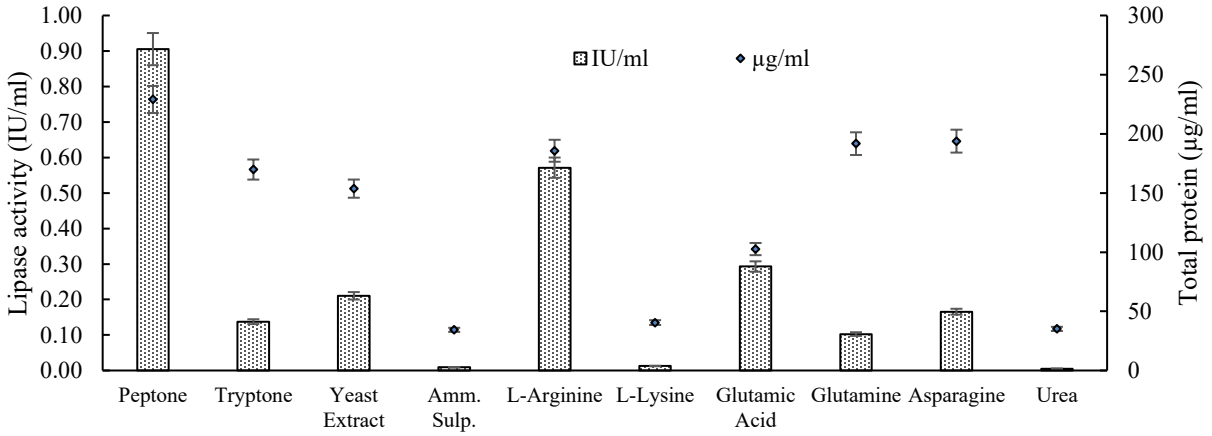

Figure 5.4: A small scale (250ml), shake flask, media supplementation optimization experiment for H3 was performed by replacing the nitrogen source in basal lipase producing medium (without peptone) with 1% (w/v) of different nitrogen sources. 2.5% (v/v) of inoculum was used for lipase production at 28°C for 2 days under continuous shaking at 200rpm. Peptone represents the control (basal lipase producing media). Amm. sulp. represents 1% (w/v) of ammonium sulfate. Data represented here are the mean of three independent determinants with standard deviations as error bars.

Having observed dramatic difference in lipase and overall protein concentration with specific nitrogen sources we looked at the inclusion levels of these compounds in was studied in greater detail (see below).

5.2.1.3. L-Lysine percentage (H1 lipase)

Following fermentation optimisation process (section 3.2.1.8), various concentrations of *L*-Lysine (0.25, 0.5, 1, 2.5 and 5% w/v) were used to investigate its effect on lipase production from H1. Maximal lipase production was observed in medium supplemented with 0.5% (w/v) *L*-Lysine, while maximal total protein concentration was seen in media supplemented with 5% (w/v) *L*-Lysine (Figure 5.5).

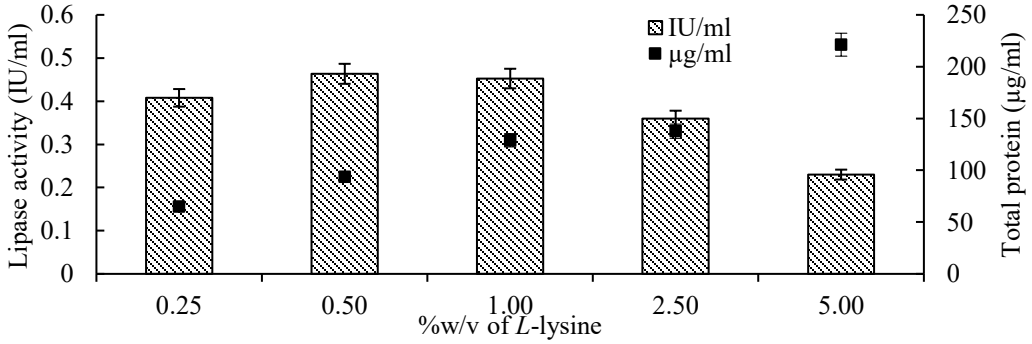

Figure 5.5: A small scale (250ml), shake flask, media supplementation optimization experiment was performed with different % (w/v) of *L*-Lysine in the production media (basal lipase producing medium without peptone). A 15% (v/v) of H1 inoculum was used for lipase production at 28°C for 6 days under continuous shaking at 200rpm. Protein concentration increased gradually with an increase in the percentage of *L*-Lysine. No statistically significant difference was observed in lipase activity of H1 at 0.5% (w/v) and 5% (w/v) of *L*-Lysine. Data represented here are the mean of three independent determinants with standard deviations as error bars**.**

5.2.1.4. Initial production media pH (H1 lipase)

Following fermentation optimisation process (section 3.2.1.8), effect of varying pH (ranging from pH 5±0.2 to pH 9±0.2) was evaluated for lipase production and total protein production. Maximum lipase activity of 0.46±0.02 IU/mL was achieved when the initial pH of the production media was 6.5±0.2. However, maximum protein concentration of 264.2±9.2µg/mL was achieved at an initial pH of 6.0±0.2. Above pH 7.0±0.2, there was a significant reduction ($p \leq 0.05$, t-test) in the production of lipase and total protein, whereas pH 9.0±0.2 resulted in the production of only 0.03±0.01 IU/mL of lipase and 89.17±3.9µg/mL of total protein (Figure 5.6).

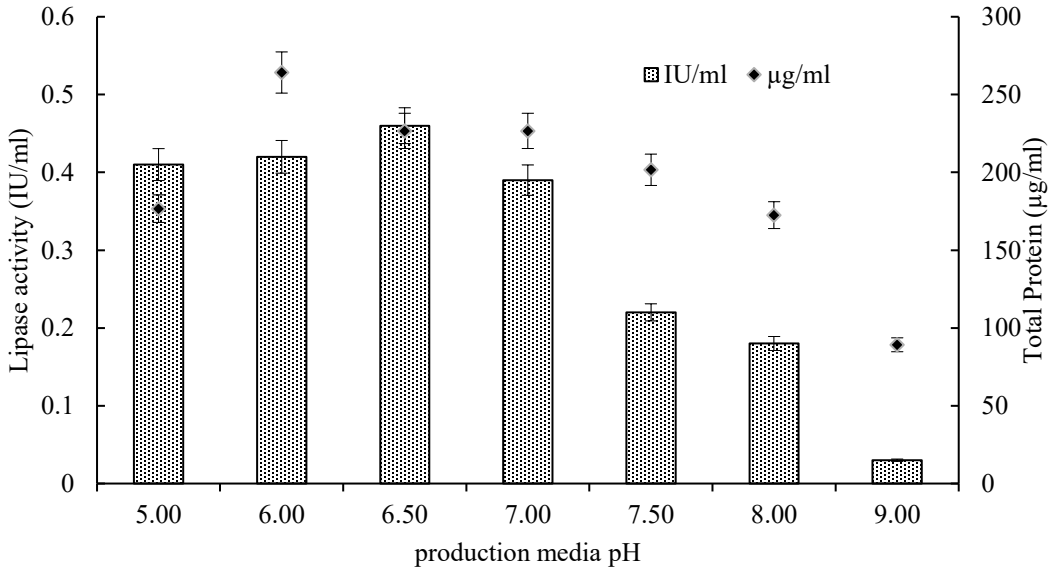

Figure 5.6: A small scale (250ml), shake flask, media supplementation optimization experiment was performed by adjusting the pH of lipase producing media containing 1% (w/v) of *L*-Lysine with HCl. A 15% (v/v) inoculum was used in the lipase production at 28°C for 6 days under continuous shaking at 200rpm. Data represented here are the mean of three independent determinants with standard deviations as error bars**.**

5.2.1.5. Fermentation temperature

Following fermentation optimisation process (section 3.2.1.8), fermentation with optimal media conditions for H1 and H3 at 35°C and 40°C, 200rpm, showed reduced production of lipase and total protein compared to 28°C (Figure 5.7 a, b). It was noted that 28°C was the ideal fermentation temperature for both bacterial strains (H1 and H3), generating lipase activity of 0.46±0.023 IU/mL

and 0.91±0.08IU/ml, with a total protein concentration of 226.67±9.23µg/mL and 229 ±9.00 µg/ml respectively.

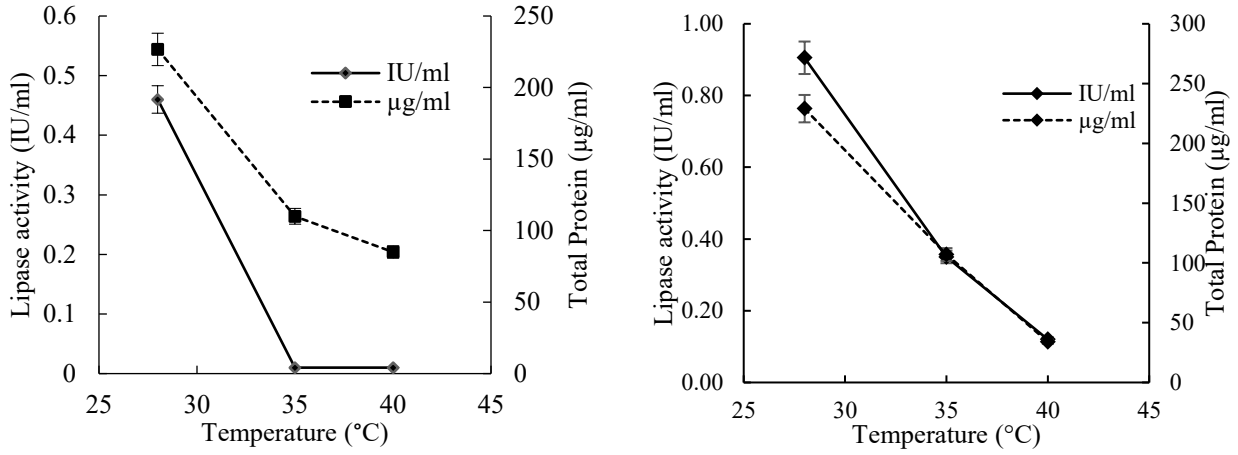

Figure 5.7: A small scale (250ml), shake flask experiment was performed in lipase producing media containing (a) 1% (w/v) of *L*-Lysine at pH 6.5±0.2 for H1. A 15% (v/v) inoculum was used for lipase production at 28°C, 35°C and 40°C for 6 days under continuous shaking at 200rpm. (b) 1% (w/v) of Peptone for H3 at 6.8±0.2. In both cases, a 2.5% (v/v) inoculum was used for lipase production at 28°C, 35°C and 40°C for 2 days under continuous shaking at 200rpm. 28°C was found to be ideal for maximum lipase production for both bacterial strains. Data represented here are the mean of three determinants with standard deviations as error bars.

Following the optimized fermentation conditions for maximum lipase production (summarized in table 5.1) from H1 (*P. reinekei*) and H3 (*P. brenneri*); extracellular lipase were purified (section 5.2.2) for further study.

Table 5.1: Consolidated table representing optimized fermentation conditions for maximum lipase production from H1 (*P. reinekei*) and H3 (*P. brenneri*)

Bacterial strain	Inoculum percentage (v/v)	Nitrogen source and percentage (w/v)	Media pH	Fermentation temperature, rpm	Fermentation time
H1 (*P. reinekei*)	15%	*L*-Lysine (1%)	6.5±0.2	28°C, 200rpm	6 days
H3 (*P. brenneri*)	2.5%	Peptone (1%)	6.8±0.2	28°C, 200rpm	2 days

5.2.2. Downstream

5.2.2.1. Purification of H1

The isolation of purified lipase from the culture filtrate was achieved by a two-step procedure (Table 5.2). The first purification step; an anion exchange Q-Sepharose HP (negative

chromatography step) resulted in 76.95% overall yield with a specific activity of 259.32 IU/mg. This first negative chromatographic step involved anion exchange on Q-Sepharose HP column which removed contaminant proteins from the lipase-rich solution.

The second chromatography step, an anion exchange on Q-Sepharose HP column, in the presence of 250mM NaCl, was required for the capture and isolation of pure lipase (Figure 5.8). Pure lipase was eluted from the second chromatography step of Q Sepharose column by stepwise elution in elution buffer containing 500mM NaCl. Following the purification procedure (Section 3.2.2.4.1), lipase specific activity of 4.23IU/mg was achieved, with an overall yield of 13.72%. Enzyme preparations, after freeze drying, were stored at 4°C for stability studies.

Table 5.2: Purification of lipase from *P. reinekei* (H1) cell free supernatant by a two-step purification procedure. Anion exchanger Q-Sepharose HP was used in negative absorption (chromatography 1) and positive absorption (chromatography 2) mode to reach an overall yield of 13.72% and 4.23IU/mg specific activity.

Purification step	Total activity (IU)	Total protein (mgs)	Specific activity (IU/mg)	Purification (fold)	Yield (%)
Cell free supernatant	75.1	82.48	0.91	1.00	100.00
Dialysate	64.2	82.06	0.79	0.98	97.13
Chromatography 1	49.4	47.60	1.04	1.14	67.66
Chromatography 2	6.8	1.60	4.23	4.65	13.72

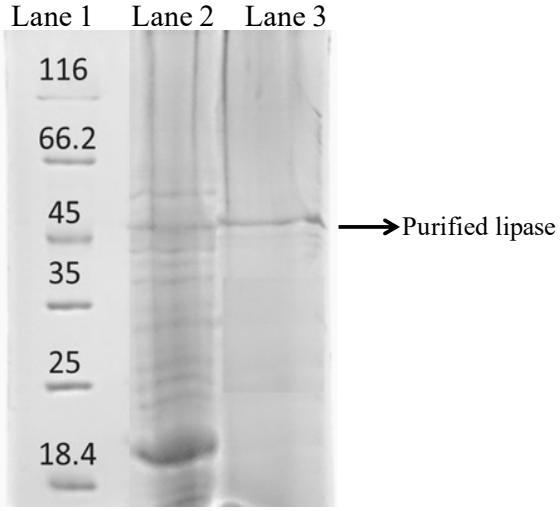

Figure 5.8: A12% (v/v) reducing SDS-PAGE of purified H1 lipase. Lane 1: molecular weight marker, Lane 2: CFS10X (i.e. cell free supernatant at 10-fold concentration), Lane 3: PL10X (i.e. purified lipase after the second chromatography step following 10-fold concentration (by ultrafiltration). Initial protein concentration of cell free supernatant was 158.3µg/mL and the purified lipase was a solution at 59.6µg/ml. An equal concentration of protein was loaded onto the gel in lanes 2 and 3. Purified lipase was estimated to be~55kDa.

Based on the molecular weight migration of markers (Appendix G), the molecular weight from reducing SDS-PAGE of purified lipase was estimated to be ~55kDa.

5.2.2.2. Zymogram for lipase activity for H1

To confirm that the purified enzyme was, indeed, the main protein band seen on the SDS gel; a non-reducing SDS-PAGE of the purified lipase was carried out. The gel displayed one active band with molecular mass of ~55kDa (Figure 5.9), corresponding with that observed by reducing SDS-PAGE. A MUF-butyrate *in situ* enzyme assay was used to visualize the purified enzyme on non-reducing SDS-PAGE. The hydrolysing activity of purified lipase coincided with the protein band of ~55kDa.

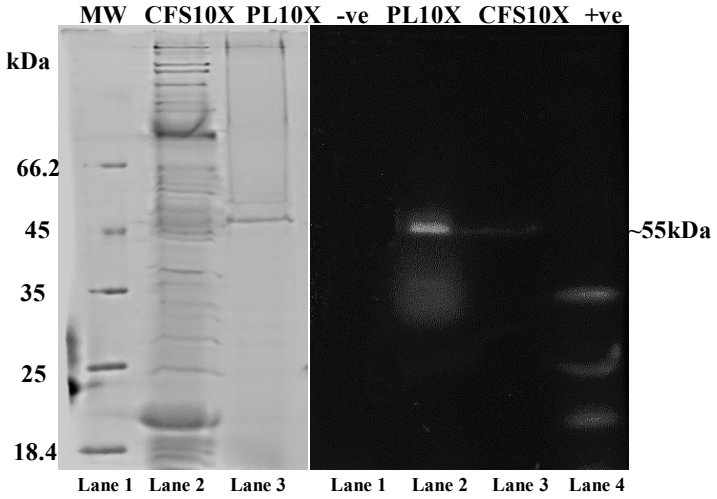

Figure 5.9: 12% (v/v) non-reducing SDS-PAGE gel (A) Stained with Coomassie Brilliant Blue. Lane 1: MW: molecular weight marker, lane 2: 10XCFS i.e. 10-fold concentrated cell free supernatant (158.3µg/mL initial concentration); 10XPL i.e. 10-fold concentrated purified lipase (initial concentration 59.6µg/mL). (B) Zymogram of 12% (v/v) non-reducing SDS-PAGE. Lane 1: negative control (1mg/ml BSA); Lane 2: 10XPL i.e. 10-fold concentrated purified lipase (initial concentration 59.6µg/mL); Lane 3: 10XCFS i.e. 10-fold concentrated cell free supernatant (158.3µg/mL initial concentration); Lane 4: lipase from *M.miehei* as positive control at 30mg/mL concentration. 20µL of each sample was loaded on the gel. The estimated size of purified lipase was ~55kDa.

5.2.2.3. Partial purification of H3

Partial lipase purification from the culture filtrate was achieved by a two-step procedure (Table 5.3, Section 3.2.2.4.2). Lipase was eluted from the chromatography column with an elution buffer containing 750mM NaCl. Following the purification procedure (Section 3.2.2.4.2) a lipase with

specific activity of 3.18IU/mg was achieved, with an overall yield of 56.89%. Enzyme preparations after freeze drying were later stored at 4°C for stability studies.

Table 5.3: Partial purification of lipase from *P. brenneri* (H3). Anion exchanger Q-Sepharose HP (Chrometography 1) was used as mode of purification to get an overall yield of 56.89 and 3.18IU/mg specific activity.

Purification step	Total activity (IU)	Total protein (mgs)	Specific activity (IU/mg)	Purification (fold)	Yield (%)
Cell free supernatant	120.9	86.1	1.40	1	100
Dialysate	114.7	58.5	1.96	1.40	94.86
Alkaline precipitation	102.8	51.2	2.01	1.43	89.57
Chromatography 1	58.5	18.4	3.18	2.26	56.89

5.2.3. Characterisation of H1 and H3 purified lipases

5.2.3.1. Effect of pH

Purified lipase from *P. reinekei* (H1) and *P. brenneri* (H3) were stored at 4°C at different pHs. Both were found to be active over a pH range of 5.0±0.2 to 9.0±0.2 with ~100% residual activity after 24h of incubation at 4ºC. In the same storage conditions, porcine pancreas lipase (PPL) (Sigma, the standard control lipase), showed ≥80% residual activity only at pH 4.0±0.2 and pH 5.0±0.2 (Figure 5.10a), while a significant loss ($p \leq 0.05$, t-test) in activity was observed below pH 4.0±0.2 and above pH 5.0±0.2. At 28°C, purified H1 lipase showed stability between pH 5.0±0.2 and 8.0±0.2 after 24h of incubation; while significant loss ($p \leq 0.05$, t-test) in lipolytic activity was observed below pH 5.0±0.2 and above pH 9.0±0.2. Lipase from H3 showed similar results at 28°C (Figure 5.10b). The PPL had no residual activity above pH 6.0±0.2 after 24h of incubation at 28°C. The lipolytic activity of purified H1 lipase was maximal at pH 7.0±0.2 at 4°C and pH 5.0±0.2 at 28°C; while lipolytic activity of H3 lipase was maximal at pH 8.0±0.2 at both 4°C and 28°C.

5.2.3.2. Effect of temperature

The effect of temperature on the stability of lipase is shown in Figure 5.11. Purified H1 lipase from *P. reinekei* was characterised as a mesophilic enzyme since it retained 90% of activity at 40°C, even after 24h of incubation. Although H1 lipase had 111.35% of activity at 50°C after 30mins of incubation, a significant loss of activity ($p \leq 0.05$, t-test) was observed after 1hr incubation at this

temperature. Lipase from *P. brenneri* (H3) showed ~80% of residual activity at 70°C and showed only 47% of residual activity at 80°C. The standard (porcine pancreas lipase) showed a significant ($p \leq 0.05$, t-test) loss in activity at all temperatures above 30°C within 30mins of incubation; 13% of activity was lost at 40°C, while 40% at 50°C after 30mins of incubation.

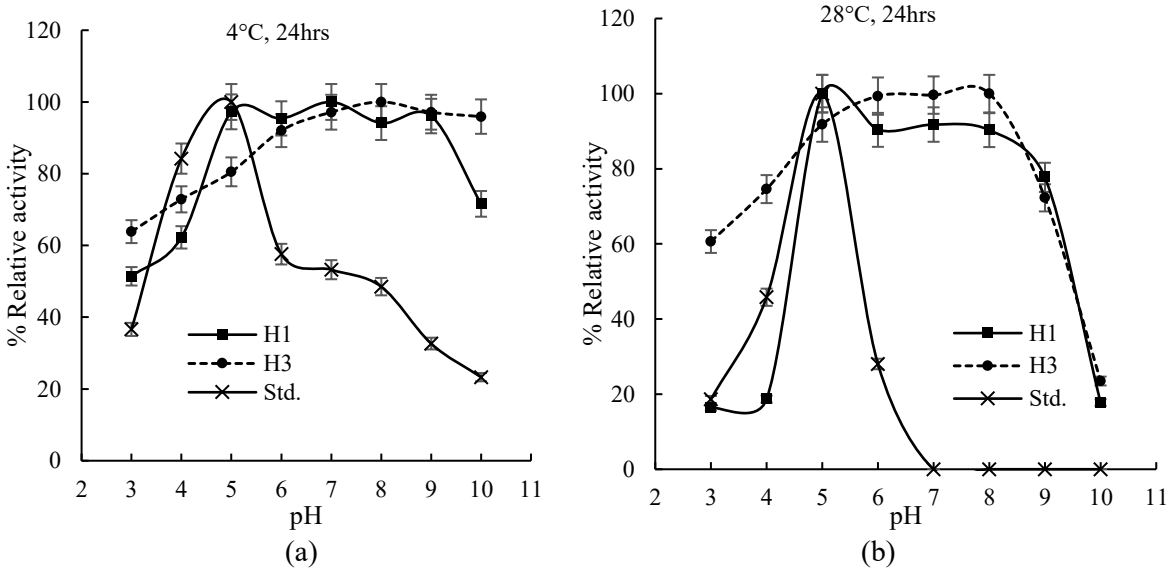

Figure 5.10: A plot of residual activities, as a proxy for pH stability, of purified lipase from H1, H3 and the standard (porcine pancreas lipase), measured after 24h incubation at 4°C (a) and 28°C (b) in the presence of different pH buffers (pH 3 to pH10). Residual lipase activity was calculated by comparison to the activity in 50mM Tris-HCl buffer, pH 7.0±0.2 without pre-incubation. Data represented here are the mean of three different experiments and error bars represents standard deviation.

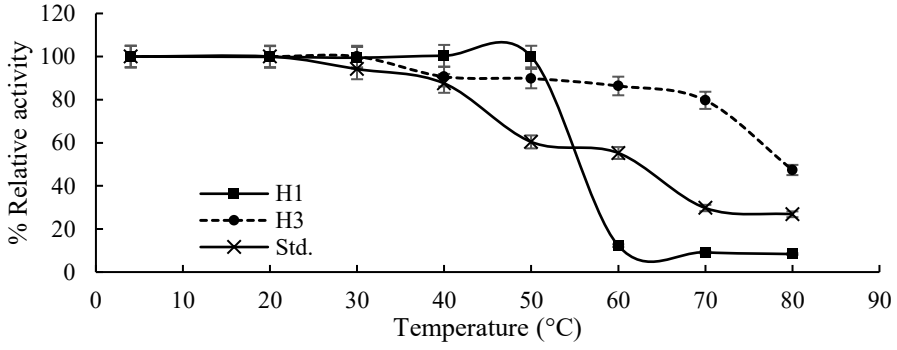

Figure 5.11: Thermal stability of standard and purified lipase from H1 (*P. reinekei*) and H3 (*P. brenneri*) was studied by incubating the enzymes at various temperatures (20, 30, 40, 50, 60, 70 and 80°C) for 30mins. All the enzyme samples were prepared in 50 mM Tris-HCl buffer pH 7.0±0.2. Residual activity (%) at each temperature was calculated relative to that at 0h as 100%. Data represented here are the mean of three different experiments and error bars represents standard deviation.

5.2.3.3. Half life

The half-lives of the purified lipases from H1 and H3 were estimated by incubating the enzyme samples at 45°C and 60°C respectively (Figure 5.12). By first order thermal deactivation, the half-life of the lipase from H1 at 45°C and H3 at 60°C was 89mins and 190mins respectively according to eq. (1) and eq. (2); where A_t stands for enzyme activity after t time, A_0 is initial enzyme activity (at t=0mins); k is decay rate constant and $T_{1/2}$ is half life of the enzyme.

$$ln\, A_t = ln\, A_0 - k_d\, \mathrm{t} \qquad (1)$$

$$T_{1/2} = \frac{\ln 0.5}{-k_d} \qquad (2)$$

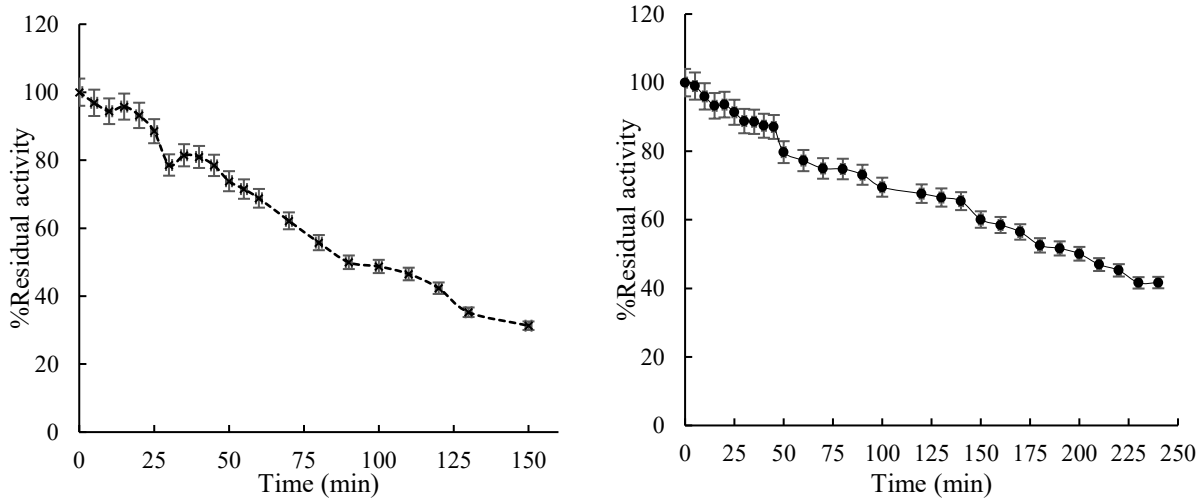

Figure 5.12: Half-life of purified lipase from H1 (a; *P. reinekei*) and H3 (b; *P. brenneri*) was measured by incubating the enzymes at 45 and 60°C respectively in 50 mM Tris-HCl buffer pH 7.0±0.2. Residual activity (%) at each time-point was calculated relative to that at 0hr as 100%. Data represented here are the mean of three different experiments and the error bars represent the standard deviation.

5.2.3.4. Optimum temperature for activity

The optimal temperature for lipolytic activity of purified lipase from H1 and H3 was estimated using *p*-NPP as substrate (Section 3.2.3.3); and incubating the reaction at various temperatures (4°C-70°C). Optimal temperature for lipase from H1 was calculated to be 37°C (Figure 5.13a); while for lipase from H3, the enzyme showed optimal lipolytic activity from 28°C to 50°C (Figure 5.13b).

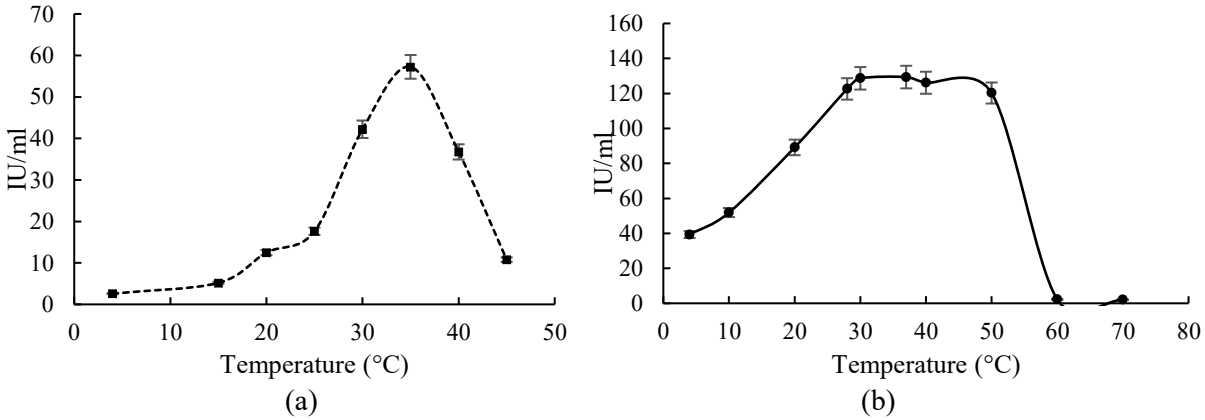

Figure 5.13: Optimal temperature for lipolytic activity of purified lipase from (a) H1 (from *P. reinekei*) and (b) H3 (from *P. brenneri*) was studied by incubating the enzymes with *p*-NPP substrate at different temperatures. Lipolytic activity was calculated after 30mins of incubation at the respective incubation temperature. Data represented here are the mean of three different experiments and the error bars represent the standard deviation.

5.2.3.5. Effect of metal ions and effectors

The effects of a 10mM of different metal ions and effector molecules on purified lipase from H1 (*P. reinekei)* and H3 (*P. brenneri*) were assessed (Table 5.4), along-with lipase standard (porcine pancreas lipase). EDTA had the strongest effect on lipolytic activity loss for all three lipases (H1, H3 and Standard). A significant loss ($p \leq 0.05$, t-test) in lipolytic activity was also observed in presence of polysorbate80 for lipase from H1; conversely, in the presence of SDS, significant activity loss was noted in H3 ($p \leq 0.05$, t-test). Porcine pancreas lipase (PPL) showed significant loss ($p \leq 0.05$, t-test) of activity in the presence of all detergents (polysorbate 80, SDS and Triton X-100). Lipases from all three sources were stable in the presence of 10mM Co^{2+} and Mn^{3+}; however, a significant loss ($p \leq 0.05$, t-test) in activity in the presence of 10mM Zn^{2+} was noted. For Fe^{3+}, only lipase from H1 was found to be stable while lipase from H3 and procine pancreas lipase (PPL) demonstrated significant change (log $p \leq 0.05$, t-test) lipolytic activity (see Table 5.4).

Table 5.4: The effect of various metal ions and effector molecules/chemicals (at a final concentration of 10mM, except urea which was tested at a final concentration of 1M) on the stability/activity of standard and purified lipases from H1 and H3 was studied. All enzyme samples were prepared in 50mM Tris-HCl buffer pH 7.0±0.2 and were incubated with respective metal ions and effector molecules/chemicals at 28°C for 24h (Section 3.2.4.3). Relative activity (%) was calculated with reference to that of enzyme solution at same temperature, but without effector, after 24h of incubation. Data represented here are the mean of three different experiments and error bars represent standard deviation. The symbols *, **, ***, **** represent significant ($p \leq 0.05$, t-test), very significant ($p \leq 0.01$, t-test), extremely significant ($p \leq 0.001$, t-test) and extremely significant ($p < 0.0001$, t-test) change respectively.

Additive	% Relative activity (H1)	% Relative activity (H3)	% Relative activity (Std.)
Control (no additive)	100.00 ± 0.00	100.00 ± 0.00	100.00 ± 0.00
$CaCl_2$	99.92 ± 2.65	106.03 ± 2.76	64.56 ± 2.14**
$MgCl_2$	94.67 ± 1.57	93.52 ± 2.32	62.81 ± 2.02**
KCl	95.30 ± 1.16	103.12 ± 2.24	55.35 ± 2.09***
NaCl	100.95 ± 2.23	99.84 ± 2.18	55.00 ± 2.37***
$CoCl_2$	95.84 ± 2.12	91.14 ± 2.92	110.26 ± 2.32
$MnCl_3$	103.078 ± 2.93	94.55 ± 2.13	94.30 ± 2.61
$FeCl_3$	102.95 ± 2.24	6.68 ± 1.86****	115.70 ± 2.65*
$ZnSO_4$	81.75 ±2.66**	0.00****	142.46 ± 2.77***
EDTA	26.25 ± 1.39****	0.00****	40.96 ± 1.49****
Urea (1M)	84.16 ± 2.87*	61.39 ± 2.24**	47.46 ± 2.14***
4-mercaptaethanol	122.22 ± 2.22**	103.10 ± 2.13	20.88 ± 2.72****
Poly-80	62.25 ± 2.39**	98.29 ± 2.11	45.88 ± 2.29****
Triton X-100	100 ± 1.50	89.94 ± 2.75	191.05 ± 2.26***
SDS	110.03 ± 2.17	59.70 ± 1.46**	54.47 ± 2.36***

5.2.3.6. Effect of solvents

An extremely significant loss ($p \leq 0.001$, t-test) in lipolytic activity was observed for lipases from all three sources (H1, H3 and Standard) irrespective of the incubation temperature (28°C or 40°C) and time (1h and 24h) in the presence of more than 30% (v/v) methanol and ethanol. No significant loss in lipolytic activity was observed for lipases from H1 and H3 in 10% (v/v) methanol at 28°C even after 24h of incubation. Moreover, at 40°C after 24h incubation, no significant loss in lipolytic activity was observed for the H3 lipase in the presence of 10% (v/v) and 20% (v/v) ethanol (Table 5.6). A significant ($p \leq 0.01$, t-test) to extremely significant ($p \leq 0.001$, t-test) gain in lipolytic activity was observed in presence of *n*-hexane, cyclohexane and *n*-heptane, irrespective of incubation time and temperature. Tables 5.5 and 5.6 show the effect of various concentrations of solvents on the stability of lipase from H1, H3 and PPL with respect to incubation time and temperature.

5.2.3.7. Substrate specificity

Lipase from H1 (*P. reinekei*) showed a maximum activity with short chain phenyl ester *p*NP-Octanoate (*C8:0*) and *p*NP-Decanoate (*C10:0*). The activity reduced with increased chain length; from *C10:0* to *C16:0*, with no, or minimal, activity observed for short chain phenyl esters (*C2:0*, *C4:0*) (Figure 5.14). Lipase from H3 (*P. brenneri*) showed maximum activity towards *p*NP-Dodecanoate (*C12:0*); however, the no significant difference in activity was observed towards *p*NP-Myristate (*C14:0*), *p*NP-Decanoate (*C10:0*), *p*NP-Octanoate (*C8:0*) and *p*NP-Palmitate (*C16:0*). Lipolytic activity reduced with reduction in phenyl ester chain length from *C4:0* to *C2:0* (Figure 5.14)

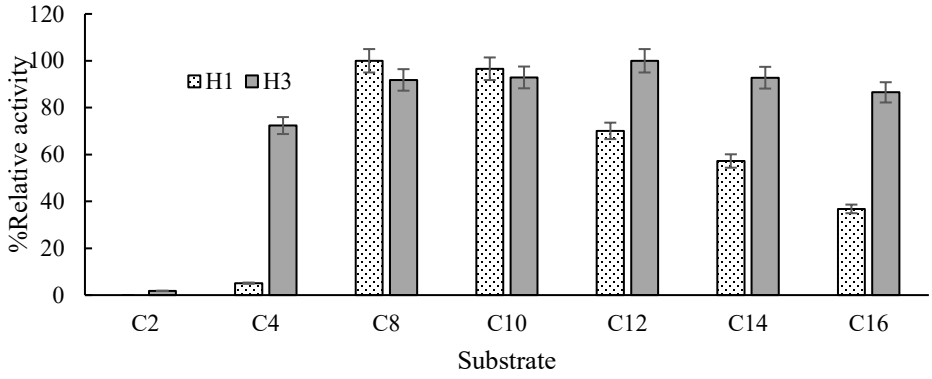

Figure 5.14: Substrate specificity of purified lipase from H1 (*P. reinekei*) and H3 (*P.* brenneri) towards a range of *p*-NP esters (*C2:0-C16:0*). Catalytic specificity was monitored using standard assay conditions reported via the spectrophotometric assay (Section 3.2.3.3). The data represented are the mean of three independent experiments and the standard deviations are noted as error bars.

Table 5.5: The effect of solvents on the stability/activity of the PPL and purified lipase from H1 and H3 was studied. All enzyme samples were prepared in 50mM Tris-HCl buffer pH 7.0±0.2 and were incubated with the respective solvent concentration, at 28°C for 1h and 24h. Relative activity (%) was calculated with reference to to that of same enzyme solution at same temperature, but no additive, at respective time point (1h and 24h). Data represented here are the mean of three different experiments and error bars represents standard deviation. The symbols *, **, ***, **** represent significant ($p \leq 0.05$, t-test), very significant ($p \leq 0.01$, t-test), extremely significant ($p \leq 0.001$, t-test) and extremely significant ($p < 0.0001$, t-test) change respectively.

Condition	Additive	% Relative activity (H1)	% Relative activity (H3)	% Relative activity (PPL)
28°C 1h	Control (no additive)	100.00 ± 0.00	100.00 ± 0.00	100.00 ± 0.00
	10% Methanol	96.24 ± 2.53	97.94 ± 2.59	70.64 ± 2.62**
	20% Methanol	90.19 ± 2.48*	92.49 ± 2.45	64.68 ± 2.91**
	30% Methanol	78.19 ± 2.04**	76.79 ± 2.52**	60.03 ± 2.73***
	40% Methanol	39.23 ± 1.93****	39.95 ± 1.69****	48.89 ± 1.52****
	50% Methanol	31.52 ± 1.02****	31.74 ± 1.08****	37.20 ± 1.22****
	10% Ethanol	97.57 ± 2.39	116.06 ± 2.38*	72.81 ± 2.13**
	20% Ethanol	87.90 ± 2.52*	93.63 ± 2.07	67.69 ± 2.88**
	30% Ethanol	72.29 ± 2.88**	73.57 ± 2.51**	64.07 ± 2.57***
	40% Ethanol	21.69 ± 1.51****	21.25 ± 1.09****	56.23 ± 2.45***
	50% Ethanol	22.38 ± 1.44****	21.62 ± 1.55****	37.68 ± 1.40****
	50% *n*-hexane	243.64 ± 3.65****	138.38 ± 2.21***	92.12 ± 2.05
	50% Cyclohexane	138.72 ± 2.29***	133.18 ± 2.04***	86.40 ± 2.61*
	50% *n*-heptane	181.14 ± 2.77***	138.25 ± 2.66***	121.03 ± 2.75**
40°C 1h	Control (no additive)	100.00 ± 0.00	100.00 ± 0.00	100.00 ± 0.00
	10% Methanol	97.19 ± 2.87	97.62 ± 2.62	46.82 ± 1.89****
	20% Methanol	69.02 ± 2.45**	78.90 ± 2.65**	42.99 ± 1.63****
	30% Methanol	17.32 ± 1.09****	55.35 ± 2.21***	36.34 ± 1.49****
	40% Methanol	15.14 ± 1.18****	30.79 ± 1.44****	28.41 ± 1.80****
	50% Methanol	14.87 ± 1.65****	10.92 ± 1.45****	25.12 ± 1.89****
	10% Ethanol	82.86 ± 2.00*	87.33 ± 2.89*	48.29 ± 1.71****
	20% Ethanol	11.87 ± 1.37****	35.00 ± 1.40****	43.55 ± 1.48****
	30% Ethanol	17.05 ± 1.45****	13.13 ± 1.69****	40.93 ± 1.86****
	40% Ethanol	15.90 ± 1.09****	11.62 ± 1.24****	28.24 ± 1.11****
	50% Ethanol	17.24 ± 1.66****	10.95 ± 1.16****	16.04 ± 1.81****
	50% *n*-hexane	198.14 ± 2.07**	114.81 ± 2.01*	75.30 ± 1.83**
	50% Cyclohexane	197.34 ± 2.67**	118.83 ± 2.44*	68.79 ± 2.16**
	50% *n*-Heptane	192.66 ± 2.33**	122.46 ± 2.98*	78.69 ± 2.69**

Table 5.6: The effect of solvents on the stability/activity of PPL and purified lipase from H1 and H3 was studied. All enzyme samples were prepared in 50mM Tris-HCl buffer pH 7.0±0.2 and were incubated with a given solvent concentration, at 40°C, for 1h and 24h. Relative activity (%) was measured relative to that of same enzyme solution at the same temperature, but without any additive, at respective time point (1h and 24h). Data represented here are the mean of three different experiments and error bars represents standard deviation. *, **, ***, **** represent significant ($p \leq 0.05$, t-test), very significant ($p \leq 0.01$, t-test), extremely significant ($p \leq 0.001$, t-test) and extremely significant ($p < 0.0001$, t-test) change respectively.

Condition	Additive	% Relative activity (H1)	% Relative activity (H3)	% Relative activity (Std.)
28°C 24h	Control (no additive)	100.00 ± 0.00	100.00 ± 0.00	100.00 ± 0.00
	10% Methanol	92.71 ± 2.36	98.64 ± 2.12	37.47 ± 1.60****
	20% Methanol	97.86 ± 2.42	80.019 ± 2.59*	31.01 ± 1.11****
	30% Methanol	70.61 ± 2.21**	65.01 ± 2.94**	24.09 ± 1.30****
	40% Methanol	24.55 ± 1.49****	27.80 ± 1.07****	18.17 ± 1.04****
	50% Methanol	25.75 ± 1.58****	17.64 ± 1.27****	13.89 ± 1.15****
	10% Ethanol	92.27 ± 2.02	84.45 ± 2.33*	30.23 ± 1.22****
	20% Ethanol	92.07 ± 2.54	16.60 ± 1.99****	22.26 ± 1.07****
	30% Ethanol	24.50 ± 1.33****	18.00 ± 1.08****	24.58 ± 1.38****
	40% Ethanol	23.70 ± 1.18****	17.70 ± 1.55****	20.89 ± 0.18****
	50% Ethanol	25.51 ± 1.72****	17.34 ± 1.72****	15.59 ± 1.08****
	50% *n*-hexane	193.28 ± 2.93**	131.02 ± 2.99**	73.45 ± 1.38**
	50% Cyclohexane	275.95 ± 2.14***	122.48 ± 2.74 *	68.89 ± 2.67***
	50% *n*-heptane	324.37 ± 2.96***	128.80 ± 2.71**	61.85 ± 2.61***
40°C 24h	Control (no additive)	100.00 ± 0.00	100.00 ± 0.00	100.00 ± 0.00
	10% Methanol	89.29 ± 2.79*	102.50 ± 2.02	25.77 ± 1.48****
	20% Methanol	36.23 ± 1.32****	91.55 ± 2.40	17.43 ± 2.32****
	30% Methanol	26.5 ± 1.59****	6.10 ± 0.12****	15.13 ± 1.84****
	40% Methanol	21.67 ± 1.26****	1.77 ± 0.69****	14.04 ± 0.79****
	50% Methanol	36.23 ± 2.39****	1.75 ± 0.49****	13.96 ± 1.01****
	10% Ethanol	44.89 ± 2.65***	103.02 ± 2.78	20.72 ± 1.77****
	20% Ethanol	37.77 ± 1.97****	53.15 ± 2.22***	15.92 ± 1.07****
	30% Ethanol	33.97 ± 1.61****	1.26 ± 0.13****	13.42 ± 1.54****
	40% Ethanol	31.23 ± 1.78****	1.72 ± 0.27****	10.96 ± 1.43****
	50% Ethanol	24.94 ± 2.24****	2.17 ± 0.53****	8.73 ± 0.58****
	50% *n*-hexane	399.57 ± 4.94****	111.78 ± 2.58*	60.04 ± 1.88***
	50% Cyclohexane	461.63 ± 4.24****	114.94 ± 2.57*	52.99 ± 2.71***
	50% *n*-heptane	378.03 ± 4.14****	124.91 ± 2.04**	62.61 ± 2.40***

5.2.3.8. Enzyme kinetics

The kinetics of the purified lipase from H1 (*P. reinekei*) and H3 (*P. brenneri*) was studied using *p*NP-palmitate as the substrate of choice at 28°C (as other characterization studies were done using *p*-NPP as substrate). A Lineweaver Burk plot was used to calculate the kinetic parameters V_{max}, K_m

and K_{cat} and they were estimated to be 3.41±0.17mmoL/min/mg, 0.48±0.02mM and 2601.66/min respectively for H1 (*P. reinekei*; Figure 5.15a). For H3 (*P. brenneri*), V_{max} and K_m were estimated to be 5.17±0.12mmoL/min/mg and 0.37±0.09mM respectively (Figure 5.15b). These Lineweaver Burk plots and kinetic data were verified using the kinetic modelling function in *Graphpad* (*Prisim Software*, San Diego, CA, version 7). Due to the absence of molecular weight information, K_{cat} for H3 was not calculated.

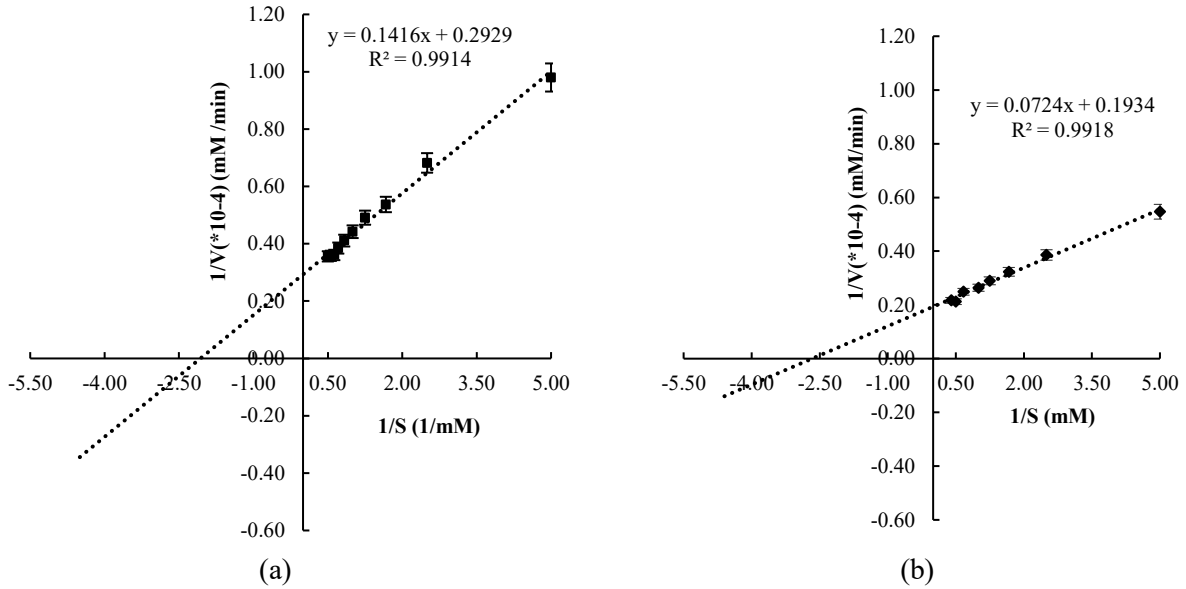

Figure 5.15: Lineweaver Burk plots for the purified lipase from (a) H1 (*P. reinekei*) and (b) H3 (*P. brenneri*) using *p*NP-Palmitate as substrate over the substrate concentration range 0.2–2mM under standard assay conditions (Section 3.2.3.3). The data represented here are the mean of three independent experiments and the standard deviations are noted as error bars.

Consolidated summary of the characterisation details for purified lipase from H1 (*P. reinekei*) and H3 (*P. brenneri*) has been provided in Table 5.7.

5.2.3.9. MS analysis for amino acid sequence identification

Mass spectrophotometric analysis of the purified lipase from *P. reinekei* revealed four conserved peptide sequences: AGYTTAQVEVLGK; LLEIGIGFR; VLNIGYENDPVFR; ANTWVQDLNR. Primers designed using these peptide sequences generated polymerase chain reaction sequences which were similar to lipases from *P. reinekei,* as well as lipases from *P. fluorescens, Pseudomonas sp.* PMAC 25886, *P. yamanorum,* LipAMS8 from *Pseudomonas* sp. AMS8 and *Pseudomonas* sp. PAMC25886 (Figure 5.16). Examination of a phylogenetic tree of the amino acid sequences by BlastP in NCBI revealed the location of lipase from *P. reinekei* relative to other lipases from *Pseudomonas* species (Figure 5.17).

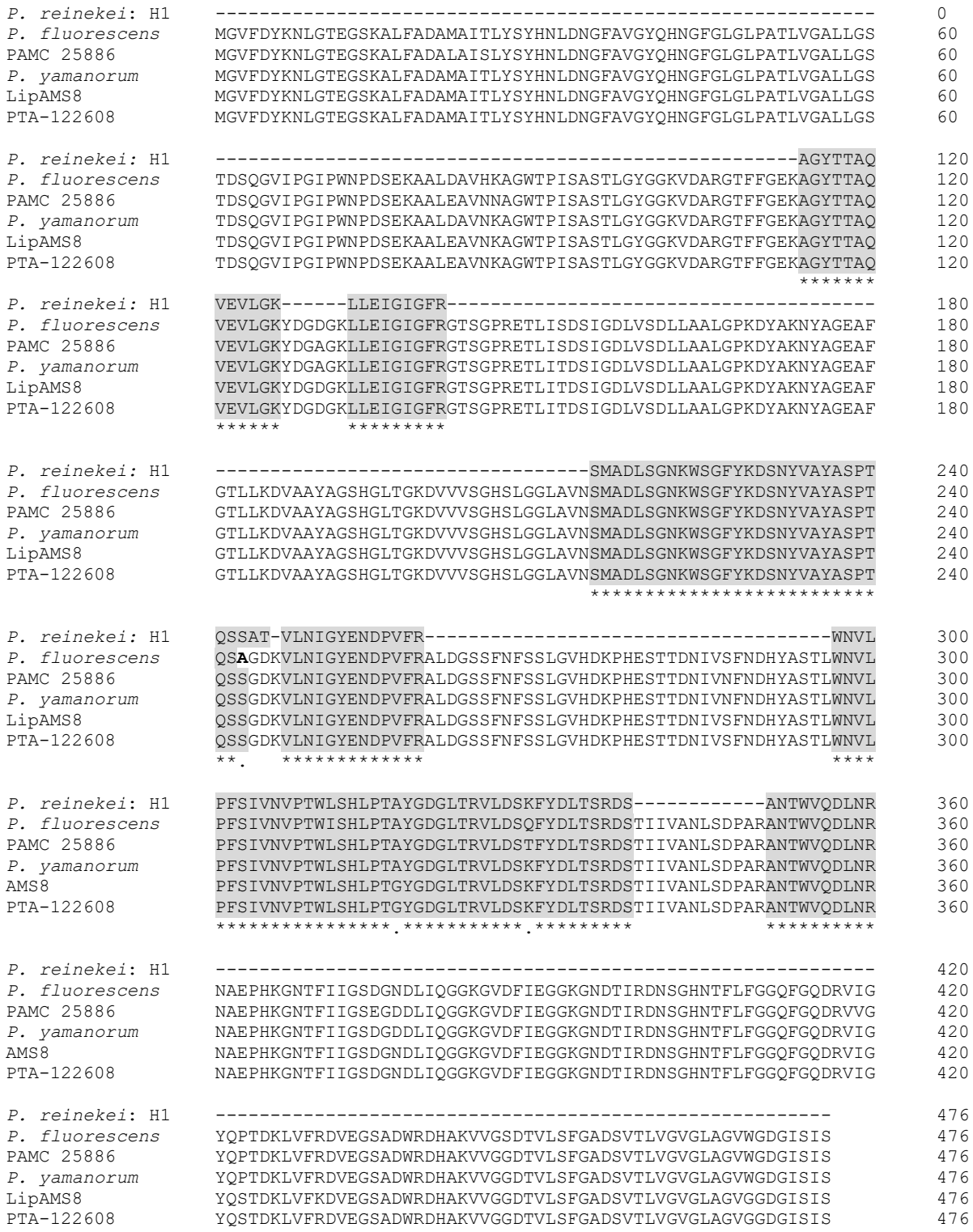

Figure 5.16: An alignment of *P. reinekei* (H1) lipase from NCBI with lipase from *P. fluorescens, Pseudomonas sp.* PMAC 25886, *P. yamanorum,* LipAMS8 from *Pseudomonas* sp. AMS8 and *Pseudomonas* sp. PAMC25886.

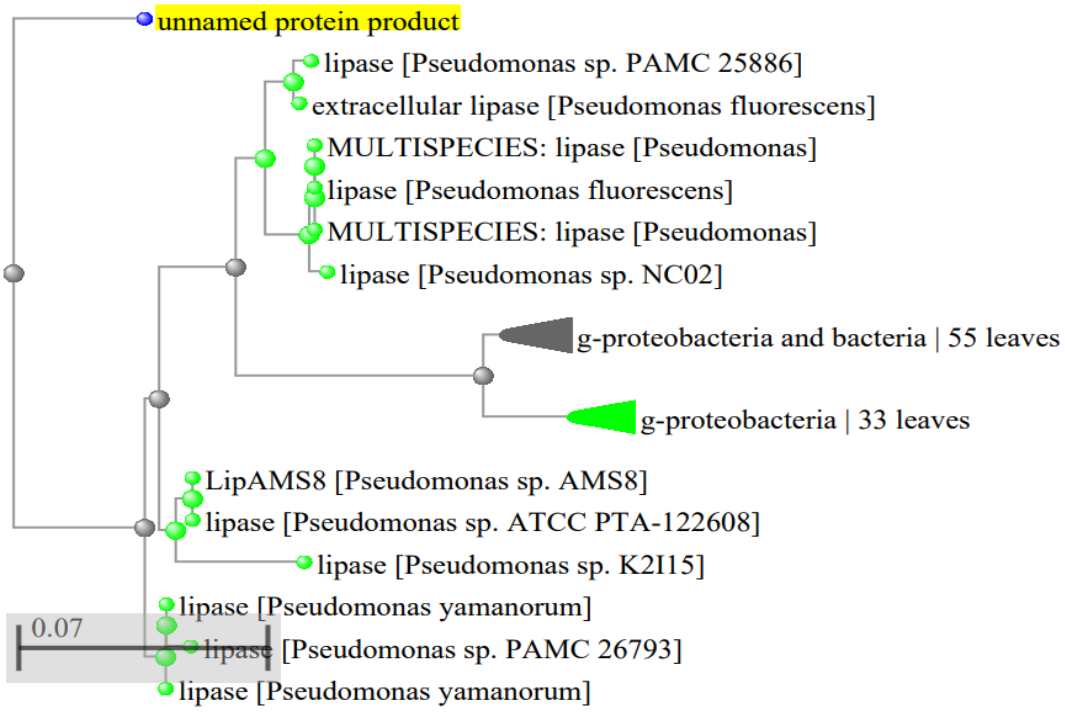

Figure 5.17: A distance tree based on conserved amino acid sequences in *P. reinekei* lipase generated via a BlastP alignment. The homology of *P. reinekei* lipase (highlighted in yellow and reported as 'unnamed protein product') to lipases from different *Pseudomonas* sp. is noted as within the same clade. 0.07 in the figure represents 7% genetic variation for the length of the scale.

MS analysis of lipase from H3 (*P. brenneri*) did not reveal any similarities to the available lipase sequences in the database.

Table 5.7: Consolidated summary of characterization details of lipase from H1 (P. reinekei) and H3 P. brenneri) along with standard (porcine pancreas lipase).

Condition	H1 (*P. reinekei*) lipase	H3 (*P. brenneri*) lipase
pH (Maximum activity/ stability)	pH 7.0±0.2 at 4°C and pH 5.0±0.2 at 28°C	pH 8.0±0.2 at both 4°C and 28°C.
Temperature (30mins incubation)	Stable @ 50°C	Stable @ 70°C
Half life	@ 45°C, 89mins	@ 60°C, 190mins
Optimum temperature for activity	37°C	28°C to 50°C
Metal ions and effector molecules	EDTA, Urea, Poly 80	Unstable in FeCl3, ZnSO4, EDTA, Urea and SDS
Solvents	Activation in hexane, heptane and cyclohexane	Activation in hexane, heptane and cyclohexane
Substrate specificity	Maximum for C8:0 and C10:0	Maximum for C8:0, C10:0, C12:0, C14:0 and C16:0
Enzyme Kinetics	Vmax=3.41±0.17mmoL/min/mg, Km=0.48±0.02mM and Kcat=2601.66/min	Vmax=5.17±0.12mmoL/min/mg, Km= 0.37±0.09mM

5.3. DISCUSSION

5.3.1. Upstream

Microbial lipases are typically extracellular and are preferable for biotechnological applications as they can be easily recovered from the fermentation broth. However, optimization of media and growth conditions are vital to the development of a successful fermentation process (Padhiar, Das and Bhattacharya, 2011). The formulation of a cost-effective medium is required to reduce the final cost of the enzyme produced. Optimization of the concentration of each component that constitutes a cultivation medium can be a time-consuming procedure (Veerapagu *et al.*, 2013). Specific media components may also need to be considered; for example, the production of lipases generally require the presence of inducers, which are lipid substrates like oils, triacylglycerols, fatty acids or hydrolysable esters (Salihu and Alam, 2012). However, the production of lipases is affected by media composition; as well as physicochemical factors such as time, initial inoculum, nitrogen source, pH, temperature etc (Andualema and Gessesse, 2012). Hence, submerged fermentation is preferable for microbial lipase production since it permits enhanced monitoring of process parameters (temperature, pH etc.; (Padhiar, Das and Bhattacharya, 2011) and this was the approach adopted in this study.

5.3.1.1. Fermentation time and inoculum percentage

The percentage of inoculum (i.e. the initial cell count) during the fermentation process plays an important role in lipase production. The finite volume of a culture medium results in limited nutrients and the rate of nutrient consumption is dependent on bacteria cell population/growth stage (Randa *et al.*, 2009). At a suitable inoculum size, the nutrient and oxygen levels are appropriate for bacteria growth and maximum lipase production. Conversely, if the inoculum size is too small, insufficient biomass will lead to reduced levels of lipase secreted over the culture period. Hence, to ensure high lipase production in a limited medium volume, the initial bacterial inoculum should be optimized; however, the optimum percentage of inoculum varies amongst bacterial strains. *Serratia marcescens* ECU1010 produced a maximum concentration of lipase when 10% (v/v) of seed culture was inoculated into the production media (Long, Xu and Pan, 2007). Conversely, a 5% (v/v) inoculum was sufficient for optimal lipase production from *Thermus thermophiles* HB27

(Dominguez *et al.*, 2005). For *P. stutzeri* MTCC 5618, a 1% (v/v) inoculum resulted in 83.33% lipase activity yield and increased inoculum percentage from 3 to 6% (v/v) resulted in decrease in enzyme activity (Thakur, Tewari and Sharma, 2014). In the present investigation, H1 (*Pseudomonas reinekei*), displayed increased lipase production with increased inoculum percentage. A 15% (v/v) inoculum was the highest inoculum tested, as inocula above this percentage would unduly dilute the production media and result in inconclusive results. There is no reported inoculum above 10% (v/v) in the literature. In this study, a 15% (v/v) inoculum resulted in 0.05±0.008IU/mL of lipase after 6 days of fermentation, which was highest amongst all the inoculum percentages examined (Figure 5.1).

For H3 (*P. brenneri*), lipase production increased with increased inocula from 1% (v/v) to 2.5% (v/v); however, further increase in inoculum decreased lipase production. A high inoculum concentration might have resulted in oxygen deprivation and nutrient depletion resulting in poor enzyme yield (Davis *et al.*, 2005). The more concentrated the cells in production media, the more the competition for media substrate and vice-versa (Thakur, Tewari and Sharma, 2014). Hence for H3, maximum lipase activity (0.92±0.08 IU/mL) was attained using 2.5% (v/v) inoculum after 2 days of fermentation (Figure 5.2).

The onset of lipase production is organism-specific, but, in general, lipases are produced during late logarithmic or stationary phase (Gupta *et al.*, 2016). Cultivation periods from 5h to 168h have been reported for the different lipase producing organisms. For example, the fermentation time for *Pseudomonas putida* 922 was 48h (Fatima and Khan, 2015); *P. aeruginosa* JCM5962 produced highest lipase after four days of fermentation (Sachan and Singh, 2017). Lipases from *Serratia marcesecens* (Sachan and Singh, 2017) and *Pseudoalteromonas* sp. WP27 (Joseph, Upadhyaya and Ramteke, 2011) were produced after six and fourteen days of fermentation respectively. In the present case, H1 (*P. reinekei*) produced maximum lipase after six days of fermentation (Figure 5.1); while for H3 (*P. brenneri*) two days of fermentation were sufficient (Figure 5.2). Further cultivation of both the lipase producing strains (H1 and H3) resulted in decreased lipase activity. This could be due to secretion of other proteins at the late logarithmic phase leading to an apparent decrease in lipase specific activity or could be due to enzyme denaturation/inactivation by extracellular proteases (Bora and Bora, 2012).

5.3.1.2. Nitrogen source

Both organic and inorganic nitrogen sources have traditionally been used for lipase production. Microorganisms give high lipase yields when organic nitrogen sources like peptone and yeast extracts are provided (Rajeshkumar, Mahendran and Balakrishnan, 2015). In the present study, 1% (w/v) peptone was found to be the best nitrogen source for lipase production from H3 (*P. brenneri*; Figure 5.4). Similarly 1% (w/v) peptone was noted as the best nitrogen source for lipase production by *Pseudomonas gessardii* (Veerapagu *et al.*, 2013). A slightly higher, 2% (w/v) peptone increased lipase production in *Aspergillus wentii*, *Mucor racemosus* and *R. nigricans* (Salihu and Alam, 2012). While 0.5% (w/v) concentration of yeast extract resulted in optimal lipase production in *R. arrhizus* MTCC2233 (Rajendran and Thangavelu, 2009) and *P. stutzeri* MTCC 5618 (Thakur, Tewari and Sharma, 2014). A combination of tryptone, amino acids and ammonium sulfate was found to be best supplementation for maximum lipase production in *P. fluorescens* (Kulkarni and Gadre, 2002). However, in this present study for H1 (*P. reinekei*), no significant increase ($p \leq 0.05$, t-test) in lipase production was seen when organic sources of nitrogen (peptone, yeast extract and tryptone) were used (Figure 5.3).

Inorganic nitrogen sources, like NH_4Cl, have been found as useful in lipase production from *C. cylindracea* NRRL Y-17506 (Brozzoli *et al.*, 2009). For *Rhodotorula glutinis* ammonium phosphate favoured enhanced lipase production (Papaparaskevas *et al.*, 1992). For *P. citrinum,* however, lipase production was higher in the presence of peptone compared to corn steep liquor or soybean meal; while urea and ammonium sulfate inhibited lipase synthesis (Sharma, Yusuf and Uttam Chand, 2001)**.** A similar nitrogen source preference might be present for lipase from *P. reinekei* and *P. brenneri* where only 0.01±0.001IU/mL lipase production was observed when ammonium sulfate was added to the production media (Figure 5.3 and 5.4).

Media supplementation with specific amino acids; such as Alanine, Glycine, Lysine and Serine, have previously been shown to stimulate lipase production (*Streptococcus faecalis;* (Chander and Ranganathan, 1975). Lipase production was supported in the presence of Arginine, Lysine, Aspartic acid and Glutamic acid for *Pseudomonas fragi* (Alford and Pierce, 1963). Tryptone combined with Lysine was the most effective inducer for lipase production in *Pseudomonas fluorescens* (Al-Saleh, Zahran and Zahran, 1999). A 5.0mM *L*-Arginine, Threonine, and *L*-Lysine supplementation was

noted as the optimal nitrogen source for lipase production in *Pseudomonas fluorescens* (Makhzoum, Knapp and Owusu, 1995).

In case of H3 (*P. brenneri*); 1% (w/v) peptone was the best nitrogen source (resulting in lipase production to 0.91±0.053 IU/mL); followed by Arginine (0.57±0.018 IU/mL) amongst tested nitrogen sources. For lipase from H1 (*P. reinekei*), a 1% (w/v; 68mM) *L*-Lysine supplement was the best nitrogen source, resulting in production of 0.46±0.023 IU/mL of lipase (significant gain, $p \leq 0.05$, t-test; Figure 5.3). *L*-Arginine (57.4mM), on the other hand, generated more total protein than lipase activity. In comparison, the total protein profile of *P. reinekei* when grown in *L*-Lysine and *L*-Arginine, resulted in different protein bands as visualised after SDS-PAGE (Appendix D). This could be due to the activation of different metabolic pathways; accounting for higher total protein production in *L*-Arginine supplemented media.

To increase lipase production in some microbial species, high nitrogen concentrations are required (Lima *et al.*, 2003). For *Penicillium chrysogenum* an increase in concentration of ammonium nitrate and corn steep liquor from 2.4% (w/v) to 6.6% (w/v) resulted in a corresponding increase in lipase production (Burkert, Maugeri and MI Rodrigues, 2004). The combined effect of various parameters (source and concentration), such as nitrogen and carbon, on lipase production from species like *Penicillium chrysogenum* (Burkert, Maugeri and MI Rodrigues, 2004); *Trichosporon asahii* MSR54 (Kumar and Gupta, 2008), *Stenotrophomonas maltophilia* (Hasan-Beikdashti *et al.*, 2012) has been reported. In the present study, lipase production from H1 (*P. reinekei*) was influenced by different concentrations of *L*-Lysine. Increased *L*-Lysine concentrations (above 1%, w/v) resulted in a significant decrease in lipase production. There was no significant difference ($p > 0.05$, t-test) in lipase production for 0.25%, 0.5% and 1% (w/v) *L*-Lysine (Section 5.2.1.3, Figure 5.4); however, the total protein produced in these production media formulations varied. At lower concentrations (w/v) of *L*-Lysine, a lower total protein concentration was observed, but higher lipase activity, was noted. Though there was no significant difference ($p > 0.05$, t-test) in lipase activity between 0.5% (w/v) and 1% (w/v) *L*-Lysine formulations (Figure 5.5); 1% (w/v) *L*-Lysine showed higher total protein concentration, and henceforth, was used as the primary nitrogen source. The total protein concentration is contributed by other vital proteins, not just the lipase alone. Since, higher total protein concentration correlated with maximum lipase production and resulted in reduced upstream

batch volumes, a 1% (w/v) *L*-Lysine was used as a media supplement for H1 (*P. reinekei*) lipase production.

5.3.1.3. Media pH

Enzymes remain active at a favourable pH range during fermentation. A drastic alteration of media pH can result in the loss of enzyme activity by disrupting microbial membrane transport mechanisms (Section 2.5.1; (Veerapagu *et al.*, 2013). A change in environmental pH directly affects the structure, stability, activity and production of lipases. For example, *Pseudomonas putida* 922 produced maximum lipase after 48h of incubation in production media at pH 10 (Fatima and Khan, 2015), whereas *P. stutzeri* MTCC 5618 produced maximum lipase with production media at pH 9.0 (Thakur, Tewari and Sharma, 2014). Similarly, a lipase from *Fusarium globulosum* was produced at neutral pH after 96h of fermentation (Gulati *et al.*, 2005). A pH of 7.0±0.2 was found to be optimum for lipase production in *P. gessardii* (Veerapagu *et al.*, 2013), *P. fluorescens* (Kulkarni and Gadre, 2002) and *P. aeruginosa* (Padhiar, Das and Bhattacharya, 2011). In the present study, for lipase from H1 (*P. reinekei*) and due to the production media contained *L*-Lysine and sodium phosphate for buffering; the media pH can be adjusted based on the buffering capacity (pI 9.74 and pKa 2.18, 8.95, 10.53) of *L*-lysine. However; maximum lipase production was observed when the pH of the production media was pH 6.5±0.2. A decrease in lipase production was observed with increase in pH above 7.0±0.2 (Figure 5.6). Similar observations were noted for lipases produced from *B. licheniformis* MTCC 10498, where maximum lipase production was achieved at pH 7.5, while alkaline conditions (pH 9.0) resulted in decreased lipase production (Sharma, Sharma and Kanwar, 2012). It is a common observation that fungal strains produce high lipase titre under acidic conditions, whereas bacterial strains produce high lipase titre in alkaline or neutral conditions (Thakur, Tewari and Sharma, 2014). For the lipase production media of H3 (*P. brenneri*), there was only one buffer component (sodium phosphate), whose composition generated a pH of 6.8±0.2; hence different pH values on lipase production from *P. brenneri* was not studied.

5.3.1.4. Fermentation temperature

Lipase production is species specific, for example, *P. putida* 922 is a mesophilic bacterium and showed maximum lipase production at 30°C, pH 10 after 48h of fermentation (Fatima and Khan, 2015). Similarly, 30°C was the optimum temperature for production of lipase from *P. fluorescens* (Kulkarni and Gadre, 2002). *Pseudomonas gessardii* produced maximum lipase at 37°C with 1% (w/v) peptone, pH 7.0 (Veerapagu *et al.*, 2013). Generally, the temperature required for lipase production corresponds to the growth conditions of the microorganism. In this present study, and by varying the fermentation temperature of the production medium, the optimum temperature for lipase production was identified as 28°C for both H1 and H3 (Figure 5.7a, b). Reduced lipase activity in the culture supernatant above 28°C is likely due to the thermolability of *P. reinekei* and *P. brenneri* bacterial cells; as these soil-based *Pseudomonas* sp. were adapted to colder regions it was expected they will produce maximum lipase at the temperatures they were adapted to. Due to unavailability of suitable fermentation equipment, the effect of lower temperatures (<28°C) on lipase production from H1 (*P. reinekei*) and H3 (*P. brenneri*) was not investigated further.

Following lengthy media and fermentation optimisation maximum production of lipase from H1 (*P. reinekei*) was achieved by using 15%(v/v) inoculum was used to initiate fermentation in a basal lipase producing media containing 1% (w/v) *L*-Lysine at pH 6.5±0.2. The fermentation was carried out at 28°C for 6 days, with constant shaking at 200rpm. For lipase production from H3 (*P. brenneri*); a 2.5% (v/v) inoculum was used to initiate fermentation in a basal lipase producing media containing 1% (w/v) peptone at pH 6.8±0.2. The fermentation was executed at 28°C for 2 days, with constant shaking at 200rpm.

5.3.2. Downstream Processing

5.3.2.1. Overview

Since most microbial lipases are extracellular, the first step for their isolation from culture broth typically involves removal of the bacterial cell mass. Bacterial cells can be separated by centrifugation or filtration (Rajendran, Palanisamy and Thangavelu, 2009). In this study, *P. reinekei* and *P. brenneri* cells from the respective fermentation broth were removed by centrifugation at 5,000**g* for 20mins at 4°C. Proteins present in a cell free supernatant were subsequently concentrated. A concentration step reduces the overall process cost, process time and yield losses

(Gronemeyer, Ditz and Strube, 2014). Typically, protein concentration can be achieved either by ultrafiltration or by precipitation (Saxena *et al.*, 2003). Ultrafiltration can be an expensive and time-consuming process (Gronemeyer, Ditz and Strube, 2014), making precipitation a better alternate. Proteins can be precipitated by production of perturbations in the buffer (pH, ionic strength, and temperature; (Gronemeyer, Ditz and Strube, 2014). Alternatively, the addition of salt, acid, solvent and temperature can also achieve protein precipitation (Wingfield, 2001). The concentration of salt required to precipitate a protein depends on the number, and distribution of, non-ionic polar groups on the surface of the protein. It also depends on the number and distribution of exposed hydrophobic residues on the protein surface. The size and shape of the protein also determines the relative ease of its precipitation (Englard and Seifter, 1990). When salt is added to a protein solution, the surface tension of water increases, increasing protein solubility due to enhanced hydrophobic interaction between protein and water (Kramer *et al.*, 2012), initially responsible for "*salting in*". With an increase in salt, the hydrophobicity increases even more where proteins decreases their surface area in order to minimize contact with the solvent, this self-association leads to precipitation i.e. "*salting out*" (Wingfield, 2001; Stenesh, 2013). Ammonium sulfate is the most commonly used precipitant as it does not generate a large amount of heat during precipitation reactions and the saturated solution (4.04M at 20°C), has a density of 1.235 g/cm^3 that does not readily interfere with protein sedimentation and is relatively inexpensive (Englard and Seifter, 1990). In this study, ammonium sulfate was utilised as the initial precipitant and was tested for the precipitation of lipase from H1 (*P. reinekei*), as well as from H3 (*P. brenneri*). However, no protein precipitation was observed even after addition of saturating ammonium sulfate (60% w/v) at room temperature (Appendix E, Table E.1 a, b). Typically, low temperature ammonium sulfate precipitation can provide high protein yields of up to 87% (Saxena *et al.*, 2003); however, with a 4°C overnight (16 hrs) salting out a ~20% and ~28% lipase yield was obtained from H1 (*P. reinekei*) and H3 (*P. brenneri*) respectively, in this study. Salt induced precipitation carried out at low temperatures (4°C) can result in increased yield. Proteins tend to be less soluble at lower temperatures resulting in enhanced salting out (Ghosh, 2006). In this study, the initial protein concentration in the cell free supernatant was quite low (0.1mg/mL) and with only ~20-28% yield attained with ammonium sulfate precipitation; this method was not considered further as a pre-purification step.

Organic solvents are also commonly used for protein precipitation including acetone, methanol, ethanol and butanol; all of these have both hydrophobic and polar domains (Deutscher, 1990). These solvents compete for water with the polar groups of the protein. In large volumes, these solvents reduce the effective concentration of water, and thus reduce protein hydration, decreasing solubility, resulting in precipitation (Fogarty and Laage, 2013). In this study, a 50% (v/v) solution of cold acetone was initially trialled for lipase precipitation from H1 (*P. reinekei*) and H3 (*P. brenneri*). The use of solvents can denature proteins, especially at temperatures above 0°C (Englard and Seifter, 1990); and this was observed in this study where precipitated proteins from cell free supernatant of both lipase producing strains (H1 and H3) underwent irreversible precipitation, indicating denaturation (Appendix E, Table E.1). Acetone, therefore, was rejected as a protein precipitant.

Polyethylene glycol (PEG) is a non-denaturing water-soluble polymer; and is a known protein precipitant (Atha and Ingham, 1981). The PEG concentration requirement for protein precipitation is unique for a given protein-polymer pair, with influencing factors including the size of protein and polymer (Ingham, 1984). Large proteins can be precipitated by lower concentrations of smaller PEGs, while high concentrations of larger PEGs can be used to precipitate small proteins (Sim *et al.*, 2012). In this study, PEG 10,000 (50% w/v) was investigated for its efficiency in precipitating proteins from cell free supernatant of lipase from H1 (*P. reinekei*) and H3 (*P. brenneri*). No precipitation was observed after addition of 50% (w/v) PEG 10,000 in cell free supernatant (Appendix E, Table E.1a, b) of both the lipase producing strains (H1 and H3).

In all precipitation steps, low initial protein concentration in the cell free supernatant could be the reason for poor precipitation. Precipitation is mostly a crude separation step and is often followed by chromatographic separation (Saxena *et al.*, 2003). Since precipitation of proteins from H1 (*P. reinekei*) and H3 (*P. brenneri*) cell free supernatant was not successful; no pre-purification step was used before chromatographic purification.

Commercial enzyme applications do not always need a homogeneous preparation of the enzyme (Panesar, 2010). However, a certain degree of purity is often required, depending upon the final

application (ICH, 1996). There are many methods of classical protein purification (Walls and Loughran, 2017); however, the most frequently employed anion and cation exchange type purification systems for lipase purification are diethylaminoethyl (DEAE) group-based resins (Kamarudin *et al.*, 2014) and carboxymethyl (CM) group-based resins respectively (Saxena *et al.*, 2003). Strong anion exchangers based on triethylaminoethyl (TEAE), trimethylaminoethyl (TMAE) and Q-Sepharose (Kordel *et al.*, 1991; De Pascale *et al.*, 2008; Yang *et al.*, 2012; Masomian *et al.*, 2013; Pereira *et al.*, 2015; W. Yang *et al.*, 2016) have also been used in lipase purification. Since lipases are hydrophobic in nature, the purification of lipases can also be carried out by affinity chromatography (Patel, Nambiar and Madamwar, 2014; Wi *et al.*, 2014; Ganasen *et al.*, 2016; Kaur *et al.*, 2016) and hydrophobic interaction chromatography (Mander *et al.*, 2012; Kamarudin *et al.*, 2014; Kumar, Parshad and Gupta, 2014; Bakir and Metin, 2016; Xie *et al.*, 2016). Due to expensive matrices and limited reusability of affinity chromatography matrices, ion exchange for lipase purification is usually preferred (Gupta, Gupta and Rathi, 2004).

The charge on the protein affects its behaviour in ion exchange chromatography (Khan, 2012). With an increase in the pH of a solution, acidic and basic groups in proteins undergo deprotonation. Carboxyl groups (R-COOH) convert to carboxylate anions (R-COO-) while ammonium groups ($R\text{-}NH_3^+$) are converted to amino groups ($R\text{-}NH_2$) giving the protein an overall negative charge. Conversely, with a decrease in the pH of the solution, carboxylate anions (R-COO-) are protonated, converting to carboxyl groups (R-COOH) while amino groups ($R\text{-}NH_2$) are converted to ($R\text{-}NH_3^+$) giving the protein an overall positive charge (Maldonado, Ribeiro and Sillero, 2010). In short, when the pH > pI, the protein will have a net negative charge; conversely when pH < pI, the protein will attain a net positive charge. The pI of a protein is dependent on its amino acid composition and hence varies from protein to protein. Since the pI of the lipase from H1 (*P. reinekei*) and H3 (*P. brenneri*) was unknown at the time of this study, the selection of appropriate purification conditions (pH, ion exchange mode) was challenging.

To work out appropriate chromatography conditions, three different chromatography modes (anion, cation and hydrophobic interaction chromatography; HIC) were tested. For anion and cation exchange, Q-Sepharose HP from GE Lifesciences and Fractogel® EMD SO3- from Merck both with 10mM sodium acetate pH 5.0 buffer were tested. While for hydrophobic interaction chromatography (HIC) Toyopearl® phenyl from Tosoh was tested. Cell free supernatant was

conditioned in the respective buffer via dialysis (dialysis for cation and anion exchanger, dialysis followed by salt addition for HIC) and loaded the onto a chromatography resin. Binding of lipase on the chromatography resin was evaluated by comparing the lipase activity in protein load and flow through samples via *p*-NPP spectrophotometric assay. No difference in lipase activity for both H1 and H3 was seen for protein load and flow through samples in the case of cation exchange. However, promising results were observed on anion exchange (Q-Sepharose) for both H1 and H3 and on hydrophobic interaction chromatography for H3 cell free supernatant.

5.3.2.2. Purification of lipase from H1

Further optimization of lipase purification from H1 (*P. reinekei*) was carried out using the Q-Sepharose HP anion exchange resin (Appendix E, Table E.2). Since lipase from H1 did not bind to the cation exchanger (pH 5.0), it could be concluded that the pI of lipase in cell free supernatant of H1 (*P. reinekei*) is above 5.0. The higher the difference between the pH and the pI, the larger will be the negative charge on the protein, and hence, the stronger the interaction between protein and the ligand on the stationary phase (resin) will be. Increasing the pH of the buffer can be a simple method to enhance the binding capacity of protein on an ion exchanger. Therefore, to increase the lipase binding capacity on Q-Sepharose, different pH conditions were screened. A variety of total binding capacities, of 48%, 47% and 44%, were observed (Appendix E, Table E.3) when 10mM Tris-HCl with pH 8.5, 9.0 and 9.5 respectively were used as buffers and the resultant samples analysed via *p*-NPP assay. Although, with an increase in pH lipase binding capacity increased, pH 9.5 is considered too harsh for protein purification as high pH can lead to protein deamidation (Cross and Schirch, 1991; Song *et al.*, 2001). Hence, pH 9.0 was used for further purification optimization of lipase from H1 (*P. reinekei*).

At 10mM Tris-HCl pH 9.0, lipase from H1 was recovered from Q-Sepharose by a 1M NaCl step elution (Section 2.3.2.4.3) indicating a strong interaction with the stationary phase. However, at this point of the purification optimisation strategy, the purity of the eluted lipase was not satisfactory (Appendix F.1). Due to high pH, it could be possible that majority of proteins in the cell free supernatant presented negative charge and selective binding/elution of lipase was over-ruled. The binding of a protein on an ion exchanger can be affected by the presence of salt in the solution. Addition of salt increases the number of ions competing with proteins for functional

groups on the stationary phase (Manz, Pamme and Iossifidis, 2004). Proteins with a lower negative charge will not bind to the resin sites due to the competitive presence of salt; while proteins with a higher negative charge will bind loosely. This can enhance selective protein binding, increasing the overall purity. The addition of 0.1M and 0.25M NaCl in the protein loading samples was investigated to identify whether it enhanced the purity of lipase in subsequent elution samples. Following salt addition, the binding capacity of lipase increased from 47% with no salt to 58.07% and 55.66% with 0.1M and 0.25M NaCl respectively. These conditions also resulted in an observed change in the Q-Sepharose resin colour (Appendix F.2). The lipase binding capacity was increased and lipase eluted from the column at 750mM NaCl step-elution in an insoluble form. This could be due to co-elution of other host cell proteins that affected lipase solubility. Therefore, a single chromatographic step was not sufficient to get the required level of purity and, hence, a two-step purification procedure was explored.

Gel filtration is the second most frequently employed purification method (Saxena *et al.*, 2003). Gel filtration has a lower capacity for loaded protein, and is mostly used as one of the last steps for 'polishing' proteins (e.g. buffer exchange); however, the technique suffers from low-resolution and is time-consuming (Edouard and Koza, 2014). Since, cation exchange and hydrophobic interaction chromatography did not provide promising results; Q-Sepharose again was used as a second step of chromatography in a two-stage purification procedure. Column 1 of Q-Sepharose with no salt generated a flow through sample that exhibited a ~52% residual lipase activity as compared to the initial loading sample. As previously observed, the addition of salt in the protein load sample enhanced the overall binding capacity of the protein. As such, 0.25M NaCl was added to the flow through from Column 1 and was subsequently used to purify the H1 lipase via a second Q-Sepharose (termed Column 2), equilibrated with 10mM Tris-HCl pH 9.0 and 0.25M NaCl. H1 lipase eluted from Column 2 when 500mM of NaCl was used within a step elution. The presence of salt in the protein load did not permit a strong interaction between the lipase and stationary phase; hence, the lipase was retrieved from the column with 500mM NaCl instead of 1M NaCl.

In summary, Column 1 of Q Sepharose was used as a negative mode of chromatography, where most of the contaminant proteins bound along with 40% of the lipase. Column 2 was used in a bind and elute mode and produced purified lipase (Section 3.2.2.4). As observed from the 12% (v/v)

reducing SDS-PAGE (Figure 5.7), a pure lipase band was visualised upon staining with Coomassie Brilliant Blue.

Proteins are relatively unstable in the aqueous state and undergo chemical and physical degradation resulting in a loss of biological activity during storage (David, 2008). Due to the lack of a stabilizer, the eluted lipase from H1 precipitated when stored overnight at 4°C and therefore required a stabilizer supplement. Sorbitol is one of the chemical chaperones commonly used as a protein stabilizer as it is known to inhibit the unfolding of native conformations into unfolded/misfolded forms (Yang and Zhang, 2013). Sorbitol and other polyols have been demonstrated to effectively reduce or inhibit aggregation of IgG solutions (Ohtake, Kita and Arakawa, 2011). Therefore, to enhance the stability of lipase and to avoid precipitation due to aggregation, two different concentrations of sorbitol were investigated. A 2% (v/v) concentration of sorbitol was found to be ineffective as precipitation was still observed, while no precipitation or change in lipase stability/activity were observed when 5% (v/v) sorbitol was used. Hence, 5% (v/v) sorbitol was added to the elution as soon as the protein was fractionated from the Q-Sepharose column.

The relative molecular mass of purified lipase was estimated as ~55kDa by molecular marker migration on both reducing and non-reducing SDS-PAGE (Appendix G) and was confirmed by zymography (Figure 5.8). Lipases typically have molecular weights in the range of 15–69 kDa (Latip *et al.*, 2016). *Pseudomonas* sp. DMVR 46 produces lipase which is ~32kDa in size (Vrutika, Shruti and Datta, 2014), while 15.5kDa and 54.97kDa lipases have been purified from *Pseudomonas aeruginosa* Ps-x (Saeed *et al.*, 2005). *Pseudomonas aeruginosa* is also known to produce lipase with molecular weight of 54kDa and 59.4kDa (Karadzic *et al.*, 2006; Singh and ChandBanerjee, 2007). To date, no literature is available on *P. reinekei* lipase(s), and in *Pseudomonas* sp. only one lipase from *Pseudomonas aeruginosa* is known (54kDa molecular weight).

The overall yield for purification was 13.72% and a 4.65-fold increase in specific activity of lipase was achieved with a 1.6mg/ml final enzyme concentration.

5.3.2.3. Purification of lipase from H3

Further optimization of lipase purification from H3 (*P. brenneri*) was carried out using Toyopearl® phenyl hydrophobic interaction resin and Q-Sepharose HP anion exchange resin. For protein binding on hydrophobic interaction chromatography, it is important to expose the hydrophobic pockets of a protein. This can be achieved through the addition of salt or decreasing the pH of the solution or a combination of both. Increasing salt concentration, from 0.75M to 0.9M ammonium sulphate and decreasing the pH of the dialysate from cell free supernatant of H3 resulted in a 48% loss of lipase activity (Appendix E, Table E.4). Clearly, the addition of ammonium sulfate resulted in activity loss as well as minimal yield; making hydrophobic interaction chromatography an unattractive option for lipase purification from H3 (*P. brenneri*). To increase the lipase binding capacity on Q-Sepharose different pH conditions were screened. At pH 9.0, protein precipitation was observed (Appendix F, Figure F.3); though no significant change in lipase activity was observed (Table 5.2); making pH 9.0 unsuitable for chromatography. Since a decrease in total protein concentration was observed at pH 9.0 without any significant loss in lipase activity; it was concluded that alkaline pH was eliminating some contaminant protein and hence was used as the first step for lipase purification from H3 (*P. brenneri*). After alkaline precipitation, the protein sample was loaded on Q-Sepharose resin at pH 8.5 in 10mM Tris-HCl pH 8.5. The lipase was subsequently recovered from Q-Sepharose by a 0.75M NaCl step elution. To estimate the purity and molecular weight of the purified lipase, various SDS, native gels with different compositions and pH were used; however due to the large number of unknown contributing factors (e.g. sample pI, hydrophobicity, size, instability of H3 in SDS: table 5.3, section 5.2.3.5 etc.) only one protein band appeared at the edge of separating gel (Appendix F, Figure F.4). Hence, only one step chromatography was used for the purification of lipase from H3 (*P. brenneri*), by which the overall yield of 56.89% and a 2.26-fold increase in specific activity of lipase was achieved.

5.3.3. Characterization

For the characterisation of lipase from H1 (*P. reinekei*) and H3 (*P. brenneri*), appropriate positive and negative controls were used in order to compare these novel enzymes in relation to a known standard. In all cases, the standard buffer was used as a negative control, while PPL from Sigma

prepared in the same testing conditions was a positive control. Attaining a specific activity equal to purified lipases (i.e. H1: 4.23IU/mg and H3: 3.18IU/mg) for porcine pancreas lipase was not feasible due to limited availability and solubility of the enzyme; hence a concentration of 30mg/L (equivalent to 1.98IU/mg) was used throughout the characterization study as a positive control.

5.3.3.1. Effect of pH

Purified lipase from H1 (*P. reinekei*) remained active over short storage periods (<1 week) in cold storage conditions (4°C), over a broad range of pH (5.0±0.2 to 9.0±0.2). However, at 28°C significant loss of activity was seen at pH 3.0±0.2, 4.0±0.2 and pH 10±0.2. Lipase from H1 (*P. reinekei*) and H3 (*P. brenneri*) had an optimum pH of 5.0±0.2 and 8.0±0.2 respectively; while both were active over a broad pH range between 5.0±0.2 and 9.0±0.2 (Figure 5.10). Generally, *Pseudomonas* lipases have neutral or alkaline pH optima (Qamsari, Kasra and Nejad, 2011), with an exception being *P. gessardii,* which has an acidic optimum at pH 5.0 and was found to be active even at pH 2.0 (Ramani *et al.*, 2010). Given that the purified lipases from H1 and H3 were stable from pH 5.0-9.0, they can be used in a variety of applications beyond biodiesel production, in industries such as detergents, leather and fine chemicals (Salihu and Alam, 2012). An optimal pH of 5.0, makes lipase from H1 (*P.reinekei*) ideal for oleochemical and food industries, as well as for the hydrolysis or modification of triacylglycerols to improve nutritional properties of food (Almeida, Tauk-Tornisielo and Carmona, 2013); while with an optimal pH of 8.0, the lipase from H3 can be used in detergents formulations as well as for flavour synthesis and bioremediation (Salihu and Alam, 2015). The positive control, PPL, was also found to be stable in acidic pH conditions. The maximum activity of standard porcine lipase was observed only at pH 5.0±0.2, above which the lipase lost its activity significantly ($p \leq 0.05$, t-test).

5.3.3.2. Effect of Temperature

P. reinekei (H1) purified lipase was, however, not thermostable and lost 70% of its activity at temperatures greater than 50°C within one hour of incubation (Figure 5.11). However, the lipase retained 90% activity at 40°C, even after 24h. Conversely, lipase from H3 (*P. brenneri*) was found to be thermostable with a half-life of 189 mins at 60°C (Figure 5.12b). Lipases from *Pseudomonas*

species have broad temperature optima from 4°C to 90°C. Lipase from *Pseudomonas* sp. PF 16 had an optimum temperature of 4°C (Xiuling *et al.*, 2015); while a lipase from *Pseudomonas* sp. AG-8 showed optimum activity at 45°C (Sharma, Tiwari and Hoondal, 2001). Lipases from other *Pseudomonas* sp. have been known to be active at 90°C (Rathi *et al.*, 2000). The optimum temperature for catalysis by the lipase from H1 (*P. reinekei*) was found to be 37°C (Figure 5.13a); indicating the mesophilic character of this enzyme. Lipase from H3 (*P. brenneri*), however; showed optimal enzyme activity over a wide temperature range (28°C-50°C; Figure 5.13b) indicating some thermostability. Thermostability is a desirable characteristic for enzymes that are used in applications operating at high temperatures. Kinetic resolution of 1,1-dipheyl-2-propanol catalysed by *Burkholderia cepacian* lipase, for example, is sometimes performed at 120°C (Ema *et al.*, 2003). Maximum methyl esters were produced via an acylation of acetyl groups from starch and methanol in presence of *Thermomyces lanuginosus* lipase at 50°C (Alissandratos *et al.*, 2010). Since, the lipase from H1 (*P. reinekei*) was not thermostable, it cannot be used directly (without further modifications) for such applications; lipase from H3 (*P. brenneri*), however; can be used due to its thermostability.

Lipase from H1 (*P.reinekei*) could be useful in transesterification reactions as most lipase catalysed transesterification reactions are performed between 30-60°C (Heitz *et al.*, 2016). In this mode of catalysis, depending on the transesterification time, solvent system and reaction time, optimum yields of biodiesel can be attained. For example, reactions catalysed at 40°C have generated 70% of biodiesel with 8h of reaction time (Shah, Sharma and Gupta, 2004) and 80% of biodiesel with 12h of reaction time at 30°C (Du, Xu and L, 2003) when different reaction conditions were employed. The lipase from H1 (*P. reinekei*) was highly stable at 40°C, with 90% of activity even after 24h of incubation, and showed 89mins of half-life at 45°C (Figure 5.12a). Also, since most lipases used in transesterification reactions are immobilized (Heitz *et al.*, 2016), physical modification methods like immobilization can be used to further enhance the thermal and solvent stability of *P. reinekei* lipase. In comparison, the PPL from porcine pancreas was not thermostable and showed significantly ($p \leq 0.05$, t-test) less stability than purified lipase from H1 (*P. reinekei*) and H3 (*P. brenneri*) above 40°C. The loss of stability for PPL could be due to the physical form

of the enzyme; as lyophilized enzymes are known to be more stable than soluble (Wong and Whitesides, 2013).

5.3.3.3. Effect of metal ions and effectors

To investigate the possible influencing effect of selected modifiers on lipase purified from H1 (*P. reinekei*) and H3 (*P. brenneri*) different metal ions, inhibitors and compounds commonly used as enzyme modifiers were analysed (Table 5.3). The lipase from H3 (*P. brenneri*) lost significant lipolytic activity in the presence of Fe^{3+} and Zn^{2+}, however; for H1 (*P. reinekei*) lipase significant loss in activity was seen only in the presence of Zn^{2+}. Surprisingly, Zn^{2+} ions have been reported to increase the lipolytic activity for a lipase from *Pseudomonas stutzeri*, *Streptomyces* sp. OC119-7 and *Pseudomonas aeruginosa* KM110 (Qamsari, Kasra and Nejad, 2011; Ayaz, Ugur and Boran, 2014; Parwata, Asyari and Hertadi, 2014). It has been reported that Zn^{2+} forms a complex with ionized free fatty acids derived from the hydrolysis of *p*NPP; which reduces the solubility of free fatty acids inside the lipid-water interface; removing them from the active site, opening the way for new substrate molecules to enter the enzyme active site (Qamsari, Kasra and Nejad, 2011). The loss of lipolytic activity from lipase from H1 (*P. reinekei*) and H3 (*P. brenneri*) in $ZnSO_4$ could be explained due to presence of SO_4^{2-} ions, rather than because of Zn^{2+}. The activity of H1 (*P. reinekei*) and H3 (*P. brenneri*) lipase was unaffected by the presence of Ca^{2+}, Mg^{2+}, K^{+}, Na^{+}, Co^{2+}, Mn^{3+} ions. This suggested that lipases from H1 (*P. reinekei*) and H3 (*P. brenneri*) are unaffected by metal ions which have been shown to stabilize some enzymes (Rahman *et al.*, 2005). The presence of Ca^{2+} and Mg^{2+} ions has been reported to enhance the hydrolytic activity of lipases (Posner and Morales, 1972; Rukman and Henny, 2015). Enhanced activity in the presence of Ca^{2+} and Mg^{2+} is contributed due to presence of negative change on the catalytic triads of most lipases (due to negatively charged carboxylate side-chain aspartyl or glutamyl residues), which are brought together by folding of the polypeptide chain. These polypeptide chains become cross-linked by the Ca^{2+}/Mg^{2+} bridge, and the enzyme-Ca^{2+}/Mg^{2+} complex thus becomes more rigid and stable (Kyu Kim *et al.*, 1997).

Though no significant effect of metal ions was observed on lipase from H1 (*P. reinekei*) and H3 (*P. brenneri*); activity was significantly affected in the presence of the chelating agent EDTA,

indicating that both lipases require metal ions. The activity of lipase from *P. aeruginosa* AAU2 has been reported to be unaffected by EDTA (Bose and Keharia, 2013); however lipase from *Pseudomonas putida* 3SK, *Pseudomonas stutzeri, Pseudomonas* sp. DMVR46 displayed higher activity in presence of Ca^{2+} ions (Lee and Rhee, 1993; Parwata, Asyari and Hertadi, 2014; Patel, Nambiar and Madamwar, 2014).

Significant loss in lipolytic activity for lipase from H1 (*P. reinekei*) and H3 (*P. brenneri*) was observed in the presence of 1M urea. Urea molecules interrupt the intra-chain hydrogen bonds in the enzyme and caused direct denaturation (Monhemi *et al.*, 2014). However, lipase from *Pseudomonas* sp. *AG-8* and *Pseudomonas* sp. 42A2 has been shown to be stable in 6M urea (Sharma, Tiwari and Hoondal, 2001; Bofill *et al.*, 2010).

Non-ionic detergents do not interact extensively with the protein surface and are therefore considered mild; ionic detergents on the other hand, in particular SDS, binds non-specifically to the enzyme surface, leading to unfolding (Mogensen, Sehgal and Otzen, 2005). Interestingly, in the presence of 10mM (0.28% w/v) SDS an enhanced activity of lipase from H1 (*P. reinekei*) was noted (see Table 5.3). However, lipase from *Pseudomonas aeruginosa* KM10 has been observed to lose 29% of activity in the presence of 1% (w/v or 34.68mM) SDS (Qamsari, Kasra and Nejad, 2011) and lipase from *Pseudomonas aeruginosa* SRT9 lost 71% activity after 30 mins with 1% (w/v) SDS (Borkar, Bodade, Srinivasa R. Rao, *et al.*, 2009). These losses in activity are in line with lipolytic activity loss from lipase of H3 (*P. brenneri*; see Table 5.3). An enhanced activity of lipase from H1 (*P. reinekei*) could be explained by the concentration of SDS. Below the Critical Micelle Concentration CMC (8.2mM or 0.24% w/v) SDS binds to the lid of lipase and activates it by conformational changes and the enzyme requires less interfacial activation (Salameh and Wiegel, 2010). Besides direct activation or inactivation, detergents may also alter the hydrophobicity of the enzyme and affect micelle formation (ratio of free-to micellar substrate), and thus the availability of substrate to the enzyme (Kubler *et al.*, 2017).

Purified lipase from H1 (*P. reinekei*) and H3 (*P. brenneri*) upon treatment with 4-mercaptoethanol showed no loss in lipolytic activity. This suggests an absence of disulfide bonds in both the purified

lipases. Conversely, a significant increase in lipolytic activity of H1 (*P. reinekei*) lipase, similar to that previously observed with lipases from *Streptomyces bambergiensis* OC 25-4 (Ugur *et al.*, 2014) and *Pseudomonas aeruginosa* BN-1 (Syed *et al.*, 2010), was observed in presence of 4-mercaptoethanol. Also, no loss in activity has been observed for lipases, for example, from *P. stutzeri* LC2-8 at 0.05mg/ml 4-mercaptoethanol (Cao *et al.*, 2012). Lipases from other *Pseudomonas* strains, for example, *Pseudomonas aeruginosa* AAU2, *Pseudomonas* sp. DMVR46 (Bose and Keharia, 2013; Patel, Nambiar and Madamwar, 2014) have shown a reduction in lipolytic activity after incubation with 4-mercaptoethanol, indicating the presence of disulphide bonds in these lipases.

No significant change ($p \leq 0.05$, t-test) in activity was observed in H3 (*P. brenneri*) lipase in the presence of detergents such as Triton X-100 and Polysorbate-80 (Tween 80). However, for the lipase from H1 (*P. reinekei*) a significant decrease in activity was observed in the presence of Polysorbate-80. The effect of detergents on a lipase can be correlated to their hydrophilic/lipophilic balance (HLB), which is defined as the way a detergent distributes between polar and non-polar phases (Bhunia and Dey, 2012). Thus, non-ionic surfactants with low HLB value (Triton X-100: HLB 13.5; and Tween 80: HLB 15) are less detrimental than SDS with a higher HLB of 40 (Bose and Keharia, 2013). The stability in surfactants is desirable for lipases for their potential application in detergent formulations. Purified lipases from H1 (*P. reinekei*) and H3 (*P. brenneri*) presented in this study exhibit inherent stability towards surfactant and detergents which add novel properties for their potential application in detergent formulation.

5.3.3.4. Effect of solvents

The application of lipases for bioconversions within an organic solvent system is advantageous from a biotechnological viewpoint; hence the activity and stability in solvents are considered critical attributes in a lipase. For the production and properties of biodiesel following a transesterification, the choice of the solvent alcohol is crucial because of the associated costs, and the effect on the catalyst itself. Short-chain alcohols, such as methanol and ethanol, are widely used with methanol being preferable due to low cost (Lotti *et al.*, 2015). Lipases from *Pseudomonas* sp. (*P. cepacia* and *P. flourescens*) alone contribute to 21% of worldwide biodiesel production (Heitz

et al., 2016). Hence, to use the lipases from H1 (*P. reinekei*) or H3 (*P. brenneri*) for biodiesel production it is important to understand their lipolytic behaviour in both methanol and ethanol. Other solvents such as cyclohexane, *n*-hexane and *n*-heptane have also been used in biodiesel production and have resulted in enhanced yields (Nie *et al.*, 2006). *P. reinekei* and *P. brenneri,* and their lipases, have proven to be stable in methanol, ethanol, cyclohexane, *n*-hexane and *n*-heptane (see Chapter 4).

To consider fully the potential application of lipase from H1 (*P. reinekei*) and H3 (*P. brenneri*) in biodiesel production, the effect of methanol, ethanol, *n*-hexane, cyclohexane and *n*-heptane on the lipolytic activity of *P.reinekei* and *P. brenneri* lipase at 28°C and 40°C was investigated (Section 5.2.3.6). As indicated by the initial temperature tolerance characterisation (Section 5.2.3.2), lipase from H1 (*P. reinekei*) was not stable >40°C after 45mins (Section 5.2.3.2) making it inappropriate for analysing the effect of solvents at higher temperatures. Since most lipase catalysed transesterification reactions are performed at low temperatures (see Section 5.3.3.2); lipase from H1 (*P. reinekei*) could be used for biodiesel synthesis.

In the present study, the lipase from H1 (*P. reinekei*) retained more than 65% activity in the presence of 30% (v/v) methanol at 28°C (Table 5.5) however, above 30% (v/v) methanol significant effects on lipolytic activity were observed. Similar trends were seen for the lipase from H3 (*P. brenneri*). At 40°C, the lipase from H1 (*P. reinekei*) was stable only in 10% (v/v) methanol and 10% (v/v) ethanol; however, the lipase from H3 (*P. brenneri*) showed higher stability under the same conditions. The loss in activity is most likely the combined effect of solvent as well as temperature. Polar organic solvents, such as methanol or ethanol, are responsible for lipase inactivation either via enzymatic structural changes or by stripping essential water required for enzyme activity (Section 2.6.1.1). The effect on lipolytic activity of various lipases from *Pseudomonas* sp. due to methanol and ethanol has been reported in the literature. A lipase from *Pseudomonas aeruginosa* AAU2 lost 90% of activity in 25% (v/v) methanol after 24h of incubation at 37°C (Bose and Keharia, 2013). Similarly, *Pseudomonas* sp. DMVR46 lipase retained only 8.9% and 30.5% of its activity in methanol and ethanol respectively when 3:1 enzyme:solvent mix was used at 37°C within 4h (Patel, Nambiar and Madamwar, 2014). However, a few lipases have been

reported to be stabilized, and/or activated, in hydrophilic solvents (Cao *et al.*, 2012). Lipases from Antarctic *Pseudomonas* lost only 10% of its activity in the presence of 25% (v/v) methanol, while it showed 101.9% activity in 25% (v/v) ethanol (Ganasen *et al.*, 2016). Similarly, in 25% (v/v) methanol and ethanol a lipase from *Pseudomonas stutzeri* LC2-8 showed enhanced activity of 121% and 168% respectively (Cao *et al.*, 2012); while at 50% (v/v) methanol and ethanol enhanced activity of 112% and 105% respectively (Parwata, Asyari and Hertadi, 2014). The activation of lipases in the presence of some hydrophilic organic solvents could be explained by the interactions of certain amino acid residues with the organic solvent, changing lipase conformation from closed to open form and thereby enhancing lipase activity (Cao *et al.*, 2012). Parwata and colleagues (Parwata, Asyari and Hertadi, 2014) postulated that the ability of a lipase to maintain the essential hydration layer was due to the presence of polar/charged amino acid residues which interact strongly with water molecules. Other researchers have suggested lipase activation is found in hydrophilic organic solvents due to the disruption of aggregates formed between the hydrophobic patches of the lipase (Sugihara *et al.*, 1992).

Despite the negative effects of methanol/ethanol on lipase activity/stability; lipases are widely used for biodiesel production. By varying the transesterification process parameters; methanol/ethanol concentration; enzyme concentration; reaction time and temperature, it is possible to reduce the adverse and destabilising effects of methanol. In the case of *Pseudomonas aeruginosa* AAU2 lipase, biodiesel was produced by using a reaction mixture of 1:4 molar ratio (jatropha oil:methanol); 300U of lipase at 40°C and step wise addition of methanol (Bose and Keharia, 2013). Similarly, lipase from *Pseudomonas fluorescens* produced higher biodiesel yields when 3:1 (methanol: oil) was used at 35°C, methanol tolerance was tackled by step-wise methanol addition (Guldhe *et al.*, 2015). By using the stability data of lipase from H1 (*P. reinekei*) and H3 (*P. brenneri*) in different concentrations of methanol and ethanol and at different temperatures it may be possible to formulate a novel reaction mixture for biodiesel production (see Chapter 8).

Hydrophobic organic solvents with higher log P possess a reduced ability to strip essential water from the enzyme than hydrophilic solvents (low log P; Section 2.6.1.1). Hence, lipases tend to be more stable and active in high log P solvents (cyclohexane, *n*-hexane, *n*-heptane log P of 3.2, 3.86, 4.39 respectively). In the present investigation, a 2- to 4-fold increase in lipolytic activity was observed for H1 (*P.reinekei*) and H3 (*P. brenneri*) lipase in the presence of 50% (v/v) hydrophobic

solvents (cyclohexane, *n*-hexane and *n*-heptane) irrespective of incubation temperature after 24h of incubation (see Table 5.4, 5.5). The activation by hydrophobic solvents could be due to the interaction of solvent with hydrophobic amino acid residues present in the lid/flap covering the catalytic site of the enzyme, thereby maintaining the enzyme in a flexible open conformation and consequently increasing its activity (Bose and Keharia, 2013). Similar observations have been found in a lipase from *Pseudomonas stutzeri*, where the activity increased to 111% when it was incubated in 50% (v/v) *n*-hexane at 37°C for 30min (Parwata, Asyari and Hertadi, 2014).

5.3.3.5. Substrate specificity and enzyme kinetics

Substrate specificity of lipases provides useful information for the rapid selection of enzyme/substrate partnerships to catalyse desired reactions. Lipase from H3 (*P. brenneri*) showed wide substrate specificity (from medium length to long chain phenyl esters i.e. C8:0 to C16:0; Figure 5.14), however; lipase from H1 (*P. reinekei*) showed greater specificity towards medium chain phenyl esters (C8:0-C10:0). None, or minimal, hydrolysis was seen from both the lipase sources (H1 and H3) towards C2:0. Lipase from H1 (*P. reinekei*) displayed a similar substrate specificity to a lipase from *Pseudomonas stutzeri* LC2-8 (Cao *et al.*, 2012). A preference for long chain fatty esters is a desirable characteristic for lipases and has been seen in many lipases (X. Li *et al.*, 2014). Since both the lipases displayed specificity towards medium and long chain fatty acid phenyl esters, they are ideal candidates for transesterification involving oils from vegetable sources or from microalgae (see Chapter 8).

The low K_m for the lipases from H1 (0.48±0.02mM) and H3 (0.37±0.09mM) indicates a high affinity of these enzymes towards *p*NP-Palmitate. Higher kinetic parameters of lipase from H3 towards pNPP, compared to lipase from H1, aligns with the substrate specificity results; where lipase from H3 showed higher activity towards pNPP than lipase from H1 (Figure 5.14). High substrate specificity (K_m of 0.440mmol/L) and kinetic activity (V_{max} of 556nmol/mL/min) of lipase from *Geobacillus thermodenitrificans* AV-5 have also been reported using *p*-nitrophenyl laurate as substrate (Christopher *et al.*, 2015). Conversely, lower values of K_m (0.338mM) have also been observed for lipase from Bacillus sp. (Jain and Mishra, 2015) using *p*-NP butyrate as substrate. K_m values as low as 0.037mM and a V_{max} of as high as 188.6mmoL/L/min using *p*-NPP hydrolysis have also been reported for lipases from *Pseudomonas aeruginosa* SRT 9 (Borkar, Bodade,

Srinivasa R Rao, *et al.*, 2009). In this study, the low K_m values (0.48±0.02mM and 0.37±0.09mM), coupled with higher specificity towards long chain esters for *P. reinekei* (H1) lipase and H3 (*P. brenneri*) lipase, are beneficial for biodiesel synthesis.

5.4. CONCLUSION

A high titre of lipase from H1 (*P. reinekei*) can be obtained using 1% (w/v) supplementation of *L-Lysine* in basal lipase producing media, at pH 6.5±0.2; while for lipase from H3 (*P. brenneri*) 1% (w/v) peptone in basal lipase producing media at pH 6.8±0.2 will generate a high titre. An initial inoculum of 15% (v/v) and 2.5% (v/v) is required, followed by a 6-day and 2-day fermentation for lipase production from H1 (*P. reinekei*) and H3 (*P. brenneri*) respectively at 28°C, with constant shaking at 200rpm.

The lipase from the H1 (*P. reinekei*) cell free supernatant can be isolated by a two-step chromatography process, using Q-Sepharose in both negative and positive modes of chromatography with an overall yield of 13.72%. It is important to have 5% (w/v) sorbitol in the final purified lipase solution to avoid protein precipitation. However, partially purified lipase from H3 (*P. brenneri*) cell free supernatant can be isolated by alkaline precipitation followed by bind and elute Q-Sepharose chromatography purification with an overall yield of 56.89%.

The novel, purified lipase from H1 (*P. reinekei*) had a molecular mass of ~55kDa and an optimum pH of 5.0±0.2; however, the lipase is stable between pH 5.0-9.0. The purified lipase from H1 (*P. reinekei*) was not thermostable, although it showed half-life of 89mins at 40°C. The partially purified lipase from H3 (*P. brenneri*) was thermostable with half-life of 190mins at 60°C and was very stable between pH 5.0-9.0. Both lipases (from H1 and H3) require metal ions for their activity and were not affected by the presence of common ions or detergents. Similarly, the presence of common detergents and reducing agents such as 4-mercaptaethanol, did not affect these lipases. The purified lipases were stable in different concentrations (up to 50% v/v) of common organic solvents at 28°C and 40°C. The presence of cyclohexane, *n*-hexane and *n*-heptane in solution enhanced their lipolytic activity. Both lipases also displayed specificity towards medium and higher phenyl esters making these lipases a strong potential candidate for biodiesel production.

Chapter 6: Lipase entrapment

6.1. INTRODUCTION AND OBJECTIVES

With the advance of recombinant DNA technology and high-throughput screening, the cost of finding and employing a reaction-specific enzyme has been significantly reduced. However, most enzymes lose their activity during long-term reaction(s) and/or storage, mainly due to denaturation (Homaei, Sariri and Stevanto, 2013). Furthermore, a significant challenge for industrial application(s) of enzyme(s) is the recovery of enzymes from reaction media for their repeated use, and to enhance product purification. On the other hand, once immobilized or entrapped, the stability of an enzyme is often enhanced; possibly due to a more fixed tertiary structure (Bagi, Simon and Szajáni, 1997; Anwar *et al.*, 2009; Shikha, Thakur and Bhattacharyya, 2017) or the inability of denaturants to interact with the enzyme (Kanmani *et al.*, 2015). Various enzyme immobilization methods such as adsorption, covalent bonding, entrapment, and cross-linking have been developed (Mohamad *et al.*, 2015). Covalently linking an enzyme to an insoluble carrier, via activated functional groups, typically generates a robust immobilized enzyme (Homaei, Sariri and Stevanto, 2013). However, covalently bonded enzymes face loss of their molecular dynamics and changes in their conformation; often resulting in limited accessibility of the active site (Lee and Nhan, 2018). Conversely, physical adsorption relies mainly on van der Waals forces, hydrogen bonding, hydrophobic interaction and electrostatic interactions between the enzyme and the surface of insoluble carriers. This kind of adsorption can circumvent enzyme deactivation which is often caused during covalent attachment and cross-linking methods due to structural/chemical modifications in enzyme structure (Marcela *et al.*, 2016).

With recent advances in nanotechnology various nanomaterials have been developed for enzyme immobilization. Nanoparticles not only have a very high surface area (giving high enzyme loading) and low diffusion resistance (yielding effective catalysis) but also have unique properties (e.g. optical, electrical, thermal, mechanical: (Lazar and Szabo, 2018). However, the limiting factor for their use in enzyme immobilization is the requirement for high-speed centrifugation in their separation from solutions (for re-use). Magnetic nanoparticles have, however, been employed for lipase immobilization (Ansil, Katja and Mayumi, 2003; Wu *et al.*, 2009). Alternatively, gold

nanoparticles (AuNPs) are more appealing for biotechnological and medical applications due to their inert, nontoxic and biocompatible nature (Khan *et al.*, 2014). The surface of AuNPs can be easily modified for specific applications. For applications in biocatalysis the possibility to attach enzymes on supports through stable interactions e.g. electrostatic interactions, could be useful (Venditti *et al.*, 2015). Several natural polymeric materials like cellulose, alginate, collagen, chitosan and starch, and some conductive polymers such as polyaniline and Nafion have been used for encapsulating/entrapping enzymes (Chang *et al.*, 2018). Enzymes entrapped inside these solid particles are protected from the external harsh reaction environment and, as a result, the stability of the enzyme is enhanced/unaffected. A disadvantage of this method of enzyme immobilization is the lower apparent activity of the enzyme due to the mass transfer resistance in the encapsulated matrix (Hari Krishna and Karanth, 2002; Won *et al.*, 2005; Talekar and Chavare, 2012; Sharma, Sharma and Majumdar, 2014; Badgujar, Pai and Bhanage, 2016; Ugur Nigiz, 2016).

The overall aim of this chapter was

- to immobilize/entrap lipases from three different sources i.e. *P. reinekei* (H1), *P. brenneri* (H3) and PPL (standard-commercial enzyme preparation)
- to examine effect of entrapment/immobilization on stability/activity of entrapped lipase compared to free lipase (see Chapter 5).

6.2. RESULTS

6.2.1. Gold Nanoparticles

6.2.1.1. Properties of nanoparticles: size and charge

The size (Figure 6.1a) of synthesized gold nanoparticles varied from 11.7-78.82nm, with an average size of 24.49nm (Figure 6.1a) and an average charge of -30.8mV noted, as determined by the Nanoseries Zeta-sizer (Figure 6.1b). The concentration of AuNPs was estimated to be 235mg/L by atomic absorption spectroscopy (see Appendix H). Figure 6.1(c) shows the absorption spectra of synthesized AuNPs from which λ_{max} of the synthesized gold nanoparticles was estimated to be 524nm. The size distribution and shape of AuNPs was validated by Scanning Electron Microscopy (SEM), performed in the FOCAS Research Institute, TU Dublin. The shape of the synthesized AuNPs was observed to be spherical (Figure 6.2).

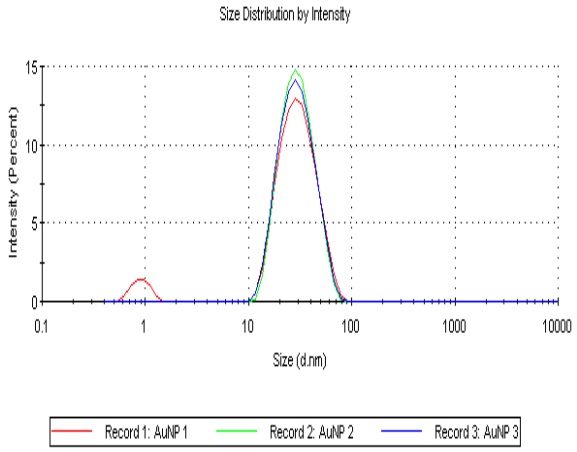

(a)

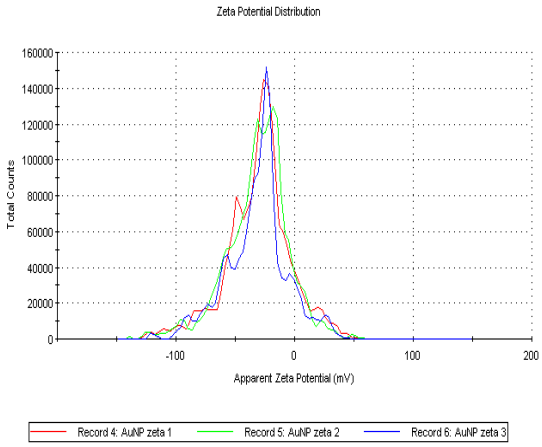

(b)

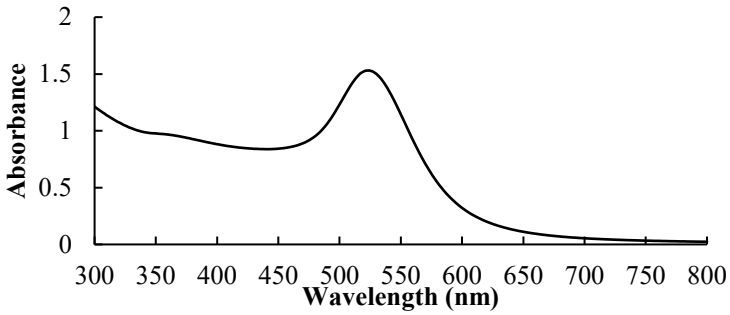

(c)

Figure 6.1: Properties of synthesized AuNPs (a) Size diztribution by intensity where x-axis represents size (nm), y axis is intensity (%) , (b) charge/ zeta potential distribution, x-axis is zeta potential (mV), y-axis is total count and (c) absorbance distribution of synthesized AuNPs using the *Nanoseries Zeta-sizer* and absorbance spectrophotometer respectively. Figure (a, b) represents data of three different AuNPs representative samples, while figure (c) represents average of three different AuNP samples.

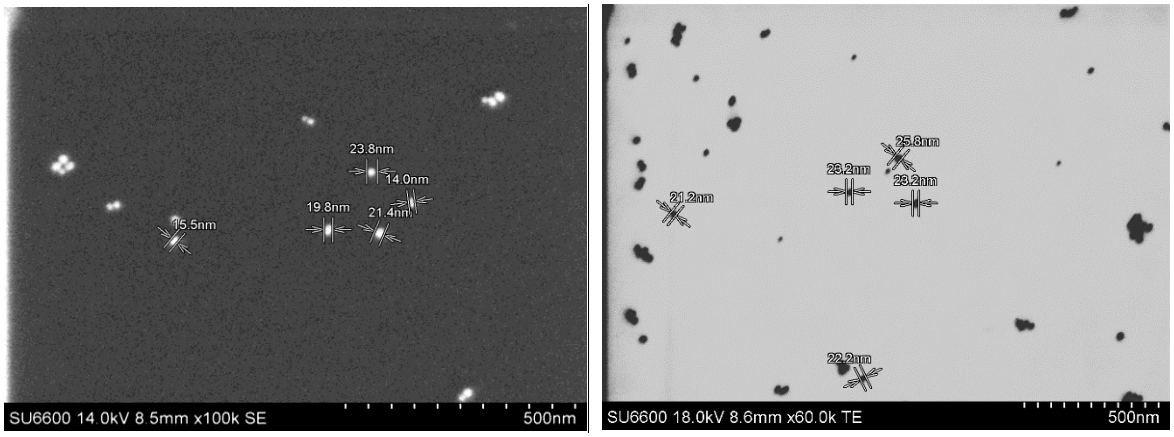

Figure 6.2: Scanning Electron Microscopy of gold nanoparticles. The AuNPs appeared spherical in shape from SEM analysis. SEM of AuNPs confirm the size of the particles lay in the range between 11.7-78.82nm as estimated by the *Nanoseries Zeta-sizer*.

6.2.1.2.Effect of solvents

The effect of 20% (v/v) methanol, 20% (v/v) ethanol and 50% (v/v) *n*-hexane, 50% (v/v) *n*-heptane and 50% (v/v) cyclohexane on the stability of AuNPs (synthesized as per section 3.2.5.1.1) was determined by incubating the AuNPs in these solvents for 30mins at room temperature. Changes in size, charge and λ_{max} for each solvent was verified via the Nanoseries Zeta-sizer and spectrophotometer using wavelength scanning from 300-800nm respectively. Figure 6.3 (a, b) represents the change in size; Figure 6.3 (c, d) represents change in charge; Figure 6.3 (e) shows the change in absorbance spectra; while Figure 6.3 (f) represents change in morphology of AuNPs in the presence of different solvents. Table 6.1 shows the change in size, charge and λ_{max} of AuNPs after addition of 20% (v/v) methanol, ethanol. Due to the formation of an insoluble bilayer in presence of *n*-hexane, *n*-heptane and cyclohexane; the AuNPs treated with these solvents were not examined further.

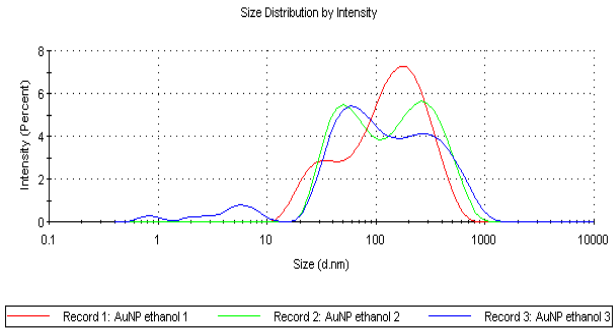

(a)

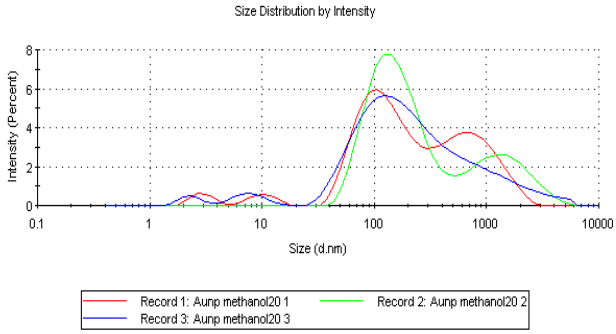

(b)

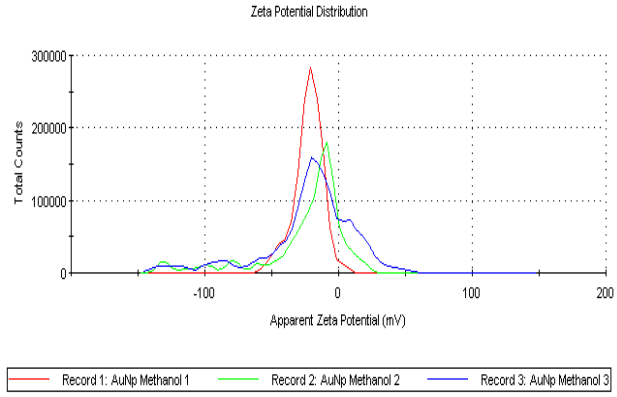

(c)

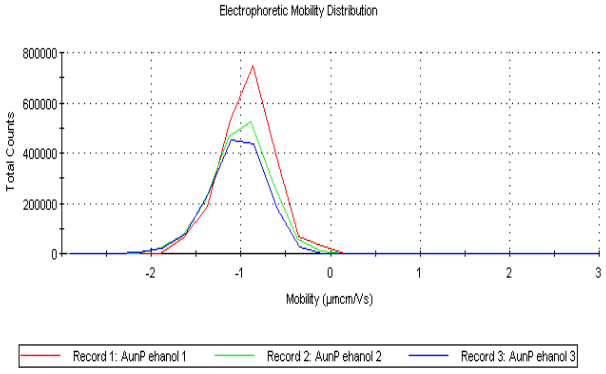

(d)

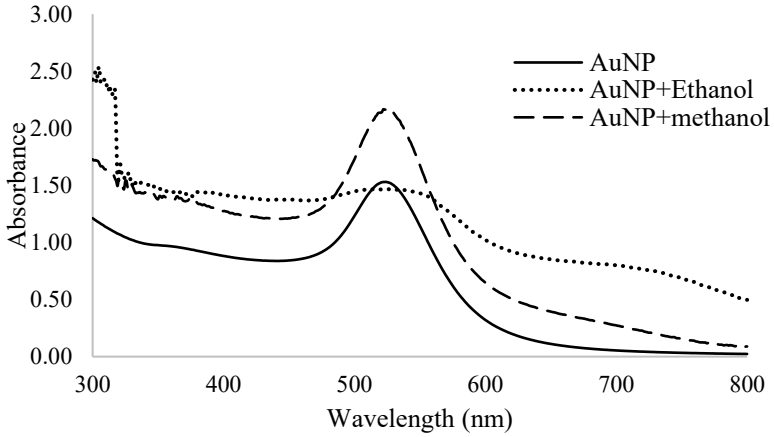

(e)

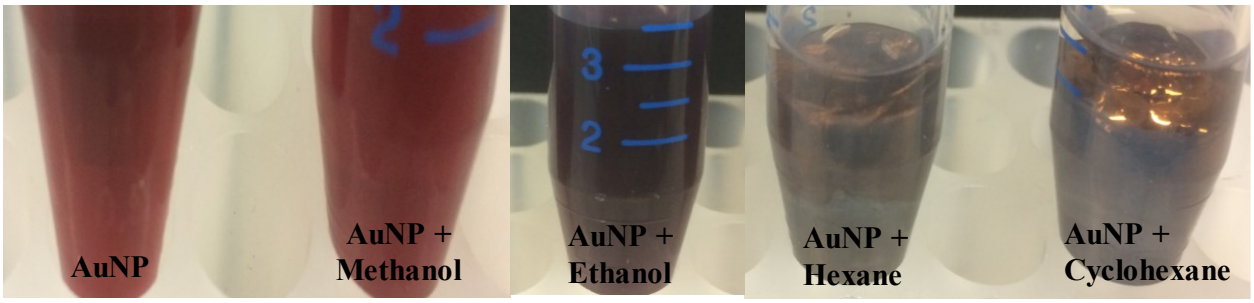

(f)

Figure 6.3: Overview of the effect of selected solvents on gold nanoparticles. (a, b) represents change in size where x-axis is size in nm and y-axis is intensity (%) (c, d) change in charge where x-axis is zeta potential (mV) and y-axis is total counts; (e) is the absorbance distribution profile of AuNPs in the presence of 20% methanol (v/v) and 20% ethanol (v/v) respectively. The graphs (a, b, c, d) represents three different representatives of AuNPs. (f): represent the change in AuNPs appearance after addition of 20% (v/v) methanol, ethanol and 50% (v/v) Hexane, cyclohexane respectively.

Table 6.1: Summary of change in size (Z-average nm), charge (zeta potential) and λ_{max} of AuNPs after addition of methanol and ethanol. An increase in particle size was observed for both methanol and ethanol. Similarly, change in charge (zeta potential) and λ_{max} was observed indicating effect of solvents on stability of AuNPs.

Component	Z-average(nm)	Zeta Potential	λ_{max}
AuNPs	24.49	-30.8mV	524
20% (v/v) Methanol	74.31	-52mV	305
20% (v/v) Ethanol	131.2	-24.6mV	522

6.2.1.3.Physical adsorption and covalent binding of lipase onto glutathione reduced AuNPs

6.2.1.3.1. Physical adsorption

A change in AuNPs colour from pink to blue was observed after addition of lipase. Figure 6.4(a), (b) and (c) represents the size, charge and λ_{max} of AuNPs after addition of lipase solution. After addition of the lipase, the size of the AuNPs increased from 24.49nm to 331.2nm, while a shift in zeta potential was also observed (Table 6.2). Although a change in size and zeta potential is an indication of physical change in AuNPs that could be ascribed to physical adsorption of lipase, no significant ($p \geq 0.05$, t-test) change in free lipase activity was observed after treatment of enzyme with AuNPs. The immobilization efficiency (measured as per section 3.2.5.1.4) was zero. This indicated no physical adsorption between lipase and AuNPs.

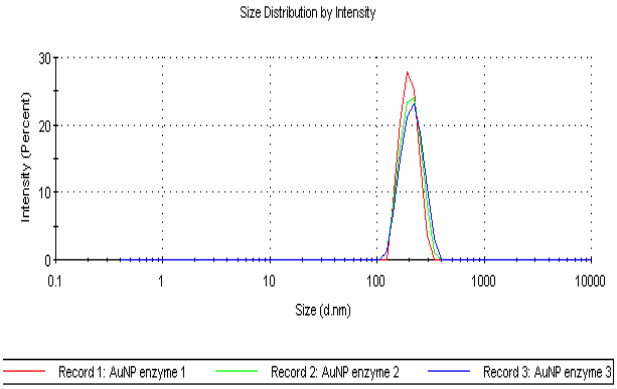

(a)

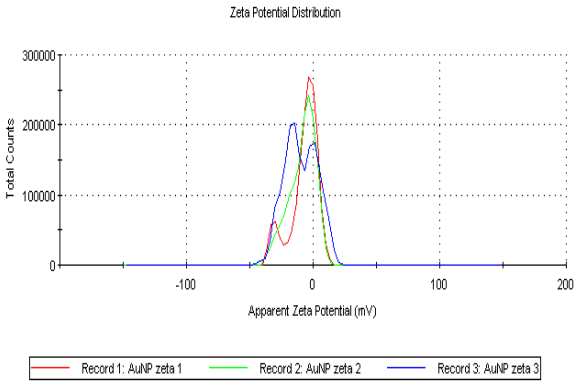

(b)

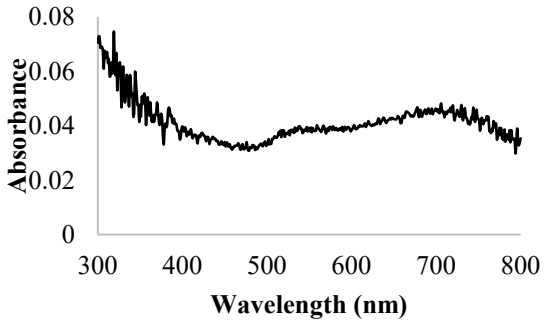

(c)

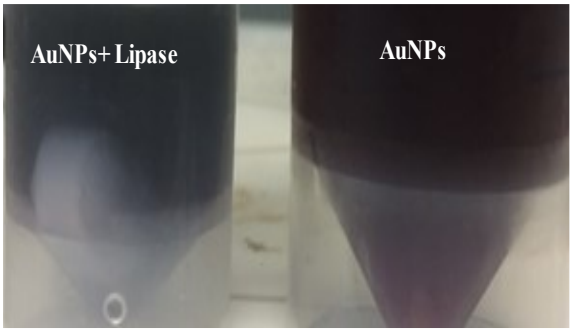

(d)

Figure 6.4: Overview of the effect of attempted lipase adsorption on gold nanoparticles. (a) Size distribution by intensity, x-axis is size (nm) while y-axis is intensity (percent); (b) charge distribution (zeta potential distribution), x-axis represents zeta potential (mV) while y-axis represents total count and (c) absorbance spectrum of AuNPs after addition of enzyme solution (lipase); (d): Change in AuNPs appearance from ruby red to blue after addition of enzyme solution (lipase) indicates change in AuNPs properties.

Table 6.2: Summary of size, charge and λmax of AuNPs after addition of enzyme solution (lipase). A change in all the physical and chemical properties was observed after treatment of AuNPs with lipase. However, no change in lipase activity before and after the reaction indicates failure of lipase physical adsorption on AuNPs.

Component	Z-average(nm)	Zeta	λ_{max}
AuNPs	24.49	-30.8mV	524
AuNPs+ lipase	331.2	-8.45mV	319

The absence of physical adsorption of lipase on AuNPs prompted the requirement for lipase immobilization on AuNPs via covalent binding.

6.2.1.3.2. Covalent binding of lipase on AuNPs modified with GSH

NHS-EDC activated GSH-AuNPs were incubated with the lipase solution in 1:1 ratio (enzyme concentration: AuNPs concentration) as described in Section 3.2.5.1.3. Precipitation of AuNPs was immediately observed. Figure 6.5 shows the precipitated AuNPs after addition of lipase solution. No significant difference ($p \geq 0.05$, t-test) in lipase activity was observed in the AuNPs free solution before and after immobilization, indicating a lack of covalent bonding between lipase and AuNPs.

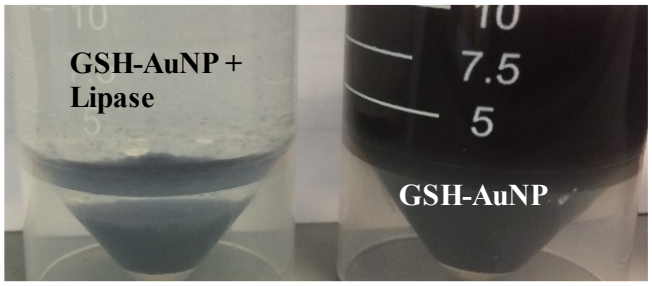

Figure 6.5: Precipitation of glutathione reduced-AuNPs (GSH-AuNPs; left) dispersed in phosphate buffer pH 9.0 was observed immediately after addition of enzyme solution (lipase) in GSH-AuNP (right) indicating the inability of lipase to bind covalently on AuNPs.

Enzyme was not binding to the AuNPs surface either via physical adsorption or via covalent binding. In that case another mode of entrapment was explored.

6.2.2. Enzyme entrapment and characterisation

The entrapment of the enzyme in alginate beads was attempted. This support matrix does not require covalent modification of the enzyme. The entrapment was carried out as described in Section 3.2.5.2.

6.2.2.1. *Reaction time*

Enzyme loaded calcium alginate beads (curing as shown in Figure 6.6) were incubated with *p*-NPP substrate for 60mins. Figure 6.7 represents the formation of yellow color due to liberation of p-NP from p-NPP by lipase entrapped in alginate beads. The rate of product (*p*-NP) formation was compared between the free and entrapped enzyme. Figure 6.8 represent the time course liberation of p-NP (product) from *p*-NPP (substrate) by free and entrapped lipases.

Figure 6.6: The curing of calcium alginate beads with time in $CaCl_2$ solution. With increased incubation (15mins, 30mins and 60mins depicted in the images from left to right), the beads turned from clear to opaque due to hardening. All the enzyme entrapped, and non-enzyme entrapped calcium alginate beads, were left to cure in $CaCl_2$ solution for 60mins before further washing and storage.

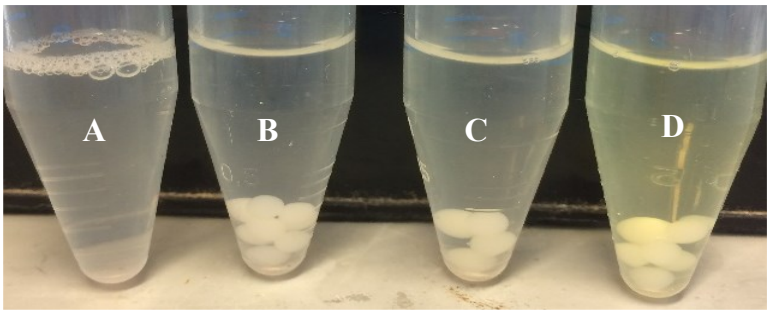

Figure 6.7: Formation of *p*-NP after degradation of *p*-NPP from the lipase entrapped in calcium alginate beads. 60 minutes of incubation, (A)-lipase substrate without any additives, (B): Lipase substrate incubated with calcium alginate beads without any enzyme (-ve control), (C): lipase substrate incubated with calcium alginate beads entrapping porcine pancreas lipase (+ve control), (D): lipase substrate incubated with calcium alginate beads entrapping *P.reinekei* lipase. Clear evidence of *p*NP formation can be observed as development of yellow colour.

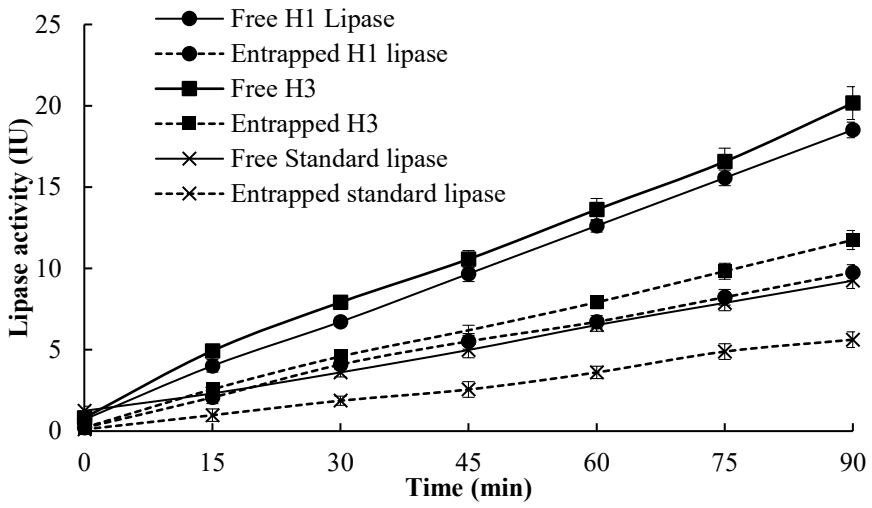

Figure 6.8: *p*-NPP spectrophotometric determination of optimal time required to obtain equal lipase activity between free lipase and lipase entrapped in calcium alginate beads. 60 mins of incubation time for enzyme entrapped in calcium alginate beads resulted in the same activity as 30 mins of free enzyme. Standard lipase is positive control (PPL) while p-NPP substrate was used as negative control. No spectrophotometric absorbance was obtained for negative control.

A 60mins incubation of entrapped lipase resulted in equal amounts of product synthesis (with the same enzyme activity) as for a 30mins free lipase reaction (Figure 6.8); a difference of approximately two-fold in activity. Hence, for the comparison of lipase activity between free and entrapped enzyme, an incubation time of 60mins was chosen for all further experiments.

6.2.2.2. *Effect of pH*

No significant difference ($p \geq 0.05$, t-test) in the pH stability of lipase was observed when entrapped lipase activity was compared to free lipase activity. Figure 6.9 (a, b, c) represents the stability of entrapped H1 (*P. reinekei*), H3 (*P. brenerri*) and porcine pancreas lipase (standard) at various pH values compared to the stability of free lipase.

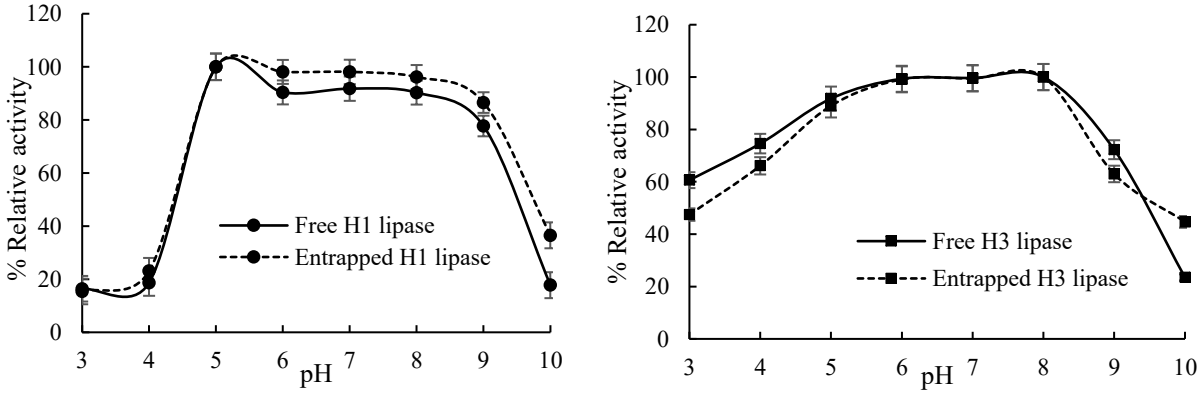

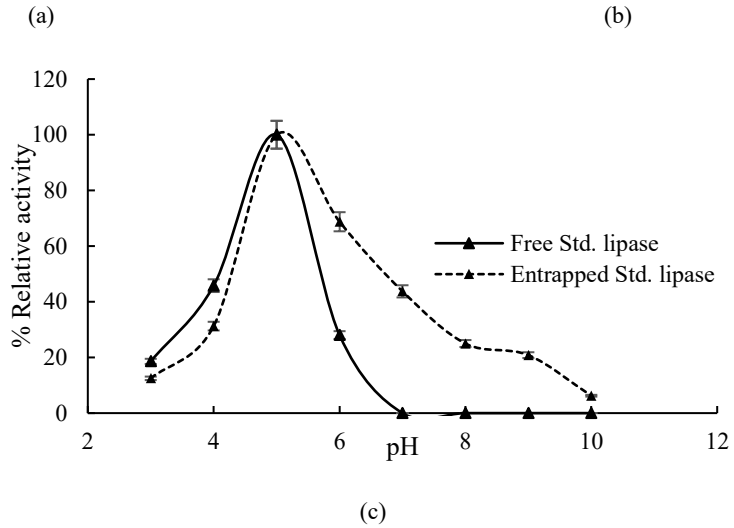

Figure 6.9: For pH stability studies, residual activities of entrapped H1 lipase (*P. reinekei*; a), entrapped H3 lipase (*P. brenneri*; b) and entrapped PPL (standard; c) were measured after 24h of incubation at 28°C in the presence of different pH buffers (pH 3.0±0.2 to pH10±0.2, section 3.2.4.1). % relative activity was calculated relative to highest activity obtained. Data represented here is the comparison of free and entrapped lipase, while values are the mean of three assays and error bars represent standard deviation.

Significantly enhanced stability ($p<0.05$, t-test) was observed for porcine pancreas lipase (standard) from pH 6.0 to pH 9.0 after entrapment (Figure 6.9 c).

6.2.2.3. *Thermostability*

The stability of entrapped lipase was examined following incubation at three different temperatures for one hour (Figure 6.10).

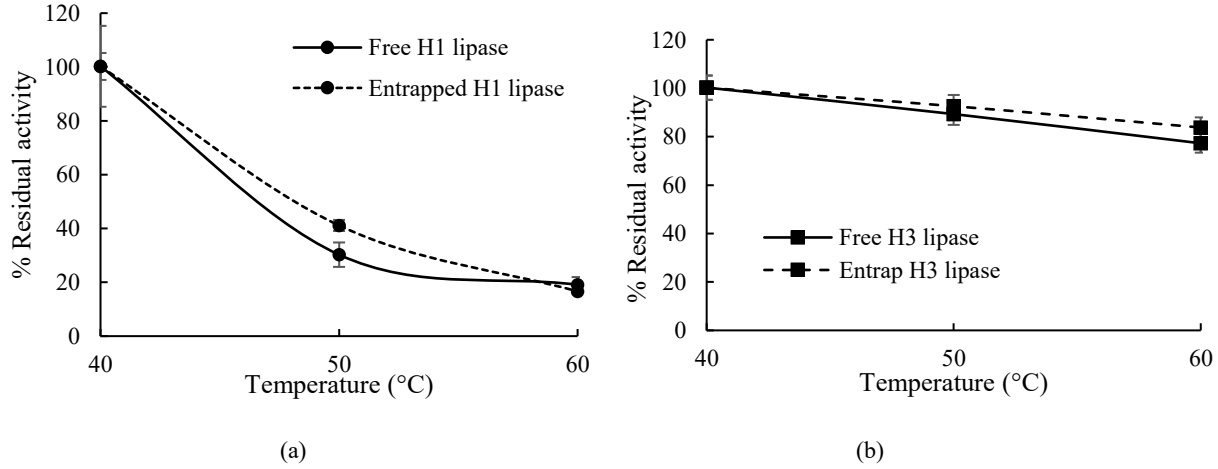

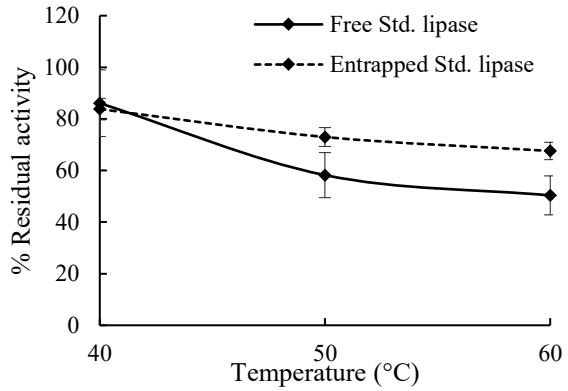

(c)

Figure 6.10: Thermal stability of entrapped purified lipase from H1 (*P. reinekei*; a), H3 (*P. brenneri*; b) and porcine pancreas lipase (standard; c) and was studied by incubating the entrapped enzymes at 40, 50, 60°C for 1h in Tris-HCl pH 7.0±0.2. Residual activity: the activity (%) at each temperature was measured and compared to that at 0hr. Data represented here are the mean of three assay values and error bars represent standard deviation.

The entrapped lipase was found to be stable, with no significant difference ($p \geq 0.5$, t-test) in stability at 40°C, 50°C and 60°C when compared to free lipase.

6.2.2.4. *Effect of additives*

A significant change ($p \leq 0.5$, t-test) in stability of entrapped lipase from all three sources (H1, H3 and porcine pancreas) was observed in the presence of EDTA and detergents (Poly 80, triton X-100 and SDS). Entrapment of lipase in calcium alginate beads enhanced the stability of lipase in the presence of EDTA. The effect of different concentrations of EDTA on the stability of lipase was estimated. Figure 6.11 represents the loss in lipase activity from entrapped lipase in the presence of different concentrations of EDTA. A 50% loss in relative activity was observed in the presence of 5.0mM EDTA. Further increase in EDTA concentration resulted in complete loss of lipase activity from the entrapped enzyme.

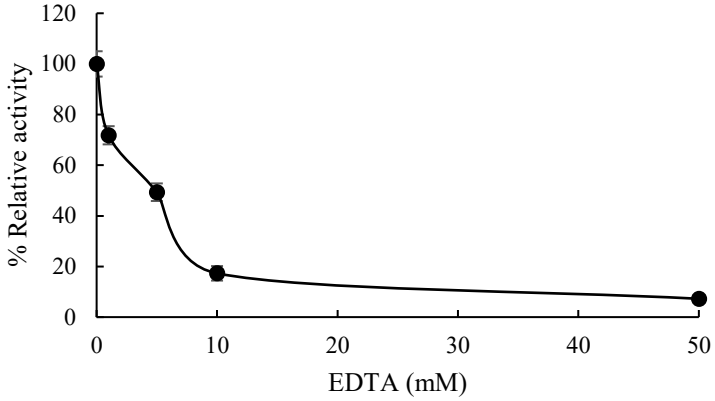

Figure 6.11: The effect of various concentration of EDTA on the stability of entrapped H1 lipase. All samples were prepared in 50 mM Tris-HCl buffer pH 7.0±0.2 with different concentrations of EDTA and were incubated at 28°C for 24h. Relative activity (%) was calculated relative to that of entrapped enzyme with same conditions but no EDTA after 24h of incubation. Data represented here are the mean of three assay values and error bars represent standard deviation.

In the presence of 10mM detergents (Polysorbate 80, Triton X-100 and SDS), significant ($p \leq 0.01$, $p < 0.0001$, t-test) reductions in enzyme activity were observed for all three sources of entrapped lipase (H1, H3 and porcine pancreas; Table 6.3a). The loss of activity from entrapped lipase in the presence of detergents was also reported in the surrounding buffer (Table 6.3b).

Entrapment of lipase in calcium alginate beads also enhanced lipase stability towards 1M urea. A significant ($p \leq 0.5$, t-test) increase in lipase stability was observed for all three lipase sources (H1, H3 and porcine pancreas) after incubation in 1M urea. The effect of metal ions; such as Co^{2+}, Mn^{3+}, Fe^{3+}, Zn2+ was observed in entrapped lipase from H3 (*P. brenneri*). An extremely significant ($p < 0.0001$, t-test) increase in lipase activity was observed after entrapment of lipase from H3 in the presence of 10mM $FeCl_3$ (Table 6.3a). No other significant changes (increase/decrease) in stability/activity were observed after entrapment of lipase(s) in the presence of other additives (Table 6.3a).

Table 6.3a: The effect of various metal ions and effector molecules/chemicals on the stability of entrapped and free purified lipase from H1 (*P. reinekei*), H3 (*P. brenneri*) and lipase from porcine pancreas (standard). All samples were prepared in 50 mM Tris-HCl buffer pH 7.0±0.2 and were incubated with 10mM concentration of respective additive (except EDTA and Urea) at 28°C for 24h. Relative activity (%) was calculated relative to that of entrapped enzyme at same temperature but no additive after 24h of incubation. Data represented here are the mean of three assay values, with standard deviations noted. The symbols *p ≤ 0.05, **p ≤ 0.01, ***P<0.001, ****p < 0.0001 represents significant, very significant and extremely significant change in lipase stability (after entrapment) based on t-test.

% Relative activity						
	Lipase from H1 (*P. reinekei*)		Lipase from H3 (*P. brenneri*)		Porcine Pancreas Lipase (Standard)	
Additive	Free	Entrapped	Free	Entrapped	Free	Entrapped
Control (no Additive)	100.00 ± 0.00	100.00 ± 0.00	100.00 ± 0.00	100.00 ± 0.00	100.00 ± 0.00	100.00 ± 0.00
$CaCl_2$	99.92 ± 2.65	97.78 ± 2.77	106.03 ± 2.76	103.03 ± 2.37	64.56 ± 2.14	75 ± 2.99
$MgCl_2$	94.67 ± 1.57	104.21 ± 2.06	93.52 ± 2.32	100.21 ± 2.49	62.81 ± 2.02	60 ± 2.65
KCl	95.30 ± 1.16	94.76 ± 2.19	103.12 ± 2.24	101.76 ± 2.19	55.35 ± 2.09	53 ± 1.33
NaCl	100.95 ± 2.23	104.76 ± 2.19	99.84 ± 2.18	104.76 ± 2.19	55.00 ± 2.37	46.5 ± 1.85
EDTA (1mM)	26.25 ± 1.39	75.29 ± 2.65*	0.00	71.82 ± 2.09***	40.96 ± 1.49	50 ± 2.43
4-Mercaptaethanol	122.22 ± 2.22	123.17 ± 2.46	103.10 ± 2.13	123.17 ± 2.46	20.88 ± 2.72	50 ± 2.73*
Polysorbate-80	62.25 ± 2.39	33.25 ± 2.39**	98.29 ± 2.11	38.25 ± 2.39****	45.88 ± 2.29	25 ± 1.21**
Triton X-100	100 ± 1.50	45.16 ± 1.87****	89.94 ± 2.75	42.16 ± 2.87****	91.05 ± 2.26	3.50 ± 1.37****
SDS	110.03 ± 2.17	4.60 ± 1.31****	59.70 ± 1.46	9.60± 1.32****	54.47 ± 2.36	15.5 ± 1.31***
Urea (1M)	84.16 ± 2.87	99.31 ± 2.35*	61.39 ± 2.24	94.03 ± 2.95**	47.46 ± 2.14	67.46 ± 2.09*
$CoCl_2$	95.84 ± 2.12	91.94 ± 2.42	91.14 ± 2.92	80.61 ± 2.34*	110.26 ± 2.32	90.26 ± 2.47*
$MnCl_3$	103.078 ± 2.93	106.54 ± 2.14	94.55 ± 2.13	121.54 ± 2.06*	94.30 ± 2.61	99.30 ± 2.82
$FeCl_3$	102.95 ± 2.24	98.55 ± 2.63	6.68 ± 1.86	128.56 ± 2.47****	115.70 ± 2.65	105.70 ± 2.93
$ZnSO_4$	81.75 ±2.66	82.05 ± 2.13	0.00	37.06 ± 1.95*	142.46 ± 2.77	121.46 ± 2.14*

Table 6.3b: The effect of various detergents on the leaching of lipase from calcium alginate beads containing entrapped purified lipase from H1 (*P. reinekei*), H3 (*P. brenneri*) and lipase from porcine pancreas (standard). All samples were prepared in 50 mM Tris-HCl buffer pH 7.0±0.2 and were incubated with 10mM concentration of respective detergent at 28°C for 24h.

Lipase source	Detergent	Initial activity (%)	% Activity retained in beads	% Activity in buffer
H1 (*P. reinekei*)	Triton X-100	100.00 ± 0.00	12.42 ± 1.22	37.82 ± 1.44
	Poly-80	100.00 ± 0.00	37.18 ± 1.17	62.16 ± 1.05
	SDS	100.00 ± 0.00	18.26 ± 1.38	62.59 ± 1.55
H3 (*P. brenneri*)	Triton X-100	100.00 ± 0.00	18.59 ± 1.32	30.71 ± 1.09
	Poly-80	100.00 ± 0.00	38.43 ± 1.05	61.41 ± 1.21
	SDS	100.00 ± 0.00	15.68 ± 1.28	54.87 ± 1.98
Std. (Porcine Pancreas)	Triton X-100	100.00 ± 0.00	10.17 ± 1.66	34.22 ± 1.61
	Poly-80	100.00 ± 0.00	30.09 ± 1.54	60.19 ± 1.08
	SDS	100.00 ± 0.00	16.44 ± 1.88	57.24 ± 1.03

6.2.2.5. *Effect of solvents*

A significant loss ($p \leq 0.5$, t-test) in activity was observed for entrapped lipase from all three sources (H1, H3 and porcine pancreas; see Table 6.4) in the presence of methanol after 24h of incubation at 28°C (Table 6.4). At 40°C, no significant ($p \geq 0.5$, t-test) change in stability for entrapped H3 lipase was observed in the presence of methanol or ethanol irrespective of their concentrations. However, free lipase in the presence of *n*-hexane, *n*-heptane and cyclohexane (50% v/v) displayed significant loss of activity, but after entrapment no loss in lipolytic activity was observed for lipase from H1 and H3. This was an extremely significant ($p \leq 0.0001$, t-test) difference in stability/activity when compared to their free forms.

Table 6.4: The effect of various solvents on the stability of entrapped and free purified lipases from H1 (*P. reinekei*) and H3 (*P. brenneri*) was examined along with porcine pancreatic lipase (standard). All samples were incubated in solvents at 28°C and 40°C for 24h. Relative activity (%) was calculated relative to that of entrapped lipase after 24h of incubation at same temperature but without the corresponding organic solvent. Data represented here are the mean of three assays with standard deviation. *p ≤ 0.05, **p ≤ 0.01, ***p≤0.001, ****p < 0.0001 represents significant, very significant and extremely significant difference in lipase stability (after entrapment) based on t-test.

% Relative activity							
		Lipase from H1 (*P. reinekei*)		Lipase from H3 (*P. brenneri*)		Std. Lipase (Porcine pancreas)	
Condition	Additive	Free	Entrapped	Free	Entrapped	Free	Entrapped
28°C 24h	Control (no additive)	100.00 ± 0.00	100.00 ± 0.00	100.00 ± 0.00	100.00 ± 0.00	100.00 ± 0.00	100.00 ± 0.00
	10% Methanol	92.71 ± 2.36	91.12± 2.31	98.64 ± 2.12	99.64± 2.24	37.47 ± 1.60	56.04 ± 2.60*
	20% Methanol	97.86 ± 2.42	78.26 ± 2.27*	80.019 ± 2.59	70.92 ± 2.90*	31.01 ± 1.11	51.08 ± 2.18*
	30% Methanol	70.61 ± 2.21	57.32 ± 2.49*	65.01 ± 2.94	51.01 ± 2.94*	24.09 ± 1.30	50.54 ± 2.05*
	10% Ethanol	92.27 ± 2.02	76.41 ± 2.33*	84.45 ± 2.33	73.45 ± 2.33*	30.23 ± 1.22	48.65 ± 1.86
	20% Ethanol	92.07 ± 2.54	54.75 ± 2.83***	16.60 ± 1.99	0.00	22.26 ± 1.07	39.82 ± 1.98
	30% Ethanol	24.50 ± 1.33	56.85 ± 2.78	18.00 ± 1.08	0.00	24.58 ± 1.38	35.59 ± 1.55
	50% Hexane	193.28 ± 2.93	97.83 ± 2.61****	131.02 ± 2.99	93.02 ± 2.95***	73.45 ± 1.38	70.45 ± 2.38
	50% Cyclohexane	275.95 ± 2.14	95.65 ± 2.21****	122.48 ± 2.74	102.77 ± 2.35***	68.89 ± 2.67	66.89 ± 2.68
	50% heptane	324.37 ± 2.96	96.74 ± 2.91****	128.80 ± 2.71	98.97 ± 2.13***	61.85 ± 2.61	58.85 ± 2.86
40°C 24h	Control (no additive)	100.00	100.00	100.00	100.00	100.00	100.00
	10% Methanol	89.29 ± 2.79	85.86 ± 2.95	102.50 ± 2.02	101.00± 2.09	25.77 ± 1.48	57.48 ± 2.74
	20% Methanol	36.23 ± 1.32	55.11 ± 1.86*	91.55 ± 2.40	89.55 ± 2.44	17.43 ± 2.32	37.48± 2.42
	30% Methanol	26.5 ± 1.59	50.00 ± 1.21*	6.10 ± 0.12	26.10 ± 1.21	15.13 ± 1.84	30.81 ± 2.08
	10% Ethanol	44.89 ± 2.65	74.64 ± 2.76*	103.023 ± 2.78	103.03 ± 2.66	20.72 ± 1.77	32.70 ± 2.27
	20% Ethanol	37.77 ± 1.97	65.62 ± 2.52*	53.15 ± 2.22	69.29 ± 2.09	15.92 ± 1.07	26.13 ± 2.61
	30% Ethanol	33.97 ± 1.61	52.03 ± 2.89*	1.26 ± 0.13	31.31 ± 2.11**	13.42 ± 1.54	15.41 ± 1.54
	50% Hexane	399.57 ± 4.94	97.83 ± 2.61****	111.78 ± 2.58	101.44 ± 2.69**	60.04 ± 1.88	55.04 ± 2.81
	50% Cyclohexane	461.63 ± 4.24	95.65 ± 2.22****	114.94 ± 2.57	104.94 ± 2.04**	52.99 ± 2.71	50.99 ± 2.71
	50% Heptane	378.03 ± 4.14	96.74 ± 2.91****	124.91 ± 2.04	104.38 ± 2.21**	62.61 ± 2.40	60.61 ± 2.70

6.2.2.6. *Reusability*

No significant change ($p \geq 0.05$, t-test) in lipase activity was observed till 3 cycles of reuse (Figure 6.12). However; after the 3rd cycle, significant loss (log $p \leq 0.05$, t-test) of lipase activity was observed from the calcium alginate beads (see Figure 6.12).

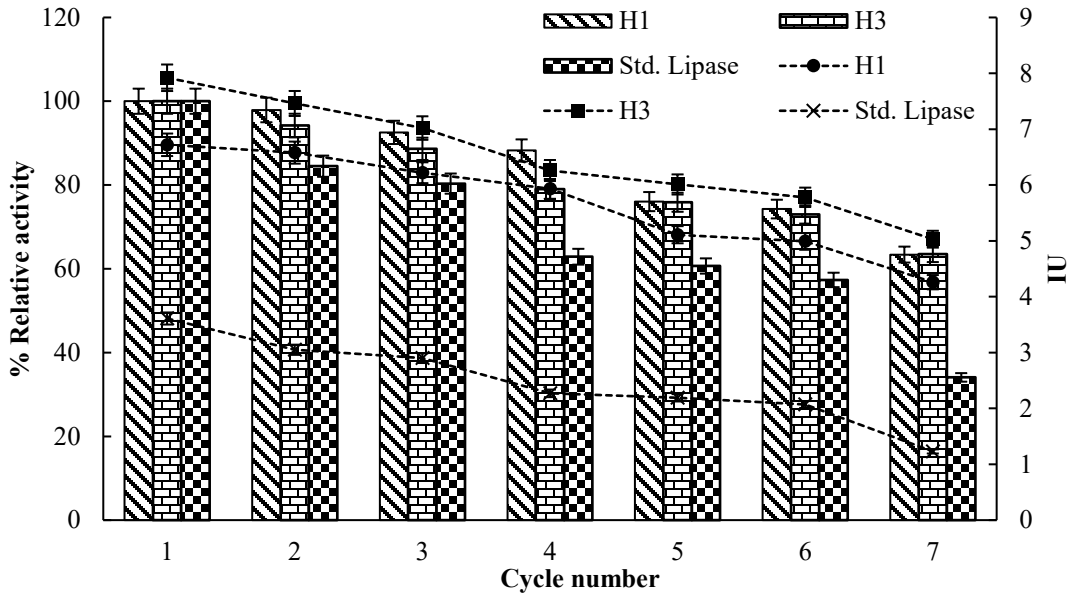

Figure 6.12: The effect of reusability on the activity of entrapped lipase was checked over 7 cycles. Enzyme activity was calculated in terms of remaining IU. % Relative activity at each time point was compared relative to lipase activity of unused lipase entrapped alginate beads. Data represented here are the mean of three different experiments and error bars represent standard deviation.

6.2.2.7. *Storage Stability*

No significant change ($p \geq 0.05$, t-test) in lipase activity was observed for the entrapped lipase from all sources (H1, H3 and porcine pancreas) after 18 days of storage at 4°C (Figure 6.13). The activity of entrapped lipase(s) in calcium alginate beads was maintained for 18 days of storage at 4°C.

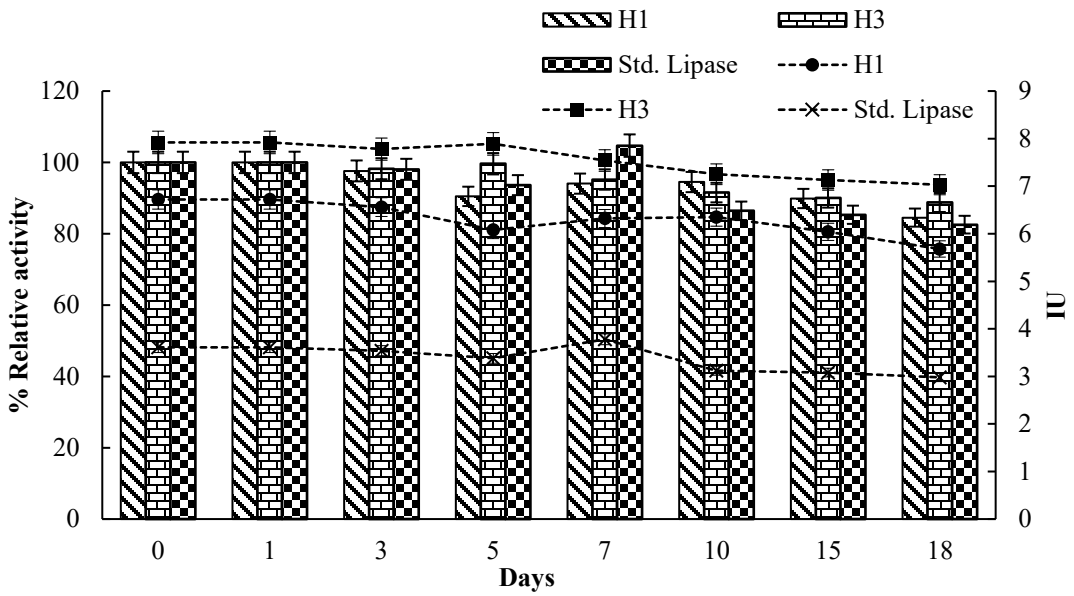

Figure 6.13: The effect of storage stability on the activity of entrapped lipase was checked over the course of 18 days. Enzyme activity was calculated in terms of IU. % Relative activity at each time point was compared relative to lipase activity of unused lipase entrapped alginate beads. Data reported here are the mean of three different experiments and error bars represent standard deviation.

6.3.DISCUSSION

The high cost of soluble enzymes often limits their use for commercial purposes. Immobilization can provide enzyme reusability, thereby reducing product isolation costs. Apart from reusability, immobilization also provides operational flexibility and often improves enzymatic thermal and chemical stability.

6.3.1. Gold nanoparticles for immobilization

Gold nanoparticles (AuNPs) have been widely used for biomedical applications, for diagnostics as well as in the area of therapeutics (Yi-Cheun, Brian and Vincet, 2012). AuNPs are of special interest for redox enzyme immobilization for biosensor and biofuel cell applications (Keith, 2017). Immobilization of enzyme(s) on AuNPs also extends their application(s) in industrial processes, for biotransformations and for enzyme directed synthesis. Binding of analytes to AuNPs changes their physiochemical properties, leading to detectable signals (fluorometric and colorimetric; (Uehara, 2010); hence they are of interest

for biosensors and other applications. Lipase sensors have been extensively explored for the detection of triglycerides and cholesterol and for applications such as the hydrolysis and synthesis of esters from glycerol and long chain fatty acids. Indeed, lipase(s) are among the most frequently used biocatalysts.

The physiological appearance (colour) of AuNPs depends on their size and shape. The AuNPs synthesized in this study were spherical in shape with an average size of 24.49nm (as confirmed by SEM, see Section 6.2.1.1). Spherical AuNPs provide a large surface-to-volume ratio for the attachment of enzymes (Venditti *et al.*, 2015). Small size AuNPs are brown in colour and with the increase in their size colour changes from brown to orange to red to purple (Martin *et al.*, 2010). The colour of AuNPs synthesized in this study was wine red with absorption maximum of 524nm; which falls in the absorption range of AuNPs (500-550nm) observed by other workers (Yi-Cheun, Brian and Vincet, 2012). Apart from size, the physiological properties of AuNPs are also influenced by shape, solvent, surface ligand and temperature. Small AuNPs provide a higher surface to volume ratio for enzyme loading - with a decrease in particle size, the surface tension increases. As with a decrease in particle size, a greater percentage of atoms exist on the surface. Hence, the smaller the particle, the higher the surface energy and the higher the particle aggregation will be. Therefore, small AuNPs aggregate more readily than larger AuNPs in order to lower the free energy of the system (Zhang, 2014).

In this study, the size, absorption and charge of AuNPs changed after treatment with organic solvents (Section 6.2.1.2). Ethanol is known to decrease the surface charge of citrate stabilized gold nanoparticles as it strips the citrate molecules from the AuNPs, decreasing the zeta potential, resulting in AuNP aggregation (Lazar and Szabo, 2018). Aggregation of AuNPs results in significant red-shifting of the surface plasmon resonance (SPR) frequency, broadening the surface plasmon band and changing the solution colour from red to purple/blue (Yi-Cheun, Brian and Vincet, 2012). However, in this study, after treatment with methanol, no significant colour change in AuNPs was visible to the naked eye; although, a change in zeta potential, size and absorption indicated aggregation of AuNPs (Section 6.2.1.2). Addition of an organic solvent also changes the polarity of the AuNPs, directly

affecting their size and zeta potential (Lazar and Szabo, 2018). In this study, in the presence of hexane, heptane and cyclohexane, AuNPs separated from the aqueous phase forming a separate monolayer (Section 6.2.1.2). It has previously been demonstrated that if hexane droplets, containing charged AuNPs, are mixed with a larger toluene droplet, nanoparticles immediately float to the air-toluene interface forming a close-packed monolayer film. These properties of AuNPs have been used for the generation of nanoparticle monolayers as biosensors (Martin *et al.*, 2010).

The pH and ionic strength of the AuNP solution effect their stability because these two parameters determine the surface charge (positive or negative; charge density and accumulation). Neutralisation of surface charge is one of the primary modes whereby pH and ionic strength promote AuNP aggregation. AuNP surfaces have surface functional groups (e.g., hydroxide and oxide groups), which can be exchanged with H^+ or OH^-, and therefore, low pH (i.e. excess H^+) results in an overall positive surface charge, while high pH (i.e. excess OH^-) renders a negative surface charge (Zhang, 2014). Hence, the addition of an enzyme for physical adsorption, in either high or low pH (in comparison to the overall charge of the AuNPs) could trigger AuNP aggregation (see Section 6.2.1.3.2). Enzymatic immobilization onto AuNPs can be achieved by physical adsorption or by the formation of a covalent bond. Physical adsorption, or non-covalent conjugation, binds enzymes to the AuNP via electrostatic interactions or hydrophobic interactions. Physical adsorption, a simpler process, displays greater enzyme leaching from the support (AuNPs in this study). In the current study, changes in AuNPs size (to 331.2nm), zeta potential (-8.45mV) and adsorption (319nm) after the addition of lipase (Section 6.2.1.3.1) indicated the adsorption on to the AuNPs surface. However, the absence of any changes in lipase activity in free solution before and after immobilization indicated that no adsorption was achieved. The change in size, charge and adsorption of AuNPs after addition of lipase could be explained due to a change in the surface charge of the AuNPs. A change in pH has also been shown to affect AuNPs coated with bovine serum albumin (BSA) where the AuNP's stability was contributed by steric stabilization due to adsorbed BSA layers (Brewer *et al.*, 2005). Temperature also influences aggregation kinetics by affecting Brownian motion of particles and collision frequency. Increasing temperature increases the kinetic energy of the AuNPs, thereby increasing

collisions, further increasing aggregation rates (Zhang, 2014). Hence, all the enzyme immobilization trials (adsorption or covalent bonding) were attempted at cold temperatures (<10°C).

Enhancing the electrostatic, steric or electrosteric repulsive forces between AuNPs, by surface coatings or functional ligands, can prevent aggregation and can provide other surface functionality (e.g. increase in enzyme/load ratio; (Yi-Cheun, Brian and Vincet, 2012). Surfactants, polymers and polyelectrolytes are the three main types of compounds for coating AuNPs (Zhang, 2014). Adsorbed, or covalently bound, surfactants increase surface charge and electrostatic repulsion or reduce interfacial energy between particle and solvent; eliminating aggregation (Zhang, 2014). Synthetic (e.g., polyethylene glycol) or naturally occurring polymers (e.g., biomacromolecules, such as proteins and polysaccharides) affect the dispersion of AuNPs, increasing AuNPs stability. Covalent conjugation of polymers or polyelectrolytes generates more stable AuNPs which are more desirable when stable enzyme immobilization is required (Yi-Cheun, Brian and Vincet, 2012). Replacement of citrate from AuNPs with glutathione is one method of stabilizing AuNPs against aggregation and was carried out in this study (Section 6.2.1.3.2). This simultaneously provided a functional group (-COOH) for covalent binding to an enzyme (with free -NH_2 group).

Matching the protein's diameter and the AuNPs pore diameter is a critical factor in attaining a high loading of enzyme on AuNPs (Du *et al.*, 2013). The pore size of AuNPs, and the adsorption time, play a significant role in enzyme loading, leaching, activity and reusability. For example, the 35nm pore size of AuNPs prepared by chemical dealloying of AgAu alloy foils in HNO_3 have been successfully used for the adsorption/entrapment of lipase (from *Pseudomonas cepacia;* (Wang *et al.*, 2011). Also, AuNPs with pore size 35-100nm (7-20 times bigger than the dimension of enzyme) have been used for entrapment (Du *et al.*, 2013). Adjusting the pore size of the AuNPs to suit enzyme immobilization can enhance the thermal stability of the enzyme (Keith, 2017). In the current study, the diameter of the lipase and the pore size of AuNPs was not determined. Hence, optimization of immobilization/entrapment using pore size as a parameter was not attempted. Immobilization of enzymes on solid surfaces produces a variety of effects ranging from the reversal and strong inhibition (affected

protein structure due to tighter or irreversible binding), to positively enhancing enzyme stability/function. These effects are enzyme dependent and are influenced by the physical and chemical properties of the support surfaces (AuNPs). Covalent binding of enzyme to AuNPs, may block the substrate binding site, or may interfere with the necessary conformational changes required for enzyme activity. Hence, to achieve an appropriate enzyme orientation, it is necessary to understand the distribution of different functional groups on enzyme's surface. Therefore, computational methods are required to analyse the structure of the enzyme. The exposed acidic amino acid residues on the enzyme surface can be exploited for conjugation with AuNPs. Improper orientation after immobilization ultimately affects activity; therefore, it is important to understand the structure of the enzyme before immobilization. EDC/NHS coupling (see Section 6.2.1.3.2) is a very simple method for the conjugation of enzyme to AuNPs; where carbodiimides mediate the formation of an amide bond between carboxy and amine groups (on AuNPs surface and enzyme respectively). If knowledge of available Asp and Glu residues on the enzyme surface is available via enzyme model/crystal structure, the ratio of EDC and NHS to enzyme concentration can be maintained (Shikha, Thakur and Bhattacharyya, 2017). Several enzymes have been conjugated using this strategy. One such example is a lipase from *B. cepacia* immobilized by covalent EDC-NHS coupling to AuNPs synthesised by reduction of $HAuCl_4$ solution with $NaBH_4$ and capping with cysteamine-HCl (Shikha, Thakur and Bhattacharyya, 2017). Another example includes covalent coupling of a lipase from porcine pancreas where AuNPs were synthesized using chemical dealloying of AgAu foils (X. N. Yang *et al.*, 2016). Hence, it can be concluded that enzyme immobilization on AuNPs require thorough investigation using suitable functional and computational tests (Bailes *et al.*, 2012).

Confirmation of lipase/enzyme immobilization on AuNPs can be achieved by characterising changes in size and zeta potential. A shift in absorbance, an increase in particle size and/or a change in zeta potential (reduction) can confirm enzyme immobilization. Since larger nanoparticles have an absorbance at a higher wavelength than smaller ones of the same shape and morphology, a redshift of the spectrum (<10nm) can be used to confirm enzyme immobilization. Zeta potential values of AuNPs conjugated with enzyme are lower than unconjugated AuNPs; lower values indicate masking of AuNPs-NH_2 with lipase molecules

(Shikha, Thakur and Bhattacharyya, 2017). In the current study, due to precipitation of GSH reduced AuNPs after attempted NHS-EDC enzyme coupling, no physiochemical properties could be examined. Also, the observation of no change in lipolytic activity in AuNPs free solution before and after immobilization confirmed a lack of enzyme binding on the AuNPs surface (Section 6.2.1.3.2). A possible explanation for precipitation of AuNPs could be higher hydrophobicity of lipase(s) or higher concentrations of NHS-EDC due to the unavailability of a lipase crystal structure or could be due to several other factors (pH, enzyme concentration etc.). The process of AuNPs synthesis might also affect the surface charge properties of AuNPs, which can directly, or indirectly, affect the final covalent coupling of lipase onto the AuNP surface. Since, no citrate GSH reduced AuNPs have been cited in the literature for covalent coupling of lipases, it is difficult to explain the reason for the inability of lipase to covalently bind or physically adsorb on AuNPs surface. Due to all these findings, no further trials were carried out to immobilize lipase on AuNPs rather, an entrapment method of immobilisation, was explored.

6.3.2. Entrapment and characterisation

Enzyme entrapment in porous matrices (alginate and acrylamide beads) has been reported as a rapid, nontoxic, inexpensive and versatile technique (Datta, Christena and Rajaram, 2013). This technique offers good mechanical strength, high porosity for substrate and product diffusion. Alginate is by far the most widely used polymer for enzyme entrapment (Zhang *et al.*, 2013). Alginate is an anionic linear copolymer composed of 1,4-linked β-D-mannuronic acid and α-L-guluronic acid in different proportions and sequential arrangements. Porous alginate beads are synthesized by crosslinking the carboxyl group of the α-L-guluronic acid with a cationic crosslinker ($CaCl_2$ or $BaCl_2$). Calcium alginate is most commonly used due to its natural biocompatibility, ease of formation, and mild physiological gelation conditions. Enzymes are entrapped by drop-wise addition of sodium alginate solution containing the enzyme to a solution of $CaCl_2$. The cation acts as a cross-linking agent for the alginate biopolymer and the droplets precipitate as beads with the enzyme entrapped within (Won *et al.*, 2005).

The pore size of the beads and the amount of entrapped enzyme can be controlled by changing the concentration of sodium alginate. The capacity to retain enzyme inside the beads (i.e. to reduce leaching) increases with increasing concentration of sodium alginate but, conversely, the activity of immobilized enzyme decreases. An increase in sodium alginate concentrations causes extensive cross linking of the matrix, resulting in reduced pore size of beads and causing reduced mass transfer or diffusion of substrate to the enzyme active site. Some workers (Talekar and Chavare, 2012) report that appropriate enzyme entrapment inside calcium alginate beads also depends on the concentration and contact time between alginate and $CaCl_2$. Bhushan and co-workers (Bhushan *et al.*, 2008) also reported that the maximum activity of entrapped lipase was achieved at 1.5% (w/v) alginate and decreased with an increase in the amount of alginate used. For comparison, for some proteases the maximum percent entrapped activity was observed at 2% (w/v) sodium alginate; maximum entrapped enzyme leakage occurred at 1% (w/v) sodium alginate while at 3% and 4% (w/v) sodium alginate the entrapped activity of the enzyme was low (Anwar *et al.*, 2009). Enzyme entrapment efficiency was unaltered by $CaCl_2$ concentration (0.05–0.3M; (Won *et al.*, 2005). Previous studies have shown 0.2M $CaCl_2$ to retain the highest activity of entrapped enzyme; however, above 0.3M $CaCl_2$, enzyme activity decreases, as the pH of $CaCl_2$ solution changes it affects the activity of entrapped enzyme (Anwar *et al.*, 2009). Hence for the entrapment of lipase(s) from *P. reinekei*, *P. brenneri* and porcine pancreas the final concentration of sodium alginate was maintained at 2% (w/v; see Section 6.2.2) with 0.2M $CaCl_2$ as a cross-linking agent.

Curing time, the time required to attain maximum calcium alginate beads hardness, is an important parameter as it ensures stable beads, which should reduce enzyme leakage and increase yield. Generally, the amount of the enzyme entrapped increases with embedding/curing time. However, it has been reported in some cases that a prolonged interaction of enzyme in alginate beads with Ca^{2+} in the solution could lead to a significant decrease in activity (Zhang *et al.*, 2013). A curing time of 60-90 mins has been considered ideal for immobilization with further increase in curing time reported to have no additional benefits in terms of immobilization yield or enzyme stability (Talekar & Chavare 2012, Zhang et al. 2013). Lower curing time generates soft and fragile beads, resulting in enzyme leaching

and hence low immobilization yield (Talekar and Chavare, 2012). Hence, in this study, a curing time of 60mins was chosen for the synthesis of calcium alginate beads entrapping lipase from *P. reinekei* (H1), *P. brenneri* (H3) and porcine pancreas (standard; Section 6.2.2.1).

Drying of calcium alginate beads to remove excess water can also affect the entrapped enzyme activity; with too long a drying time causing a loss of bound water in enzyme molecules, resulting in lower enzymatic activity. Generally, 10h drying time is considered sufficient to maintain the catalytic activity of the enzyme beads (Zhang *et al.*, 2013). For this reason, in this study, calcium alginate beads were dried for 10h in a vacuum desiccator at room temperature.

Mass transfer (which ultimately determines the rate of enzymatic reaction) depends on the form of enzyme immobilization. The molecular transport between the reaction mixture and the surface of the enzyme through a boundary layer governs the external mass transfer rate. The external mass transfer rate is inversely proportional to the thickness of the boundary layer and is, therefore, the limiting factor for enzymatic reaction. Internal mass transfer occurs within the pores of the enzyme and the carrier, whereas, the external mass transfer is affected by the concentration of alginate beads. The higher the concentration of alginate, the lower the bead porosity and, hence, the lower the enzyme activity due to limited mass transfer. Entrapment based immobilization can also affect the flexibility of the enzyme, as well as the accessibility of the substrate(s) to the enzyme active site. Important parameters influencing internal mass transfer are particle size, pore size and the effective diffusion coefficient of the substrate within the pores of the support (Won *et al.*, 2005; Talekar and Chavare, 2012; Kumar, Yadav and Negi, 2014). A 60min incubation of calcium alginate beads entrapping lipase from *P. reinekei* (H1), *P. brenneri* (H3) and porcine pancreas (standard) generated equivalent lipolytic activity comparable to that of free lipase from the respective source, however, a two-fold difference in the reaction time was noted (Section 6.2.2.1). For all calcium alginate immobilisation characterisation studies, a 60min incubation with the substrate was used in order to compare it with free lipase enzymatic activity (which typically employed a 30mins incubation).

Immobilization can result in a shift in optimum pH due to conformational changes in the enzyme. As a result of changes in the degree of ionization of amino acid residues at the active site, leading to changes in electrostatic potential (Ψ), the optimum pH of many enzymes may shift to a higher pH if they are entrapped in a carrier that is anionic and towards low pH if it is cationic (Palmer and Bonner, 2008). This shift in optimum pH may be due to changes in acidic and basic amino acid side chain ionization in the microenvironment around the active site (Talekar and Chavare, 2012). This property of the calcium alginate carrier also has an effect on the optimal pH of enzymatic activity (Zhang *et al.*, 2013). The carboxyl moiety of glucuronic and mannuronic acids is the acidic group present in alginate. The pKa of guluronic acid is 3.65, and the pKa of mannuronic acid is 3.38. Therefore, the alginate gels are usually negatively charged at neutral pH values. If the enzyme solution is positively charged (pH of the solution < pI of the enzyme); the enzyme could be easily adsorbed on the alginate network (facilitated by the overall negative charge on the enzyme), thus reducing enzyme leakage (Zhang *et al.*, 2013). This charged surface of alginate beads and entrapped enzyme produces a charged microenvironment, which can ultimately affect the pH stability of the entrapped enzyme (Anwar *et al.*, 2009). However; in this study, no statistically significant change in lipase stability/activity was observed in the different pH solutions tested (Section 6.2.2.2) compared to free lipase. The optimum pH of lipase before and after entrapment was not changed for all the three lipases examined. Similar observations have been made for immobilized proteases where the optimum pH of free and immobilized enzyme remained same (pH 7.5; (Anwar *et al.*, 2009). Bhushan and colleagues (2008) have also reported no loss in enzyme activity for immobilized lipase at pH 7.0; however, a loss in activity was observed at lower pH values after prolonged incubation (96h); indicating a shift in optimum pH of the enzyme after entrapment.

In general, entrapment restricts the overall flexibility of the enzyme, thereby increasing enzyme thermal stability through enzyme rigidity. It has been suggested that immobilization creates a microenvironment that protects the hydrogen bonding patterns in lipases at higher temperatures (Knezevic *et al.*, 2002). Thus, at higher temperatures enzyme unfolding might be reduced to some extent through immobilization. In most cases, immobilization results in a broadening of the functional temperature range for enzyme activity compared to the free

enzyme (Zhang *et al.*, 2013). However, in the current study, calcium alginate beads entrapping lipases from *P. reinekei* (H1), *P. brenneri* (H3) and porcine pancreas (standard) respectively showed no significant increase in thermostability compared to their free forms (Section 6.2.2.3). Since free forms of lipase from H1 (*P. reinekei*) and Porcine pancreas (Standard) were unstable above 50°C and free form of lipase from H3 (*P. brenneri*) was unstable above 60°C (Chapter 5, Section 5.2.3.2); thermostability of their calcium alginate entrapped forms was not explored at higher temperatures and prolonged durations. To understand the significance of lipase entrapment in calcium alginate beads in terms of thermostability; an incubation at higher temperatures (>60°C) and prolonged time (>45mins) would have been required. No significant change in thermostability of calcium alginate entrapped lipase from H1 (*P. reinekei*), H3 (*P. brenneri*) and porcine pancreas (standard) was observed at 40°C, 50°C and 60°C could be due to short incubation time (45mins).

In the presence of 1mM EDTA, there was a significant increase in stability for all the three entrapped lipases compared to their free forms (Section 6.2.2.4). The enhanced stability could be due to chelation of Ca^{2+} ions present in alginate beads instead of metal ions required for the stability/activity of the lipases, as established in Chapter 5. With increased concentrations of EDTA, the stability of entrapped lipases decreased (Figure 6.11), indicating that the chelation of divalent metal ions associated with the enzyme, along with the Ca^{2+} ions of calcium alginate beads, eventually becomes critical for enzyme stability. Metal ions at lower concentration are known to inhibit the activity of immobilized enzymes; 3.0 mM of various metal ions (Ca, Mg, K, Na, Cu) decreased the lipolytic activity of entrapped rice bran lipase (Kanmani *et al.*, 2015). In the current study, no statistically significant changes in lipolytic activity were observed in calcium alginate entrapped lipase from *P. reinekei* (H1), *P. brenneri* (H3) or porcine pancreas (standard) respectively in presence of 10mM of a variety of metal ions. Since the free form of these enzymes were also stable in 10mM of metal ions (Chapter 5, Section 5.2.3.5), no loss of lipolytic activity after entrapment suggests that entrapped forms of these lipases (H1 and H3) could be used in presence of these metal ions.

Kanmani and co-workers (2015) noted a decrease in calcium alginate entrapped rice bran lipase activity in presence of 1% (v/v) Triton X-100 and Tween 80; while activity increased

in the presence of SDS. A loss of lipolytic activity was also observed in the present study when a calcium alginate entrapped lipase from *P. reinekei* (H1), *P. brenneri* (H3) and porcine pancreas (lipase standard; Section 6.2.2.4) were incubated with 10mM Poly 80, Triton X-100 and SDS respectively. Observed loss of lipolytic activity from calcium alginate entrapped lipase in presence of detergents was because of lipase leaching from calcium alginate beads; as lipolytic activity was observed in the calcium alginate bead free solution. One possible explanation of enzyme leaching could be hydrolysis of calcium alginate beads into calcium chloride and alginic acid in the presence of detergents; causing them to lose integrity and thus permitting the entrapped lipase to leach from the beads (Sharma, Sharma and Majumdar, 2014).

A statistically significant loss of activity was observed in the presence of different solvent concentrations (see Section 6.2.2.5) at 28°C for calcium alginate entrapped lipase from all the sources (*P. reinekei*, H1; *P. brenneri*, H3, and porcine pancreas, lipase standard). Similar observations have been made for rice bran lipase in the presence of 10% (v/v) propanol, where only 58% relative activity was reported in entrapped lipase (Kanmani *et al.*, 2015). The ability to retain the lipase inside the alginate beads decreases with an increase in the hydrophilic character of the solvent (Hertzberg, Kvittingen and Anthonsent, 1992). Non polar solvents, such as petroleum ether and *n*-hexane, also inhibited the activity of rice bran lipase (Kanmani *et al.*, 2015). The possible reason behind loss of lipolytic activity in the presence of polar solvents has not been reported to date, a logical explanation could be stripping of essential water molecules from the enzyme, resulting in instability (as detailed in Section 2.6.1). Although no loss of activity was observed for calcium alginate entrapped lipase from all the sources (*P. reinekei*, H1; *P. brenneri*, H3, and porcine pancreas, lipase standard) in the presence of non-polar solvents; no gain in relative activity compared to free lipase was observed. As the non-polar solvents are known to bind to the lid of the lipase, keeping it in an open confirmation and further enhancing the lipolytic activity (see Section 2.6.1.2); entrapment might hinder this interaction due to reduced structural flexibility. As the enzyme in alginate beads cannot move as freely as the enzyme in solution, non-polar solvents cannot interact with the enzyme lid and hence activation of lipolytic activity was observed (see Table 6.4).

Finally, no significant loss of activity was observed till 3 cycles of reuse with lipase entrapped calcium alginate beads (Section 6.2.2.6), however after the 3rd cycle a statistically significant ($p>0.5$, t-test) loss of lipolytic activity was observed. This decrease in activity could be due to loss of enzyme from the carrier, i.e., due to repetitive washing of beads at the end of each cycle (Kumar, Yadav and Negi, 2014). Another possible reason could be the damage to beads from repeated washing, as reported in case of entrapped lipase from *Candida rugosa* (Knezevic *et al.*, 2002). This limitation can be overcome by coating the surface of alginate bead with chitosan or silicate (Won *et al.*, 2005). Storage stability of calcium alginate beads confirmed their stability at 4°C for 18 days with no statistically significant loss in lipolytic activity. The current study is the first reported storage stability in literature, suggesting that calcium alginate beads entrapped lipase can be re-used for 3 cycles and can be stored at 4°C, for a minimum of 18 days (see Section 6.2.2.7).

6.4.CONCLUSION

Immobilization on AuNPs was carried out as a 'proof of principle' exploration. The precipitation of AuNPs in presence of lipase(s) resulted in inadequate immobilization of the lipases of choice and the AuNPs. Therefore, calcium alginate entrapment was explored as an alternative technique for lipase immobilization. Entrapment of lipase from H1 (*P. reinekei*), H3 (*P. brenneri*) and PPL (as a commercial lipase standard) in calcium alginate beads reduced the rate of reaction by two-fold, probably due to mass transfer limitations. No significant change in the stability of calcium alginate lipase compared to their respective free form was observed at different pH and temperatures. However, the calcium alginate entrapped lipase showed significant stability in presence of 1mM EDTA; this stability decreased with increase in EDTA concentrations. Though stability of lipase(s) after calcium alginate entrapment in presence of organic solvents was also negatively affected; entrapment cannot be considered as an immobilization method to enhance thermal or solvent stability of enzymes. However, the advantage of enzyme recovery from the reaction is a tempting parameter to explore calcium alginate entrapped lipase(s) for synthesis of biodiesel by enzymatic transesterification.

Chapter 7: Culturing of microalgae for TAGs (triacylglycerides)

7.1. INTRODUCTION AND OBJECTIVES

Microalgae cover unicellular and multicellular microorganisms capable of year-round photosynthetic production. They are highly adapted towards their surrounding environment, do not require fertile land and hence can be grown almost anywhere, even on waste- water, sewage or saltwater. They are fast growing photosynthesizing organisms, which can complete an entire growth cycle in a few days, if adequate amount(s) of sunlight, water and other nutrients are available. Wastewater from municipal sources, dairy/poultry industry and other agricultural practices has highly concentrated nutrients and is unsuitable feed for terrestrial crops as leached nutrients from soil can result in eutrophication of surface waters. By contrast, culturing of microalgae in wastewater not only provides an inexpensive and alternative method to treat wastewater, but also substantially reduces the need for chemical fertilizers (Lam and Lee, 2012). The lipid content in microalgae generally varies from 20-40% biomass dry weight, however, lipid content as high as 85% biomass dry weight has also been reported in certain microalgal strains (Mairet *et al.*, 2011). Optimizing the metabolic pathway of microalgae cells can increase the lipid content (Lowrey, Brooks and McGinn, 2015). Therefore**,** utilising a short harvesting cycle, coupled to metabolic pathway optimisation to produce higher lipid content and with continuous harvesting suggests that microalgae may be very good candidates for sustainable fuel production, which is been explored in this Chapter (Miao and Wu, 2006).

The overall objectives of this chapter were:

- To obtain maximum biomass of *Chlorella emersonii* and *Pseudokirchneriella subcapitata* after culturing in simulated secondary treated wastewater
- To develop a Nile Red based assay for lipid quantification (TAGs) in *Chlorella emersonii* and *Pseudokirchneriella subcapitata*
- To determine the cultivation time required for maximum TAGs production in nitrogen deficient media.

7.2. RESULTS

7.2.1. Biomass generation

Growth curves in different simulated secondaty treated wastewater culturing conditions for *Chlorella emersonii* and *Pseudokirchneriella subcapitata* are shown in Figure 7.1 (a, b) and Figure 7.2 (a, b) respectively. A mixotrophic mode of culturing resulted in the maximum biomass for both the microalgal strains. To obtain a higher biomass, a 5-day and 8-day mixotrophic culturing mode was found to be optimum for *Chlorella emersonii* and *Pseudokirchneriella subcapitata* respectively. A minimum biomass was observed for both microalgal strains using a heterotrophic mode of culturing. A 10-day autotrophic mode of culturing for *Pseudokirchneriella subcapitata* resulted in an equivalent biomass generation as that of 8 days in mixotrophic culturing. Therefore, a mixotrophic mode of culturing was used to obtain maximum biomass in the minimum timeframe.

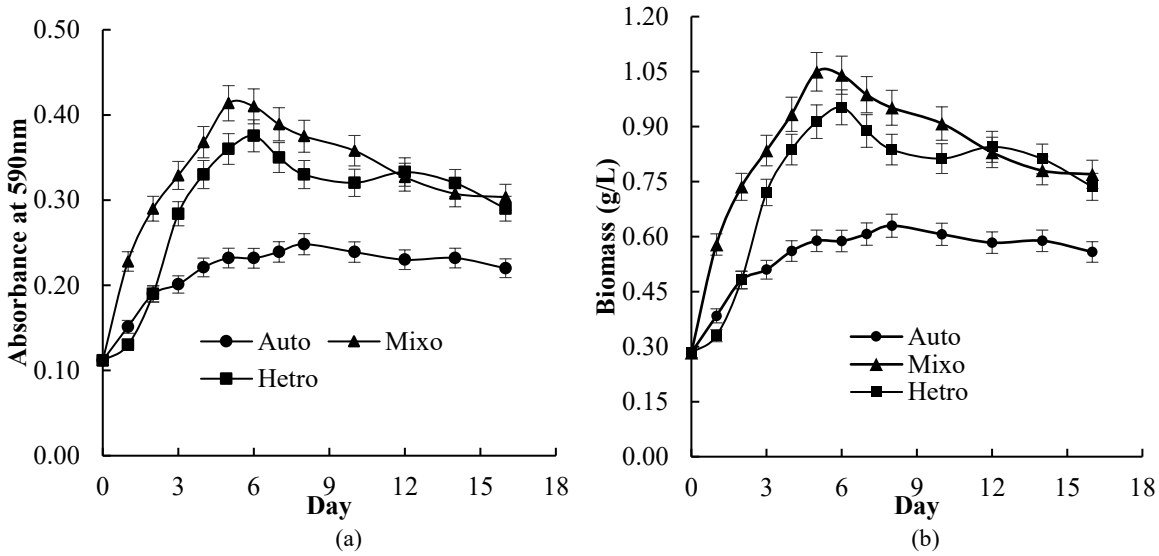

Figure 7.1: (a, b) Growth curve of *Chlorella emersonii* following three different modes of culturing. The maximum biomass (measured as per Section 3.2.6.5) was produced after 5 days of culturing in mixotrophic mode. Data represented here are the average of three independent trials, with the standard deviation shown as error bars. (c) A difference in physiological appearance of culture after 15 days of growth represents loss of chlorophyll in mixotrophic and heterotrophic mode.

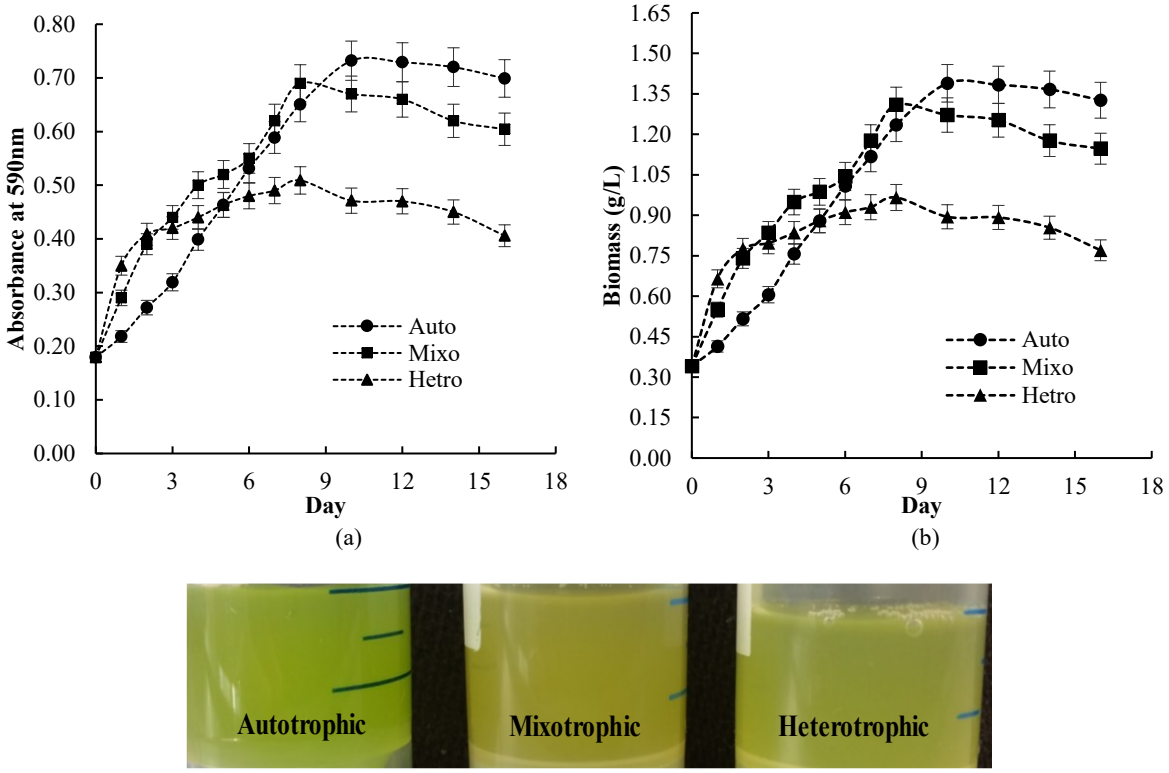

Figure 7.2: (a, b) Growth curve of *Pseudokirchneriella subcapitata* following three different modes of culturing. The maximum biomass (measured as per Section 3.2.6.5) was produced after 8 days of culturing in mixotrophic mode and 10 days of culturing in autotrophic mode. The data represented here are the average of three independent trials, with standard deviation shown as error bars. (c) A difference in physiological appearance of culture after 15 days of growth represents loss of chlorophyll in mixotrophic and heterotrophic mode.

Furthermore, a difference in physiological appearance was observed for both the cultures under different growth conditions (Figure 7.1(c), 7.2(c)), indicating a reduced production of chlorophyll in mixotrophic and heterotrophic mode.

7.2.2. Nile red assay for neutral lipids estimation

7.2.2.1.Solvent concentration and assay excitation wavelength

Different concentrations of DMSO and acetone, with fixed concentration of Nile Red (10µg/ml), were examined to understand the concentration of solvent required to penetrate the microalgal cells. In the case of DMSO, a 20% (v/v) concentration generated maximum fluorescence intensity for both the microalgal strains (Figure 7.3, 7.4). However, a 10% (v/v) and 20% (v/v) concentration of acetone generated maximum fluorescence intensity for *Pseudokirchneriella subcapitata* and *Chlorella emersonii* respectively (Figure 7.3(b), 7.4(b)).

In 20% (v/v) DMSO, an excitation wavelength of 530nm and an emission wavelength of 580nm were selected as the most appropriate for the generation of maximum intensity for the estimation of neutral lipids in both the microalgal strains (Figure 7.3, 7.4).

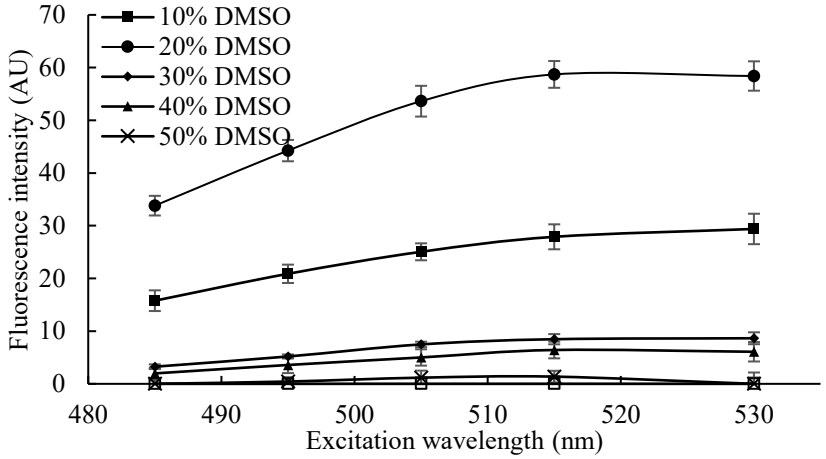

Figure 7.3: The effect of different concentrations (10-60% v/v) of DMSO on the fluorescence intensity of neutral lipids from *Chlorella emersonii.* A constant concentration of Nile Red was maintained (10µg/ml) for all the solvents. Different excitation wavelengths resulted in different fluorescence intensities with 530nm being the wavelength for maximum fluorescence intensity after 30mins of incubation at room temperature. Data represented here are the average of three independent experiments with five assay values each and the error bars shown are the standard deviation.

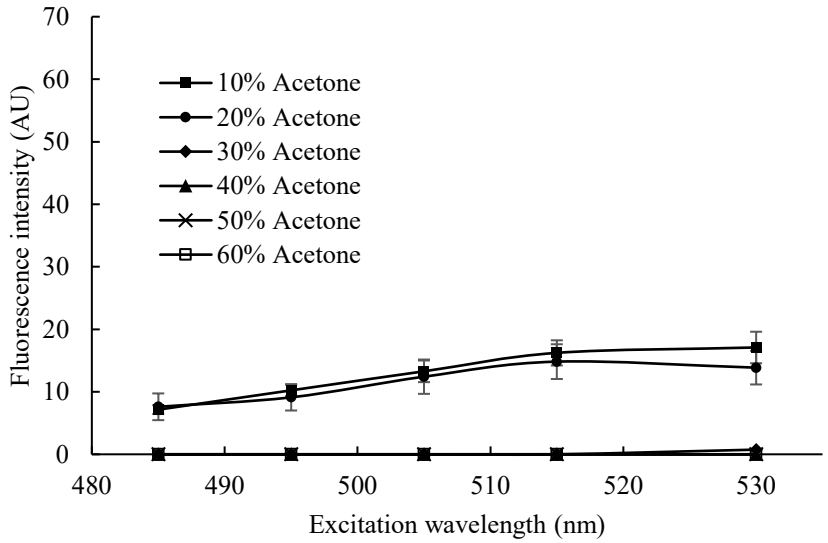

Figure 7.4: The effect of different concentrations (10-60% v/v) of acetone on the fluorescence intensity of neutral lipids from *Chlorella emersonii.* A constant concentration of Nile Red was maintained (10µg/ml) for all the solvents. Different excitation wavelengths resulted in different fluorescence intensities with 530nm being the wavelength for maximum fluorescence intensity after 30mins of incubation at room temperature. Data represented here are the average of three different experiments with five assay values each and the error bars shown are the standard deviation.

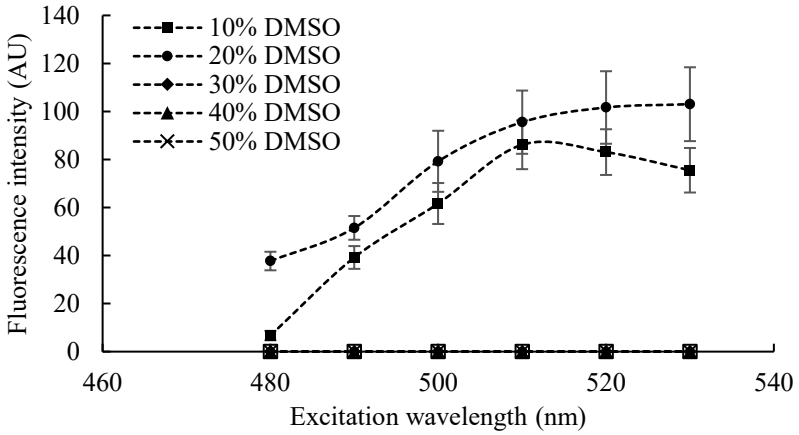

Figure 7.5: The effect of different concentrations (10-60% v/v) of DMSO on the fluorescence intensity of neutral lipids from *Pseudokirchneriella subcapitata.* A constant concentration of Nile Red was maintained (10µg/ml) for all the solvents. Different excitation wavelengths resulted in different fluorescence intensities with 530nm being the wavelength for maximum fluorescence intensity after 30mins of incubation at room temperature. Data represented here is the average of three independent experiments with five assay values each and the error bars shown are the standard deviation.

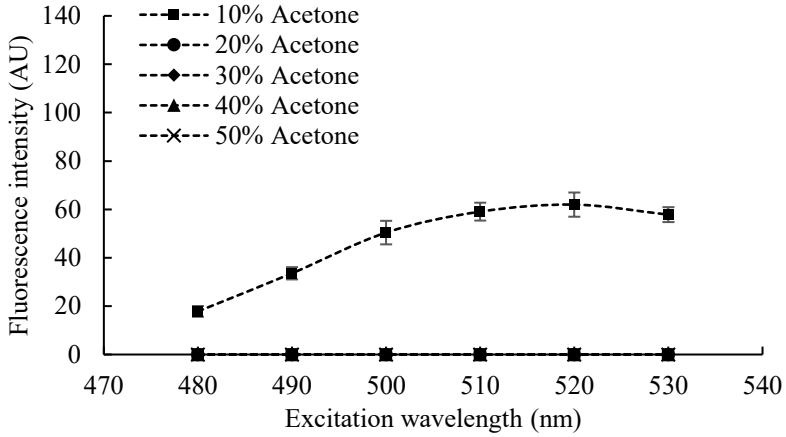

Figure 7.6: The effect of different concentrations (10-60% v/v) of Acetone on the fluorescence intensity of neutral lipids from *Pseudokirchneriella subcapitata.* A constant concentration of Nile Red was maintained (10µg/ml) for all the solvents. Different excitation wavelengths resulted in different fluorescence intensities with 530nm being the wavelength for maximum fluorescence intensity after 30mins of incubation at room temperature. Data represented here is the average of three independent experiments with five assay values each and the error bars shown are the standard deviation.

7.2.2.2.Dye concentration

A maximum fluorescence intensity was observed with 10µg/ml concentration of Nile Red in the case of *Chlorella emersonii* (Figure 7.5 (a)) and 5µg/ml for *Pseudokirchneriella subcapitata* (Figure 7.5 (b)). With a further increase in dye concentration, a decrease in fluorescence intensity was observed for both the microalgal strains (*Chlorella emersonii* and *Pseudokirchneriella subcapitata)*. However, for *Pseudokirchneriella subcapitata*, there was

no significant difference (log p≥0.5, t-test) in fluorescence intensity between 5µg/ml and 10µg/ml Nile red dye. A concentration of 10µg/ml and 5 µg/ml Nile Red dye in 20% (v/v) DMSO was selected as the optimal parameters for neutral lipid quantification in *Chlorella emersonii* and *Pseudokirchneriella subcapitata* respectively.

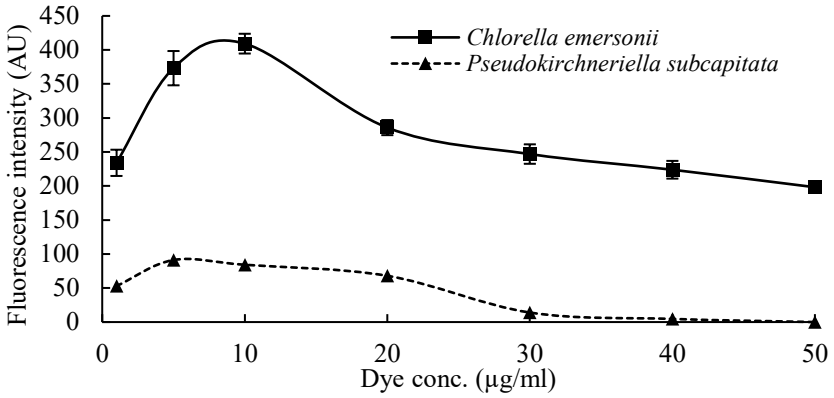

(a)

Figure 7.7: Fluorescence intensity from neutral lipids of *Chlorella emersonii* and *Pseudokirchneriella subcapitata* utilising different dye concentrations (1-50µg/ml) in 20% (v/v) of DMSO, with an excitation wavelength of 530nm and an emission wavelength of 580nm. Microalgal strains were incubated at 40°C for 60mins before measuring fluorescence intensity. The data represented here are the average of three independent experiments with five assay values each and the error bars shown are the standard deviation.

7.2.2.3.Effect of incubation time

An increase in fluorescence intensity was observed with incubation time for both the microalgal strains (*Chlorella emersonii* and *Pseudokirchneriella subcapitata*) till 60mins and 40mins respectively (Figure 7.6 a, b). However, further incubation resulted in saturation or no significant change in fluorescence intensity (log P≥0.5, t-test). Since a minimum incubation of 60mins is required to attain maximum fluorescence intensity for *Chlorella emersonii* and no significant change was observed in fluorescence intensity for *Pseudokirchneriella subcapitata* after 40mins of incubation (Figure 7.6 a, b); a 60mins incubation at 40°C was selected as the incubation parameters for neutral lipids estimation for both the microalgal strains.

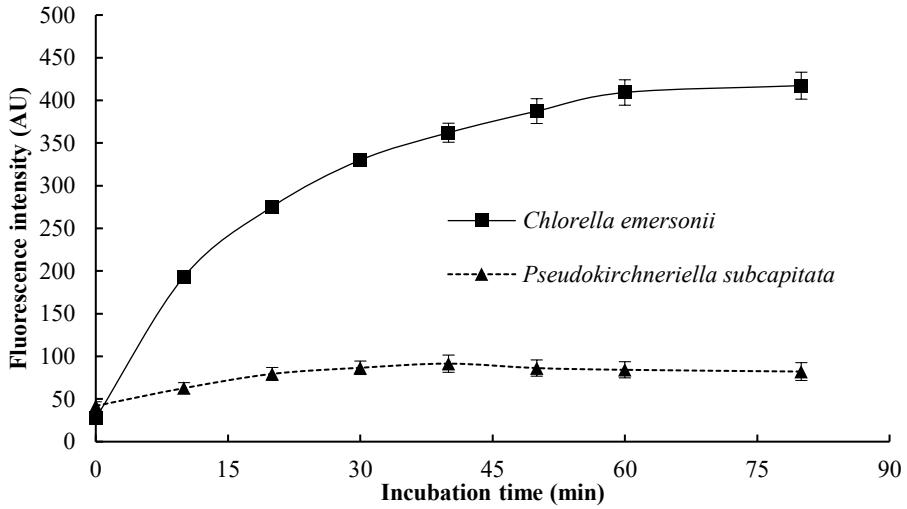

Figure 7.8: The effect of incubation time on the fluorescence intensity of neutral lipids from *Chlorella emersonii* and *Pseudokirchneriella subcapitata* when microalgal cells were incubated at 40°C with 10µg/ml and 5µg/ml of Nile Red dye in 20% (v/v) of DMSO respectively. A maximum fluorescence intensity in *Chlorella emersonii* was observed after 60mins of incubation and for *Pseudokirchneriella subcapitata* 40mins of incubation was ideal. Data represented here are the average of three independent experiments with five assay values each and the error bars shown are the standard deviation.

7.2.2.4.Effect of cell concentration on fluorescence intensity

A linear relationship was observed between fluorescence intensity and number of cells with an OD_{590nm} between 0.2-0.7, and this was used for staining *Chlorella emersonii* and *Pseudokirchneriella subcapitata* with 10µg/ml and 5µg/ml Nile Red dye in 20% (v/v) DMSO respectively. Below an OD_{590nm} of 0.2 and above 0.7, a saturation in fluorescence intensity was observed (Figure 7.9).

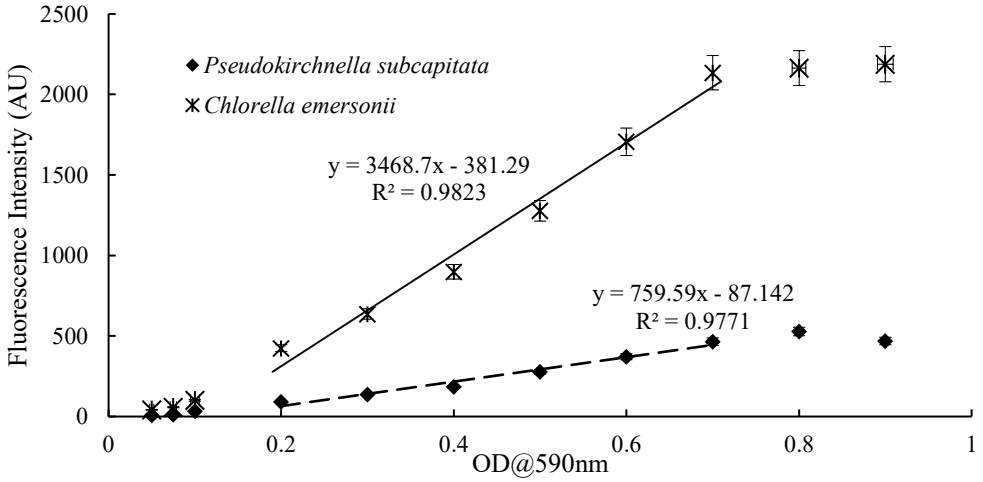

Figure 7.9: The relationship between fluorescence intensity and number of cells (OD_{590nm}) when *Chlorella emersonii* and *Pseudokirchneriella subcapitata* were stained with 10µg/ml and 5µg/ml Nile red dye in 20% (v/v) DMSO respectively. Fluorescence was recorded after 40min and 60min of incubation at 40°C respectively. Data represented here is the mean of three independent experiments and the error bars shown are the standard deviation.

7.2.2.5.Microscopic analysis for presence of neutral lipids

Microscopic examination of microalgal cells indicated the shape of *Chlorella emersonii* to be spherical and *Pseudokirchneriella subcapitata* to be sickle shaped (Figure 7.10 (a), 7.11 (a)). Treatment of *Chlorella emersonii* and *Pseudokirchneriella subcapitata* with 20% (v/v) DMSO containing 10µg/ml and 5µg/ml Nile red respectively generated fluorescence when the cells were observed in the green excitation zone (530nm) and a red emission zone (604nm; Figure 7.10 (c), 7.11 (c)). The presence of fluorescence after the excitation of Nile Red treated microalgal cells indicated the presence of neutral lipids in the microalgal strains.

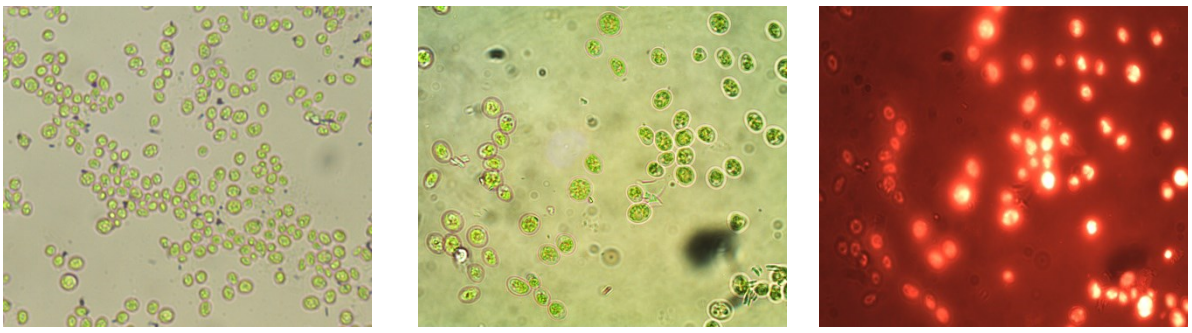

(a) (b) (c)

Figure 7.10: Microscopic observation of *Chlorella emersonii* under (a) 40X and (b) 100X magnification. Microalgal cells containing neutral lipids present in *Chlorella emersonii* after incubation with 20% (v/v) DMSO with 10µg/ml of Nile Red dye after fluorescence excitation under 100X magnification (c). Cells without any fluorescence have either no neutral lipid or too few lipids to be observed visually.

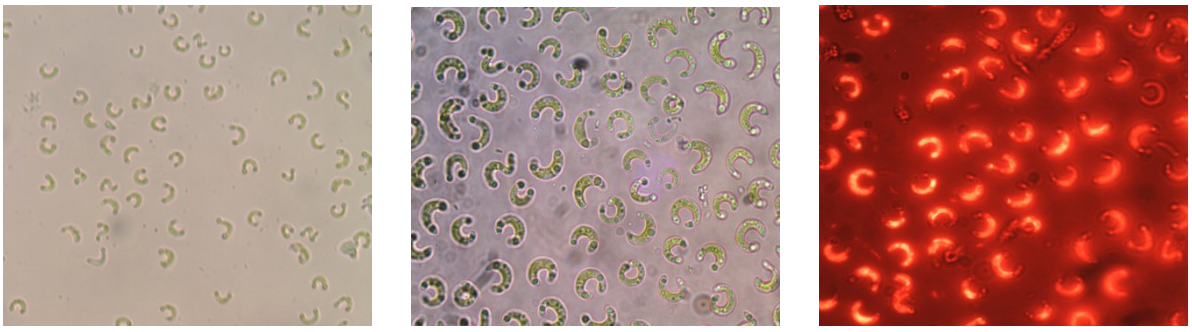

(a) (b) (c)

Figure 7.11: Microscopic observation of *Pseudokirchneriella subcapitata* under (a) 40X and (b) 100X. Microalgal cells containing neutral lipids present in *Pseudokirchneriella subcapitata* after incubation with 20% (v/v) DMSO with 5µg/ml of Nile Red dye after fluorescence excitation under 100X magnification (c). Cells without any fluorescence have either no neutral lipid or too few lipids to be observed visually.

7.2.3. Neutral lipid production profile

The presence of 1% (w/v) glucose in nitrogen deficient wastewater media enhanced the production of neutral lipids in both the microalgal strains (Figure 7.12 (a), (b)). Fluoresence intensity for presence of neutral lipids generated from *Chlorella emersonii* in absence of nitrogen alone was noted as 384.08±23.44AU after 6 days; in the presence of glucose: 848.81±45.52AU after 13 days. For *Pseudokirchneriella subcapitata* 286.05±19.00AU were produced after 13 days in the absence of nitrogen, and 445.94±10.89AU in the presence of glucose after 21days of incubation. Therefore, an incubation time of 13 days and 21 days in nitrogen deficient wastewater containing 1% (w/v) glucose was selected as the lipid production condition for *Chlorella emersonii* and *Pseudokirchneriella subcapitata* respectively. Figure 7.13 (a), (b) represent the loss of pigmentation due to absence of nitrogen in *Chlorella emersonii* and *Pseudokirchneriella subcapitata* respectively.

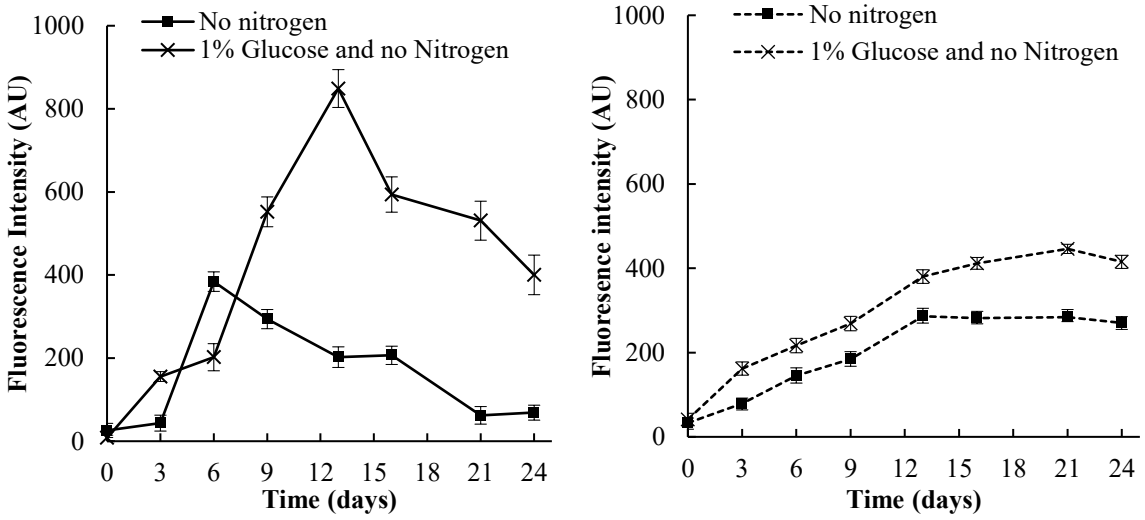

Figure 7.12 (a), (b): The effect of nitrogen deficient media with and without 1% (w/v) glucose on the production of neutral lipids in (a) *Chlorella emersonii* and (b) *Pseudokirchneriella subcapitata* as determined by the Nile Red assay. The data represented here is the average of three independent experiments with five assay values and the error bars shown are the standard deviation.

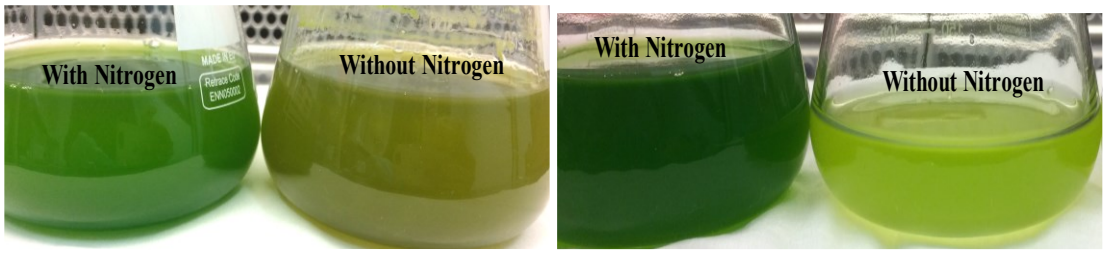

(a) (b)

Figure 7.13 (a), (b): Images (a), (b) show the appearance of *Chlorella emersonii* and *Pseudokirchneriella subcapitata* in the presence or absence of nitrogen.

7.2.4. Neutral lipid content

Using the standard curve generated by a five-point calibration of triolein (see Appendix J), the concentration of triacylglycerols in *Chlorella emersonii* and *Pseudokirchneriella subcapitata* after 13 and 21 days of culturing (Section 7.2.3) was estimated to be 0.61±0.017mg/mg and 0.31±0.006mg/mg of dry biomass respectively.

7.3. DISCUSSION

7.3.1. Biomass generation and neutral lipid production

The primary hurdle in commercialization of biodiesel from microalgae is the high cost of biomass production (Mondal *et al.*, 2017). Biomass and intracellular lipid yields can be increased through metabolic pathway optimization during cultivation, including the exploration of alternative substrates (Su *et al.*, 2011; Kim *et al.*, 2019). Carbon is essential for the growth and development of any living organism; and its form dictates the metabolic pathway in which it will be assimilated. Carbon is fixed by two primary avenues in microalgae: autotrophic (photosynthetic growth and fixation of inorganic carbon; i.e. carbon dioxide through the Calvin-Bensen cycle), and heterotrophic (assimilation of organic carbon in the absence of light). Another form of metabolic processing, referred to as mixotrophic, or photoheterotrophic, also exists in microalgae. Mixotrophic cultivation improves the efficient use of light or eliminates its requirement by cells; CO_2 and organic carbon are used in photosynthetic and respiratory metabolism simultaneously, resulting in a synergistic effect of the two processes (Yeesang and Cheirsilp, 2014). Mixotrophic growth conditions of

microalgae have shown promising results for increasing both biomass and lipid content (Lee *et al.*, 1996; Yamane *et al.*, 2001; Lowrey, Brooks and McGinn, 2015; Ratnapuram, Vutukuru and Yadavalli, 2018). Alternative carbon sources, that are compatible with heterotrophic and mixotrophic microalgae culture, include wastewater. Wastewater not only provides nitrogen, phosphate, minerals, and other trace metals for the growth and development of microalgae; it also has a high concentration of organic carbon which can support microalgal heterotrophic and mixotrophic growth. Microalgae are adapted for wastewater treatment as they can use inorganic nitrogen and phosphorus for their growth, and can also remove heavy metals and xenobiotic substances; thereby purifying wastewater (Yeesang and Cheirsilp, 2014). Mixotrophic cultivation does suffer from many disadvantages; such as increased costs associated with an organic carbon (mostly glucose) requirement; a reduction in pigmentation and therefore production of high value phytochemicals (Yamane *et al.*, 2001; Mata, Martins and Caetano, 2010; Bhatnagar *et al.*, 2011); a requirement of sterile media (bacterial contamination due to organic carbon; Chen et al. 2011); release of CO_2 due to respiration during growth (Yang, Hua and Shimizu, 2000; Perez-Garcia *et al.*, 2011); and a reduced energy conversion efficiency compared to autotrophic growth (Yang, Hua and Shimizu, 2000).

Despite of all these disadvantages, various studies focus on implementing mixotrophic culturing for the generation of microalgal biomass. For example, a maximum biomass concentration of 11.1g/L was observed in mixotrophic conditions (utilising glucose as organic carbon) for *Chlorella sorokiniana*, compared to a 2.2g/L yield in photoautotrophic conditions for the same species (Lee *et al.*, 1996). A maximum biomass of 2.46g/L was also obtained for *Botryococcus braunii* cultured in mixotrophic conditions, where 5g/L of glucose was used as an organic carbon source (Yeesang and Cheirsilp, 2014). Similarly, *Chlamydomonas globosa*, *Chlorella minutissima* and *Scenedesmus bijuga* cultured mixotrophically in treated and untreated wastewater resulted in 3 to 10 fold increase in biomass in comparison to photoautotrophic conditions (Bhatnagar *et al.*, 2011). High biomass from mixotrophic conditions has also been achieved from *Euglena gracilis* in presence of glucose (1.2% w/v) resulting in 15-19% biomass increase (Yamane *et al.*, 2001). Similarly, *Chlorella sorokiniana,* grown in the presence of 0.1M glucose in an outdoor enclosed tubular

photobioreactor resulted in biomass of 206gm/m^2/day (Lee *et al.*, 1996). Furthermore, nine days culturing in 40g/L glucose resulted in maximum biomass for *C. protothecoides* (Shen *et al.*, 2009). In this study, for both *Chlorella emersonii* and *Pseudokirchneriella subcapitata*, the highest biomass was also observed in mixotrophic growth conditions (with 1% w/v glucose) after five and eight days of cultivation respectively (Section 7.2.1). Though various sources of organic carbon (glucose, acetate, sucrose etc.) have been used for mixotrophic and heterotrophic growth conditions, the most prevalent source is glucose ($C_6H_{12}O_6$) due to its availability (Perez-Garcia *et al.*, 2011). Also, since glucose is one of the final photosynthesis products; it may be considered that any photosynthetic microorganism must be able to incorporate it in its metabolism (Yeesang and Cheirsilp, 2014). Hence, in the current study, glucose was used as a source of organic carbon for mixotrophic and heterotrophic growth conditions for the microalgae strains.

There are limited studies conducted to date using wastewater for mixotrophic or heterotrophic cultivation of microalgae. Concerns about the availability and form of organic carbon, as well as the presence of competitive microorganisms (i.e., non-symbiotic bacteria) are among the factors responsible for the limited mixotrophic/heterotrophic studies to date (Lowrey, Brooks and McGinn, 2015). In this study, the reduced biomass produced through the autotrophic culturing mode for both the microalgal strains (*Chlorella emersonii* and *Pseudokirchneriella subcapitata*; Section 7.2.1) could be due to cellular self-shading, resulting in reduced light availability (Yeesang and Cheirsilp, 2014). It is well known that photoautotrophic conditions generate low cell density over long cultivation times (Mohamed, Wei and Ariff, 2011; Abreu *et al.*, 2012); which was also observed in the current study of *Chlorella emersonii* and *Pseudokirchneriella subcapitata* (Section 7.2.1). Based on the results of this current study and the literature for other microalgae strains; mixotrophic cultivation of *Chlorella emersonii* and *Pseudokirchneriella subcapitata* was proposed as potential alternative for microalgae biomass production.

The ability of microalgae to survive or proliferate over a wide range of environmental conditions can be due to unusual cellular lipids as well as an ability of microalgae to modify lipid metabolism in response to altered environmental conditions (Thompson, 1996; Wada and Murata, 1998; Gouveia and Oliveira, 2009). Under optimal growth conditions,

microalgae can synthesize glycerol-based polar membrane lipids (between 5–20% of dry cell weight; DCW, Hu et al. 2008); under unfavourable/stress conditions many microalgae alter their lipid biosynthetic pathways towards the formation and accumulation of neutral lipids (between 20–50% DCW), mainly in the form of sterols, sterol esters, monoacylglycerol (MAG), diacylglycerol (DAG) and triacylglycerol (TAG). TAGs do not perform any structural role in microalgae cells as they are densely packed in the cytoplasm, but they instead serve as a carbon and energy source (Hu *et al.*, 2008).

Many naturally occurring microalgal strains used for neutral lipid production suffer from low cellular lipid content or low biomass, and therefore, metabolic engineering of microalgae to increase lipid production has been explored in the past (Y. Li *et al.*, 2010). Shen and colleagues (Shen *et al.*, 2009) have demonstrated that limiting certain nutrients (e.g. nitrogen) can result in higher lipid production and storage in microalgal cells, as the microalgal cells respond to the stress conditions imposed. Using this approach; the total lipid content in microalgae can vary between 1–85% (DCW); however, values >40% are typically achieved under nutrient limitation. Spoehr and Milner (Spoehr and Milner, 1949), first demonstrated that lipid content could be increased (from 5% to 85%) in nitrogen starved *Chlorella pyrenoidosa* culture, and since then nutrient deficiency/depletion (particularly nitrogen) has been regarded as the most efficient approach to increase lipid content in algae (Rodolfi *et al.*, 2009). Building on this, the accumulation of neutral lipids (particularly TAGs) in nitrogen deficiency/starvation has been reported in numerous microalgal species and strains; for example, *Chlorella* sp. (Hsieh and Wu, 2009); *Neochloris oleoabundans* (Gouveia and Oliveira, 2009), *Nannochloropsis oculate* (Su *et al.*, 2011) and *Nannochloropsis* (Rodolfi *et al.*, 2009) have shown an increase in neutral lipid content of between 1.5 to 5 fold under nitrogen starvation/depletion.

Additionally, decreasing nitrate (from 35.3mM to 0.2mM) resulted in increased neutral lipid formation from 9% of dry weight to 43% in *Chlorococcum* sp. (Harwati, 2013). Total neutral lipid content produced by *C. protothecoides* in a low-nitrate-concentration medium was at least 23% higher than that in media with a higher nitrogen concentration (Shen *et al.*, 2009). In the current study, the depletion of the nitrogen source from simulated wastewater media in cultivation of *Chlorella emersonii* and *Pseudokirchneriella subcapitata* resulted in

production of maximum neutral lipids after 6 and 12 days of incubation respectively (Section 7.2.4). The increase in lipid production under nitrogen limited conditions is typically due to the disorganization of lipid-synthesizing enzymes and is less than compared to carbohydrate synthesizing enzymes; thus, the major proportion of carbon is bound in lipids (Becker, 1994). Ultimately, the lipid content of microalgae is one of the most important parameters in determining the economic viability of microalgae-based biodiesel production. However, an increased microalgae lipid content does not always correlate with a high total lipid production as higher lipid content is often associated with low biomass productivity (Y. Li *et al.*, 2008). Therefore, it is important to explore culture optimisation considering both biomass production and neutral lipid accumulation.

A high concentration of the appropriate nutrients is necessary for a high growth rate (i.e. maximum biomass); but accumulation of a large concentration of lipids normally cannot take place during increased growth. Culturing under nitrogen deficient conditions leads to higher lipid accumulation, but with lower biomass, and vice-versa. A possible explanation for this vice-versa phenomenon may be the starch synthesis pathway. In high nitrogen cultures, microalgae cells synthesise starch to support their growth; while in limited nitrogen, the starch synthesis pathway is blocked, and fixed carbon is redirected into fatty acid synthesis, and therefore lipid accumulation. Simultaneously, starch which is the carbon and energy source will get exhausted and the photosynthetic efficiency of microalgae cells will reduce (Y. Li *et al.*, 2010). Therefore, the observed change in physiological appearance in nitrogen starved *Chlorella emersonii* and *Pseudokirchneriella subcapitata* in this study could be due to a loss of chlorophyll and a reduction in photosynthetic efficiency (Figure 7.9 c, d). Therefore, in nitrogen deficient conditions, microalgae growth will be retarded, and less biomass will be produced. Due to reduced biomass production there is a possibility that the overall lipid productivity might even be lower in the nitrogen deficient conditions (Huang *et al.*, 2010).

In order to balance the challenges associated with simultaneous production of biomass and neutral lipids; a two-stage cultivation process can be followed, as in this study. The first step of cultivation focuses on microalgal biomass generation by providing optimum nutrients. In the second stage the biomass from first stage is harvested, washed with deionized water to remove any traces of nitrogen or other nutrients from stage one and then biomass is grown in

nitrogen deficient media. A similar two stage cultivation process has been successfully used for the generation of high lipid content from *Nannochloropsis oculata* where biomass generation at first stage was done in the presence of 1.7μM urea followed by a second stage cultivation with no nitrogen. With this two stage process, a 2.82 fold increase in lipid content was generated compared to the traditional single stage batch cultivation systems (Su *et al.*, 2011). Ratnapuram and co-workers (Ratnapuram, Vutukuru and Yadavalli, 2018) demonstrated that for *Chlorella pyrenoidosa* a neutral lipid yield of 284g/kg dry biomass was achievable. Here, the first stage of biomass generation was mixotrophic growth in 3g/L glucose. This was followed by a second stage of lipid generation in stress conditions involving a decrease in light intensity, nitrogen starvation, bicarbonate and glucose supplementation generated. The absence of nutrients (nitrogen or phosphorous) in stage two of cultivation reduces the biomass however; incorporation of an organic carbon source, like glucose or sodium acetate, is known to enhance lipid production along with biomass. For example, the addition of 4g/L sodium acetate in nitrogen and phosphorous deficient media increased total lipid content by 93% in *Chlamydomonas reinhardtii* (Yang *et al.*, 2018). Similarly, it has been reported that supplementation of glucose in reduced nitrogen media enhanced the lipid accumulation to 47.67% of dry weight in *Chlorella kessleri* (Wang, Chen and Qin, 2012). Heterotrophic lipid generation conditions in *Chlorella protothecoides* also demonstrated an increase in lipid content from 15% to 55% of dry biomass (Miao and Wu, 2006). Lipid accumulation in heterotrophic/mixotrophic conditions is usually induced by resource exhaustion, either due to high-density cultures or extended growth periods (Perez-Garcia *et al.*, 2011). This mirrors the key observations in the current study. Following the two-step cultivation for *Chlorella emersonii* and *Pseudokirchneriella subcapitata* an increase in lipid content was observed when 10g/L of glucose was added in a nitrogen starved environment (Section 7.2.3). In autotrophic nitrogen deficient media, 6 days and 13 days of cultivation generated maximum neutral lipid content, however; in a mixotrophic condition a 45% and 64% increase in neutral lipid content was achieved after 13 days and 21 days of cultivation for *Chlorella emersonii* and *Pseudokirchneriella subcapitata* respectively (Figure 7.9 a, b). Most microalgae grow at temperatures between 20 and 24°C. However, the optimal growth temperature varies by species, strain culture and composition of the culture medium. For the

growth and lipid production of *Chlorella emersonii* and *Pseudokirchneriella subcapitata*, 18°C with 16h:8h light dark cycle was noted as optimal and echoes the supplier-suggested conditions (see Section 3.2.6.5).

Optical density was the primary instrument used for measuring biomass to estimate growth; however, this technique is also strain specific and can be influenced by the pigments synthesized by the microalgae. For example, an optical density measurement at 750nm has been used to measure biomass for determining growth rate in *Chlorella sorokiniana*, *M. reisseri* (Radzun *et al.*, 2015). For *Chlorella minutissima* 680nm was used for measuring growth (Tang *et al.*, 2011). For *Neochloris oleoabundans*, biomass was monitored by measuring optical density at 600nm (Y. Li *et al.*, 2008). For *Chlorella vulgaris* (Morschett, Wiechert and Oldiges, 2016) and for many other microalgal strains (Rodolfi *et al.*, 2009) an optical density at 750nm was used to measure biomass. 682nm was used for monitoring cell growth of *Nannochloropsis oculata* (Su *et al.*, 2011) while for *Chlorella pyrenoidosa* an optical density of 647nm and 664nm was used (Ratnapuram, Vutukuru and Yadavalli, 2018). In this study, for both *Chlorella emersonii* and *Pseudokirchneriella subcapitata*, a linear relationship between cell number and OD_{590nm} was observed; hence an optical density of 590nm was used for checking biomass and generating growth curves (Section 7.2.1) One unit of optical density at 590nm was noted to correspond to 10^7 cells/ml; this approach was validated by a simultaneous microscope haemocytometer-based count.

7.3.2. Nile red assay for neutral lipid estimation

Fluorescent dyes offer a useful method for the measurement of intracellular lipids. They are inexpensive and require simple optical measurement instrumentation while simultaneously providing the opportunity of high throughput application. BODIPY® 505/515 (4,4-difluoro-1,3,5,7-tetramethyl-4-bora-3a,4a-diaza-s- indacene) and Nile Red (9-diethylamino- 5-benzo [α] phenoxazinone) are the most common lipophilic dyes. These dyes have been used for the detection of intracellular lipids by fluorescence microscopy, spectrofluorometry and flow cytometry (Cirulis *et al.*, 2012). Nile Red is a more suitable dye for spectrofluorometric applications as BODIPY® staining suffers from strong dye background fluorescence (Govender *et al.*, 2012a). Nile Red is a hydrophobic (and therefore has poor solubility and

fluorescence in water) and metachromatic dye with colour emission from deep red to strong yellow/gold based in solvent. Hence, the spectral properties (excitation and emission characteristics) of Nile Red are highly dependent on the polarity of microenvironment (Greenspan, Mayer and Fowler, 1985; Ghoneim, 2000; Lakowicz J.R., 2006; Elsey *et al.*, 2007). The peak emission is blue shifted as the surrounding polarity decreases (Cooksey *et al.*, 1987a; Alonzo and Mayzaud, 1999; Elsey *et al.*, 2007). The blueshift being 632 nm for ethanol, 600 nm for chloroform and 576 nm for hexane (Greenspan and Fowler, 1985; Elsey *et al.*, 2007; Mutanda *et al.*, 2011). Therefore, considerable variation in the excitation and emission wavelengths is required for different classes of hydrophobic molecules. Short excitation wavelengths (450-500 nm) and yellow/gold emission wavelengths (≤580 nm) favour detection of highly hydrophobic environments like neutral lipids (TAGs; (Greenspan and Fowler, 1985). As lipids increase in polarity (diacylglycerols and monoacylglycerols) the maximum Nile Red emission shifts to 610 and 640 nm accordingly (Cirulis *et al.*, 2012); hence longer excitation wavelengths (515-560 nm) and red emission wavelengths (≥590 nm) favour a general fluorescence for polar lipids (intracellular membrane phospholipids (Greenspan and Fowler, 1985). Based on these observations; Nile Red, at an excitation/emission wavelengths of 450nm to 500≥528nm, has been used for staining and detecting lipid vesicles in smooth muscle cells and in cultured macrophages (Greenspan and Fowler, 1985; Greenspan, Mayer and Fowler, 1985). Nile Red has also been used in ligand-hydrophobic protein surface interactions at 570/610nm wavelengths (Sackett and Wolff, 1987). However, the most common use of Nile Red though is staining of intracellular neutral lipids (TAGs) in microbial cells by using wavelengths 488/565 to 585nm (Kimura, Yamaoka and Kamisaka, 2004); in microalgae with 488 to 600nm (Cooksey *et al.*, 1987a) and for microalgal total lipids with 490/585nm (Lee, Yoon and Oh, 1998). A high correlation between neutral lipid content (as per the gravimetric method) and Nile Red fluorescence has been established and the assay is used as the quantitative analysis method of choice for neutral lipid quantification in a variety of microalgae, such as *Chlorella* sp. (Chen *et al.*, 2009; Huang, Chen and Chen, 2009). Therefore, the Nile Red assay is a suitable choice for neutral lipid estimation in *Chlorella emersonii* and *Pseudokirchneriella subcapitata* in present study. To enhance neutral lipid staining by Nile Red, solvents such as acetone, dimethylsulfoxide

(DMSO), ethanol, isopropanol, hexane or chloroform have been used; with DMSO and acetone being the most commonly used solvents (Cooksey *et al.*, 1987b; Chen *et al.*, 2009; Satpati and Pal, 2015).

In this study, a standard and bespoke Nile Red assay was developed and optimised for the microalgae strains at hand and to reduce background interference. Intracellular neutral lipids can be detected via a Nile Red fluorescence signal with a maximum emission at 570-580 nm; however, proteins and other microalgal pigments (e.g. chlorophyll) can interfere with fluorescence intensity (Cirulis *et al.*, 2012). Green microalgae species contain chlorophyll (1-4% of the dry weight) which increases the fluorescence background (Chen et al. 2011; Cirulis et al. 2012; Satpati & Pal 2015). Therefore, for accurate quantification of neutral lipids; optimal excitation and emission wavelengths for each microalgal strain must be identified. Neither significant background fluorescence, nor Nile Red (600–750 nm), nor chlorophyll mediated cellular autofluorescence (650–750 nm) have been reported to interfere at this wavelength (Morschett, Wiechert and Oldiges, 2016). By choosing an excitation/emission setup of 480/570–580 nm, Nile Red was successfully used for staining neutral lipids from *Chlorella vulgaris* under nutrient starvation conditions (Morschett, Wiechert and Oldiges, 2016). Irrespective of DMSO and acetone concentrations, an excitation emission wavelength of 530/580nm was found to be optimum for neutral lipid detection in *Chlorella emersonii* and *Pseudokirchneriella subcapitata* (Section 7.2.2.1), which follows the observations noted in key literature references sources (Chen *et al.*, 2009; Cirulis *et al.*, 2012; Isleten-Hosoglu, Gultepe and Elibol, 2012; Halim and Webley, 2015; Satpati and Pal, 2015). Low DMSO concentrations (between 5-25% v/v) have been extensively used in effective lipid staining (Chen *et al.*, 2009; Doan and Obbard, 2011; Govender *et al.*, 2012b). Outside this concentration range, the fluorescence efficiency decreased (Chen *et al.*, 2009). For effective neutral lipid detection a final concentration of 5% (v/v) DMSO was used for *Pseudochlorococcum* sp. and *Scenedesmus dimorphus* (Chen et al. 2011), whilst 15% (v/v) DMSO was used for *Nannochloropsis* sp. (Doan and Obbard, 2011); and 25% (v/v) DMSO for *Chlorella vulgaris* (Chen *et al.*, 2009). In this study, for both *Chlorella emersonii* and *Pseudokirchneriella subcapitata*, 20% (v/v) DMSO was found to be optimum for attaining maximum fluorescence intensity (Section 7.2.2.1). With increased DMSO concentrations

resulting in a decrease in fluorescence intensity, echoing seminal literature sources (Chen *et al.*, 2009; Cirulis *et al.*, 2012; Satpati and Pal, 2015). The decrease in fluorescence intensity at higher DMSO concentrations could be due to cell lysis/low cell survival and enhanced cellular debris (Pick & Rachutin-Zalogin 2012; Cirulis et al. 2012). For example, *Nannochloropsis* sp. exposed to DMSO concentration varying from 7% to 10% (v/v), respectively reported lower cell survival; and cultures exposed to 15% (v/v) DMSO collapsed, demonstrating DMSO toxic effect (Doan and Obbard, 2011).

Nile Red dissolved in acetone generated lower fluorescence intensity (Figure 7.3, 7.4). In addition to being sensitive towards polar environments, fluorescence from Nile Red is also affected by the volatility of the solvent. Acetone can be used as a solvent for Nile Red neutral lipid determination; however, due to its volatility; the solution is unstable and its repeated use over long periods generates concentration variations (Pick and Rachutin-Zalogin, 2012). Nile Red fluorescence intensity is also dependent on dye concentration, cell concentration, incubation time and temperature due to quenching issues (Lakowicz J.R., 2006; Pick and Rachutin-Zalogin, 2012). To finalise the optimum Nile Red concentration for neutral lipid detection, it is important to keep the concentration of the solvent constant, while varying only dye concentration.

In the current study, an increase in fluorescence intensity was observed with an increase in Nile Red concentration (10µg/ml i.e. 0.03µM and 5 µg/ml i.e. 0.015µM for *Chlorella emersonii* and *Pseudokirchneriella subcapitata* respectively); however, with higher dye concentrations, the fluorescence intensity decreased (Section 7.2.22). Overall, the mean fluorescence intensity increased with increasing concentration of dye (>1µg/ml), indicating that at low Nile Red concentrations cellular lipids were not saturated (Cirulis *et al.*, 2012). Furthermore, at low Nile Red concentrations (~0.5µM), quenching is minor compared to high concentrations (>5µM; Pick & Rachutin-Zalogin 2012). Using triolein (TO) as a standard of triacylglycerol, it has been demonstrated that when the Nile Red concentration is low compared to lipid droplets, the dye is less accessible to all the lipid droplets (Pick and Rachutin-Zalogin, 2012). Conversely, with increased Nile Red concentrations, the dye not only interacts with neutral lipids but also with phospholipidic coat and hydrophobic protein surfaces; generating a redshift of emission peak which interferes with neutral lipid

fluorescence (Bertozzini *et al.*, 2011). A concentration dependent aggregation and precipitation of Nile Red has also been reported (Pick and Rachutin-Zalogin, 2012). An optimum concentration of Nile Red (generally between 0.01 to 100µg/mL) is required to stain each individual microalgal species (Chen *et al.*, 2009; Huang, Chen and Chen, 2009; Govender *et al.*, 2012b). For example, 0.7µg/mL of Nile Red in DMSO (0.165g/ml, or 15% v/v) was found to be optimal for neutral lipid quantification in *Nannochloropsis* sp. (Doan and Obbard, 2011), whereas, 0.5µg/mL of Nile Red in 20% (v/v) DMSO for *C. vulgaris* (Chen *et al.*, 2009). In this study, for the estimation of neutral lipids in *Chlorella emersonii* and *Pseudokirchneriella subcapitata* a concentration of 10µg/ml and 5 µg/ml was observed to be optimal (Section 7.2.2.2, Figure 7.5).

For the detection and quantification of neutral lipids from *Chlorella emersonii* and *Pseudokirchneriella subcapitata*, an incubation temperature of 40°C was used (Section 7.2.2.3) as very few studies have investigated the effect of temperature on neutral lipid staining via Nile Red. Staining of neutral lipids in *Chlorella vulgaris* was checked at incubation temperatures between 20°C and 80°C, and a temperature of 40°C was the most appropriate for staining (Chen *et al.*, 2009). For *Chlorococcum infusionum* and *C. ellipsoidea* an optimum temperature for Nile Red staining was 30-40°C and 40-50°C respectively (Satpati and Pal, 2015). It has been hypothesized that though higher temperature facilitates Nile Red permeation into microalgal cells (Rumin *et al.*, 2015), it also is responsible for fluorescence quenching and changes in lipid accumulation (Chen *et al.*, 2009; Satpati and Pal, 2015).

The intensity of Nile Red fluorescence is generally not constant over time in microalgae (Cooksey *et al.*, 1987a; Elsey *et al.*, 2007; Pick and Rachutin-Zalogin, 2012); maximum fluorescence is not attained at the same time for all microalgal species and shape, quenching of the fluorescence curve is species specific (Cooksey *et al.*, 1987a; Pick and Rachutin-Zalogin, 2012). After the addition of Nile Red to microalgal cells, fluorescence increases to reach a peak and then plateaus or decreases with time. A 60min and 40min incubation at 40°C with 10µg/ml and 5µg/ml Nile red (20% v/v DMSO) was used to identify the maximum fluorescence intensity in the case of *Chlorella emersonii* and *Pseudokirchneriella subcapitata* respectively. It was noted that increased incubation resulted in decreased fluorescence intensity in *Chlorella emersonii*; while fluorescence plateaued in the case of

Pseudokirchneriella subcapitata (Section 7.2.2.3, Figure 7.6). Similar observations have been made in Nile Red neutral lipid staining for *Dunaliella salina, Dunaliella parva, Dunaliella bardawil* and *Nanochloris atomus* (Pick and Rachutin-Zalogin, 2012); and *Chlorella vulgaris* (Chen *et al.*, 2009). Conversely, to obtain the maximum fluorescence intensity; a 5min incubation was sufficient in case of *Nannochloropsis* sp. (Doan and Obbard, 2011), a 15min incubation time for *Tetraselmis suecica* (Montero, Aristizabal and Reina, 2011), and 20min for *Chlorella vulgaris* and *S. dimorphus* (Cirulis *et al.*, 2012). For *Chlorella ellipsoidea* and *Chlorococcum infusionum*; maximum staining efficiency was recorded at 5µg/mL Nile Red in 40% (v/v) DMSO after 15min of incubation at 40 °C (Satpati and Pal, 2015). It has been suggested that after long incubations, fluorescence quenching occurs due to interaction of dye and cell compounds rather than enzymatic degradation of dye (Pick and Rachutin-Zalogin, 2012). Fluorescence and staining kinetics, in addition to microalgae species, depend on the size and quantity of lipid droplets within microalgae (Pick and Rachutin-Zalogin, 2012). The difference in staining time is also dependent on the composition and structure of the microalgal cell wall. Robust and thick cell walls (particularly in green algae and nutrient starved microalgae) act as a barrier; preventing efficient penetration of Nile Red in cells and neutral lipid staining (Doan and Obbard, 2011; Guzman *et al.*, 2011; Pick and Rachutin-Zalogin, 2012).

Although appropriate staining conditions (dye concentration, temperature, organic solvents) have been established for different microalgae, their applicability remains dependent on the cell concentration. A decrease in fluorescence (or saturation) has been reported below and above the threshold of cell concentration for neutral lipid staining at fixed Nile Red concentrations. Therefore, it is important to establish a linear correlation between microalgae concentration and fluorescence intensity between these thresholds. The optimum range of cell concentration is species specific and varies between $5x10^4$ to $1x10^6$ cell/mL, as observed with *Chlorella vulgaris* (Chen *et al.*, 2009; Isleten-Hosoglu, Gultepe and Elibol, 2012) and *Scenedesmus dimorphus* (Cirulis *et al.*, 2012). A linear relationship between fluorescence intensity and cell concentration was observed between 0.2-0.7 OD_{590nm} (at 1OD unit = 10^7cells/ml) for both *Chlorella emersonii* and *Pseudokirchneriella subcapitata* (Section 7.2.2.5, Figure 7.7), above and below this range saturation in fluorescence intensity was

observed. For *C. saccharophila* florescence intensity was linear over the cell turbidity of 0.03-0.10 OD_{750nm} (Isleten-Hosoglu, Gultepe and Elibol, 2012). For *C. vulgaris*; a linear relationship between cell concentration and fluorescence intensity of *Chlorella vulgaris* was established between $5x10^4$cells/ml and $4x10^5$cells/ml (Chen *et al.*, 2009) and $3x10^5$ cells/mL (OD_{750nm}=0.06) was used in optimization of staining procedure (Huang, Chen and Chen, 2009). In general, as microalgal biomass increases, fluorescence signal saturation occurs and is possibly caused by one or a combination of the following; limited dye transport to lipid droplets, adsorption to other hydrophobic compartments like membrane phospholipids, depletion of Nile Red or a negative effect in the cell permeation/staining reaction. Furthermore, Nile Red diffusion from hydrophobic cell membrane via the aqueous cytoplasm towards the liposomes, as well as its uptake by the liposomes itself, could be rate limiting step (Morschett, Wiechert and Oldiges, 2016).

Neutral lipid content of 0.61±0.017mg/mg and 0.31±0.006mg/mg of dry biomass for *Chlorella emersonii* and *Pseudokirchneriella subcapitata* was obtained after 13 days and 21 days cultivation respectively in nitrogen deficient simulated wastewater media supplemented with 10g/L glucose. This corresponds to 60% and 30% of neutral lipid in dry biomass for *Chlorella emersonii* and *Pseudokirchneriella subcapitata* respectively.

7.4. CONCLUSION

Mixotrophic culturing mode containing 10g/L glucose (1% w/v) in simulated wastewater was found to be optimum for generation of maximum biomass from *Chlorella emersonii* and *Pseudokirchneriella subcapitata* after 5 and 8-days cultivation respectively. Estimation of neutral lipids was carried out using an adapted and optimised Nile Red assay, where 20% (v/v) DMSO was found to be an ideal solvent for penetration of dye in microalgae cells. In brief, 10µg/ml and 5µg/ml Nile Red, in 20% (v/v) DMSO, was the optimal concentration required to obtain maximum fluorescence intensity at 40°C after 60mins and 40mins of incubation with 530/580nm excitation/emission wavelength for *Chlorella emersonii* and *Pseudokirchneriella subcapitata* respectively. Maximum Nile Red fluorescence intensity of 848.81±45.52AU and 445.94±10.89AU was obtained for *Chlorella emersonii* and *Pseudokirchneriella subcapitata* in nitrogen depleted simulated wastewater with 1% (w/v)

(10g/L) glucose after 13days and 21 days of cultivation. Finally, neutral lipid content of 0.61±0.017mg/mg of biomass and 0.31±0.006mg/mg of dry biomass for *Chlorella emersonii* and *Pseudokirchneriella subcapitata* was obtained.

Chapter 8: Enzymatic Transesterification of Olive Oil and microalgal TAGs to produce biodiesel

8.1. INTRODUCTION AND OBJECTIVES

Converting a biological lipid into biodiesel is carried out by a transesterification process. The process involves reaction of the triglyceride molecules present in oils/fats with alcohol to produce esters and glycerol in the presence of a catalyst (acid/alkali or enzyme; see Section 2.8.3). This chapter focuses on the production of biodiesel using an enzyme catalysed transesterification reaction encompassing two different feedstocks: commercially available olive oil (as a standard) and *in-situ* synthesized lipids from microalgae (developed in Chapter 7). By using lipase (both free form and immobilised) from *P. reinekei* (H1), *P. brenneri* (H3) and porcine pancreas (lipase standard; Chapter 5); the overall objectives of this chapter are:

- Parameter optimisation for the synthesis of biodiesel using olive oil as feedstock (including; reaction temperature, oil: methanol molar ratio and reaction time)
- Comparison of the rate of biodiesel synthesis between the free and the calcium alginate entrapped lipase (from Chapter 6) utilising the optimised conditions of olive oil feed stock
- *In-situ* transesterification of neutral lipids from *Chlorella emersonii* and *Pseudokirchneriella subcapitata* (from Chapter 7) for biodiesel synthesis.
- Comparison of olive oil and microalgae synthesized biodiesel, via TLC and GC, with a standardised FAME mix and standard biodiesel for composition and quality determination respectively.

8.2. RESULTS

8.2.1. Synthesis of Fatty Acid Methyl esters (FAMEs) using olive oil

8.2.1.1. Effect of incubation temperature

The transesterification reaction (Section 3.2.7.1), at 40°C, resulted in the synthesis of FAMEs; however, at 30°C no FAMEs were synthesised. The observation was the same for all lipase sources (*P. reinekei*, H1; *P. Brenneri*, H3; and Porcine Pancreas Lipase, PPL, standard). Figure 8.1 is the result of olive oil transesterification reaction utilising different lipase sources.

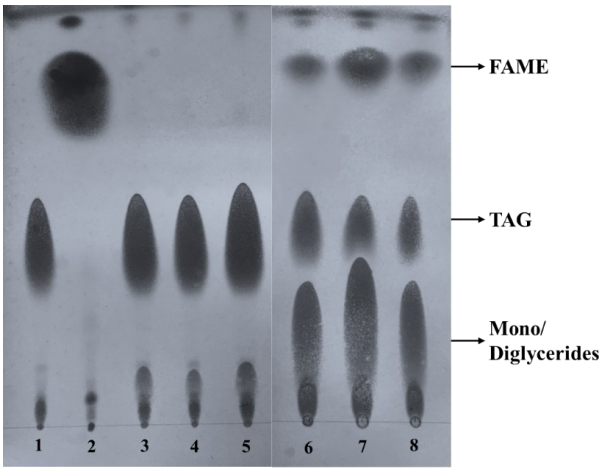

Figure 8.1: TLC (Section 3.2.7.2) plate depicting enzyme synthesized FAMEs using three different lipase sources. FAMEs were synthesized via transesterification (Section 3.2.7.1) of olive oil using lipase from *P. reinekei* (H1; Lanes 3 and 6), *P. brenneri* (H3; Lanes 4 and 7) and PPL (standard; Lanes 5 and 8) after 48h incubation at 40°C (6,7,8) and 30°C (3, 4, 5). Lane 1 and 2 represent olive oil and FAME standard respectively. FAMEs were observed only at 40°C incubation (Lane 6,7,8).

Lipase from all three sources (*P. reinekei*, *P. brenneri*, PPL) catalysed transesterification of olive oil at 40°C. Since no FAMEs were generated at 30°C after 48h incubation, 30°C was not used for further transesterification reaction optimisations.

8.2.1.2. Effect of solvent to oil ratio

A ratio of 1:12 (olive oil: methanol) was found to be optimum for FAMEs production in H1 (*P. reinekei* lipase) and PPL catalysed transesterification reactions. However, for H3 (*P. brenneri* lipase), 1:9 (olive oil: methanol) was the lowest molar ratio required for transesterification reaction. Enhanced synthesis of FAMEs was not observed with increased olive oil to methanol ratio. Figure 8.2 represents the synthesis of FAMEs after

transesterification of olive oil in the presence of different molar ratios of methanol when catalysed via *P. reinekei* (H1; Figure 8.2a), *P. brenneri* (H3; Figure 8.2b) and Porcine Pancreas Lipase (Standard; Figure 8.2c).

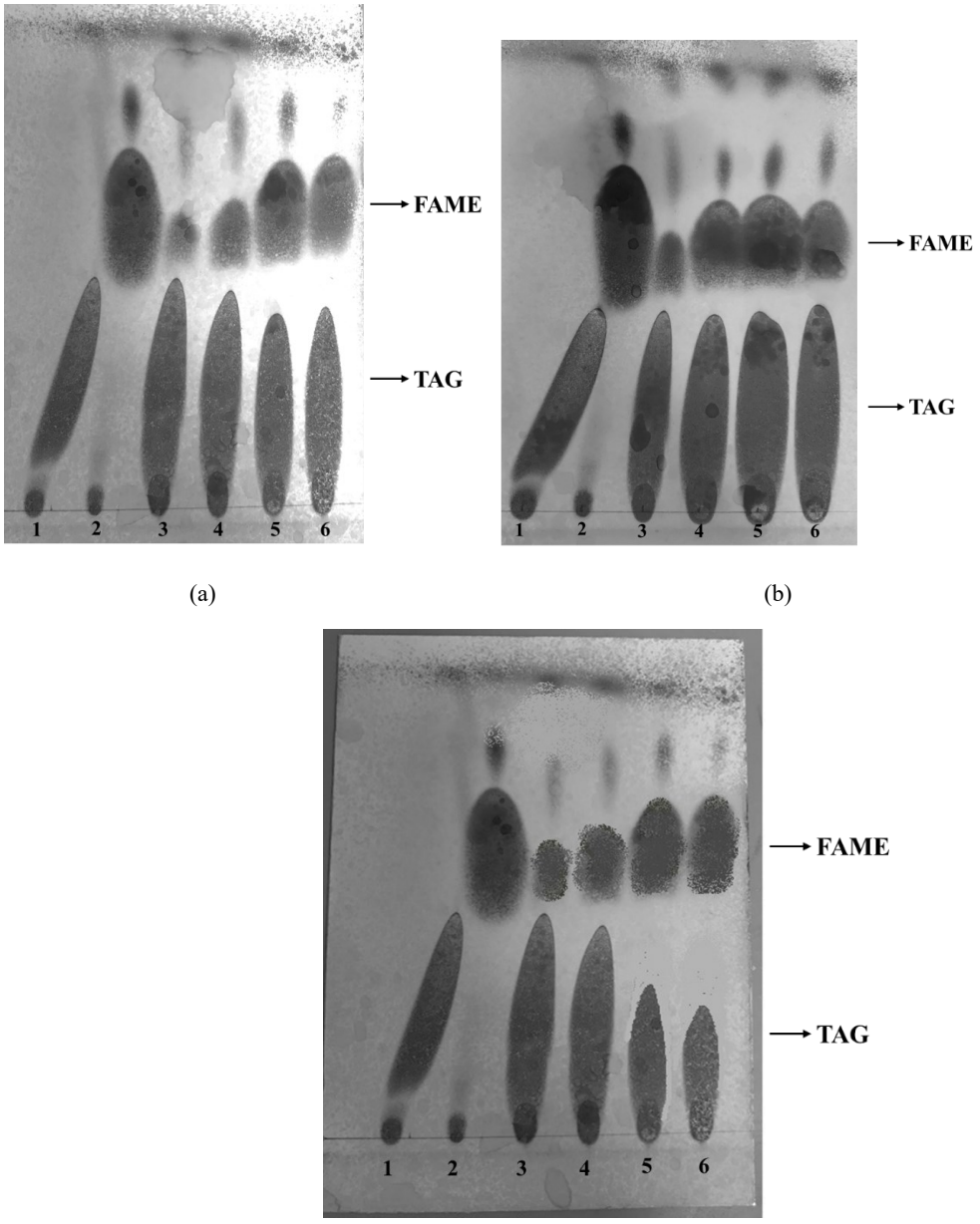

Figure 8.2: TLC (Section 3.2.7.2) plate depeciting synthesized FAMEs, via an enzyme catalysed transesterification reaction of olive oil using various molar ratios of methanol after 72h of incubation at 40°C, 120rpm in shaker water bath. (a) represents catalysis with *P. reinekei* (H1) lipase; (b) with *P. brenneri* (H3) lipase and (c) with porcine pancreas lipase (standard). Lane 1 is Olive oil, lane 2 is the FAME standard, lanes 3, 4, 5, 6 represents a molar ratio (methanol: olive oil) of 6:1, 9:1, 12:1 and 15:1 respectively.

A molar ratio of 1:12 was further used for transesterification optimisation while using lipase from H1 (*P. reinekei*) and PPL. However, for lipase from H3 (*P. brenneri*) a molar ratio of 1:9 (olive oil: methanol) was selected. All the further transesterification optimisation trials were performed at 40°C.

8.2.1.3. Incubation time

A minimum incubation of 72h was required to achieve the maximum transesterification yield irrespective of lipase source (*P. reinekei* H1, *P. brenneri* H3 or PPL). FAMEs were not generated after 28h of incubation, after 48h the quantity, as per TLC, was low. Figure 8.3 a, b, c represents the synthesis of FAMEs after 24h, 48h and 72h incubation at 40°C.

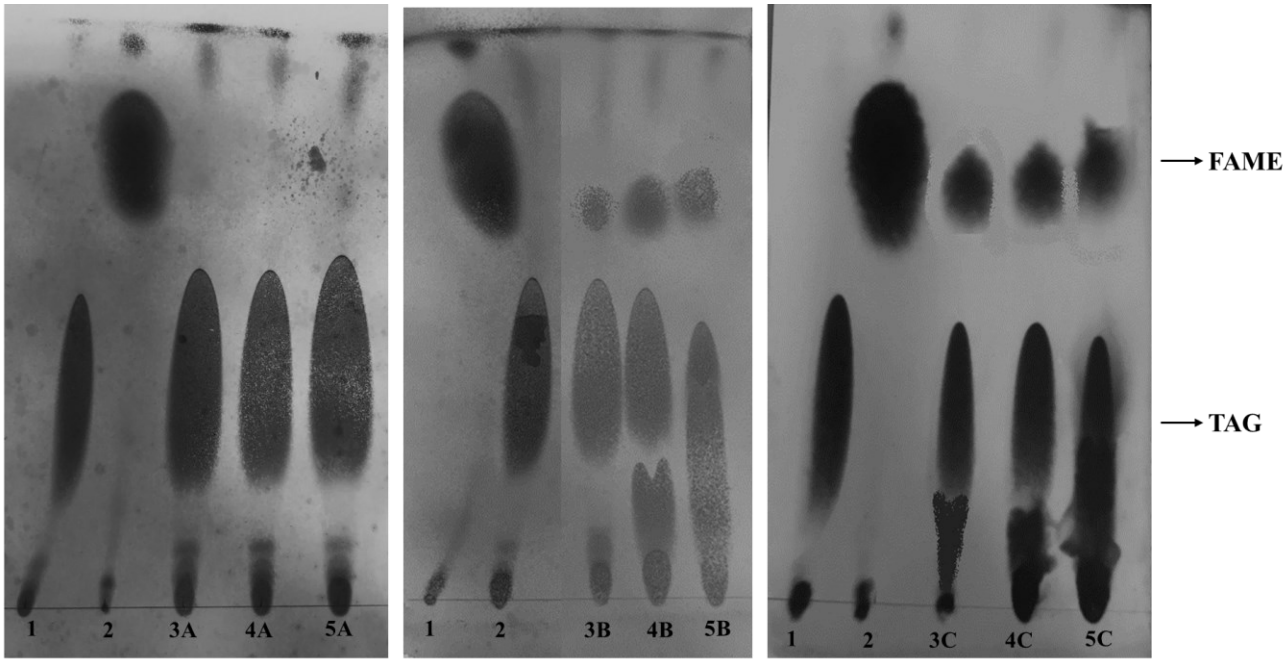

(a) (b) (c)

Figure 8.3: TLC (section 3.2.7.2) plate depecting synthesized FAMEs from olive oil via transesterification over a period of (a) 24h, (b) 48h and (c) 72h. Lanes 1 and 2 represent olive oil and the FAME standard. Lanes 3A, 3B, 3C are enzyme catalysed transesterifications using lipase from *P. reinekei* (H1) over 24, 48 and 72h respectively. Lanes 4A, 4B, 4C are enzyme catalysed transesterifications using lipase from *P. brenneri* (H3) over 24, 48 and 72h respectively. Lanes 5A, 5B, 5C are enzyme catalysed transesterifications using lipase from porcine pancreas (standard) over 24, 48 and 72h respectively.

Using a molar ratio of 1:12 (Olive oil:Methanol) for transesterification reactions of olive oil with lipase from H1 (*P. reinekei*) or PPL; and a molar ratio of 1:9 (Olive oil: methanol) for

transesterification reaction with lipase from H3 (*P. brenneri*); a 72h incubation time at 40°C was found to be optimal under tested conditions.

8.2.1.4. Free lipase vs. entrapped lipase

It was observed that free lipase generated more FAMEs, as detected via TLC, compared to calcium entrapped lipase after 72h of transesterification reaction at 40°C (Figure 8.4).

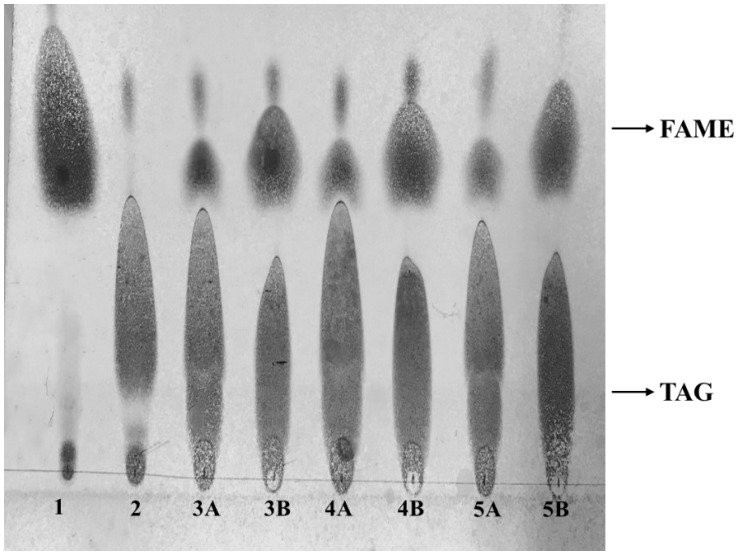

Figure 8.4: TLC (section 3.2.7.2) plate depecting synthesized FAMEs from olive oil using free and calcium alginate entrapped lipase. Samples represented here are the products of transesterification after 72h of incubation at 40°C. Lanes 1 and 2 represent FAME standard and olive oil. Lanes 3A, 4A, 5A are calcium alginate entrapped lipase, while lanes 3B, 4B and 5B are free (in solution) forms from *P. reinekei* (H1), *P. brenerri* (H3) and porcine pancreas (standard) respectively.

A reduced FAMEs concentration, as observed via TLC (Figure 8.4) using calcium alginate entrapped lipases (Chapter 6), indicated less FAMEs synthesis compared to free lipases used in respective transesterification.

8.2.1.5. GC analysis of FAME(s) from olive oil

GC allows identification and as well as quantification of FAMEs synthesized. However due to lack of internal standard, quantification of FAMEs generated in-house was not excecuted via GC. FAMEs synthesized from the transesterification reaction of olive oil were only identified via GC and were represented as a mixed composition of FAMEs as compared with a FAME standard mix (Appendix L). GC profiles of the FAMEs generated are represented in

Figure 8.5, 8.6, 8.7, while Table 8.1 represent the composition of the FAMEs in terms of C18:0 and C20:0.

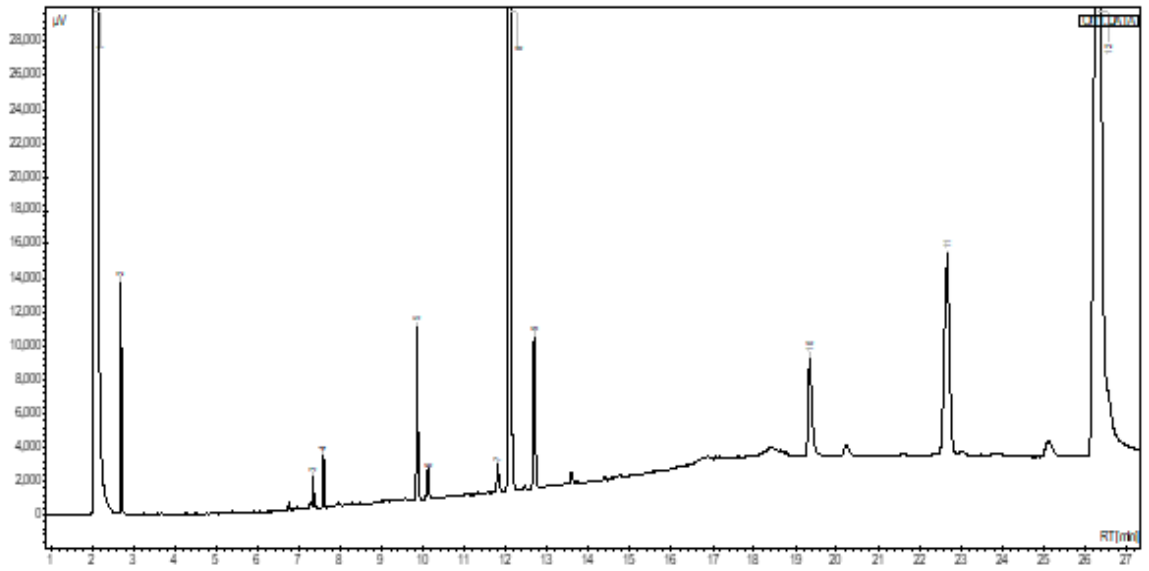

Figure 8.5: GC chromatogram of FAMEs synthesized from the transesterification reaction of olive oil using lipase from H1 (*P. reinekei*). 1: Solvent; 2: Capric acid (C10:0); 3: Myristoleic acid (C14:1); 4: Pentadecanoic acid (C15:0); 5: cis-10-heptadecenoic acid (C17:1); 6: stearic acid (C18:0); 7: linolelaidic acid (C18:2n6t); 8: linoleic acid (C18:2n6c); 9: γ-linolenic acid (C18:3n6); 10: cis-13,16-docosadienoic acid (C22:2); 11: lignoceric acid (C24:0); 12: nervonic acid (C24:1n9). GC and peak identification were done as per section 3.2.7.3.

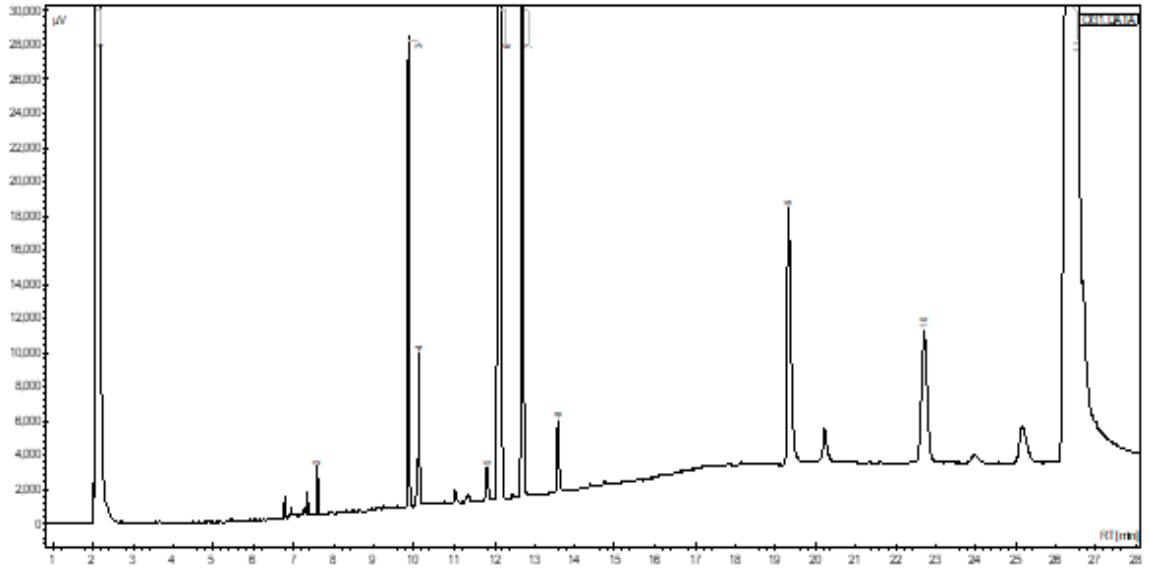

Figure 8.6: GC chromatogram of FAMEs synthesized from the transesterification reaction of olive oil using lipase from H3 (*P. brenneri*). 1: Solvent; 2: Pentadecanoic acid (C15:0); 3: cis-10-heptadecenoic acid (C17:1); 4: stearic acid (C18:0); 5: linolelaidic acid (C18:2n6t); 6: linoleic acid (C18:2n6c); 7: γ-linolenic acid (C18:3n6); 8: arachidic acid (C20:0); 9: cis-13,16-docosadienoic acid (C22:2); 10: lignoceric acid (C24:0); 11: nervonic acid (C24:1n9). GC and peak identification were done as per section 3.2.7.3.

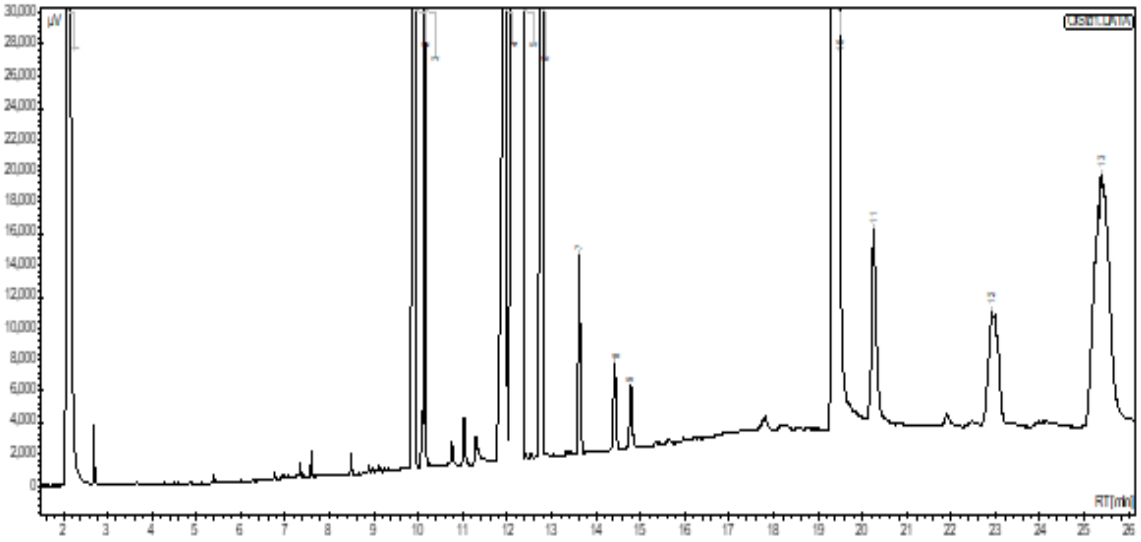

Figure 8.7: GC chromatogram of FAMEs synthesized from the transesterification reaction of olive oil using lipase from porcine pancreas (standard). 1: Solvent; 2: cis-10-heptadedenoic acid (C17:1); 3: stearic acid (C18:0); 4: linoleic acid (C18:2n6c); 5: γ-linolenic acid (C18:3n6); 6: α-linolenic acid (C18:3n3); 7: arachidic acid (C20:0); 8: cis-11-eicosenoic acid (C10:1n9); 9: cis-11,14-eicosadienoic acid (C20:2); 10: cis-13,16-docosadienoic acid (C22:2); 11: tricosanoic acid (C23:0); 12: lignoceric acid (C24:0); 13: nervonic acid (C24:1n9). GC and peak identification were done as per section 3.2.7.3.

The yield of biodiesel (%), as calculated as per Section 3.2.7.4, over five different batches was 80±5% (Table 8.1).

Table 8.1: A summary table for different batches of FAMEs generated using lipase from H1 (*P. reinekei*), H3 (*P. brenneri*) and porcine pancreas lipase for transesterification of olive oil. Average yield of the transesterification reaction was noted to be 80%.

Lipase (500IU)	Molar ratio (Oil: Methanol)	Batch	Olive oil used (gms)	Methanol (ml)	FAMEs generated (gms)	% Yield	Average Yield
H1 (*P. reinekei*)	1:12	1	1.25	2.15	0.94	75	77.2
		2	1.17	2	0.97	83	
		3	1.28	2.2	1.10	86	
		4	1.26	2.17	0.91	72	
		5	1.25	2.15	0.87	70	
H3 (*P. brenneri*)	1:9	1	1.25	1.61	1.10	88	82.4
		2	1.27	1.64	1.08	85	
		3	1.28	1.65	1.02	80	
		4	1.28	1.65	1.00	78	
		5	1.27	1.64	1.03	81	
PPL (Standard)	1:12	1	1.26	2.17	1.14	90	79.4
		2	1.26	2.17	0.87	69	
		3	1.26	2.17	0.98	78	
		4	1.26	2.17	1.01	80	
		5	1.28	2.2	1.02	80	

The composition of FAMEs synthesized was represented as percentage of saturated and unsaturated FAMEs (see Table 8.2). Unsaturated fatty acid methyl esters were a major component of the synthesized FAMEs, while the percentage of saturated fatty acid methyl esters was below 15%. On comparison to a biodiesel standard; the synthesized FAMEs, irrespective of lipase source, contained a lower percentage of C18:0 and C20:0. However, the percentage of unsaturated C18, in all the synthesized FAMEs, was comparable to the biodiesel standard.

Table 8.2: Composition of FAMEs synthesized using lipase from *P. reinekei* (H1), *P. brenneri* (H3) and standard lipase (porcine pancreas) by transesterification of olive oil at 40°C after 72h of incubation, 120rpm in shaker water bath. Data represented here are from one GC run, the standard deviation was 10% based on analytical method variation. *Unsat*. denotes unsaturated fatty acid methyl esters, *sat*. denotes saturated fatty acid methyl esters.

Component	C18:0	C18 (unsat.)	C20:0	C20 (unsat.)	Other sat. FAME	Other unsat. FAME
Biodiesel standard	4.16	60.37	18.44	8.72	7.74	0.57
P. reinekei (H1) FAMEs	0.41	30.4	0	0	13.28	55.92
P. brenneri (H3) FAMEs	1.08	48.6	0.72	0	3.7	45.89
Porcine pancreas (PPL) FAMEs	1.09	68.6	0.54	0.29	2.09	27.48

8.2.2. Synthesis of FAME(s) using microalgal biomass

8.2.2.1. Lipase catalysed transesterification

In-situ transesterification of *Pseudokirchneriella subcapitata* and *Chlorella emersonii* lyophilised biomass containing TAGs and free lipase from *P. reinekei* (H1), *P. brenerri* (H3) and porcine pancreas (standard) resulted in FAME generation after 48h and 72h of incubation (Figure 8.8). The solvent layer containing the FAMEs was separated, as per Section 3.2.7.1, and was used for GC analysis.

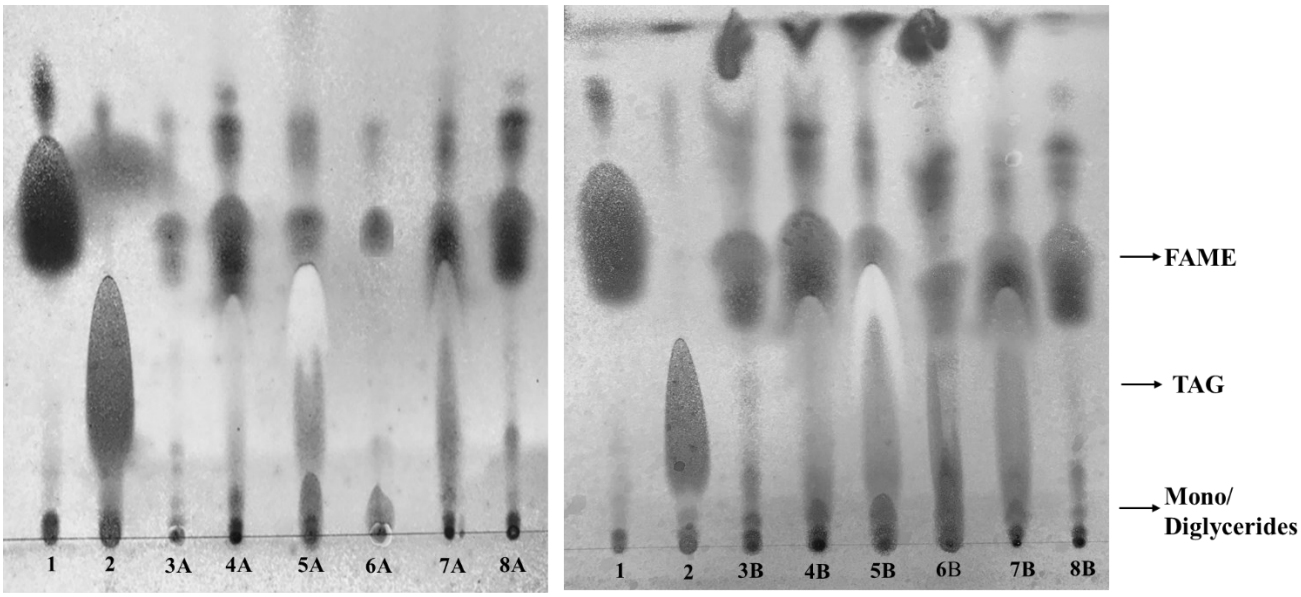

Figure 8.8: TLC (section 3.2.7.2) plate representing synthesized FAMEs via lipase catalysed transesterification of TAGs from *Pseudokirchneriella subcapitata* and *Chlorella emersonii* after 48h and 72h of incubation at 40°C. Lanes 1 and 2 represent the FAME standard and olive oil. Lanes 3 and 4 are the transesterification reactions of *Pseudokirchneriella subcapitata* and *Chlorella emersonii* respectively catalysed by lipase from *P. reinekei* (H1). Lanes 5 and 6 are the transesterification reactions of *Pseudokirchneriella subcapitata* and *Chlorella emersonii* respectively catalysed by lipase from *P. brenneri* (H3). Lanes 7 and 8 are the transesterification reactions of *Pseudokirchneriella subcapitata* and *Chlorella emersonii* respectively catalysed by lipase from porcine pancreas (standard). A, B are products of transesterification reactions after 48h and 72h of incubation respectively.

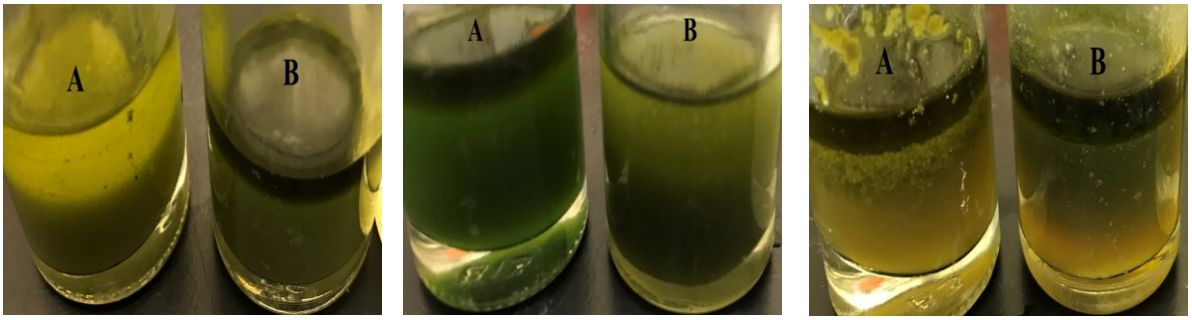

(a) (b) (c)

Figure 8.9: The upper oil layer from (A) *Pseudokirchneriella subcapitata* and (B) *Chlorella emersonii* formed after transesterification reaction catalysed by lipase from (a) *P. reinekei* (H1); (b) *P. brenneri* (H3) and (c) porcine pancreas lipase (standard) after 72h of incubation at 40°C.

Figure 8.9 represents the solvent layers formed after transesterification of biomass from *Pseudokirchneriella subcapitata* and *Chlorella emersonii* using different lipase sources (H1, H3 and PPL). The upper solvent layer (hexane) contains FAME generated after transesterification, while the lower layer contains biomass and transesterification byproducts.

8.2.2.2. GC analysis of FAMEs from microalgae

FAMEs synthesized from the transesterification reaction of neutral lipids (TAGs) from *Chlorella emersonii* and *Pseudokirchneriella subcapitata* were examined via GC and represented a broad composition of fatty acid methyl esters as compared with FAME standard mix (Appendix L). GC profiles of the FAMEs generated are represented in Figures 8.10, 8.11, 8.12, 8.13, 8.14, 8.15; Table 8.2 represent the FAME composition in terms of saturated and unsaturated fatty esters, along with standard biodiesel (Appendix K).

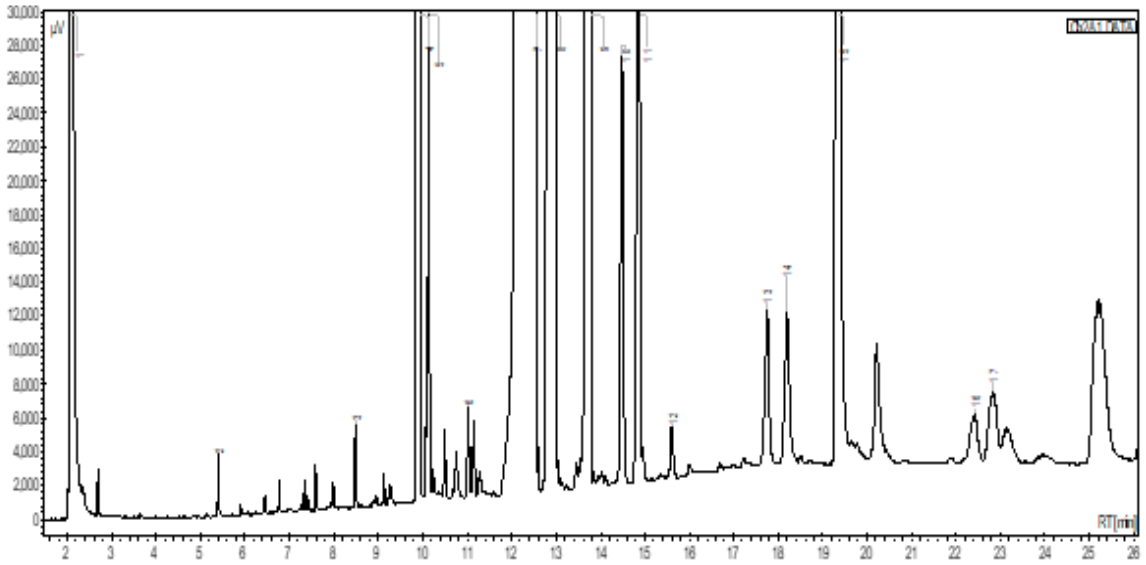

Figure 8.10: GC chromatogram of FAMEs synthesized from the transesterification reaction of *Chlorella emersonii* using lipase from H1 (*P. reinekei*). 1: Solvent; 2: lauric acid (C12:0); 3: cis-10-pentadedenoic acid (C15:1); 4: cis-10-heptadedenoic acid (C17:1); 5: stearic acid (C18:0); 6: oleic acid (C18:1n9c); 7: γ-linolenic acid (C18:3n6); 8: α-linolenic acid (C18:3n3); 9: arachidic acid (C20:0); 10: cis-11-eicosenoic acid (C10:1n9); 11: cis-11,14-eicosadienoic acid (C20:2); 12: cis-8,11,14-eicosatienoic acid (C12:3n6); 13: cis-5,8,11,14,17-eicosapentaenoic acid (C20:5n3); 14: behenic acid (C22:0); 15: cis-13,16-docosadienoic acid (C22:2); 16: tricosanoic acid (C23:0); 17: lignoceric acid (C24:0). GC and peak identification were executed as per section 3.2.7.3.

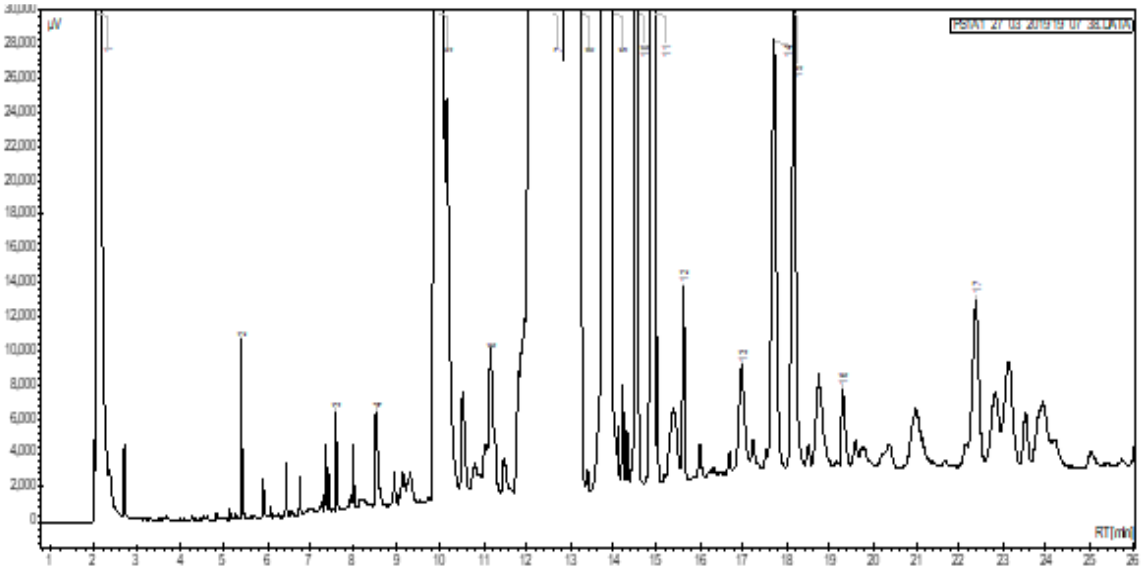

Figure 8.11: GC chromatogram of FAMEs synthesized from the transesterification reaction of *Chlorella emersonii* using lipase from H3 (*P. brenneri*). 1: Solvent; 2: capric acid (C10:0); 3: lauric acid (C12:0); 4: tridecanoic acid (C13:0); 5: myristoleic acid (C14:1); 6: cis-10-pentadedenoic acid (C15:1); 7: cis-10-heptadedenoic acid (C17:1); 8: oleic acid (C18:1n9c); 9: γ-linolenic acid (C18:3n6); 10: cis-11-eicosenoic acid (C10:1n9); 11: cis-11,14-eicosadienoic acid (C20:2); 12: cis-8,11,14-eicosatienoic acid (C12:3n6); 13: heneicosanoic acid (C21:0); 14: cis-5,8,11,14,17-eicosapentaenoic acid (C20:5n3); 15: behenic acid (C22:0); 16: erucic acid (C22:1n9); 17: tricosanoic acid (C23:0); 18: lignoceric acid (C24:0). GC and peak identification were executed as per section 3.2.7.3.

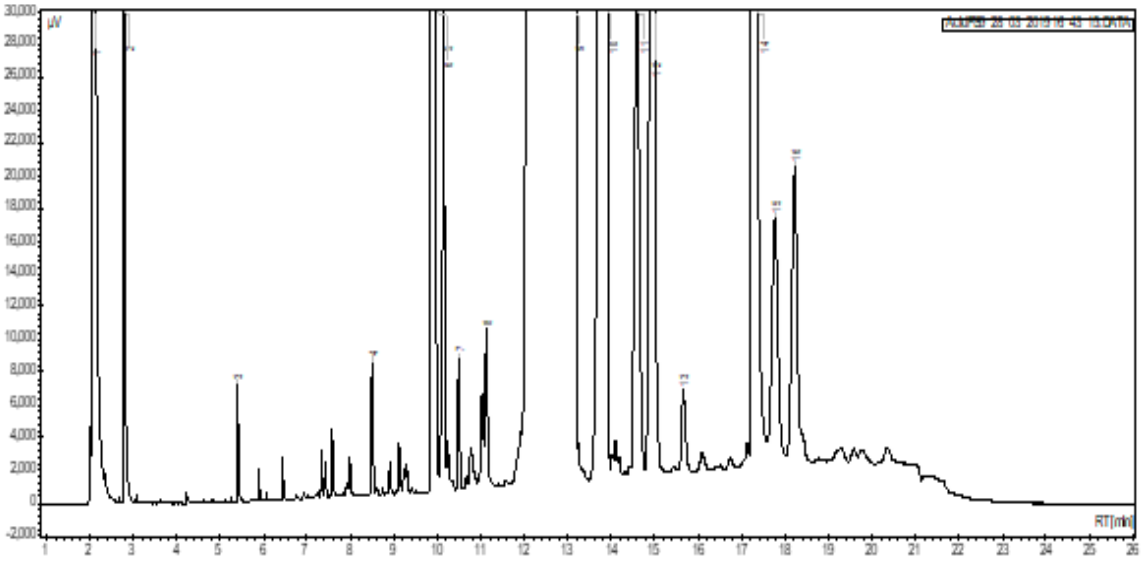

Figure 8.12: GC chromatogram of FAMEs synthesized from the transesterification reaction of *Chlorella emersonii* using lipase from porcine pancreas (standard). 1: Solvent; 2: capric acid (C10:0); 3: lauric acid (C12:0); 4: cis-10-pentadedenoic acid (C15:1); 5: cis-10-heptadedenoic acid (C17:1); 6: stearic acid (C18:0); 7: elaidic acid (C18:1n9t); 8: oleic acid (C18:1n9c); 9: α-linolenic acid (C18:3n3); 10: arachidic acid (C20:0); 11: cis-11-eicosenoic acid (C10:1n9); 12: cis-11,14-eicosadienoic acid (C20:2); 13: heneicosanoic acid (C21:0); 14: arachidonic acid (C20:4n6); 15: cis-5,8,11,14,17-eicosapentaenoic acid (C20:5n3); 16: behenic acid (C22:0). GC and peak identification were executed as per section 3.2.7.3.

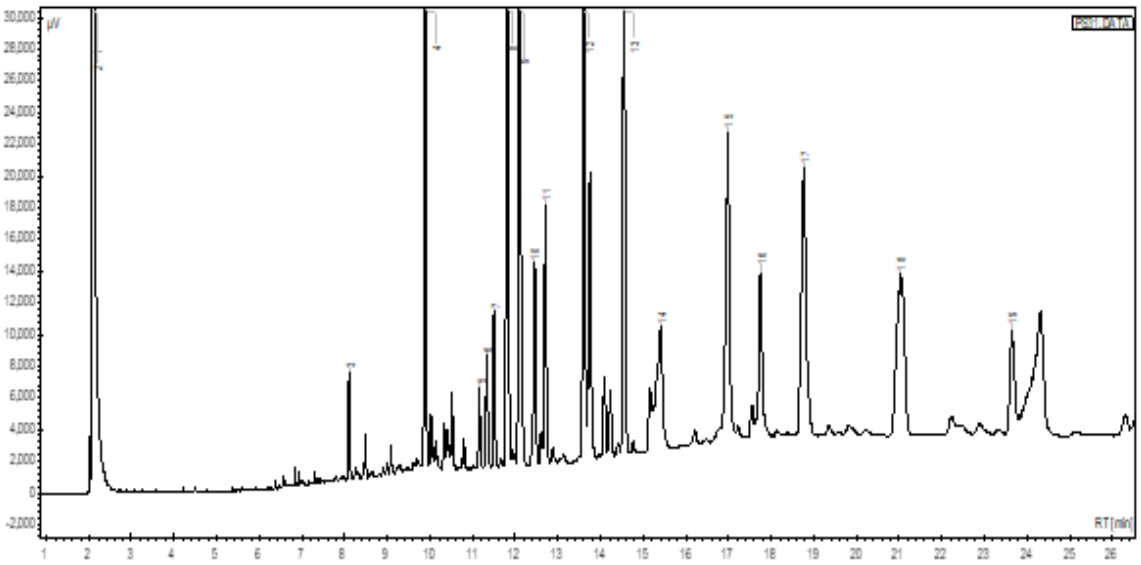

Figure 8.13: GC chromatogram of FAME synthesized from the transesterification reaction of *Pseudokirchneriella subcapitata* using lipase from H1 (*P. reinekei*). 1: Solvent; 2: caproic acid (C6:0); 3: pentadecanoic acid (C15:0); 4: cis-10-heptadedenoic acid (C17:1); 5: stearic acid (C18:0); 6: elaidic acid (C18:1n9t); 7: oleic acid (C18:1n9c); 8: linolelaidic acid (C18:2n6t); 9: linoleic acid (C18:2n6c); 10: γ-linolenic acid (C18:3n6); 11: α-linolenic acid (C18:3n3); 12: arachidic acid (C20:0); 13: cis-11,14-eicosadienoic acid (C20:2); 14: cis-8,11,14-eicosatienoic acid (C12:3n6); 15: arachidonic acid (C20:4n6); 16: cis-5,8,11,14,17-eicosapentaenoic acid (C20:5n3); 17: erucic acid (C22:1n9); 18: tricosanoic acid (C23:0); 19: cis-4,7,10,13,16,19-docosahaenoic acid (C22:6n3). GC and peak identification were executed as per section 3.2.7.3.

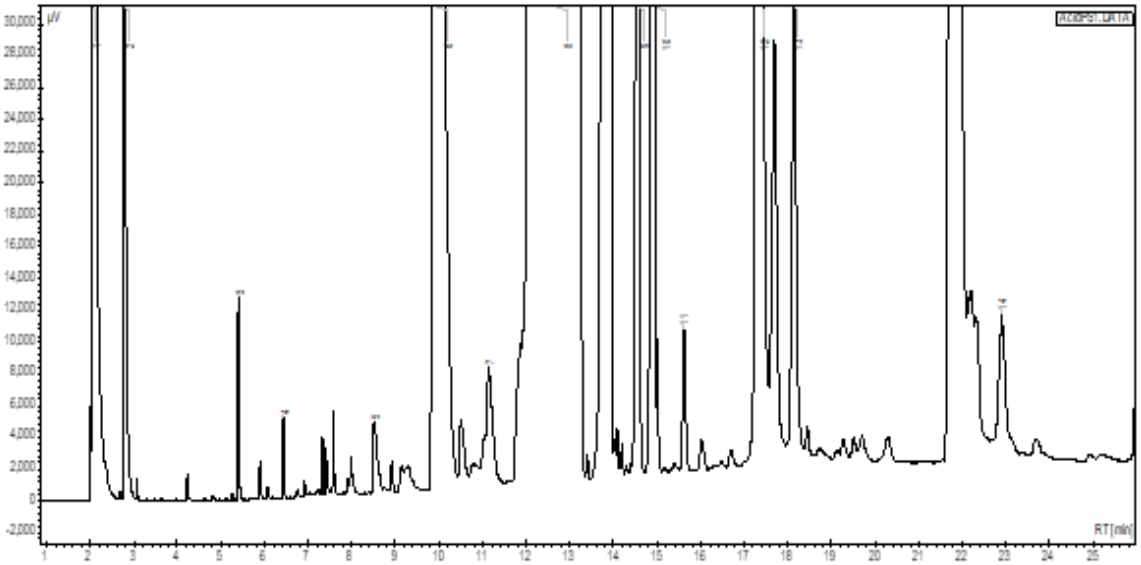

Figure 8.14: GC chromatogram of FAME synthesized from the transesterification reaction of *Pseudokirchneriella subcapitata* using lipase from H3 (*P. brenneri*). 1: Solvent; 2: capric acid (C10:0); 3: lauric acid (C12:0); 4: tridecanoic acid (C13:0); 5: cis-10-pentadedenoic acid (C15:1); 6: cis-10-heptadedenoic acid (C17:1); 7: oleic acid (C18:1n9c); 8: γ-linolenic acid (C18:3n6); 9: cis-11-eicosenoic acid (C10:1n9); 10: cis-11,14-eicosadienoic acid (C20:2); 11: cis-8,11,14-eicosatienoic acid (C12:3n6); 12: cis-5,8,11,14,17-eicosapentaenoic acid (C20:5n3); 13: behenic acid (C22:0); 14: lignoceric acid (C24:0). GC and peak identification were executed as per section 3.2.7.3.

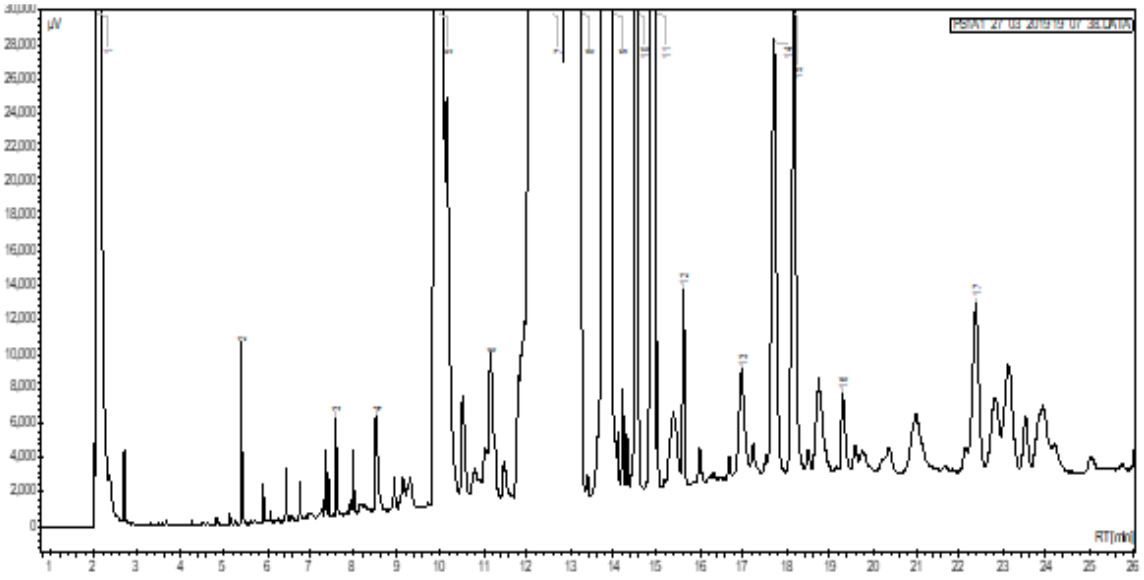

Figure 8.15: GC chromatogram of FAME synthesized from the transesterification reaction of *Pseudokirchneriella subcapitata* using lipase from porcine pancreas (standard). 1: Solvent; 2: lauric acid (C12:0); 3: myristoleic acid (C14:1); 4: cis-10-pentadecanoic acid (C15:1); 5: cis-10-heptadedenoic acid (C17:1); 6: oleic acid (C18:1n9c); 7: γ-linolenic acid (C18:3n6); 8: α-linolenic acid (C18:3n3); 9: arachidic acid (C20:0); 10: cis-11-eicosenoic acid (C10:1n9); 11: cis-11,14-eicosadienoic acid (C20:2); 12: cis-8,11,14-eicosatienoic acid (C12:3n6); 13: arachidonic acid (C20:4n6); 14: cis-5,8,11,14,17-eicosapentaenoic acid (C20:5n3); 15: behenic acid (C22:0); 16: cis-13,16-docosadienoic acid (C22:2); 18: lignoceric acid (C24:0). GC and peak identification were executed as per section 3.2.7.3.

The biodiesel yield, from *in-situ* transesterification, was not calculated. First, in the absence of internal standard, the yield could not be easily estimated. Secondly, while using the *in-situ* transesterification reaction, efficiency of lipid extraction could not be measured. Hence either way, the yield of FAMEs generated after transesterification of neutral lipids from *Chlorella emersonii* and *Pseudokirchnella* using lipase from H1 (*P. reinekei*), H3 (*P. brenneri*) or PPL was not estimated. The composition of FAMEs synthesized was represented as percentage of saturated and unsaturated fatty acid methyl esters (see Table 8.3). Unsaturated fatty acid methyl esters contributed majorly to the synthesized FAMEs, while the percentage of saturated fatty acid methyl esters was below 15%. On comparison with a biodiesel standard; synthesized FAME(s), irrespective of lipase source, contained the lower percentage of C18:0 and C20:0. However, unsaturated C18, in all the synthesized FAMEs, was comparable to biodiesel standard.

Table 8.3: Composition of FAMEs synthesized using lipase from *P. reinekei* (H1), *P. brenneri* (H3) and Standard (porcine pancreas) by transesterification of neutral lipids from *Chlorella emersonii*, *Pseudokirchneriella subcapitata* at 40°C after 72h of incubation, 120rpm in shaker water bath. Data represented here are from one GC run, standard deviation was 10% based on analytical method variation obtained after three repeats of FAME mix. *Unsat*. denotes unsaturated fatty acid methyl esters, *sat*. denotes saturated fatty acid methyl esters.

Source	Catalysed by lipase from	C18:0	C18 unsat.	C20:0	C20 unsat.	Other sat.	Other unsat.
Biodiesel standard		4.16	60.37	18.44	8.72	7.74	0.57
Chlorella emersonii	*P. reinekei* (H1)	0.4	82.09	7.1	1.45	0.59	8.38
Pseudokirchnella subcapitata		0.73	30.39	5.83	17.75	22.59	22.72
Chlorella emersonii	*P. brenneri* (H3)	0	56.72	0.93	10.35	10.39	21.61
Pseudokirchnella subcapitata		0	77	0	10.9	4.1	8.1
Chlorella emersonii	Porcine pancreas (PPL, Std.)	0.59	49.91	21.81	10.94	3.79	12.96
Pseudokirchnella subcapitata		0.00	63.11	19.91	4.16	1.04	11.79

Transesterification of neutral lipids from *Chlorella emersonii* generated approx. 82%, 57% and 50% of C18 unsaturated FAMEs when lipase from H1 (*P. reinekei*), H3 (*P. brenneri*) and PPL were used respectively. While for *Pseudokirchnella subcapitata* neutral lipid transesterification approx. 30%, 77% and 63% of C18 unsaturated FAME(s) when lipase from H1 (*P. reinekei*), H3 (*P. brenneri*) and PPL were used respectively. The highest percentage of saturated C20 FAMEs were from *Pseudokirchnella subcapitata* when PPL was used for transesterification; conversely, other saturated FAMEs were obtained (to approximately 23%) from *Pseudokirchnella subcapitata* neutral lipids while using H1 (*P. reinekei*) lipase.

8.3. DISCUSSION

To explore the optimal parameters (i.e. minimum solvent, temperature and incubation time) required for transesterification reaction of microalgal neutral lipids; transesterification trials were initially carried out on olive oil. Previous studies on unused and used olive oil as raw materials for transesterification have shown no major difference in the biodiesel generated

from both raw materials (Coggon, Vasudevan and Sanchez, 2007). Therefore, the transesterification reaction parameters identified (Section 8.2.1) using lipase from H1 (*P. reinekei*), H3 (*P. brenneri*) and PPL (standard) could be used for the generation of biodiesel from either olive oil or waste olive oil.

Reaction temperature is one of the factors known to affect biodiesel/FAMEs synthesis; where the rate of the reaction increases with increased temperature (Sanchez and Vasudevan, 2006; Guldhe *et al.*, 2015; Kia-Kojouri *et al.*, 2016). Due to the lower thermostability of the lipase from H1 (*P. reinekei;* Chapter 5, Section 5.2.3.2) and H3 (*P. brenneri,* Chapter 5, Section 5.2.3.2) respectively, characterisation trials of these two lipases were carried out at 28°C and 40°C; with similar temperatures (30°C and 40°C) to those used for the olive oil transesterification reaction. After 72h of incubation at 40°C FAMEs generated were successfully synthesized by all the three different lipase sources as characterised by TLC and GC (Section 8.2.1.1); however, 30°C was insufficient for FAME generation after 72h incubation. Similarly, lipase LipSB25-4 isolated from *Streptomyces bambergiensis* OC 25-4 demonstrated biodiesel production using olive oil only after 48h of reaction at 40°C (Ugur *et al.*, 2014).

The rate of transesterification is also driven by oil to alcohol molar ratio. Methanol is a commonly used alcohol for the transesterification due to its availability and solubility (Musa, 2016). Generally, for complete conversion of an oil to methyl esters (biodiesel/FAME), at least a 3-fold molar ratio of alcohol is required in the reaction mixture (Bose and Keharia, 2013). A higher molar ratio of alcohol to oil is required to increase the contact between oil and alcohol; and, to drive the reaction towards ester synthesis. An increased alcohol to oil ratio results in enhanced biodiesel yield in a shorter time (Helwani *et al.*, 2009). This can be used to explain the higher transesterification of olive oil to biodiesel in 12:1, 9:1, 12:1 (methanol: olive oil) compared to 6:1 transesterification reaction catalysed by H1 (*P. reinekei*), H3 (*P. brenneri*) and standard (porcine pancreas lipase) respectively (Section 8.2.1.2). Similar trends in enhanced transesterification yields with increased alcohol: oil molar ratio have been observed in soyabean oil transesterification using *Pseudomonas cepacia* lipase where the biodiesel yield was increased to 7.5:1 (methanol: oil) molar ratio,

but further increase in methanol: oil ratio showed no enhanced biodiesel production (Noureddini, Gao and Philkana, 2005). Likewise, biodiesel production increased with increased methanol to oil ratio (from 6:1 to 9:1) for the transesterification of sardine oil using *Aspergillus niger* lipase, while a further molar increase did not increase biodiesel synthesis (Arumugam and Ponnusami, 2017). For transesterification of rapeseed oil using porcine pancreas lipase at 37°C with 48hr incubation, biodiesel synthesis increased with increased molar ratio (from 3:1 to 9:1); however, further increase in methanol oil ratio did not increase biodiesel synthesis (Kia-Kojouri *et al.*, 2016). Interestingly, the optimal methanol to oil ratio varies based on the oil source and source enzyme; for *Geobacillus thermodenitrificans* lipase a 3:1 molar ratio of methanol and coconut oil generated biodiesel at 65°C incubation after 48h of reaction (Christopher *et al.*, 2015).

In terms of entrapped versus free lipase bioconversion rates; lower yields of biodiesel formation were observed from olive oil transesterification using calcium alginate entrapped lipase of H1 (*P. reinekei*), H3 (*P. brenneri*) and standard (porcine pancreas lipase) compared to their free forms (Section 8.2.1.4). Immobilized and entrapped enzymes tend to have restricted access to the active site for substrates, primarily due to lower diffusion rates (see Chapter 6, Section 6.2.2.1). Therefore, it was expected that the entrapped lipase would generate lower biodiesel yields compared to the free form. These observations have also been reported in literature where lower yields of biodiesel were observed from acrylic resin immobilized lipase from *Candida Antarctica* compared to its free form for jatropha oil transesterification at 40°C, 24h of incubation 3:1 methanol to oil ratio (Bueso *et al.*, 2015). Likewise, *Pseudomonas cepacia* lipase entrapped in calcium alginate beads showed half of the transesterification activity after encapsulation (Yadav and Jadhav, 2005). Though the entrapped lipase can be recovered from the reaction and reused, higher reaction times for biodiesel generation due to poor bioconversion rates for the enzyme entrapment makes the process less economical. Subsequently, for the microalgal neutral lipid *in situ* transesterification reactions the free form of the lipases of interest was used.

The combination of oil extraction and biodiesel conversion, or *in-situ* transesterification, involves mixing of the oil/lipid-bearing biomass with the solvent of choice in the presence of a catalyst, and sometimes co-solvents (Baumgartner *et al.*, 2013; Hidalgo *et al.*, 2013). *In*

situ transesterification, is simply the omission of the extraction step in traditional transesterification process; instead the entire biomass is used as the feedstock for the reaction (Griffiths, Hille and Harrison, 2010). This process simplifies the biodiesel synthesis process from microalgae and improves biodiesel yield due to elimination of oil extraction step that incurs oil loss (Section 2.8.4). Oil extraction yield from dry microalgal cells is higher than that of wet microalgal cells (Guldhe *et al.*, 2014). This, combined with the inhibitory nature of water on the transesterification reaction (Sathish, Smith and Sims, 2013), resulted in the selection of an enzymatic *in-situ* transesterification of *Chlorella emersonii* and *Pseudokirchneriella subcapitata* employing dried biomass. The first part of this biomass preparation is microalgae harvesting; techniques such as centrifugation, filtration, flotation, chemical flocculation or their combination are commonplace (Guldhe *et al.*, 2014). Flocculation techniques however are time consuming and have a high risk of decomposition of the desired products. Filtration and centrifugation on the other hand are more efficient and safer for small scale processes. Biomass drying after microalgae harvesting can be achieved through sun drying, spray drying, fluidized bed drying, or freeze drying (Harwati, 2013). However, due to the small scale of this exploratory study; harvesting and drying of biomass from *Chlorella emersonii* and *Pseudokirchneriella subcapitata* was achieved using centrifugation followed by freeze drying.

Alcohol is required for *in-situ* transesterification during the oil extraction step and the transesterification of microalgal neutral lipids step (see Section 2.8.4); therefore larger quantities of alcohol are used in *in-situ* transesterification reactions compared to commercial biodiesel production process (Dianursanti, Religia and Wijanarko, 2015; Park, Park and Lee, 2015) . Short-chain alcohols, especially methanol, have poor oil solubility, which generates a new liquid phase causing enzyme inactivation and lower biodiesel yields (Dianursanti, Religia and Wijanarko, 2015). For *in-situ* transesterification, the use of co-solvent is considered to increase biodiesel yield. Co-solvents are also expected to aid oil extraction from microalgal cells and enhance the contact of microalgal oils with the esterification reagent (Cao *et al.*, 2013). Hexane and *t*-butanol are the most commonly used co-solvents during *in-situ* enzymatic transesterification reactions (Heitz *et al.*, 2016); however, other solvents like pentane and diethyl ether have also been used (Park, Park and Lee, 2015). As the lipase from

H1 (*P. reinekei*) and H3 (*P. brenneri*) showed enhanced lipolytic activity in *n*-hexane, *n*-heptane and cyclohexane (Section 5.2.3.6), any of these solvents could be used as the co-solvent of choice for the *in-situ* transesterification reaction of *Chlorella emersonii* and *Pseudokirchneriella subcapitata* neutral lipids. The use of *n*-hexane with methanol 1:1 (v/v) has been reported to increase FAME conversion by 94% (Dianursanti, Religia and Wijanarko, 2015), and therefore, a 1:1 (v/v) ratio of methanol and *n*-hexane were used for *in-situ* biodiesel/FAMEs synthesis from *Chlorella emersonii* and *Pseudokirchneriella subcapitata* in this study.

Gas Chromatography of biodiesel generated from *in-situ* enzymatic transesterification of neutral lipids from *Chlorella emersonii* and *Pseudokirchneriella subcapitata* showed a higher percentage of C18 unsaturated fatty acid methyl esters; irrespective of the lipase used for the transesterification reaction (see Table 8.2). It has been previously demonstrated that nitrogen deficiency induces accumulation of C16:0 and C18 unsaturated FAMEs in microalgae strains (Rodolfi *et al.*, 2009; Tang *et al.*, 2011). Increased accumulation of C18 unsaturated fatty acid methyl esters under nitrogen starvation condition has also been reported in *Nannochloropsis* sp. (Rodolfi *et al.*, 2009), *Chlorella minutissima* UTEX 2341 (Tang *et al.*, 2011) and *Nannochloropsis oculata* (Su *et al.*, 2011). In this current study, since the two microalgal strains i.e. *Chlorella emersonii* and *Pseudokirchneriella subcapitata* were nitrogen starved (Section 7.2.3) for the synthesis of neutral lipids; and based on the existing literature, it was expected that a higher percentage of C18 unsaturated fatty acids would be observed in the corresponding biodiesel.

Since the properties of FAMEs/biodiesel generated from enzymatic transesterification of olive oil and *in-situ* transesterification reaction of neutral lipids from *Chlorella emersonii* and *Pseudokirchneriella subcapitata* were not analysed; the composition of the FAMEs (based on GC analysis) can, alternatively, be used to determine fuel properties (Ved and Padam, 2013). The cetane number (CN) provides information about the ignition delay time of a diesel fuel upon injection into a combustion chamber (Cataluna and Silva, 2012). A biodiesel CN depends on the distribution of fatty acids in the feedstock oil. A higher CN value has been observed in saturated FAMEs; whilst the CN is in the medium range in mono-saturated FAMEs (A. I. Bamgboye and Hansen, 2008). The CN is directly related to the degree of

saturation and chain length of the fatty acid feedstock; it decreases with increasing unsaturation (and vice versa) and increases with increasing chain length (A.I. Bamgboye and Hansen, 2008). Biodiesel with a low CN causes increased gaseous and particulate exhaust emissions (PM) due to incomplete combustion. Biodiesel has higher CN values than fossil fuels, which is considered a significant advantage in terms of engine performance and emissions, allowing biodiesel fuelled engines to run smoothly with less noise (Pinzi *et al.*, 2009). Transesterification of olive oil and neutral lipids from *Chlorella emersonii* and *Pseudokirchneriella subcapitata* generated a higher percentage of unsaturated fatty acid esters in the FAMEs (Table 8.1 and 8.2 respectively), indicating the CN of the generated FAME could be high. However, without analysis, the same cannot be confirmed for this study.

Other important biodiesel properties include heat of combustion for estimating fuel consumption: the greater the heat of consumption, the lower the fuel consumption. Short chain saturated compounds have the lowest heat of combustion, but greater fuel consumption (Knothe, 2008). Likewise, biodiesel viscosity is an important consideration, which deceases with increase in unsaturation (Allen *et al.*, 1999). The composition of biodiesel also determines its cold flow properties. Cloud point (CP) and pour point (PP) are the two main properties which determine the use and stability of biodiesel at lower, close to freezing, temperatures. CP is the temperature below which biodiesel becomes cloudy and clogs engine filters; while PP is the temperature below which biodiesel turns into semi-solid and losses its flow properties (Dwivedi and Sharma, 2013). Since unsaturated fatty esters have lower melting points; to improve the low-temperature properties of biodiesel, a higher percentage of unsaturated fatty esters is required. Long chain saturated fatty esters significantly increases the cloud and pour points (Pinzi *et al.*, 2009). However, biodiesel with a higher percentage of unsaturated FAMEs suffers from a higher oxidation rate (Falk and Pittroff, 2004) and low cetane numbers (Knothe, 2008), which is undesirable. Therefore, for attaining low-temperature and oxidative stability, an optimum percentage of saturated and unsaturated esters is required; which again depends on the type of fatty esters in the biodiesel.

To ensure satisfactory performance of biodiesel with respect to low temperature operability and oxidative stability, biodiesel should contain relatively low concentrations of both long-

chain saturated FAMEs and poly-unsaturated FAMEs. Although the relationship between carbon chain length, low temperature properties and oxidative stability is quite strong for pure FAMEs compounds, the effects appear elusive when complex mixtures of FAMEs are considered in actual biodiesel samples (Refaat, 2009; Pinzi *et al.*, 2013; Monirul *et al.*, 2015). In this study, the biodiesel generated from enzymatic transesterification of olive oil and neutral lipids from *Chlorella emersonii* and *Pseudokirchneriella subcapitata* have a higher percentage of unsaturated fatty esters (Table 8.1 and 8.2) and lower percentage of saturated fatty esters (compared to standard biodiesel). A higher percentage of unsaturated fatty esters can contribute towards lower oxidation stability, but good CP and PP properties. Also, the composition of FAMEs/biodiesel generated after transesterification reaction depends on the feedstock; a change in the fatty acid composition of neutral lipids in *Chlorella emersonii* and *Pseudokirchneriella subcapitata* can affect the final composition of FAME(s) generated. The composition of the fatty acids synthesized by microalgae can be varied by changing the cultivation conditions. For example with *B. braunii* different composition of fatty acids were observed under different culturing conditions (Hidalgo *et al.*, 2013). Hu and co-workers (Hu *et al.*, 2008) also reported an increase in the relative proportions of both saturated and monounsaturated fatty acids (C16:0 and C18:1) and the decrease in the proportion of polyunsaturated fatty acids with growth-phase transition from the logarithmic to the stationary phase and from change in growth temperature from 25°C to 32°C.

Though the purity of biodiesel generated from enzymatic transesterification is high, the commercial use of these fuels can only be determined after experimental determination of CP, PP and oxidative stability. The properties can be further improved through blending the fuels generated with commercial/other biodiesel or by altering the growth conditions of *Chlorella emersonii* and *Pseudokirchneriella subcapitata*.

8.4. CONCLUSION

A 72h incubation, at 40°C, is required for the transesterification of olive oil using 500IU/g of oil when lipase from H1 (*P. reinekei*), H3 (*P. brenneri*) and porcine pancreas (standard) were used. A molar ratio of 1:12 for olive oil: methanol was required for transesterification using

lipase from H1 (*P. reinekei*) and porcine pancreas (Standard) while 1:9 for lipase from H3 (*P. brenneri*). Limited mass transfer using calcium alginate entrapped lipase restricted its usage for microalgae neutral lipid transesterification. *In-situ* transesterification of neutral lipids from *Chlorella emersonii*, *Pseudokirchneriella subcapitata* generated FAMEs which were composed primarily of unsaturated fatty acid methyl esters. Though the final transesterification product is pure, the analysis of analytical properties can provide a clearer picture of potential commercial applications.

Chapter 9: Overall Conclusions and Future Perspectives

This chapter provides an overall conclusion of the results detailed in the preceding chapters which have not been examined previously. Futhermore, it will provide an overview of the progress made in this research in conjunction with the significant findings to date. At the outset, this work aimed to identify novel solvent stable lipases which could be useful for biotechnological applications. By 16S rRNA sequencing five novel extracellular lipase producing strains; of which three from *Pseudomonas* genus could provide an opportunity in many biotechnological applications (Silby *et al.*, 2011). The work in this thesis attempts to address one of the biotechnological applications of lipase from *Pseudomonas* sp. strains H1 and H3 identified as *Pseudomonas reinekei* and *Pseudomonas brenneri* respectively.

Purification of lipases from these two *Pseudomonas* strains was done by by-passing the first step of ammonium sulfate precipitation and utilizing chromatographic methods. A unique way of implementing positive and negative mode of purification using same chromatographic resin provides a "thinking out of the box" approach in protein purification.

Specificity towards medium and long chain fatty acid phenyl esters and higher stability/activity of lipase(s) from both H1 (*P. reinekei*) and H3 (*P. brenneri*) made them ideal candidates for the transesterification of vegetable oils and microalgae neutral lipids. The mass spectrophotometry analysis of purified lipase from H1 (*P. reinekei*) revealed its resemblance to lipases from *P. fluorescens* and *P. yamanorum.* However, a lack of similarities for H3 (*P. brenneri*) lipase with the available lipase database indicated its novelty. Due to the unavailability of gene sequence for lipases from H1 (*P. reinekei*) and H3 (*P. brenneri*), media optimisation rather than molecular cloning via recombinant DNA technology was exploted to attain higher yields of lipase.

Though entrapment in calcium alginate did not prove to enhance the stability of the lipases from H1 (*P. reinekei*) and H3 (*P. brenneri*) under stressful temperature and pH conditions; their stability enhanced in presence of selected metal ions.

Chlorella emersonii is known to produce high lipid content (63% of biomass; (Illman, Scragg and Shales, 2000) while *Pseudokirchneriella subcapitata* is associated with lower lipid content (36.7% of biomass; (Islam *et al.*, 2013). In the current study by following metabolic engineering, a total yield of 0.61±0.017mg/mg of biomass and 0.31±0.006mg/mg of neutral lipids in dry biomass was achieved respectively for the microalgae of choice; *Chlorella emersonii* and *Pseudokirchneriella subcapitata.* Quantification of neutral lipids generated by *Chlorella emersonii* and *Pseudokirchneriella subcapitata* was done by Nile red fluorescence spectrophotometer assay developed and validated in-house. FAMEs generated after the transesterification reaction of olive oil and lipids from *Chlorella emersonii* and *Pseudokirchneriella subcapitata* were mainly comprised of unsaturated fatty acid methyl esters (with the majority being C18 and C20 unsaturated fatty acids). Although, the quality of FAMEs generated from enzymatic transesterification was high (as per GC), the commercial use of these fuels can only be determined after the estimation of CN, CP, PP and oxidative stability. In conclusion this work has identified and purified two exciting and novel lipases from *Pseudomonas* genus which are thermo and organo-stable and can be used in various biotechnological applications.

9.1. Future Perspectives

There are many avenues for expanding the research work described in this thesis. The major issues which could be addressed in future are as follows:

1. Of five organic solvent stable lipase producing strains, only two lipases i.e. H1 (*P. reinekei*) and H3 (*P. brenneri*) were optimally produced, purified and extensively characterised. Several new lipases described in this work are worth exploring for optimal production, purification and characterisation. *Listeria monocytogenes* is one of the interesting solvent stable lipase producing strain which is known to be involved in severe illnesses and outbreaks of food-borne infections. Exploration of lipases from this strain could provide an insight on the lipase related virulence factors in *Listeria monocytogenes.*
2. Significant stabilities of purified lipases from H1 (*P. reinekei*) and H3 (*P. brenneri*) in non-polar organic solvents (Log P>2.0) are promising for application in various food,

flavour industries and in pharmaceutical synthesis (as detailed in Sections 2.7.1 and 2.7.2).

3. In this work, abortive attempts to immobilize lipase(s) from H1 (*P. reinekei*) and H3 (*P. brenneri*) on gold nanoparticles were carried out. With the knowledge of molecular structures of these lipases; successful attempts could be made for their immobilization on AuNPs. This will not only further improve the properties of these lipases, but also will enhance application of lipases in various biomedical fields, especially as biosensors for the detection of triglycerides and cholesterol (as outlined in Section 6.3.1).
4. With the knowledge of gene sequence of lipase from H1 (*P. reinekei*) and H3 (*P. brenneri*); improved expression of these enzymes could be achieved by cloning them into a more suitable host such as *E. coli*; which is a useful tool for the expression (and secretion) of lipases (Burdette *et al.*, 2018). Improving the heterologous expression of these lipases will provide enough soluble protein for easy purification and application. The same can be further used for obtaining the crystallographic analysis of these lipases, facilitating immobilization on AuNPs (as mentioned earlier).
5. Homology models of lipase from H1 (*P. reinekei*) and H3 (*P. brenneri*) can be obtained to get structural insights of these enzymes, which can be very useful in designing rational mutagenesis experiments to improve different properties such as thermostabilities, regio- or strereo-selectivities or organic solvent stabilities.

References

Abdulmalek E, Hamidon N. F. and Abdul Rahman M. B. 2016. Optimization and characterization of lipase catalysed synthesis of xylose caproate ester in organic solvents. Journal of Molecular Catalysis B: Enzymatic, 132: 1–4.

Abreu A. P., Fernandes B., Vicente A.A., Teixeira J., Dragoneet G. 2012. Mixotrophic cultivation of *Chlorella vulgaris* using industrial dairy waste as organic carbon source. Bioresource Technology, 118: 61–66.

Adlercreutz P. 2013. Immobilisation and application of lipases in organic media. Applied and Environmental Microbiology, 42: 6406–6436.

Adrio J. L. and Demain A. L. 2014. Microbial enzymes: tools for biotechnological processes. Biomolecules, 4(1): 117–139.

Affleck R., Xu Z. F., Suzawa V., Focht K., Clark D. S., Dordick J.S. 1992. Enzymatic catalysis and dynamics in low-water environments. Proceedings of the National Academy of Sciences of the United States of America. National Academy of Sciences, 89(3): 1100–4.

Agency I. E. (2010) Sustainable Production of Second-Generation Biofuels: Potential and perspectives in major economies and developing countries.

Ahmad A.L., Mat Yasin N.H., Derek C.J.C, Lim J.K. 2011. Microalgae as a sustainable energy source for biodiesel production: A review. Renewable and Sustainable Energy Reviews, 15(1): 584–593.

Ahmed E.H., Raghavendra T. and Madamwar D. 2010. An alkaline lipase from organic solvent tolerant *Acinetobacter* sp. EH28: Application for ethyl caprylate synthesis. Bioresource Technology, 101(10): 3628–3634.

Akella S. and Mitra C. K. 2007. Electrochemical studies of glucose oxidase immobilized on glutathione coated gold nanoparticles. Indian Journal of Biochemistry and Biophysics, 44(2): 82–87.

Al-Saleh A. A., Zahran A. S. and Zahran S. A. 1999. Synthesis of extracellular lipase by a strain of *Pseudomonas fluorescens* isolated from raw camel milk. Food Microbiology, 16: 149–156.

Alford J. A. and Pierce D. A. 1963. Production of Lipase by *Pseudomonas Fragi* in a Synthetic Medium. Journal of Bacteriology, 86: 24–29.

Alina Maria B. 2014. *Listeria Monocytogenes* – characterization of strains isolated from clinical severe cases. Journal of Medicine and Life, 7(2): 42–48.

Alissandratos A., Baudendistel N., Flitsch S.L., Hauer B., Halling P.J. 2010. Lipase-catalysed acylation of starch and determination of the degree of substitution by methanolysis and GC. BMC Biotechnology, 10(82).

Allen C.A.W., Watts K.C., Ackman R.G., Pegg M.J. 1999. Predicting the viscosity of biodiesel fuels from their fatty acid ester composition. Fuel. 78(11): 1319–1326.

Almeida de A.F., Tauk-Tornisielo S.M., Carmona E.C. 2013. Acid Lipase from *Candida viswanathii*: Production, Biochemical Properties, and Potential Application. BioMed Research International. PMID: 24350270

Alonzo F. and Mayzaud P. 1999. Spectrofluorometric quantification of neutral and polar lipids in zooplankton using Nile red. Marine Chemistry, 67(3–4): 289–301.

Anastas P.T., Bartlett L.B., Kirchhoff M.M., Williamson T.C. 2000. The role of catalysis in the design, development, and implementation of green chemistry. Catalysis Today, 55(1–2): 11–22.

Andualema B. and Gessesse, A. 2012. Microbial Lipase and Their Industrial Applications: Review. Biotechnology, 11(3): 100–118.

Ansil D., Katja L. and Mayumi N. 2003. Activity of *Candida rugosa* Lipase Immobilized on γ-Fe_2O_3 Magnetic Nanoparticles. Journal of American Chemical Society, 125(7): 1684–1685.

Antczak M.S., Kubiak A., Antczak T., Bielecki S. 2009. Enzymatic biodiesel synthesis – Key factors affecting efficiency of the process. Renewable Energy, 34(5): 1185–1194.

Anwar A., Qader Ul S.A., Raiz A., Iqbal S. and Azhar A. 2009. Calcium Alginate: A Support Material for Immobilization of Proteases from Newly Isolated Strain of *Bacillus subtilis* KIBGE-HAS. World Applied Sciences Journal, 7(10): 1281–1286.

Arakawa T., Kita Y. and Timasheff S. N. 2007. Protein precipitation and denaturation by dimethyl sulfoxide. Biophysical Chemistry, 131(1–3): 62–70.

Aravindan R., Anbumathi P. and Viruthagiri T. 2007. Lipase applications in food industry. Indian Journal of Biotechnology, 6: 141–158.

Aris M.H., Annuar M.S.M. and Ling T.C. 2016. Lipase-mediated degradation of poly- ε-caprolactone in toluene: Behavior and its action mechanism. Degradation and Stability, 133: 182–191.

Arumugam A. and Ponnusami V. 2017. Production of biodiesel by enzymatic transesterification of waste sardine oil and evaluation of its engine performance. Heliyon, 3(12).

Ashfaq A., Mohammad S., Kaifiyan M. and Maheshwari A. 2015. Evolution, impacts and sustainability assessment of renewable energy. International journal of current microbiology and applied sciences, 4(4): 610–616.

Atha D.H. and Ingham K.C. 1981. Mechanism of precipitation of proteins by polyethylene glycols. Analysis in terms of excluded volume. Journal of Biological Chemistry, 256(23): 12108–12117.

Ayaz B., Ugur A. and Boran R. 2014. Purification and characterization of organic solvent-tolerant lipase from *Streptomyces* sp. OC119-7 for biodiesel production. Biocatalysis and Agricultural Biotechnology, 4(1): 103–108.

Ben Bacha A., Moubayed N.M.S. and Al-Assaf A. 2016. An organic solvent-stable lipase from a newly isolated *Staphylococcus aureus* ALA1 strain with potential for use as an industrial biocatalyst. Biotechnology and Applied Biochemistry, 63(3): 378–390.

Badgujar K.C., Pai P.A. and Bhanage B.M. 2016. Enhanced biocatalytic activity of immobilized *Pseudomonas cepacia* lipase under sonicated condition. Bioprocess and Biosystems Engineering, 39(2): 211–221.

Bagi K., Simon L.M. and Szajáni B. 1997. Immobilization and characterization of porcine pancreas lipase. Enzyme and Microbial Technology, 20(7): 531–535.

Baharum S.N., Salleh A.B., Razak C.N.A, Basri M., Rahma M.B.A., Rahman R.N.Z.R.A. 2003. Organic solvent tolerant lipase by *Pseudomonas* sp . strain S5: stability of enzyme in organic solvent and physical factors affecting its production. Annals of Microbiology, 53: 75–83.

Bailes J., Gazi S., Ivanova R. and Soloviev M. 2012. Effect of Gold Nanoparticle Conjugation on the Activity and Stability of Functional Proteins. Nanoparticles in Biology and Medicine. Methods in Molecular Biology (Methods and Protocols), 906: 89–99.

Bakir Z.B. and Metin K. 2016. Purification and characterization of an alkali-thermostable lipase from thermophilic *Anoxybacillus Flavithermus* HBB 134. Journal of Microbiology and Biotechnology, 26(6): 1087–1097.

Balan V. 2014. Current Challenges in Commercially Producing Biofuels from Lignocellulosic Biomass. ISRN Biotechnology, 2014. Article ID: 463074.

Balat M. and Balat H. 2010. Progress in biodiesel processing. Applied Energy, 87(6): 1815–1835.

Bamgboye A.I. and Hansen A.C. 2008. Prediction of cetane number of biodiesel fuel from the fatty acid methyl ester (FAME) composition. International Agrophysics, 22: 21–29.

Banerjee A., Chatterjee K. and Madras G. 2014. Enzymatic degradation of polymers: a brief review. Materials Science and Technology, 30(5): 567–573.

Barrera-rivera K.A., Flores-carreón A. and Martinez-Richa A. 2012. Synthesis of Biodegradable Polymers Using Biocatalysis with *Yarrowia lipolytica* Lipase. Methods in Molecular Biology, 861: 485-493.

Bartling K., Thompson Judith U.S., Pfromm P.H., Czermak P., Rezac M.E. 2001. Lipase-catalyzed synthesis of geranyl acetate in n-hexane with membrane-mediated water removal. Biotechnology and Bioengineering, 75(6): 676–681.

Baumgartner T. R. da S., Burak J.A.M., Baumgartner D., Zanin G.M., Arroyo P.A. 2013. Biomass production and ester synthesis by in situ transesterification/esterification using the microalga *Spirulina platensis*. International Journal of Chemical Engineering. Article ID: 425604.

Becker E.W. 1994. Microalgae: Biotechnology and Microbiology. 10th edn. Cambridge University Press, 1994.

Bertozzini E., Galluzzi L., Penna A., Magnani M. 2011. Application of the standard addition method for the absolute quantification of neutral lipids in microalgae using Nile red', Journal of Microbiological Methods, 87(1): 17–23.

Bharathiraja, B. et al. (2014) 'Biodiesel production using chemical and biological methods – A review of process, catalyst, acyl acceptor, source and process variables', Renewable and Sustainable Energy Reviews. Pergamon, 38, pp. 368–382. doi: 10.1016/J.RSER.2014.05.084.

Bhatnagar A., Chinnasamy S., Singh M., Das K.C. 2011. Renewable biomass production by mixotrophic algae in the presence of various carbon sources and wastewaters. Applied Energy, 88(10): 3425–3431.

Bhunia B. and Dey A. 2012. Statistical Approach for Optimization of Physiochemical Requirements on Alkaline Protease Production from *Bacillus licheniformis* NCIM 2042. Enzyme Research. PMID: 22347624

Bhushan I., Parshad R., Qazi G.N., Gupta V.K. 2008. Immobilization of Lipase by Entrapment in Ca-alginate Beads. Journal of Bioactiive and Compatible polymers, 23 (6): 552–562.

Bofill C., Prim N., Mormeneo M., Manresa A., Pastor Javier F.I., Diaz P. 2010. Differential behaviour of *Pseudomonas* sp. 42A2 LipC, a lipase showing greater versatility than its counterpart LipA. Biochimie, 92(3): 307–316.

Bora L. and Bora M. 2012. Optimization of extracellular thermophilic highly alkaline lipase from thermophilic *Bacillus* sp. isolated from hotspring of Arunachal Pradesh, India. Brazilian Journal of Microbiology, 43(1): 30–42.

Borkar P.S., Bodade R.G., Rao Srinivasa R., Khobragade C.N. 2009. Purification and characterization of extracellular lipase from a new strain: *Pseudomonas aeruginosa* SRT 9. Brazilian Journal of Microbiology, 40(2): 358–366.

Bornscheuer U.T., Altenbuchner J. and Meyer H.H. 1999. Directed evolution of an esterase: screening of enzyme libraries based on pH-Indicators and a growth assay. Bioorganic & Medicinal Chemistry, 7(10): 2169–2173.

Borrelli G.M. and Trono D. 2015. Recombinant Lipases and Phospholipases and Their Use as Biocatalysts for Industrial Applications. International Journal of Molecular Sciences, 16(9): 20774–20840.

Bose A. and Keharia H. 2013. Production, characterization and applications of organic solvent tolerant lipase by *Pseudomonas aeruginosa* AAU2. Biocatalysis and Agricultural Biotechnology, 2(3): 255–266.

Brennan L. and Owende P. 2010. Biofuels from microalgae—A review of technologies for production, processing, and extractions of biofuels and co-products. Renewable and Sustainable Energy Reviews, 14(2): 557–577.

Breuer G., Evers Wendy A.C., Vree Jeroen de. H., Kleinegris Dorinde M.M., Martens Dirk E., Wijfells Rene H., Lamers Packo P. 2013. Analysis of Fatty Acid Content and Composition in Microalgae. Journal of Visualized Experiments, 80 (80).

Brewer S.H., Gloom W.R., Johnson M.C., Kang M.K., Franzen S. 2005. Probing BSA binding to citrate- coated gold nanoparticles and surfaces. Langmuir. 21(20): 9303–9307.

Brian S.R. and Sims R.C. 2013. Effect of moisture on in situ transesterification of microalgae for biodiesel production. Journal of Chemical Technology and Biotechnology, 89(1): 137–142.

Brozzoli V., Crognale S., Sampedro I., Federici F., Annibale A.D., Petruccioli M. 2009. Assessment of olive-mill wastewater as a growth medium for lipase production by *Candida cylindracea* in bench-top reactor. Bioresource Technology, 100(13): 3395–3402.

Bueso F., Moreno L., Cedeno M., Manzanarez K. 2015. Lipase-catalyzed biodiesel production and quality with *Jatropha curcas* oil: exploring its potential for Central America. Journal of Biological Engineering, 9(12).

Burdette L.A., Leach S.A., Wong H.T. and Tullman-Ercek D. 2018. Developing Gram-negative bacteria for the secretion of heterologous proteins. Microbial Cell Factories, 17(196).

Burkert J., Maugeri F. and MI Rodrigues. 2004. Optimization of extracellular lipase production by *Penicillium chrysogenum* using factorial design. Malaysian Journal of Microbiology, 7(2): 71–77.

Burlina A. and Galzigna L. 1973. Turbidimetric procedure for determination of lipase activity. Clinical Chemistry, 19(4): 384–386.

Cao H., Zhang Z., Wu X., Miao X. 2013. Direct biodiesel production from wet microalgae biomass of *Chlorella pyrenoidosa* through *In Situ* transesterification. BioMed Research International, Article ID 930686.

Cao H., Jiang Y., Zhang H. Nie K., Lei M. Dend L., Wang F., Tan T. 2017. Enhancement of methanol resistance of *Yarrowia lipolytica* lipase 2 using β-cyclodextrin as an additive: Insights from experiments and molecular dynamics simulation. Enzyme and Microbial Technology, 96: 157–162.

Cao Y., Zhuang Y., Yan C., Wu B., He B. 2012. Purification and characterization of an organic solvent-stable lipase from *Pseudomonas stutzeri* LC2-8 and its application for efficient resolution of (R, S)-1-phenylethanol. Biochemical Engineering Journal, 64: 55–60.

Cataluna R. and Silva R. da. 2012. Effect of Cetane Number on Specific Fuel Consumption and Particulate Matter and Unburned Hydrocarbon Emissions from Diesel Engines. Journal of Combustion. Article ID 738940.

Chakravorty D., parameshwaran S., Dubey V.K., Patra S. 2012. Unraveling the rationale behind organic solvent stability of lipases. Applied Biochemistry and Biotechnology, 167(3): 439–461.

Champe P., Harvey R.A. and Ferrier D.R. 2005. Biochemistry: 55-56

Chander H. and Ranganathan B. 1975. Role of amino acids on the growth and lipase production of *Streptococcus faecalis*. Experientia, 31(11): 1973–1975.

Chang H.M. 2018. Emerging Areas in Bioengineering, Volume 1. John Wiley & Sons, 2018.

Charles H. and Jack L. 1947. For Surgery, publication in Chromogenic substrates: 467–482.

Chen B., Hu J., Miller E.M., Xie W., Cai M. and Gross R.A. 2008. *Candida antarctica* Lipase B chemically immobilized on epoxy-activated micro- and nanobeads: Catalysts for polyester synthesis. Biomacromolecules, 9(2): 463–471.

Chen C.Y., Yeh K-L., Aisyah R., Lee D-J., Chang J-S. 2011. Cultivation, photobioreactor design and harvesting of microalgae for biodiesel production: A critical review. Bioresource Technology, 102(1): 71–81.

Chen G., Ying M. and Li W. 2006. Enzymatic Conversion of Waste Cooking Oils into Alternative Fuel Biodiesel. Applied Biochemistry and Biotechnology 132: 911-921.

Chen J.W. and Wu W.T. 2003. Regeneration of immobilized *Candida antarctica* lipase for transesterification. Journal of Bioscience and Bioengineering, 95(5): 466–469.

Chen W., Zhang C., Song L., Sommerfeld M., Hu Q. 2009. A high throughput Nile red method for quantitative measurement of neutral lipids in microalgae. Journal of Microbiological Methods,77(1): 41–47.

Chen W., Sommerfeld M. and Hu Q. 2011. Microwave-assisted Nile red method for in vivo quantification of neutral lipids in microalgae. Bioresource Technology,102(1): 135–141.

Chisti Y. 2007. Biodiesel from microalgae. Biotechnology Advances,25(3): 294–306.

Chong H., Geng H., Zhang H., Song H., Huang L. and Jiang R. 2014. Enhancing *E. coli* isobutanol tolerance through engineering its global transcription factor cAMP receptor protein (CRP). Biotechnology and Bioengineering, 111(4): 700–708.

Christopher L.P., Zambare V.P., Zambare A., Kumar H., Malek L. 2015. A thermo-alkaline lipase from a new thermophile *Geobacillus thermodenitrificans* AV-5 with potential application in biodiesel production. Journal of Chemical Technology and Biotechnology, 90(11): 2007–2016.

Christopher L.P., Hemanathan Kumar and Zambare V.P. 2014. Enzymatic biodiesel: Challenges and opportunities. Applied Energy,119: 497–520.

Cirulis J.T., Strasser B.C., Scott J.A. and Ross G.M. 2012. Optimization of staining conditions for microalgae with three lipophilic dyes to reduce precipitation and fluorescence variability. Journal of Quantitative cell Science, 81A (7): 618–626.

Clarridge J.E. and Alerts C. 2004. Impact of 16S rRNA gene sequence analysis for identification of bacteria on clinical microbiology and infectious diseases. Clinical Microbiology Reviews,17(4): 840–862.

Coggon R., Vasudevan P.T. and Sanchez F. 2007. Enzymatic transesterification of olive oil and its precursors. Biocatalysis and Biotransformation,25(2–4): 135–143.

Cooksey K.E., Guckert J.B., Williams S.A. and Callis P.R. 1987. Fluorometric determination of the neutral lipid content of microalgal cells using Nile Red. Journal of Microbiological Methods,6(6): 333–345.

Correa I.N.D.S., Silva Da S.S.P., Queiroz D.S., Rosas D.O., Langone M.A.P. 2016. Enzymatic synthesis of dioctyl sebacate. Journal of Molecular Catalysis B: Enzymatic, 133(supplement 1): S166–S171.

Cross R.T. and Schirch V. 1991. Effects of amino acid sequence, buffers, and ionic strength on rate and mechanism of deamidation of asparagine residues in small peptides. The journal of biological chemistry, 266(33): 22549–22556.

Dalmaso G.Z.L., Ferreira D. and Vermelho A.B. 2015. Marine extremophiles a source of hydrolases for biotechnological applications. Marine Drugs, 13(4): 1925–1965.

Dandavate V., Jinjala J., Keharia H. and Madamwar D. 2009. Production, partial purification and characterization of organic solvent tolerant lipase from *Burkholderia multivorans* V2 and its application for ester synthesis. Bioresource Technology, 100(13): 3374–3381.

Datta S., Christena L.R. and Rajaram Y.R.S. 2013. Enzyme immobilization: an overview on techniques and support materials. 3 Biotech, 3(1): 1–9.

David C.S. 2008. Protein Formulations Containing Sorbitol. Patent US20080200655A1.

David F., Sandra P. and Vickers A.K. 2005. Column Selection for the Analysis of Fatty Acid Methyl Esters. Agilent Technologies.

Davis K.E.R., Joseph S.J and Janssen P.H. 2005. Effects of Growth Medium, Inoculum Size, and Incubation Time on Culturability and Isolation of Soil Bacteria. Applied and environmental microbiology, 71(2): 826–834.

Desai J.D. and Banat I.M. 1997. Microbial production of surfactants and their commercial potential. Microbiology and Molecular Biology Reviews, 61(1): 47–64.

Deutscher M.P. 1990. Precipitation techniques. Methods in Enzymology: Guide to protein purification. 182nd edn: 289–290.

Dianursanti, Religia P. and Wijanarko A. 2015. Utilization of n-Hexane as Co-solvent to Increase Biodiesel Yield on Direct Transesterification Reaction from Marine Microalgae. Procedia Environmental Sciences, 23: 412–420.

Doan T.T.Y. and Obbard J.P. 2011. Improved Nile Red staining of *Nannochloropsis* sp. Journal of Applied Phycology, 23(5): 895–901.

Dominguez A., Pastrana L., Longo M.A., Rua M.L., Sanroman M.A. 2005. Lipolytic enzyme production by *Thermus thermophilus* HB27 in a stirred tank bioreactor. Biochemical Engineering Journal, 26(2–3): 95–99.

Dror A., Kanteev M., Kagan I., Gihaz S., Shahar A. and Fishman A. 2015. Structural insights into methanol-stable variants of lipase T6 from *Geobacillus stearothermophilus*. Applied Microbiology and Biotechnology, 99(22): 9449–9461.

Du W., Xu Y. and Liu D. 2003. Lipase-catalysed transesterification of soya bean oil for biodiesel production during continuous batch operation. Biotechnology and Applied Biochemistry, 38: 103–106.

Du X., Liu X., Li Y., Wu C., Wang X and Xu P. 2013. Efficient biocatalyst by encapsulating lipase into nanoporous gold. Nanoscale Research Letters, 8(1): 1–6.

Duchiron S.W., Pollet E., Givry S. and Averous L. 2017. Enzymatic synthesis of poly(ε-caprolactone-co-ε-thiocaprolactone). European Polymer Journal, 87: 147–158.

Dunn R.O. 2009. Effects of minor constituents on cold flow properties and performance of biodiesel. Progress in Energy and Combustion Science, 35(6): 481–489.

Dunn R.O., Ngo H.L. and Haas M.J. 2015. Branched-chain fatty acid methyl esters as cold flow improvers for biodiesel. Journal of the American Oil Chemists' Society, 92(6): 853–869.

Dwivedi G. and Sharma M.P. 2013. Cold Flow Behaviour of Biodiesel-A Review. International Journal of Renewable Energy Research, 3(4).

Edouard B.S. and Koza S.M. 2014. Advances in size-exclusion separations of proteins and polymers by UHPLC. TrAC Trends in Analytical Chemistry, 63: 85–94.

Elsey D., Jameson D., Raleigh B and Cooney M.J. 2007. Fluorescent measurement of microalgal neutral lipids. Journal of Microbiological Methods, 68(3): 639–642.

Ema T., Kageyama M., Korenaga T. and Sakai T. 2003. Highly enantioselective lipase-catalyzed reactions at high temperatures up to 120°C in organic solvent. Tetrahedron: Asymmetry, 14(24): 3943–3947.

Englard S. and Seifter S. 1990. Precipitation techniques. Methods in Enzymology, 182(C): 285–300.

Ernst O. and Zor T. 2010. Linearization of the Bradford Protein Assay. Journal of Visualized Experiments, 38: 1–6.

Falk O. and Pittroff R.M. 2004. The effect of fatty acid composition on biodiesel oxidative stability. European Journal of Lipid Science and Technology, 106(12): 837–843.

Fatima H. and Khan N. 2015. Production and Partial Characterization of Lipase from *Pseudomonas putida*. Fermentation Technology, 4(1): 1–7.

Fogarty A.C. and Laage D. 2013. Water Dynamics in Protein Hydration Shells: The Molecular Origins of the Dynamical Perturbation. The Journal of Physical Chemistry, 118: 7715–7729.

Ganasen M., Yaacob N., Rahman R.N.Z.R.A, Leow A.T.C., Basri M., Salleh A.B and Ali M.S.M. 2016. Cold-adapted organic solvent tolerant alkalophilic family I.3 lipase from an Antarctic Pseudomonas. International Journal of Biological Macromolecules, 92: 1266–1276.

Garcia M.D. and M.J. Valencia Gonazalez. 1995. Enzyme catalysis in organic solvents: a promising field for optical biosensing. Talanta, 42(11): 1763–1773.

Gekko K., Ohmae E., Kameyama K. and Takagi T. 1998. Acetonitrile-protein interactions: amino acid solubility and preferential solvation. Biochimica et Biophysica Acta (BBA) - Protein Structure and Molecular Enzymology, 1387(1–2): 195–205.

Geng H. and Jiang R. 2015. cAMP receptor protein (CRP)-mediated resistance/tolerance in bacteria: mechanism and utilization in biotechnology. Applied Microbiology and Biotechnology, 99(11): 4533–4543.

Ghaly A.E., Dave D., Brooks M.S. and Budge S. 2010. Production of Biodiesel by Enzymatic Transesterification: Review. American Journal of Biochemistry and Biotechnology, 6(2): 54–76.

Ghamgui H., Karra-cha M. and Gargouri Y. 2004. 1-Butyl oleate synthesis by immobilized lipase from *Rhizopus oryzae*: a comparative study between n -hexane and solvent-free system. Biocatalysis and Biotransformation, 35: 355–363.

Ghoneim N. 2000. Photophysics of Nile red in solution: Steady state spectroscopy. Spectrochimica Acta Part A: Molecular and Biomolecular Spectroscopy,56(5): 1003–1010.

Ghosh R. 2006. Precipitation. Principles of Bioseperations Engineering: 72.

Gilham D. and Lehner R. 2005. Techniques to measure lipase and esterase activity in vitro. Methods, 36(2): 139–147.

Glogauer A., Martini V.P., Faoro H., Couto G.H., Muller-Santos M., Monterio R.A., Mitchell D.A., Souza de E.M., Pedrosa F.O. and Krieger N. 2011. Identification and characterization of a new true lipase isolated through metagenomic approach. Microbial cell factories 10: 54.

Gog A., Roman M., Tosa M., Paizs C. and Irimie F.D. 2012. Biodiesel production using enzymatic transesterification – Current state and perspectives. Renewable Energy,39(1): 10–16.

Gouveia L. and Oliveira A.C. 2009. Microalgae as a raw material for biofuels production. Journal of industrial microbiology & biotechnology, 36(2): 269–274.

Govender T., Ramanna L., Rawat I. and Bux F. 2012. BODIPY staining, an alternative to the Nile Red fluorescence method for the evaluation of intracellular lipids in microalgae. Bioresource Technology, 114: 507–511.

Greenspan P. and Fowler S. 1985. Spectrofluorometric studies of the lipid probe, Nile red. Journal of Lipid research, 26(7): 781–789.

Greenspan P., Mayer E. and Fowler S. 1985. Nile red: a selective fluorescent stain for intracellular lipid droplets. The Journal of Cellular Biology, 100(3): 965–973.

Griffiths M.J., Hille R.P. Van and Harrison S.T.L. 2010. Selection of direct transesterification as the preferred method for assay of fatty acid content of microalgae. Lipids, 45: 1053–1060.

Gromiha M.M., Santhosh C. and Ahmad S. 2004. Structural analysis of cation–π interactions in DNA binding proteins. International Journal of Biological Macromolecules, 34(3): 203–211.

Gronemeyer P., Ditz R. and Strube J. 2014. Trends in Upstream and Downstream Process Development for Antibody Manufacturing. Bioengineering, 1(4): 188–212.

Gulati R., Isar J., Kumar V., Prasad A.K., Parmar V.S. 2005. Production of a novel alkaline lipase by *Fusarium globulosum* using neem oil, and its applications. Pure and Applied Chemistry, 77(1): 251-262.

Guldhe A., Singh B., Rawat I., Ramluckan K. and Bux F. 2014. Efficacy of drying and cell disruption techniques on lipid recovery from microalgae for biodiesel production. Fuel,128: 46–52.

Guldhe A., Singh B., Rawat I., Permaul K. and Bux F. 2015. Biocatalytic conversion of lipids from microalgae *Scenedesmus obliquus* to biodiesel using *Pseudomonas fluorescens* lipase. Fuel, 147: 117–124.

Gumel A.M., Annuar M.S.M., Heidelberg T. and Chisti Y. 2011. Lipase mediated synthesis of sugar fatty acid esters. Process Biochemistry, 46(11): 2079–2090.

Gupta R., Rathi P., Gupta N. and Bradoo S. 2010. Lipase assays for conventional and molecular screening: an overview. Biotechnology and Applied Biochemistry, 37(1): 63–71.

Gupta R., Gupta N. and Rathi P. 2004. Bacterial lipases: An overview of production, purification and biochemical properties. Applied Microbiology and Biotechnology, 64(6): 763–781.

Gupta V. K., Sharma G.D., Tuohy M.G. and Gaur R. 2016. The Handbook of Microbial Bioresources. CAB International.

Gupta V.K. and Tuohy M.G. 2013. Biofuel Technologies: Recent Developments. 1st edn. Springer-Verlag Berlin Heidelberg.

Gurung N., Ray S., Bose S. and Rai V. 2013. A broader view: Microbial enzymes and their relevance in industries, medicine, and beyond. BioMed Research International. Article ID 329121.

Guzman H.M., Valido de la A.J., Durate L.C. and Presmanes K.F. 2011. Analysis of interspecific variation in relative fatty acid composition: use of flow cytometry to estimate unsaturation index and relative polyunsaturated fatty acid content in microalgae. Journal of Applied Phycology, 23(1): 7–15.

Halder D. and Basu M. 2016. Role of *Pseudomonas stutzeri* MTCC101 in Cadmium Bioremediation. International Journal of Current Microbiology and Applied Sciences, 5(2): 139–148.

Halim R., Razif H., Micheal K. D. and Paul A.W. 2012. Microalgal cell disruption for biofuel development. Applied Energy, 91(1): 116–121.

Halim R. and Webley P.A. 2015. Nile Red Staining for Oil Determination in Microalgal Cells: A New Insight through Statistical Modelling. International Journal of Chemical Engineering. Article ID: 695061.

Halling P.J. 1997. Predicting the behaviour of lipases in low-water media. Biochemical Society transactions, 25(1): 170–4.

Hama S., Yamaji H., Fukumizu T., Numata T., Tamalampudi S., Kondo A., Noda H. and Fukuda H. 2007. Biodiesel-fuel production in a packed-bed reactor using lipase-producing *Rhizopus oryzae* cells immobilized within biomass support particles. Biochemical Engineering Journal,34(3): 273–278.

Hanaki K. and Portugal-Pereira J. 2018. The Effect of Biofuel Production on Greenhouse Gas Emission Reductions. Biofuels and Sustainability. Science for Sustainable Societies.

Hari Krishna S. and Karanth N. G. 2002. Lipases and Lipase-Catalyzed Esterification Reactions in Nonaqueous Media. Catalysis Reviews, 44(4): 161–4940.

Harwati T.U. 2013. Cultivation of Microalgae: Lipid Production, Evaluation of Antioxidant Capacity and Modeling of Growth and Lipid Production. PhD dissertation. University Carolo Wilhelmina. Germany.

Hasan-Beikdashti M., Forootanfar H., Safiarian M.S., Ameri A., Ghahremani M.H., Khoshayand M.R. and Faramarzi M.A. 2012. Optimization of culture conditions for production of lipase by a newly isolated bacterium *Stenotrophomonas maltophilia*. Journal of the Taiwan Institute of Chemical Engineers,43(5): 670–677.

Hasan F., Shah A.A. and Hameed A. 2006. Industrial applications of microbial lipases. Enzyme and Microbial Technology,39(2): 235–251.

Heitz M., Rodriguez del M.P., Brzezinski R. and Faucheux N. 2016. Enzymatic transesterification of lipids from microalgae into biodiesel: a review. AIMS Energy,4(6): 817–855.

Helwani Z., Othman M.R., Aziz N., Fernando W.J.N. and Kim J. 2009. Technologies for production of biodiesel focusing on green catalytic techniques: A review. Fuel Processing Technology, 90(12): 1502–1514.

Henderson C.M. and Block D.E. 2014. Examining the Role of Membrane Lipid Composition in Determining the Ethanol Tolerance of *Saccharomyces cerevisiae*. Applied and environmental microbiology,80(10): 2966–72.

Hertzberg S., Kvittingen L. and Anthonsent T. 1992. Alginate as immobilization matrix and stabilizing agent in a two-phase liquid system: Application in lipase-catalysed reactions. Enzyme and Microbial Technology,14(1): 42-47.

Hidalgo P., Toro C., Ciudad G. and Navia R. 2013. Advances in direct transesterification of microalgal biomass for biodiesel production. Reviews in Environmental Science and Bio/Technology, 12(2), pp. 179–199.

Homaei A.A., Sariri R. and Stevanto R. 2013. Enzyme immobilization: an update. Journal of chemical biology,6(4): 185–205.

Hospital P., Creu S. and Pau S. 1999. Direct fluorescence-based lipase activity assay. Biotechniques, 27.

Hsieh C.H. and Wu W.T. 2009. Cultivation of microalgae for oil production with a cultivation strategy of urea limitation. Bioresource Technology,100(17): 3921–3926.

Hu Q., Sommerfeld M., Jarvis E., Ghirardi M., Posewitz M., Seibert M. and Darzins Al. 2008. Microalgal triacylglycerols as feedstocks for biofuel production: Perspectives and advances. Plant Journal,54(4): 621–639.

Huang C., Luo M.T, Chen Z.F., Qi G.X., Xiong L., Lin X.Q., Wang C., Long H.Li. and Chen X.D. 2017. Combined "de novo" and "ex novo" lipid fermentation in a mix-medium of corncob acid hydrolysate and soybean oil by *Trichosporon dermatis*. Biotechnology for biofuels,10: article: 147.

Huang G.H., Chen G. and Chen F. 2009. Rapid screening method for lipid production in alga based on Nile red fluorescence. Biomass and Bioenergy,33(10): 1386–1392.

Huang G., Chen F., Wei D., Zhang XueW. And Chen G. 2010. Biodiesel production by microalgal biotechnology. Applied Energy,87(1): 38–46.

Huang J., Xia Ji, Jiang W., Li Y. and Li J. 2015. Biodiesel production from microalgae oil catalyzed by a recombinant lipase. Bioresource Technology,180: 47–53.

Hwang H.T., Qi F., Yuan C., Zhao X., Ramkrishna D., Liu D. and Varma S. 2014. Lipase-catalyzed process for biodiesel production: Protein engineering and lipase production. Biotechnology and Bioengineering,111(4): 639–653.

ICH. 1996. Guidance for industry: Q2B validation of analytical procedures: methodology, International conference on harmonisation of technical requirements for registration tripartite guideline.

Illanes A. 2016. Biocatalysis in Organic media. Chapter 3, White Biotechnology for Sustainable Chemistry: 36–51.

Illman A., Scragg, A. and Shales S. 2000. Increase in *Chlorella* strains calorific values when grown in low nitrogen medium. Enzyme and Microbial Technology, 27(8): 631–635.

Ingham K. 1984. Protein precipitation with polyethylene glycol. Methods in Enzymology, 104: 351–356.

Islam M.A., Magnusson M., Brown R.J., Ayoko G.A., Nabi Md. N. and Heimann K. 2013. Microalgal species selection for biodiesel production based on fuel properties derived from fatty acid profiles. Energies,6(11): 5676–5702.

Isleten-Hosoglu M., Gultepe I. and Elibol M. 2012. Optimization of carbon and nitrogen sources for biomass and lipid production by *Chlorella saccharophila* under heterotrophic conditions and development of Nile red fluorescence based method for quantification of its neutral lipid content. Biochemical Engineering Journal, 61: 11–19.

Iso M., Chen B., Eguchi M., Kudo T. and Shrestha S. 2001. Production of biodiesel fuel from triglycerides and alcohol using immobilized lipase. Journal of Molecular Catalysis B: Enzymatic, 16(1): 53–58.

Isobe K., Akiba T. and Yamaguchi S. 1988. Crystallization and characterization of lipase from *Penicillium cyclopium*. Agricultural and biological chemistry,52(1): 41–47.

Jaeger K.E., Ransac S., Dijkstra B.W., Colson C., Heuvel van M. and Misset O. 1994. Bacterial lipases. FEMS Microbiology Reviews,15(1): 29-63.

Jaeger K.E. and Reetzb M.T. 1998. Microbial lipases form versatile tools for biotechnology. Trends in Biotechnology,16(9): 396–403.

Jain D. and Mishra S. 2015. Multifunctional solvent stable *Bacillus* lipase mediated biotransformations in the context of food and fuel. Journal of Molecular Catalysis B: Enzymatic, 117: 21–30.

Jarvis G.N. and Thiele J.H. 1997. Qualitative Rhodamine B assay which uses tallow as a substrate for lipolytic obligately anaerobic bacteria. Journal of Microbiological Methods,29(1): 41–47.

Jassinnee M., Ong H.C., Masjuki H.H., Chong W.T., Lan M.K., Loh P.K. and Vellayan V. 2016. Microalgae biofuels as an alternative to fossil fuel for power generation. Renewable and Sustainable Energy Reviews,58: 180–197.

Jeong G.T. and Park D.H. 2008. Lipase-catalyzed transesterification of rapeseed oil for biodiesel production with tert-butanol. Applied Biochemistry and Biotechnology,148(1–3): 131–139.

Jia C., Zhao J., Feng B., Zhang X. and Xia W. 2010. A simple approach for the selective enzymatic synthesis of dilauroyl maltose in organic media. Journal of Molecular Catalysis B: Enzymatic,62(3–4): 265–269.

Jiang X.J., Hu Y., Jiang L., Gong Ji-H. and Huang H. 2013. Synthesis of vitamin E succinate from *Candida rugosa* lipase in organic medium. Chemical Research in Chinese Universities,29(2): 223–226.

Jiang Z., Yu M., Ren L., Zhou H. and Wei P. 2013. Synthesis of phytosterol esters catalyzed by immobilized lipase in organic media. Chinese Journal of Catalysis,34(12): 2255–2262.

Jones D.T., Vander Westhuizen A., Long S., Allcock E.R., Reid S.J. 1982. Solvent Production and Morphological Changes in *Clostridium acetobutylicum.* Applied and Environmental Microbiology, 43(6): 1434–1439.

Joseph B., Upadhyaya S. and Ramteke P. 2011. Production of Cold-Active Bacterial Lipases through Semisolid State Fermentation Using Oil Cakes. Enzyme Research. Article ID 796407.

Juan F.L., Garbayo I., Cuaresma M., Montero Z., Valle-del-G.M. and Vilchez C. 2016. Impact of Microalgae-Bacteria Interactions on the Production of Algal Biomass and Associated Compounds. Marine Drugs,14(5): 100.

Kai Chee Loh and Cao B. 2008. Paradigm in biodegradation using *Pseudomonas putida*—A review of proteomics studies. Enzyme and Microbial Technology,43(1): 1–12.

Kamal Z. Md., Yedavallo P., Deshmukh M.V. and Rao N.M. 2013. Lipase in aqueous-polar organic solvents: Activity, structure, and stability. Protein Science,22(7): 904–915.

Kamarudin N.H.A., Rahman R.N.Z.R.A., Ali M.M.S.M., Leow T.C., Basri M. and Salleh A.B. 2014. A new cold-adapted, organic solvent stable lipase from mesophilic *Staphylococcus epidermidis* AT2. Protein Journal,33(3): 296–307.

Kanmani P., Ramya S., Dhivya R. and Subashini D. 2015. Rice Bran Lipase: Partial Purification, Immobilization in Calcium Alginate Beads, Characterization and Application as a Detergent Additive. World Applied Sciences Journal, 33(6): 1052–1058.

Kanmani P., Kumaresan K., Aravind J., Karthikeyan S. and Balan R. 2016. Enzymatic degradation of polyhydroxyalkanoate using lipase from *Bacillus subtilis*. International Journal of Environmental Science and Technology,13(6): 1541–1552.

Kanno M., Katayama T., Tamaki H., Mitani Y., Meng X.Y., Hori T., Narihiro T., Morita N., Hoshino T., Yumoti I., Kimura N., hanada S. and Kamagata Y. 2013. Isolation of butanol- and isobutanol-tolerant bacteria and physiological characterization of their butanol tolerance. Applied and Environmental Microbiology,79(22): 6998–7005.

Kaplan A. 1970. A simple radioactive assay for triglyceride lipase. Analytical Biochemistry,33(2): 218–225.

Karadzic I., Masui A., Zivkovic L.I., and Fujiwara N. 2006. Purification and characterization of an alkaline lipase from *Pseudomonas aeruginosa* isolated from putrid mineral cutting oil as component of metalworking fluid. Journal of Bioscience and Bioengineering,102(2): 82–89.

Kaur G., Singh A., Sharma R., Sharma V., Verma S. and Sharma P.K. 2016. Cloning, expression, purification and characterization of lipase from *Bacillus licheniformis*, isolated from hot spring of Himachal. 3 Biotech 6: 49.

Keesoo L., Eisterhold M.L., Rindi F., Palanisami S. and Paul K.N. 2014. Isolation and screening of microalgae from natural habitats in the midwestern United States of America for biomass and biodiesel sources. Journal of natural science, biology and medicine,5(2): 333–339.

Keith S.J. 2017. Enzyme Immobilization on Nanoporous Gold: A Review. Biochemistry Insights,10: 1–12.

Khan A.K., Rashid R., Murtaza G. and Zahra A. 2014. Gold Nanoparticles: Synthesis and Applications in Drug Delivery. Tropical Journal of Pharmacecutical Research,13(7): 1169–1177.

Khan H.U. 2012. The role of ion exchange chromatography in purification and characterization of molecules. Ion exchange technologies, Chapter 14.

Khan Ray Dutta J. and Ganesan R. 2017. *Lactobacillus* sps. lipase mediated poly (Ɛ-caprolactone) degradation. International Journal of Biological Macromolecules,95: 126–131.

Khmelnitsky Y.L., Levashov A.V., Klyachko N.L. and Martinek K. 1988. Engineering biocatalytic systems in organic media with low water content. Enzyme and Microbial Technology,10(12): 710–724.

Khutale G.V. and Casey A. 2017. Synthesis and characterization of a multifunctional gold-doxorubicin nanoparticle system for pH triggered intracellular anticancer drug release. European Journal of Pharmaceutics and Biopharmaceutics,119: 372–380.

Kia-Kojouri M., Najafpour D.G., Banin R. and Meghdad M. 2016. Production of biodiesel from rapeseed oil by porcine pancreatic mediated transesterification reaction in organic solvent. Indian Journal of Chemical Technology,23(3): 216–220.

Kim G.V. Choi W.Y., Kang D.H., Lee S.Y. and Lee H.Y. 2014. Enhancement of Biodiesel Production from Marine Alga, *Scenedesmus* sp. through In Situ Transesterification Process Associated with Acidic Catalyst. BioMed Research International. Article ID: 391542.

Kim H.B. and Gadd M.G. 2008. Bacterial Physiology and Metabolism. Cambridge University Press. ISBN: 9780511790461.

Kim J.H. and Yoon S.H. 2014. Effects of organic solvents on transesterification of phospholipids using phospholipase A2 and lipase. Food Science and Biotechnology,23(4): 1207–1211.

Kim M., Lee B., Kim H.S., Nam K., Moon M., Oh H-M. and Chang Y.K. 2019. Increased biomass and lipid production of Ettlia sp. YC001 by optimized C and N sources in heterotrophic culture. Scientific Reports, 9(1): 1–12.

Kimura K., Yamaoka M. and Kamisaka Y. 2004. Rapid estimation of lipids in oleaginous fungi and yeasts using Nile red fluorescence. Journal of Microbiological Methods,56(3): 331–338.

Kirdi R., Akacha N.B., Bejaoui H., Messaoudi Y., Romano D., Molinari F. and Gargouri M. 2017. Mycelium-bound lipase from *Aspergillus oryzae* as efficient biocatalyst for cis-3-hexen-1-yl acetate synthesis in organic solvent. Biocatalysis and Agricultural Biotechnology,10: 13–19.

Klockgether J., Cramer N., Wiehlmann L., Devanport C.F. and Tummler B. 2011. *Pseudomonas aeruginosa* genomic structure and diversity. Frontiers in Microbiology, 2: 1–18.

Knezevic Z., Bobic S., Milutinovic A., Obradovic B., Mojovic L. and Bugarski B. 2002. Alginate-immobilized lipase by electrostatic extrusion for the purpose of palm oil hydrolysis in lecithin/isooctane system. Process Biochemistry,38(3): 313–318.

Knothe G. 2005. Dependence of biodiesel fuel properties on the structure of fatty acid alkyl esters. Fuel Processing Technology,86(10): 1059–1070.

Knothe G. 2008. "Designer" Biodiesel: Optimizing Fatty Ester Composition to Improve Fuel Properties. Energy & Fuels,22: 1358–1364.

Kobayashi S., Uyama H. and Takamoto T. 2000. Lipase-Catalyzed Degradation of Polyesters in Organic Solvents. A New Methodology of Polymer Recycling Using Enzyme as Catalyst. Biomacromolecules, 1(1): 3–5.

Kondamudi N., Mohapatra S.K. and Misra M. 2011. Quintinite as a bifunctional heterogeneous catalyst for biodiesel synthesis. Applied Catalysis A: General,393(1–2): 36–43.

Kordel M., Hofmann B., Schomburg D. and Schmid R.D. 1991. Extracellular lipase of *Pseudomonas* sp. strain ATCC 21808: purification, characterization, crystallization, and preliminary X-ray diffraction data. Journal of Bacteriology,173(15): 4836–4841.

Kouker G. and Jaeger K.E. 1987. Specific and sensitive plate assay for bacterial lipases. Applied and Environmental Microbiology,53(1): 211–213.

Kramer R.M., Shende V.R., Moti N., Pace C.N. and Scholtz M. 2012. Toward a molecular understanding of protein solubility: Increased negative surface charge correlates with increased solubility. Biophysical Journal. Biophysical Society, 102(8): 1907–1915.

Kubler D., Bergmann A., Weger L., Ingenbosch K.N. and Jocobsen K.H. 2017. Kinetics of Detergent-Induced Activation and Inhibition of a Minimal Lipase. Journal of Physical Chemistry B,121(6): 1248–1257.

Kulkarni A.G. and Kaliwal B. 2015. Bioremediation of Methomyl by Soil Isolate - *Pseudomonas aeruginosa*. Journal of Environmental Science, Toxicology and Food Technology, 8(12).

Kulkarni N. and Gadre R. 2002. Production and properties of an alkaline, thermophilic lipase from *Pseudomonas fluorescens* NS2W. Journal of Industrial microbiology & biotechnology,28(6): 344–348.

Kumar A., Ergas S., Yuan X., Sahu A., Zhang Q., Dewulf J., Malcata F.X. and Langenhove van H. 2010. Enhanced CO_2 fixation and biofuel production via microalgae: recent developments and future directions. Trends in Biotechnology,28(7): 371–380.

Kumar A., Zhang S., Wu G., Wu C.C., Chen JunP., Baskaran R. and Liu Z. 2015. Cellulose binding domain assisted immobilization of lipase (GSlip-CBD) onto cellulosic nanogel:

Characterization and application in organic medium. Colloids and Surfaces B: Biointerfaces,136: 1042–1050.

Kumar A., Dhar K., Kanwar S.S. and Arora P.K. 2016. Lipase catalysis in organic solvents: advantages and applications. Biological procedures online,18.

Kumar D., Kumar L., Nagar S., Raina C., Parshad R. and Gupta V.K. 2012. Screening, isolation and production of lipase/esterase producing *Bacillus* sp. strain DVL2 and its potential evaluation in esterification and resolution reactions. Archives of Applied Science Research, 4(4): 1763–1770.

Kumar D., Parshad R. and Gupta V.K. 2014. Application of a statistically enhanced, novel, organic solvent stable lipase from *Bacillus safensis* DVL-43. International Journal of Biological Macromolecules,66: 97–107.

Kumar S.S. and Gupta R. 2008. An extracellular lipase from *Trichosporon asahii* MSR 54: Medium optimization and enantioselective deacetylation of phenyl ethyl acetate. Process Biochemistry,43(10): 1054–1060.

Kumar S., Yadav R.K. and Negi S. 2014. A comparative study of immobilized lipase produced from *Penicillium chrysogenum* SNP5 on two different anionic carriers for its pH and thermostability. Indian Journal of Biotechnology,13: 301–305.

Kumari A., Mahapatra P., Garlapati V.K. and Banerjee R. 2009. Enzymatic transesterification of Jatropha oil. Biotechnology for biofuels, 2(1).

Kung V.L., Ozer E.A. and Hauser A.R. 2010. The Accessory Genome of *Pseudomonas aeruginosa*. Microbiology and Molecular Biology Reviews,74(4): 621–641.

Kyu Kim K., Song H.K., Shin D.H., Hwang K.Y and Suh S.W. 1997. The crystal structure of a triacylglycerol lipase from *Pseudomonas cepacia* reveals a highly open conformation in the absence of a bound inhibitor. Structure,5(2): 173–185.

Laemmli U. 1970. Cleavage of Structural Proteins during the Assembly of the Head of Bacteriophage T4. Nature, 227: 680-685.

Lakowicz J.R. 2006. Quenching of fluorescence. Lakowicz J.R. (ed.) Principles of Fluorescence Spectroscopy: 277–330.

Lalucat J., Bennasar A., Bosch R., Valdes-Garcia E. and Palleroni N.J. 2006. Biology of *Pseudomonas stutzeri*. Microbiology and Molecular Biology Reviews,70(2): 510–547.

Lam M.K. and Lee K.T. 2012. Microalgae biofuels: A critical review of issues, problems and the way forward. Biotechnology Advances,30(3): 673–690.

Latip W., Rahman R.N.Z.R.A., Leow A.T.C., Shariff F.M. and Ali M.S.M. 2016. Expression and characterization of thermotolerant lipase with broad pH profiles isolated from an Antarctic *Pseudomonas* sp strain AMS3. PeerJ, 4(2420): 1–20.

Lazar I. and Szabo H.J. 2018. Prevention of the Aggregation of Nanoparticles during the Synthesis of Nanogold-Containing. Gels,4(55).

Lazaroaie M.M. 2009. Resistance in Gram-Negative Bacteria. International journal of biomedical and biological engineering,3(6): 309–319.

Leao R.A.C., Souza S.P.de., Nogueira O.D., Silba G.M.A., Silva M.V.M., Gutarra M.L.E., Miranda L.S.M., Castro A.M., Junior I.I. and souza R.O.M.A. 2016. Consecutive lipase immobilization and glycerol carbonate production under continuous-flow conditions. Catalysis Science & Technology,6(13): 4743–4748.

Lee C.K. and Nhan A.D.A. 2018. Enzyme Immobilization on Nanoparticles: Recent Applications. Emerging areas in Bioengineering. 2018th edn, Chapter 4: 67–80.

Lee J.O., Cho K.S. and Kim O. Bin. 2014. Overproduction of AcrR increases organic solvent tolerance mediated by modulation of SoxS regulon in *Escherichia coli*. Applied Microbiology and Biotechnology,98(20): 8763–8773.

Lee K., Eisterhold M.L., Rindi F., Palanisami S. and Nam P.K. 2014. Isolation and screening of microalgae from natural habitats in the midwestern United States of America for biomass and biodiesel sources. Journal of natural science, biology and medicine,5(2): 333–339.

Lee S.J., Yoon B.D. and Oh H.M. 1998. Rapid method for the determination of lipid from the green alga *Botryococcus braunii*. Biotechnology Techniques,12(7): 553–556.

Lee S.Y. and Rhee J.S. 1993. Production and partial purification of a lipase from *Pseudomonas putida* 3SK. Enzyme and Microbial Technology,15(7): 617–623.

Lee Y.K., Ding S.Y., Hoe C.H. and Low C.S. 1996. Mixotrophic growth of *Chlorella sorokiniana* in outdoor enclosed photobioreactor. Journal of Applied Phycology,8(2): 163–169.

Li C., Tan T., Zhang H. and Feng W. 2010. Analysis of the conformational stability and activity of *Candida antarctica* lipase B in organic solvents: Insight from molecular dynamics and quantum mechanics/simulations. The Journal of Biological Chemistry, 285(37): 28434–28441.

Li L., Jiang Y., Zhang H., Feng W., Chen B. and Tan T. 2014. Theoretical and experimental studies on activity of *Yarrowia lipolytica* lipase in methanol/water mixtures. Journal of Physical Chemistry B, 118(8): 1976–1983.

Li W., Du W., Liu D. and Yao Y. 2008. Study on factors influencing stability of whole cell during biodiesel production in solvent-free and tert-butanol system. Biochemical Engineering Journal,41(2): 111–115.

Li X., Qian Po., Wu S-G. and Yu H.Y .2014. Characterization of an organic solvent-tolerant lipase from *Idiomarina* sp. W33 and its application for biodiesel production using Jatropha oil. Extremophiles,18(1): 171–178.

Li X. and Yu H.Y. 2014. Characterization of an organic solvent-tolerant lipase from *Haloarcula* sp. G41 and its application for biodiesel production. Folia Microbiologica,59(6): 455–463.

Li Y., Horsman M., Wang B., Wu N. and Lan C.Q. 2008. Effects of nitrogen sources on cell growth and lipid accumulation of green alga *Neochloris oleoabundans*. Applied Microbiology and Biotechnology,81(4): 629–636.

Li Y., Han D., Hu G., Sommerfeld M. and Hu Q. 2010. Inhibition of starch synthesis results in overproduction of lipids in *Chlamydomonas reinhardtii*. Biotechnology and bioengineering,107(2): 258–268.

Lidbury I.D.E.A., Murphy A.R.J., Scanlan D.J., Bending G.D., Jones A.M.E., Moore J.D., Goodall A., Hammond J.P. and Wellington E.M.H. 2016. Comparative genomic, proteomic and exoproteomic analyses of three *Pseudomonas* strains reveals novel insights into the phosphorus scavenging capabilities of soil bacteria. Environmental Microbiology,18(10): 3535–3549.

Lima V.M.G., Krieger N., Sarquis M.I.M., Mitchell D.A., Ramos L.P. and Fontana J.D. 2003. Effect of Nitrogen and Carbon Sources on Lipase Production by *Penicillium aurantiogriseum*. Food Technology and Biotechnology,41(2): 105–110.

Liu Y., Zhang X., Tan H., Yan Y. and Hameed B.H. 2010. Effect of pretreatment by different organic solvents on esterification activity and conformation of immobilized *Pseudomonas cepacia* lipase. Process Biochemistry,45(7): 1176–1180.

Lomolino G., Di Pierro G. and Lante A. 2012. A quantitative fluorescence-based lipase assay. Food Technology and Biotechnology,50(4): 479–482.

Long Z., Xu J. and Pan J. 2007. Significant improvement of *Serratia marcescens* lipase fermentation, by optimizing medium, induction, and oxygen supply. Applied Biochemistry and Biotechnology,142(2): 148–157.

Lotti M., Pleiss J., Valero F. and Ferrer P. 2015. Effects of methanol on lipases: Molecular, kinetic and process issues in the production of biodiesel. Biotechnology Journal,10(1): 22–30.

Lowrey J., Brooks M.S. and McGinn P.J. 2015. Heterotrophic and mixotrophic cultivation of microalgae for biodiesel production in agricultural wastewaters and associated challenges—a critical review. Journal of applied phycology,27(4): 1485–1498.

Mahanta N., Gupta A. and Khare S. 2008. Production of protease and lipase by solvent tolerant *Pseudomonas aeruginosa* PseA in solid-state fermentation using *Jatropha curcas* seed cake as substrate. Bioresource Technology,99(6): 1729–1735.

Mairet F., Bernard O., Masci P., Lacour T. and Sciandra A. 2011. Modelling neutral lipid production by the microalga *Isochrysis aff*. galbana under nitrogen limitation. Bioresource Technology, 102(1): 142–149.

Makhzoum A., Knapp J.S. and Owusu R.K. 1995. Factors Affecting Growth and Extracellular Lipase Production by *Pseudomonas Fluorescens* 2D. Food Microbiology,12(4): 277–290.

Malcata F.X., Paiva A.L., and Balcao V.M. 2000. Kinetics and mechanisms of reactions catalysed by immobilized lipases. Enzyme and Microbial Technology,27(3-5): 187-204.

Maldonado A.A., Ribeiro J.M. and Sillero A. 2010. Isoelectric point, electric charge, and nomenclature of the acid–base residues of proteins. Biochemistry and Molecular biology Education,38(4): 230–237.

Mander P., Cho S.S., Simkhada J.R., Choi Y.H., Park Da J.P. and Yoo J.C. 2012. An organic solvent – tolerant lipase from *Streptomyces* sp. CS133 for enzymatic transesterification of vegetable oils in organic media. Process Biochemistry,47(4): 635–642.

Manz A., Pamme N. and Iossifidis D. 2004. Chromatography. Bioanalytical Chemistry: 37–40.

Marcela F., Lucia C., Esther F. and Elena M. 2016. Microencapsulation of L-Ascorbic Acid by Spray Drying Using Sodium Alginate as Wall Material. Journal of Encapsulation and Adsorption Sciences,6(6): 1–8.

Martin C.J., Golubow J. and Frazier A.R. 1958. A Rapid and Sensitive Spectrophotometric Method for the Assay of Chymotrypsin. Journal of Biological Chemistry,234(2): 294–298.

Martin M.N., Basham J.I., Chando P. and Eah S.K. 2010. Charged gold nanoparticles in non-polar solvents: 10-min synthesis and 2D self-assembly. Langmuir,26(10): 7410–7417.

Masomian M., Rahman R.N.Z.R.A., Salleh A.B. and Basri M. 2013. A new thermostable and organic solvent-tolerant lipase from *Aneurinibacillus thermoaerophilus* strain HZ. Process Biochemistry,48(1): 169–175.

Mata T.M., Martins A.A. and Caetano N.S. 2010. Microalgae for biodiesel production and other applications: A review. Renewable and Sustainable Energy Reviews,14(1): 217–232.

Mateo C., Palomo J.M., Lorente G.F., Guisan J.M. and Lafuente R.F. 2007. Improvement of enzyme activity, stability and selectivity via immobilization techniques. Enzyme and Microbial Technology,40(6): 1451–1463.

Matte C.R., Bordinhao C., Poppe J.K., Rodrigues R.C., Hertz P.F., Ayub M.A.Z. 2016. Synthesis of butyl butyrate in batch and continuous enzymatic reactors using *Thermomyces*

lanuginosus lipase immobilized in Immobead 150. Journal of Molecular Catalysis B: Enzymatic,127: 67–75.

Melero J.A., Iglesias J. and Morales G. 2009. Heterogeneous acid catalysts for biodiesel production: current status and future challenges. Green Chemistry,9.

Members R. 21 (2018) Renewables 2018 Global Status Report.

Miao X. and Wu Q. 2006. Biodiesel production from heterotrophic microalgal oil. Bioresource Technology,97(6): 841–846.

Micaêlo N.M. and Soares C. M. 2007. Modeling hydration mechanisms of enzymes in nonpolar and polar organic solvents. FEBS Journal,274(9): 2424–2436.

Milano J., Ong H.C., Masjuki H.H., Chong W.T., Lam M.K., Loh P.K. and Vellayan V. 2016. Microalgae biofuels as an alternative to fossil fuel for power generation. Renewable and Sustainable Energy Reviews,58: 180–197.

Miller A.L. and Smith L.C. 1973. Activation of lipoprotein lipase by apolipoprotein Glutamic acid. The Journal of Biological Chemistry,248(9): 3359–3362.

Mo Q., Liu A., Guo H., Zhang Y. and Li M. 2016. A novel thermostable and organic solvent-tolerant lipase from *Xanthomonas oryzae* pv. oryzae YB103: screening, purification and characterization. Extremophiles,20(2): 157–165.

Mogensen J., Sehgal P. and Otzen D. 2005. Activation, inhibition, and destabilization of *Thermomyces lanuginosus* lipase by detergents. Biochemistry,44(5): 1719–1730.

Mohamad N.R., Marzuki N.H.C., Buang N.A., Huyop F. and Wahab R.A. 2015. An overview of technologies for immobilization of enzymes and surface analysis techniques for immobilized enzymes. Biotechnology & Biotechnological Equipment,29(2): 205–220.

Mohamed I.O. 2012. Lipase-catalyzed synthesis of cocoa butter equivalent from palm olein and saturated fatty acid distillate from palm oil physical refinery. Applied Biochemistry and Biotechnology,168(6): 1405–1415.

Mohamed M., Wei L. and Ariff A. 2011. Heterotrophic cultivation of microalgae for production of biodiesel. Recent Patents on Biotechnology,5(2): 95–107.

Mohr A. and Raman S. 2013. Lessons from first generation biofuels and implications for the sustainability appraisal of second generation biofuels. Energy Policy,63: 114–122.

Molina-Gutiérrez M., Hakalin N.L., Sanchez L.R., Prieto A., Martinez M.J. 2016. Green synthesis of β-sitostanol esters catalyzed by the versatile lipase/sterol esterase from *Ophiostoma piceae*. Food Chemistry,15(221): 1458-1465.

Mondal M., Goswami S., Ghosh A., Oinam G., Tiwari O.N., Das P., Gayen K., Mandal M.K., and Halder G.N. 2017. Production of biodiesel from microalgae through biological carbon capture: a review.3 Biotech,7(2): 99.

Monhemi H., Housaindokht M.R., Movahedi A.K.M. and Bozorgmehr M.R. 2014. How a protein can remain stable in a solvent with high content of urea: insights from molecular dynamics simulation of *Candida antarctica* lipase B in urea: choline chloride deep eutectic solvent. Physical Chemistry chemical physics,16(28): 14882-93.

Monirul I.M., Masjuki H.H., Kalam M.A., Zulkifli N.W.M., Rashedul H.K., Rashed M.M. Imdadul H.K. and Mosarof M.H. 2015. A comprehensive review on biodiesel cold flow properties and oxidation stability along with their improvement processes. RSC Advances,105.

Montero M.F., Aristizabal M. and Reina G.G. 2011. Isolation of high-lipid content strains of the marine microalga *Tetraselmis suecica* for biodiesel production by flow cytometry and single-cell sorting. Journal of Applied Phycology,23(6): 1053–1057.

Morschett H., Wiechert W. and Oldiges M. 2016. Automation of a Nile red staining assay enables high throughput quantification of microalgal lipid production. Microbial Cell Factories, 15.

Mukesh K.M., Reddy J.R.C., Rao B.V.S.K. and Prasad R.B.N. 2007. Lipase-mediated conversion of vegetable oils into biodiesel using ethyl acetate as acyl acceptor. Bioresource Technology,98(6): 1260–1264.

Musa I.A. 2016. The effects of alcohol to oil molar ratios and the type of alcohol on biodiesel production using transesterification process. Egyptian Journal of Petroleum,25(1): 21–31.

Mustafa B. and Gunhan A. 2005. Biomass Energy in the World, Use of Biomass and Potential Trends. Energy Sources,27(10): 931–940.

Mutanda T., Ramesh D., Karthikeyan S., Kumari S., Anandraj A., and Bux F. 2011. Bioprospecting for hyper-lipid producing microalgal strains for sustainable biofuel production. Bioresource Technology,102(1): 57–70.

Nagao T., Shimada Y., Sugihara A. and Tominaga Y. 2002. Increase in stability of *Fusarium heterosporum* lipase. Journal of Molecular Catalysis B: Enzymatic,17(3–5): 125–132.

Najafi G., Ghobadian B. and Yusaf T.F. 2011. Algae as a sustainable energy source for biofuel production in Iran: A case study', Renewable and Sustainable Energy Reviews,15(8): 3870–3876.

Narwal S.K. et al. 2016. Green synthesis of isoamyl acetate via silica immobilized novel thermophilic lipase from *Bacillus aerius.* Russian Journal of Bioorganic Chemistry,42(1): 69–73.

Nie K., Xie F., Wang F. and Tan T. 2006. Lipase catalyzed methanolysis to produce biodiesel: Optimization of the biodiesel production. Journal of Molecular Catalysis B: Enzymatic,43(1–4): 142–147.

Noureddini H., Gao X. and Philkana R.S. 2005. Immobilized *Pseudomonas cepacia* lipase for biodiesel fuel production from soybean oil. Bioresource Technology,96(7): 769–777.

Novik G., Savich V. and Kiseleva E. 2015. An Insight Into Beneficial *Pseudomonas* bacteria. Microbiology in Agriculture and Human Health: 73–105.

Ogino H., Watanabe F., Yamada M., Nakagawa S., Hirose T., Hirose T., Noguchi A., Yasuda M. and Ishikawa H. 1999. Purification and characterization of organic solvent-stable protease from organic solvent-tolerant *Pseudomonas aeruginosa* PST-01. Journal of Bioscience and Bioengineering, 87(1): 61–68.

Ogino H. and Ishikawa H. 2001. Enzymes Which Are Stable in the Presence of Organic Solvents. Journal of Bioscience and Bioengineering,91(2): 109–116.

Ohtake S., Kita Y. and Arakawa T. 2011. Interactions of formulation excipients with proteins in solution and in the dried state. Advanced Drug Delivery Reviews,63(13): 1053–1073.

Olivier J. G., Schure K.M. and Peters J.A.H.W. 2017. Trends in Global CO_2 and Total Greenhouse Gas Emissions. 2017 Report. Netherlands Environmental Assessment Agency.

Owusu P.A. and Asumadu-Sarkodie S. 2016. A review of renewable energy sources, sustainability issues and climate change mitigation. Cogent Engineering, 3(1).

Öztürk Düs H., Pollet E., Phalip V., Guvenilir Y. and Averous L. et al. 2014. Lipase catalyzed synthesis of polycaprolactone and clay-based nanohybrids. Polymer,55(7): 1648–1655.

Padhiar J., Das A. and Bhattacharya S. 2011. Optimization of process parameters influencing the submerged fermentation of extracellular lipases from *Pseudomonas aeruginosa*, *Candida albicans* and *Aspergillus flavus*. Pakistan journal of biological sciences,14(22).

Palleroni N. 1992. Introduction to the *Pseudomonadaceae*. A Handbook on the Biology of Bacteria, Ecophysiology, Isolation, Identification and Applications. Vol. III, 2nd edn: 3071–3085.

Palmer T. and Bonner P.L. 2008. Enzymes: Biochemistry, Biotechnology and Clinical Chemistry. 2nd, revised edn. Elsevier, 2007.

Panesar P.S. 2010. Enzymes in Fat Oil Flavor and Fragrance Industries. Enzymes in Food Processing: Fundamentals and Potential Applications: 202–203.

Papaparaskevas D., Christakopoulos P., Kekos D. and Macris B.J. 1992. Optimizing production of extracellular lipase from *Rhodotorula glutinis*. Biotechnology letters,14(5): 397–402.

Park J.Y., Park M.S. and Lee Y.C. 2015. Advances in direct transesterification of algal oils from wet biomass. Bioresource Technology,184: 267–275.

Parwata I.P., Asyari M. and Hertadi R. 2014. Organic Solvent-Stable Lipase from Moderate Halophilic Bacteria *Pseudomonas stutzeri* Isolated from the Mud Crater of Bleduk Kuwu, Central Java, Indonesia. Journal of Pure and Applied Microbiology, 8: 1–10.

De Pascale D. et al. 2008. The cold-active Lip1 lipase from the Antarctic bacterium *Pseudoalteromonas haloplanktis* TAC125 is a member of a new bacterial lipolytic enzyme family. Extremophiles,12(3): 311–323.

Patel J. 2001. 16S rRNA gene sequencing for bacterial pathogen identification in the clinical laboratory. Molecular Diagnosis,6(4): 313–321.

Patel N.K. and Shah S.N. 2015. Biodiesel from Plant Oils. Food, Energy, and Water: 277–307.

Patel V., Gajera H., Gupta A., Manocha L. and Madamwar D. 2015. Synthesis of ethyl caprylate in organic media using *Candida rugosa* lipase immobilized on exfoliated graphene oxide: Process parameters and reusability studies. Biochemical Engineering Journal,95: 62–70.

Patel V., Nambiar S. and Madamwar D. 2014. An extracellular solvent stable alkaline lipase from *Pseudomonas* sp. DMVR46: Partial purification, characterization and application in non-aqueous environment. Process Biochemistry,49(10): 1673–1681.

Patil K.J., Chopda M.Z. and Mahajan R.T. 2011. Lipase biodiversity. Indian Journal of Science and Technology,4(8): 971–982.

Pedrotta V. and Witholt B. 1999. Isolation and characterization of the cis-trans-unsaturated fatty acid isomerase of *Pseudomonas oleovorans* gpo12. Journal of Bacteriology,181(10): 3256–3261.

Peled N. and Krenz M.C. 1981. A new assay of microbial lipases with emulsified trioleoyl glycerol. Analytical Biochemistry,112(2): 219–222.

Pereira M.G., Facchini F.D.A., Filo L.E.C., Polizeli A.M., Vici A.C., Jorge J.A., Lorente G.F., Pessela B.C., Guisan J.M., Polizeli de M.L.T. 2015. Immobilized lipase from *Hypocrea pseudokoningii* on hydrophobic and ionic supports: Determination of thermal and organic solvent stabilities for applications in the oleochemical industry. Process Biochemistry,50(4): 561–570.

Perez-Garcia O., Escalante F.M.E., Bashan Luz E.de. and Bashan Y. 2011. Heterotrophic cultures of microalgae: Metabolism and potential products. Water Research,45(1): 11–36.

Pham V., Rediers H., Ghequire M.G.K., Naguyen H.H., Mot R.D., Vanderleyden J. and Spaepen S. 2017. The plant growth-promoting effect of the nitrogen-fixing endophyte *Pseudomonas stutzeri* A15. Archives of microbiology,199(3): 513–517.

Pick U. and Rachutin-Zalogin T. 2012. Kinetic anomalies in the interactions of Nile red with microalgae. Journal of Microbiological Methods,88(2): 189–196.

Pilissao C., De P. and Da M. 2010. Potential application of native lipases in the resolution of (RS)-phenylethylamine. Journal of the Brazilian Chemical Society,21(6): 973–977.

Pinzi S., Garcia I.L., Gimenez F.J.L., Castro de M.D.L., Dorado G. and Dorado M.P. 2009. The Ideal Vegetable Oil-based Biodiesel Composition: A Review of Social, Economical and Technical Implications. Energy Fuels,23(5): 2325–2341.

Pinzi S., Rounce P., Herreros J.M., Tsolakis A. and Dorado M.P. 2013. The effect of biodiesel fatty acid composition on combustion and diesel engine exhaust emissions. Fuel,104: 170–182.

Pogorevc M., Stecher H. and Faber K. 2002. A caveat for the use of log P values for the assessment of the biocompatibility of organic solvents. Biotechnology Letters,24(11): 857–860.

Posner I. and Morales A. 1972. Mechanisms of enzyme and substrate activation by lipoprotein lipase cofactors. The Journal of Biological Chemistry,247(8): 2255–2265.

Prakash B.S., Sanodiya B.S, Thakur G.S., Baghel R.K. and Prasad G.B.K.S. 2010. Biodiesel production with special emphasis on lipase-catalyzed transesterification. Biotechnology Letters,32(8): 1019–1030.

Puchałka J., Oberhardt M.A., Godinho M., Bielecka A., Regenhardt D., Timmis K.N., Papin J.A. and Santos dos V.A.P. 2008. Genome-scale reconstruction and analysis of the *Pseudomonas putida* KT2440 metabolic network facilitates applications in biotechnology. PLoS Computational Biology, 4(10).

Qamsari E.M., Kasra K.R. and Nejad Z.M. 2011. Isolation and identification of a novel, lipase-producing bacterium, *Pseudomonas aeruginosa* KM110. Iranian Journal of Microbiology,3(2): 92–98.

Qayed W.S., Aboraia A.S., Abdel-Rahman H.M. and Youssef A.F. 2015.Lipases-catalyzed enantioselective kinetic resolution of alcohols. Journal of Chemical and Pharmaceutical Research,7(5): 311–322.

Qin H., Yan X., Yun T. and Dong W. 2008. Biodiesel Production Catalyzed by Whole-Cell Lipase from *Rhizopus chinensis*. Chinese Journal of Catalysis,29(1): 41–46.

Rabbani M., Bagherinejad M.R., Sadeghi H.M., Shariat Z.S., Etemadifar Z., Moazen F., Rahbari M., Mafakher L. and Zaghian S. 2013. Isolation and characterization of novel thermophilic lipase-secreting bacteria. Brazilian Journal of Microbiology,44(4): 1113–1119.

Radzun K.A., Wolf J., Jakob G., Zhang E., Stephens E., Ross I. and Hankamer B. 2015. Automated nutrient screening system enables high-throughput optimisation of microalgae production conditions. Biotechnology for biofuels, 8(65).

Rahman R.N.Z.R.A., Baharum S.N., Basri M. and Salleh A.B. 2005. High-yield purification of an organic solvent-tolerant lipase from *Pseudomonas* sp. strain S5. Analytical Biochemistry,341(2): 267–274.

Rahman R.N.Z.R.A., Kamarudin N.H.A., Yunus J., Salleh A.B. and Basri M. 2010. Expression of an Organic Solvent Stable Lipase from *Staphylococcus epidermidis* AT2. International Journal of Molecular Sciences,11(9): 3195–3208.

Rajendran A., Palanisamy A. and Thangavelu V. 2009. Lipase Catalyzed Ester Synthesis for Food Processing Industries. Brazilian Archives of Biology and Technology,52(1): 207–219.

Rajendran A. and Thangavelu V. 2009. Statistical experimental design for evaluation of medium components for lipase production by *Rhizopus arrhizus* MTCC 2233. Food Science and Technology,42(5): 985–992.

Rajeshkumar M.P., Mahendran V. and Balakrishnan V. 2015. Carbon and nitrogen sources enhance lipase production in the bacteria *Bacillus subtilis* kpl13 isolated from soil samples of kolli hills, South India. International Journal of Science and Nature,6(2): 183–187.

Ramani K., Kennedy L.J., Ramakrishnan M. and Sekaran G. 2010. Purification, characterization and application of acidic lipase from *Pseudomonas gessardii* using beef tallow as a substrate for fats and oil hydrolysis. Process Biochemistry,45(10): 1683–1691.

Ramos J.L. et al. 2015. Mechanisms of solvent resistance mediated by interplay of cellular factors in *Pseudomonas putida.* FEMS Microbiology Reviews,39(4): 555–566.

Rampelotto P. 2013. Extremophiles and Extreme Environments. Life,3(3): 482–485.

Randa A.A., Rahman R.N.Z.RA., Salleh A.B. and Basri M. 2009. Optimization of physical factors affecting the production of thermo-stable organic solvent-tolerant protease from a newly isolated halo tolerant *Bacillus subtilis* strain Rand. Microbial cell factories, 8(20).

Rathi P., Bradoo S., Saxena R.K. and Gupta R. 2000. A hyper-thermostable, alkaline lipase from *Pseudomonas* sp. with the property of thermal activation. Biotechnology Letters,22(6): 495–498.

Ratnapuram H.P., Vutukuru S.S. and Yadavalli R. 2018. Mixotrophic transition induced lipid productivity in *Chlorella pyrenoidosa* under stress conditions for biodiesel production. Heliyo,4(1).

Rawat I., Kumar R., Mutanda T. and Bux. F. 2013. Biodiesel from microalgae: A critical evaluation from laboratory to large scale production. Applied Energy,103: 444–467.

Reetz M.T., Carballeira J.D. and Vogel A. 2006. Iterative saturation mutagenesis on the basis of b factors as a strategy for increasing protein thermostability. Angewandte Chemie - International Edition, 45(46): 7745–7751.

Refaat A.A. 2009. Correlation between the chemical structure of biodiesel and its physical properties. International Journal of Environment Science and Technology,6(4): 677–694.

Reis P.M., Raab T.W., Chuat J.Y., Leser M.E., Miller R., Watzke H.J. and Holmberg K. 2008. Influence of surfactants on lipase fat digestion in a model gastro-intestinal system. Food Biophysics,3(4): 370–381.

Ribeiro B.D., Castro de A.M., Coelho M.A.Z. and Freire D.M.G. 2011. Production and use of lipases in bioenergy: A review from the feedstocks to biodiesel production. Enzyme Research, Article ID: 615803.

Richard G., Nott K., Nicks F., Paqout M., Blecker C. and Fauconnier M.L. 2013. Use of lipases for the kinetic resolution of lactic acid esters in heptane or in a solvent free system. Journal of Molecular Catalysis B: Enzymatic,97: 289–296.

Rodolfi L., Zittelli G.C., Bassi N., Padovani G., Biondi N., Bonini G. and Tredici M.R. 2009. Microalgae for oil: Strain selection, induction of lipid synthesis and outdoor mass cultivation in a low-cost photobioreactor. Biotechnology and Bioengineering,102(1): 100–112.

Romero C.M., Baigori M.D., Baron A.M., Krieger N. and Pera L.M. 2014. Activity and stability of lipase preparations from *Penicillium corylophilum*: Potential use in biocatalysis. Chemical Engineering and Technology,37(11): 1987–1992.

Romo A. De. 1989. Tallow and the time capsule: Claude Bernard's discovery of the pancreatic digestion of fat. History and Philosophy of life sciences,11(2): 253–274.

Ronald H., Micheal D.K. and Paul W.A. 2012. Extraction of oil from microalgae for biodiesel production: A review. Biotechnology Advances,30(3): 709–732.

Rukman H. and Henny W. 2015. Effect of Ca^{2+} Ion to the Activity and Stability of Lipase Isolated from *Chromohalobacter japonicus* BK-AB18. Procedia Chemistry,16: 306–313.

Rumin J., Bonnefond H., Jean-Saint B., Rouxel C., Sciandra A., Bernard O., Cadoret J.P. and Bougaran G. 2015. The use of fluorescent Nile red and BODIPY for lipid measurement in microalgae. Biotechnology for Biofuels,8(1): 1–16.

Rutherford B.J., Bahl R.H., Price R.E., Szmidt H.L., Benke P.I., Mukhopadhyay A. and Keasling J.D. 2010. Functional genomic study of exogenous n-butanol stress in *Escherichia coli*. Applied and Environmental Microbiology,76(6): 1935–1945.

Sachan S. and Singh A. 2017. Production of Lipase by *Pseudomonas aeruginosa* JCM5962 (T) Under Semi-Solid State Fermentation: Potential Use of *Azadirachta indica* (Neem) Oil Cake. Bioscience Biotechnology Research Asia, 14(2): 767–773.

Sackett D. and Wolff J. 1987. Nile red as a polarity-sensitive fluorescent probe of hydrophobic protein surfaces. Analytical Biochemistry,167(2): 228–234.

Saeed H.M., Zaghloul T.I., Khalil A.I. and Abdelbaeth M.T. 2005. Purification and characterisation of two extracellular lipases from *Pseudomonas aeruginosa* Ps-x. Polish journal of microbiology,54(3): 233–240.

Sahoo R.K., Subudhi E. and Kumar M. 2014. Quantitative approach to track lipase producing *Pseudomonas* sp. S1 in nonsterilized solid state fermentation. Letters in Applied Microbiology, 58(6): 610–616.

Salameh M.A. and Wiegel J. 2010. Effects of Detergents on Activity, Thermostability and Aggregation of Two Alkalithermophilic Lipases from *Thermosyntropha lipolytica.* Open Biochemistry Journal,4: 22–28.

Salameh M. and Juergen W. 2007. Lipases from Extremophiles and Potential for Industrial Applications. Advances in Applied Microbiology,61: 253–283.

Salihu A. and Alam M.Z. 2012. Production and applications of microbial lipases: A review. Scientific Research and Essays,7(30): 2667–2677.

Salihu A. and Alam M. Z. 2015. Solvent tolerant lipases: A review. Process Biochemistry,50(1): 86–96.

Salis A., Pinna M., Monduzzi M. and Solinas V. 2005. Biodiesel production from triolein and short chain alcohols through biocatalysis. Journal of Biotechnology,119(3): 291–299.

Samad M.Y.A., Razak C.N., Salleh A.B., Yunus Zin Wan W.M., Ampon K. and Basri M. 1989. A plate assay for primary screening of lipase activity. Journal of Microbiological Methods, 9(1): 51–56.

Sanchez F. and Vasudevan P.T. 2006. Enzyme catalyzed production of biodiesel from olive oil. Applied Biochemistry and Biotechnology,135(1): 1–14.

Sathish A., Smith B.R. and Sims R.C. 2013. Effect of moisture on *in situ* transesterification of microalgae for biodiesel production. Journal of Chemical Technology and Biotechnology,89(1): 137–142.

Satpati G.G. and Pal R. 2015. Rapid detection of neutral lipid in green microalgae by flow cytometry in combination with Nile red staining—an improved technique. Annals of Microbiology,65(2): 937–949.

Saxena R.K, Sheoran A., Giri B. and Davidson W.S. 2003. Purification strategies for microbial lipases. Journal of Microbiological Methods, 52(1): 1–18.

Scott S.A., Davey M.P., Dennis J.S., Horst I., Howe J.C., LeaSmith D.J. and Smith A.G. 2010. Biodiesel from algae: challenges and prospects. Current Opinion in Biotechnology,21(3): 277–286.

Segura A., Hurtado A., Rivera B. and Lazaroaie M.M. 2008. Isolation of new toluene-tolerant marine strains of bacteria and characterization of their solvent-tolerance properties. Journal of Applied Microbiology,104(5): 1408–1416.

Segura A., Molina L., Fillet S., Krell T., Bernal P., Rojas J.S. and Ramos J.L .2012. Solvent tolerance in Gram-negative bacteria. Current Opinion in Biotechnology,23(3): 415–421.

Semwal S., Arora K.A., Badoni R.P. and Tuli D.K. 2011. Biodiesel production using heterogeneous catalysts. Bioresource Technology,102(3): 2151–2161.

Shah S., Sharma S. and Gupta M.N. 2004. Biodiesel Preparation by Lipase-Catalyzed Transesterification of Jatropha Oil. Energy Fuels,18(1): 154–159.

Sharma A.K., Tiwari R.P. and Hoondal G.S. 2001. Properties of a thermostable and solvent stable extracellular lipase from a *Pseudomonas* sp. AG-8. Journal of Basic Microbiology,41(6): 363–366.

Sharma C., Sharma P. and Kanwar S. 2012. Optimization of production conditions of lipase from *B. licheniformis* MTCC-10498. Research Journal of Recent Sciences,1(4): 25–32.

Sharma M., Sharma V. and Majumdar D.K. 2014. Entrapment of α-Amylase in Agar Beads for Biocatalysis of Macromolecular Substrate. International Scholarly Research Notices, Article ID: 936129

Sharma R., Yusuf C. and Uttam Chand B. 2001. Production, Purification, Characterization, and Applications of Lipases. Biotechnology advances,19(8): 627–662.

Sharma S. and Kanwar S.S. 2014. Organic solvent tolerant lipases and applications. The Scientific World Journal, Article ID: 625258.

Sharma Y.C., Singh B. and Korstad J. 2011. Latest developments on application of heterogenous basic catalysts for an efficient and eco-friendly synthesis of biodiesel: A review. Fuel,90(4): 1309–1324.

Shen K., Sayeed S., Antalis P., Gladitz J., Ahmed A., Dice B., Janto B., Dopico R., Keefe R., Hayes J., Johnson S., Yu S., Ehrlich N., Jocz J., Kropp L., Wong R., Wadowsky R.M., Slifkin M., Perston R.A., Erdos G., Post C.J., Ehrlich G.D. and Hu F.Z. 2006. Extensive genomic plasticity in *Pseudomonas aeruginosa* revealed by identification and distribution studies of novel genes among clinical isolates. Infection and Immunity,74(9): 5272–5283.

Shen Y., Pei Z., Yuan W. and Mao E. 2009. Effect of nitrogen and extraction method on algae lipid yield. International Journal of Agricultural and Biological Engineering,2(1): 51-57.

Shikha S., Thakur K.G. and Bhattacharyya M.S. 2017. Facile fabrication of lipase to amine functionalized gold nanoparticles to enhance stability and activity. RSC Advances,7(68): 42845–42855.

Silby M.W., Winstanley C., Godfrey Scott A.C., Levy S.B. and Jackson R.W. 2011. *Pseudomonas* genomes: Diverse and adaptable. FEMS Microbiology Reviews,35(4): 652–680.

Sim S.L., He T., Tscheliessnig A., Mueller M., Tan R.B.H. and Jungbauer A. 2012. Protein precipitation by polyethylene glycol: A generalized model based on hydrodynamic radius. Journal of Biotechnology,157(2): 315–319.

Singh M. and Chand Banerjee U. 2007. Enantioselective transesterification of (RS)-1-chloro-3-(3,4-difluorophenoxy)-2-propanol using *Pseudomonas aeruginosa* lipases. Tetrahedron: Asymmetry. Pergamon, 18(17): 2079–2085.

Singh R., Kumar M., Mittal A. and Mehta P.K. 2016. Microbial enzymes: industrial progress in 21st century. 3 Biotech, 6(2): 1–15.

Sivaramakrishnan, R. and Incharoensakdi, A. 2016. Purification and characterization of solvent tolerant lipase from *Bacillus* sp. for methyl ester production from algal oil. Journal of Bioscience and Bioengineering,121(5): 517–522.

Soares C.M., Teixeira V.H. and Baptista A.M. 2003. Protein structure and dynamics in nonaqueous solvents: insights from molecular dynamics simulation studies. Biophysical journal,84(3): 1628–1641.

Walde P. and Luisi P.L. 1989. A Continuous Assay for Lipases in Reverse Micelles Based on Fourier Transform Infrared Spectroscopy. Biochemistry, 28(8): 3353–3360.

Song Y., Schowen R.L., Borchardt R.T. and Topp E.M. 2001. Effect of pH on the rate of asparagine deamidation in polymeric formulations: pH-rate profile. Journal of Pharmaceutical Sciences,90(2): 141–156.

De Souza T.C., Fonseca de. S.T., Costa da. J.A., Rocha M.V.P., Mattos de M.C., Lafuente F.R., Goncalves L.R.B. and Santos dos C.S.J. 2016. Cashew apple bagasse as a support for the immobilization of lipase B from *Candida antarctica*: Application to the chemoenzymatic production of (*R*)-Indanol. Journal of Molecular Catalysis B: Enzymatic,130: 58–69.

Spoehr H.A. and Milner H.W. 1949. The Chemical Composition of *Chlorella*; Effect of Environmental Conditions. Plant Physiology,24(1): 120–149.

Stancu M. M. 2015. Adaptation Mechanisms to Toxic Solvents in *Shewanella Putrefaciens*. Agriculture and Agricultural Science Procedia,6: 601–607.

Stelmaschuk S. and Tigerstrom R. 1988. The use of tween 20 in a sensitive turbidimetric assay of lipolytic enzymes. Canadian Journal of Microbiology,35(4): 511-514.

Stenesh J. 2013. Proteins. Biochemistry: 68–69.

Stoytcheva M., Montero G., Zlatev R., Leon J.A. and Gochev V. 2012. Analytical methods for lipases activity determination: A review. Current Analytical Chemistry,8: 400-407.

Stuart S.A., Davey M.P., Dennis J.S., Horst I., Howe J.C., LeaSmith D.J. and Smith A.G. 2010. Biodiesel from algae: challenges and prospects. Current Opinion in Biotechnology,21(3): 277–286.

Su C.H., Chien L.J., Gomes J., Lin Y.S., Yu Y.K., Liou J.S. and Syu R.J. 2011. Factors affecting lipid accumulation by *Nannochloropsis oculata* in a two-stage cultivation process. Journal of Applied Phycology,23(5): 903–908.

Su H., Mai Z. and Zhang S. 2016. Cloning, expression and characterization of a lipase gene from marine bacterium *Pseudoalteromonas lipolytica* SCSIO 04301. Journal of Ocean University of China,15(6): 1051–1058.

Sugihara A., Ueshima M., Shimada Y., Tsunasawa S. and Tominaga Y. 1992. Purification and characterisation of a novel thermostable lipase from *Pseudomonas cepacian*. Journal of Biochemistry,112(5): 598–603.

Swarnali P. 2015. Acid catalysed transesterification. Journal of Chemical and Pharmaceutical Research,7(3): 1780–1786.

Syed M.N., Iqbal S., Bano S., Khan A.B., Qader ul-Ali S. and Azhar A. 2010. Purification and characterization of 60 kd lipase linked with chaperonin from *Pseudomonas aeruginosa* BN-1. African Journal of Biotechnology,9(45): 7724–7732.

Taher H., Zuhair Al-S., Marzouqi Al- Ali H., Hail Y. and Farid M.M. 2011. A Review of Enzymatic Transesterification of Microalgal Oil-Based Biodiesel Using Supercritical Technology. Enzyme Research, Article ID: 468292

Talekar S. and Chavare S. 2012. Optimization of immobilization of α-amylase in alginate gel and its comparative biochemical studies with free α-amylase. Recent Research in Science and Technology,4(2): 1–5.

Talha N.S. and Sulaiman S. 2016. Overview of catalysts in biodiesel production. ARPN Journal of Engineering and Applied Sciences,11(1): 439–442.

Tamalampudi S., Talukder M.R., Hama S., Numata T., Kondo A. and Fukuda H. 2008. Enzymatic production of biodiesel from Jatropha oil: A comparative study of immobilized-whole cell and commercial lipases as a biocatalyst. Biochemical Engineering Journal,39(1): 185–189.

Tamilarasan K. and Kumar M.D. 2012. Biocatalysis and Agricultural Biotechnology Purification and characterization of solvent tolerant lipase from *Bacillus sphaericus* MTCC 7542. Biocatalysis and Agricultural Biotechnology,1(4): 309–313.

Tang H., Chen M, Garcia M.E.D., Abunasser N., Ng Simon K.Y. and Salley S.O. 2011. Culture of microalgae *Chlorella minutissima* for biodiesel feedstock production. Biotechnology and Bioengineering,108(10): 2280–2287.

Thakur V., Tewari R. and Sharma R. 2014. Evaluation of Production Parameters for Maximum Lipase Production by *P. stutzeri* MTCC 5618 and Scale-Up in Bioreactor. Chinese Journal of Biology, Article ID: 208462.

Thompson G.A. 1996. Lipids and membrane function in green algae. Biochimica et Biophysica Acta (BBA) - Lipids and Lipid Metabolism,1302(1): 17–45.

Tiwari P., Kumar R. and Garg S. 2006. Transesterification, Modeling and Simulation of Batch Kinetics of Non- Edible Vegetable Oils for Biodiesel Production. American Institute of Chemical Engineers.

Tran D.T., Yeh K.L., Chen C.L. and Chang J.S. 2012. Enzymatic transesterification of microalgal oil from *Chlorella vulgaris* ESP-31 for biodiesel synthesis using immobilized *Burkholderia* lipase', Bioresource Technology,108: 119–127.

Trbojevic I.J., Velickovic D., Dimitrijevic A., Bezbradica D., Dragacevic V., Jankulovic M.G. and Milosavic N. 2016. Design of biocompatible immobilized *Candida rugosa* lipase with potential application in food industry. Journal of the Science of Food and Agriculture, 96(12): 4281–4287.

Trivedi J., Aila M., Bangwal D.P., Kaul S. and Garg M.O. 2015. Algae based biorefinery—How to make sense? Renewable and Sustainable Energy Reviews,47: 295–307.

Uehara N. 2010. Polymer-functionalized gold nanoparticles as versatile sensing materials. Analytical sciences: the International Journal of Japan Society for Analytical Chemistry,26(12): 1219–1228.

Ugo A.K., Amara A.V., Kenechuwku U. and Igwe C.N. 2017. Microbial Lipases: A Prospect for Biotechnological Industrial Catalysis for Green Products: A Review. Fermentation Technology,6(2).

Ugur A., Sarac N., Boran R., Ayaz B., Ceylan O. and Okmen G. 2014. New Lipase for Biodiesel Production: Partial Purification and Characterization of LipSB 25-4. ISRN Biochemistry, PMID: 25937966.

Ugur Nigiz F. 2016. *Rhizomucor miehei* Lipase-Immobilized Sodium Alginate Membrane Preparation and Usage in a Pervaporation Biocatalytic Membrane Reactor. Chemical and Biochemical Engineering Quarterly Journal,30(3): 381–391.

Ullah K., Ahmad M., Sofia., Sharma V.K., Lu P., Harvey A., Zafar M. and Sultana S. 2015. Assessing the potential of algal biomass opportunities for bioenergy industry: A review. Fuel,143: 414–423.

Ved K. and Padam K. 2013. Study of Physical and Chemical Properties of Biodiesel from Sorghum Oil. Research Journal of Chemical Sciences,3(9): 64–68.

Veerapagu M., Narayanan S.A., Ponmurugan K. and Jeya K.R. 2013. Screening selection identification production and optimization of Bacterial Lipase from oil spilled soil. Asian Journal of Pharmaceutical and Clinical Research,6(SUPPL.3): 62–67.

Venditti I., Palocci C., Chronopoulou L., Fratoddi I., Fontana L., Diociaiuti M. and Russo M.V. 2015. *Candida rugosa* lipase immobilization on hydrophilic charged gold nanoparticles as promising biocatalysts: Activity and stability investigations. Colloids and Surfaces B: Biointerfaces,131: 93–101.

Verger R. and de Haas G.H. 1976. Interfacial enzyme kinetics of lipolysis. Annual review of Biophysics and Bioengineering,5: 77–117.

Verma M.L., Azmi W. and Kanwar S.S. 2011. Enzymatic Synthesis of Isopropyl Acetate by Immobilized *Bacillus cereus* Lipase in Organic Medium. Enzyme Research,2011(Scheme 1): 1–7.

Vescovi V., Giordano R.L.C., Mendes A.A. and Tardioli P.W. 2017. Immobilized Lipases on Functionalized Silica Particles as Potential Biocatalysts for the Synthesis of Fructose Oleate in an Organic Solvent/Water System. Molecules,22(2): 212.

Vieira F.C.S. and Nahas E. 2005. Comparison of microbial numbers in soils by using various culture media and temperatures. Microbiological Research,160(2): 197–202.

Villeneuve P., Muderhwa J.M., Graille J. and Haas J.M. 2000. Customizing lipases for biocatalysis: a survey of chemical, physical and molecular biological approaches. Journal of Molecular Catalysis B: Enzymatic,9(4): 113–148.

Vrutika P. and Datta M. 2015. Lipase from Solvent-Tolerant *Pseudomonas* sp. DMVR46 Strain Adsorb on Multiwalled Carbon Nanotubes: Application for Enzymatic Biotransformation in Organic Solvents. Applied Biochemistry and Biotechnology,177(6): 1313–1326.

Vrutika P., Shruti N. and Datta M. 2014. An extracellular solvent stable alkaline lipase from *Pseudomonas* sp. DMVR46: Partial purification, characterization and application in non-aqueous environment. Process Biochemistry,49(10): 1673–1681.

Wada H. and Murata N. 1998. Membrane Lipids in Cyanobacteria. Lipids in Photosynthesis: Structure, Function and Genetics. 6th edn. Springer: 65–81.

Walls D. and Loughran S. 2017. Protein Chromatography: Methods and Protocols. Humana Press.

Wang M., Nie K., Yun F., Cao H., Deng Li., Wang F. and Tan T. 2015. Biodiesel with low temperature properties: Enzymatic synthesis of fusel alcohol fatty acid ester in a solvent free system. Renewable Energy, 83: 1020–1025.

Wang R., Hou M., Ge J. and Liu Z. 2015. Enzymatic Synthesis of Lutein Dipalmitate in Organic Solvents. Catalysis Letters, 145(4): 995–999.

Wang S., Meng X., Zhou H., Liu Y., Secundo F. and Liu Y. 2016. Enzyme Stability and Activity in Non-Aqueous Reaction Systems: A Mini Review. Catalysts,6(2): 32.

Wang X., Liu X., Yan X., Zhao P., Ding Y and Xu P. 2011. Enzyme-nanoporous gold biocomposite: Excellent biocatalyst with improved biocatalytic performance and stability. Plos One,6(9): 1–7.

Wang Y., Chen T. and Qin S. 2012. Heterotrophic cultivation of *Chlorella kessleri* for fatty acids production by carbon and nitrogen supplements. Biomass and Bioenergy,47: 402–409.

Wehtje E. and Adlercreutz P. 1997. Lipases have similar water activity profiles in different reactions. Biotechnology Letters,11(6): 537–540.

Wi A.R., Jeon S.J., Kim S., Park H.J., Kim D., Han S.J., Yim J.H. and Kim H.W. 2014. Characterization and a point mutational approach of a psychrophilic lipase from an arctic bacterium, *Bacillus pumilus*. Biotechnology Letters,36(6): 1295–1302.

Wingfield P.T. 2001. Protein Precipitation Using Ammonium Sulfate. Current Protocol on Protein Science. PMID: 18429073.

Won K., Kim S., Kim K.J., Park H.W. and Moon S.J. 2005. Optimization of lipase entrapment in Ca-alginate gel beads. Process Biochemistry,40: 2149–2154.

Wong C.H. and Whitesides G.M. 2013. Enzymes in Synthetic Organic Chemistry, Volume 12.

Wongwatanapaiboon J., Klinbunga S., Ruangchainikom C., Thummadetsak G., Chulalaksananukul S., Marty A. and Chulalaksananukul W. 2016. Cloning, expression, and characterization of *Aureobasidium melanogenum* lipase in *Pichia pastoris*. Bioscience, Biotechnology, and Biochemistry,80(11): 2231–2240.

Wu Y., Wang Y., Luo G. and Dai Y. 2009. In situ preparation of magnetic Fe_3O_4-chitosan nanoparticles for lipase immobilization by cross-linking and oxidation in aqueous solution. Bioresource Technology,100(14): 3459–3464.

Xie C., Wu B., Qin S. and He B. 2016. A lipase with broad solvent stability from *Burkholderia cepacia* RQ3: Isolation, characteristics and application for chiral resolution of 1-phenylethanol. Bioprocess and Biosystems Engineering,39(1): 59–66.

Xiuling J., Li S., Lin L., Zhang Q. and Wei Y. 2015. Gene cloning, sequence analysis and heterologous expression of a novel cold-active lipase from *Pseudomonas* sp. PF16. Technology and health care, 23(Suppl. 1): S109–S117.

Xun E., Wang J., Zhang H., Chen G, Yue H., Zhao J., Wang L. and Wang Z. 2013. Resolution of N-hydroxymethyl vince lactam catalyzed by lipase in organic solvent. Journal of Chemical Technology and Biotechnology,88(5): 904–909.

Yadav G.D. and Jadhav S.R. 2005. Synthesis of reusable lipases by immobilization on hexagonal mesoporous silica and encapsulation in calcium alginate: Transesterification in non-aqueous medium. Microporous and Mesoporous materials,86(1-3): 215–222.

Yamane Y., Utsunomiya T., Watanabe M. and Sasaki K. 2001. Biomass production in mixotrophic culture of *Euglena gracilis* under acidic condition and its growth energetics. Biotechnology Letters,23: 1223–1228.

Yang C., Wang F., Lan D., Whiteley C., Yang B. and Wang Y. 2012. Effects of organic solvents on activity and conformation of recombinant Candida antarctica lipase A produced by *Pichia pastoris.* Process Biochemistry,47(3): 533-537.

Yang C., Hua Q. and Shimizu K. 2000. Energetics and carbon metabolism during growth of microalgal cells under photoautotrophic, mixotrophic and cyclic light-autotrophic/dark-heterotrophic conditions. Biochemical Engineering Journal,6(2): 87–102.

Yang L., Chen J., Qin S., Zeng M., Jiang Y., Hu L., Xiao P., hao W., Hu Z., Lei A. and Wang J. 2018. Growth and lipid accumulation by different nutrients in the microalga *Chlamydomonas reinhardtii*. Biotechnology for Biofuels,11(1): 1–12.

Yang W., He Y., Xu L., Zhang H. and Yan Y. 2016. A new extracellular thermo-solvent-stable lipase from *Burkholderia ubonensis* SL-4: Identification, characterization and application for biodiesel production. Journal of Molecular Catalysis B: Enzymatic,126: 76–89.

Yang X.N., Huang X.B., Hang R.Q., Zhang X.Y., Qin L. and Tang B. 2016. Improved catalytic performance of porcine pancreas lipase immobilized onto nanoporous gold via covalent coupling. Journal of Materials Science,51(13): 6428–6435.

Yang X. and Zhang Y. 2013. Effect of temperature and sorbitol in improving the solubility of Carboxylesterases protein CpCE-1 from *Cydia pomonella* and biochemical characterization. Applied Microbiology and Biotechnology,97(24): 10423–10433.

Yao C., Cao Y., Wu S., Li S. and He B. 2013. An organic solvent and thermally stable lipase from *Burkholderia ambifaria* YCJ01: Purification, characteristics and application for chiral resolution of mandelic acid. Journal of Molecular Catalysis B: Enzymatic,85: 105–110.

Yeesang C. and Cheirsilp B. 2014. Low-Cost Production of Green Microalga *Botryococcus braunii* Biomass with High Lipid Content Through Mixotrophic and Photoautotrophic Cultivation. Applied Biochemistry and Biotechnology,174(1): 116–129.

Yeh H.J. and Chen C.Y. 2006. Toxicity assessment of pesticides to *Pseudokirchneriella subcapitata* under air-tight test environment. Journal of Hazardous Materials,131(1–3): 6–12.

Yi-Cheun Y., Brian C. and Vincet R.M. 2012. Gold Nanoparticles: Preparation, Properties, and Applications in Bionanotechnology. Nanoscale,4(6): 1871–1880.

Zaks A. 1996. New enzymatic propertied in organic media. Enzymatic Reactions in Organic Media: 70–93.

Zarevúcka M. 2012. Olive Oil as Inductor of Microbial Lipase. Olive Oil - Constituents, Quality, Health Properties and Bioconversions: 457–470.

Zarinviarsagh M., Ebrahimipour G. and Sadeghi H. 2017. Lipase and biosurfactant from *Ochrobactrum intermedium* strain MZV101 isolated by washing powder for detergent application. Lipids in Health and Science, 16(177).

Zhang S., Shang W., Yang X., Zhang S., Zhang X. and Chen J. 2013. Immobilization of lipase using alginate hydrogel beads and enzymatic evaluation in hydrolysis of p-nitrophenol butyrate. Bulletin of the Korean Chemical Society,34(9): 2741–2746.

Zhang W. 2014. Nanoparticle aggregation: Principles and Modeling. Nanomaterial. Advances in Experimental Medicine and Biology: 19–43.

Zhu L., Dong H., Zhang Y. and Li Y. 2011. Engineering the robustness of *Clostridium acetobutylicum* by introducing glutathione biosynthetic capability. Metabolic Engineering,13(4): 426–434.

Appendices

APPENDIX A

16S rRNA sequences obtained from Eurofins (Germany): 27F (forward primer)

>Culture_A3_27F.ab1

GGTGGCGGCAGCTACACATGCAGTCGAGCGGATGAGAGGAGCTTGCTCCTGGATTCAGCGGCGGACGGG
TGAGTAATGCCTAGGAATCTGCCTGGTAGTGGGGGACAACGTTTCGAAAGGAACGCTAATACCGCATAC
GTCCTACGGGAGAAAGCAGGGGACCTTCGGGCCTTGCGCTATCAGATGAGCCTAGGTCGGATTAGCTAG
TTGGTGAGGTAATGGCTCACCAAGGCGACGATCCGTAACTGGTCTGAGAGGATGATCAGTCACACTGGA
ACTGAGACACGGTCCAGACTCCTACGGGAGGCAGCAGTGGGGAATATTGGACAATGGGCGAAAGCCTGA
TCCAGCCATGCCGCGTGTGTGAAGAAGGTCTTCGGATTGTAAAGCACTTTAAGTTGGGAGGAAGGGCAG
TAACTTAATACGTTGCTGTTTTGACGTTACCGACAGAATAAGCACCGGCTAACTCTGTGCCAGCAGCCG
CGGTAATACAGAGGGTGCAAGCGTTAATCGGAATTACTGGGCGTAAAGCGCGCGTAGGTGGTTCGTTAA
GTTGGATG
TGAAATCCCCGGGCTCAACCTGGGAACTGCATTCAAAACTGTCGAGCTAGAGTATGGTAGAGGGTGGTG
GAATTTCCTGTGTAGCGGTGAAATGCGTAGATATAGGAAGGAACACCAGTGGCGAAGGCGACCACCTGG
ACTGATACTGACACTGAGGTGCGAAAGCGTGGGGAGCAAACAGGATTAGATACCCTGGTAGTCCACGCC
GTAAACGATGTCAACTAGCCGTTGGGAGCCTTGAGCTCTTAGTGGCGCAGCTAACGCATTAAGTTGACC
GCCTGGGGAGTACGGCCGCAAGGTTAAAACTCAAATGAATTGACGGGGGCCCGCACAAGCGGTGGAGCA
TGTGGTTTATTCGAGCAACGCGAGAACCTTACCAGGCCTTGACATCCAATGACTTTCAGAGATGATGTG
CCTCGGGAACATTGAGACAGTGCTGCATGGCTGTCGTCAGCTCGGTGTCGTGAGATG

>Culture_D1_27F.ab1

CTGCGCTGCTACCATGCAGTCGAGCGGCAGCATCGGCCTTTGTGCCGCATGGTGCGTACGCATGTGAAA
CTGCCCTCATGTTTCCAACTCACCGAGGGATTGCTGCTCGACAGGATGATATCCCCAAATCACATTTTA
TCGCATGAAGATAAGCATCTTCAGACCTCACTCTCATAGTGTGATCTAGCCGCTTTTAGCGACAATCCT
TAGCTGGTCTGACAGGAGAAGCTCCCCACTGGGACTGAGACGGAAGCCCCACTCCTCTGGGAGGGACCC
ATGGGGAATATTGAACAATGGGCGAACACCTGATCCTATTGGCGGCGTGAGTGTTAAAAGCCTTAGGGT
TGTAAAGCTCTTTTACCCGGGATGATAATGACAATACCGGGATAAAAAACTCCGGCTATCTCCTTGCCC
CCACCCCCGGTAATACTGAAGGAGCTATCGTTATTCGCAATTACTGTGCGCAAAGCGCACGTAGGCGGC
TTTGTGTGTTAGAGGTGAAAACTCGGAGCTCACCTCCCCAAATGCCTTTATGACTGCATCTCTTGAATC
CTGGAGAG
GTGAGTGGAATTCCGAGTGTATAGGTGAAATTCGTAGATATTCTGAAGAACACCAGTGGCGAAAGCGGC
TCACTGGACTGCTATTGACACTGAGGTGCGAAAACGTGTGGAGCAAACACGATTATATACCCTGATAGT
CCCCGCCGCATACGATGATAACGAGCTGTCGGGGCTCTTATAGCTTCTGGTGGCGCACCTCACGCATTA
ATGTTATCCACCTGGGGAGTACGGCCGCCAGATTAAACTCAAATGAATTGACGGGGGCCTGCACAAGCG
GTGGAGCATGTGGTTTAATTCCAACCAACGCGCAGAACTTACCAGCGTTTGACATGTCCGGTACGATTA
TCTGGAGACGATCTCTTTCCATCTGGGCACTGACACACAGTGCTGCATGTCTGTCGTCAACTCGTGTCG
TGAGATGATGGGTTAGACCGCGACGACAGCACCCTCCTCCTTAAGTTGTCGTCAAT

>Culture_D5_27F.ab1

GCATGCAGCGAGCTATACATGCAAGTCGAACGAACGGAGGAAGAGCTTGCTCTTCCAAAGTTAGTGGCG
GACGGGTGAGTAACACGTGGGCAACCTGCCTGTAAGTTGGGGATAACTCCGGGAAACCGGGGCTAATAC
CGAATGATAAAGTGTGGCGCATGCCACGCTTTTGAAAGATGGTTTCGGCTATCGCTTACAGATGGGCCC
GCGGTGCATTAGCTAGTTGGTAGGGTAATGGCCTACCAAGGCAACGATGCATAGCCGACCTGAGAGGGT
GATCGGCCACACTGGGACTGAGACACGGCCCAGACTCCTACGGGAGGCAGCAGTAGGGAATCTTCCGCA
ATGGACGAAAGTCTGACGGAGCAACGCCGCGTGTATGAAGAAGGTTTTCGGATCGTAAAGTACTGTTGT
TAGAGAAGAACAAGGATAAGAGTAACTGCTTGTCCCTTGACGGTATCTAACCAGAAAGCCACGGCTAAC

TACGTGCCAGCAGCCGCGGTAATACGTAGGTGGCAAGCGTTGTCCGGATTTATTGGGCGTAAAGCGCGC
GCAGGCGG
TCTTTTAAGTCTGATGTGAAAGCCCCCGGCTTAACCGGGGAGGGTCATTGGAAACTGGAAGACTGGAGT
GCAGAAGAGGAGAGTGGAATTCCACGTGTAGCGGTGAAATGCGTAGATATGTGGAGGAACACCAGTGGC
GAAGGCGACTCTCTGGTCTGTAACTGACGCTGAGGCGCGAAAGCGTGGGGAGCAAACAGGATTAGATAC
CCTGGTAGTCCACGCCGTAAACGATGAGTGCTAAGTGTTAGGGGTTTCCGCCCCTTAGTGCTGCAGCTA
ACGCATTAAGCACTCCGCCTGGGGAGTACGACCGCAAGGTTGAAACTCAAAGGAATTGACGGGGGCCCG
CACAAGCGGTGGAGCATGTGGTTTAATTCGAAGCAACGCGAAGAACCTTACCAGGTCTTGACATCCTTT
GACCACTCTGGAGACGGAGCTTCCCTTTCGGGGACAAGGTGACAGGTGGTGCATGGTTGTCGTCAG
CTCGTGTCGAT

>Culture_H1_27F.ab1
TGGATGGCGGCAGCTACACATGCAGTCGAGCGGATGAGAGGAGCTTGCTCCTGGATTCAGCGGCGGACG
GGTGAGTAATGCCTAGGAATCTGCCTGGTAGTGGGGGACAACGTTTCGAAAGGAACGCTAATACCGCAT
ACGTCCTACGGGAGAAAGCAGGGGACCTTCGGGCCTTGCGCTATCAGATGAGCCTAGGTCGGATTAGCT
AGTTGGTGAGGTAATGGCTCACCAAGGCGACGATCCGTAACTGGTCTGAGAGGATGATCAGTCACACTG
GAACTGAGACACGGTCCAGACTCCTACGGGAGGCAGCAGTGGGGAATATTGGACAATGGGCGAAAGCCT
GATCCAGCCATGCCGCGTGTGTGAAGAAGGTCTTCGGATTGTAAAGCACTTTAAGTTGGGAGGAAGGGT
TGTAGATTAATACTCTGCAATTTTGACGTTACCGACAGAATAAGCACCGGCTAACTCTGTGCCAGCAGC
CGCGGTAATACAGAGGGTGCAAGCGTTAATCGGAATTACTGGGCGTAAAGCGCGCGTAGGTGGTTCGTT
AAGTTGGA
TGTGAAATCCCCGGGCTCAACCTGGGAACTGCATTCAAAACTGTCGAGCTAGAGTATGGTAGAGGGTGG
TGGAATTTCCTGTGTAGCGGTGAAATGCGTAGATATAGGAAGGAACACCAGTGGCGAAGGCGACCACCT
GGACTGATACTGACACTGAGGTGCGAAAGCGTGTGGAGCAAACAGGATTAGATACCCTGGTAGTCCACG
CCGTAAACGATGTCAACTAGCCGTTGGGAGCCTTGAGCTCTTAGTGGCGCAGCTAACGCATTAAGTTGA
CCGCCTGGGGAGTACGGCCGCAAGGTTAAAACTCAAATGAATTGACGGGGGCCCGCACAAGCGGTGGAG
CATGTGGTTTATTTCGAAGCAACGCGAGAACTTACCAGGCCTTGACATCCAATGACTTTCAGAGATGGA
TTGTGCCTTCGGACATTGAGACAGGTGCTGCATGGCTGTCGTCAGCTCGTGTCGTGAGATGTTGGGTTA
AGTCCCGTA

>Culture_H3_27F.ab1
GGTGCGGCAGCTACACATGCAGTCGAGCGGTAGAGAGAAGCTTGCTTCTCTTGAGAGCGGCGGACGGGT
GAGTAATGCCTAGGAATCTGCCTGGTAGTGGGGGATAACGTTCGGAAACGGACGCTAATACCGCATACG
TCCTACGGGAGAAAGCAGGGGACCTTCGGGCCTTGCGCTATCAGATGAGCCTAGGTCGGATTAGCTAGT
TGGTGGGGTAATGGCTCACCAAGGCGACGATCCGTAACTGGTCTGAGAGGATGATCAGTCACACTGGAA
CTGAGACACGGTCCAGACTCCTACGGGAGGCAGCAGTGGGGAATATTGGACAATGGGCGAAAGCCTGAT
CCAGCCATGCCGCGTGTGTGAAGAAGGTCTTCGGATTGTAAAGCACTTTAAGTTGGGAGGAAGGGCAGT
AAATTAATACTTTGCTGTTTTGACGTTACCGACAGAATAAGCACCGGCTAACTCTGTGCCAGCAGCCGC
GGTAATACAGAGGGTGCAAGCGTTAATCGGAATTACTGGGCGTAAAGCGCGCGTAGGTGGTTCGTTAAG
TTGGATGT
GAAATCCCCGGGCTCAACCTGGGAACTGCATTCAAAACTGACGAGCTAGAGTATGGTAGAGGGTGGTGG
AATTTCCTGTGTAGCGGTGAAATGCGTAGATATAGGAAGGAACACCAGTGGCGAAGGCGACCACCTGGA
CTGATACTGACACTGAGGTGCGAAAGCGTGGGGAGCAAACAGGATTAGATACCCTGGTAGTCCACGCCG
TAAACGATGTCAACTAGCCGTTGGGAGCCTTGAGCTCTTAGTGGCGCAGCTAACGCATTAAGTTGACCG
CCTGGGAGTACGGCCGCAACGCTAAAACTCAAATGAATTGACGGGGGCCGCACAAGCGGTGGAGCATGT
GTTTAATTCGAAGCAACGCGAAAACCTTACCAGGCCTTGACATCAATGAACTTTCTAGAGATAGATTGT
GCCTTCGGTACATTGAGACAGGTGCTGCATGGCTGTCGTCAGCTCGTGTCGTGAGATGCTCGGTTAAGT
TCCGTACGAACGCCAA

16S rRNA sequences obtained from Eurofins (Germany): 1492R (Reverse primer)

>Culture_A3_1492R.ab1

CAAGTCTGATCAACCGTGGTACCGTCCTCCCGAAGGTTAGACTAGCTACTTCTGGTGCAACCCACTCCC
ATGGTGTGACGGGCGGTGTGTACAAGGCCCGGGAACGTATTCACCGTGACATTCTGATTCACGATTACT
AGCGATTCCGACTTCACGCAGTCGAGTTGCAGACTGCGATCCGGACTACGATCGGTTTTATGGGATTAG
CTCCACCTCGCGGCTTGGCAACCCTTTGTACCGACCATTGTAGCACGTGTGTAGCCCAGGCCGTAAGGG
CCATGATGACTTGACGTCATCCCCACCTTCCTCCGGTTTGTCACCGGCAGTCTCCTTAGAGTGCCCACC
ATAACGTGCTGGTAACTAAGGACAAGGGTTGCGCTCGTTACGGGACTTAACCCAACATCTCACGACACG
AGCTGACGACAGCCATGCAGCACCTGTCTCAATGTTCCCGAAGGCACCAATCCATCTCTGGAAAGTTCA
TTGGATGTCAAGGCCTGGTAAGGTTCTTCGCGTTGCTTCGAATTAAACCACATGCTCCACCGCTTGTGC
GGGCCCCC
GTCAATTCATTTGAGTTTTAACCTTGCGGCCGTACTCCCCAGGCGGTCAACTTAATGCGTTAGCTGCGC
CACTAAGAGCTCAAGGCTCCCAACGGCTAGTTGACATCGTTTACGGCGTGGACTACCAGGGTATCTAAT
CCTGTTTGCTCCCCACGCTTTCGCACCTCAGTGTCAGTATCAGTCCAGGTGGTCGCCTTCGCCACTGGT
GTTCCTTCCTATATCTACGCATTTCACCGCTACACAGGAAATTCCACCACCCTCTACCATACTCTAGCT
CGACAGTTTTGAATGCAGTTCCCAGTTGAGCCCGGGGATTTCACATCCAACTTAACGAACCACCTACGC
GCGCTTTACGCCCAGTAATTCCGATTACGCTTGCACCCCTCTGTATTACCGCGGCTGCTGGCACAGAGT
TAGCCGGTGCTTATTTCTGTCGGTAACGTCCA

>Culture_D1_1492R.ab1
ATAAGATCGGTATACTATCGTGGTAAGCGTGCCTCCTTAACGTGTTAGACTGACACTTGACCTTCGGTT
GCAACCCAACTCCCATGGTGTGACGGGCGGTGTGTACAAGGCCCGGGAACGTATTCACCGCGACTTGCT
GATCGGATTACTAGCGATTCCACTTCATGATCTCAGTTGCAGACTGCAATCCGAACTGAGACCGCTTTT
ATGGAATTACCTCCCCCTCCCGGATTGCCGCCCCTTGGCACCGCCCTTTGAACCAGGGGGGAACCCCAC
GCCTAAAGGGCCAGGAGAACTTGACTCCTCCCCCCCCTTCCCCCGGTTTGTCACCGGCAGTCTCCTTAA
AGTGCCCACCATAAGGTGCTGGTAACTGAGGAGGAGGGTTGCCCTCGTTGGAGTACTTACCCCAACATC
TCACAACACCAGCTGACAACCGCGATGCACCAGCTGTCTCATCGTTCCCGAAAGCACAACTCTCTCTCT
AGAAAGTTCGGTGGAGGTCAAGGCTGGGAAAGGTTCTTCCCGTTGCTTCAAATTAAACCCCAGGCCCCC
CCCCTGGT
GCGGCCCCCCGCCAATTCTTTTGAGTTTTAACCTTGCGGCCGTATTCCCCAGGCGATCAACTTATGGCG
TTACCTGCGCAACTAAGATCTCAAAGCCCCCAAAGGTAAGTTGACATCTTTTACGGGTGGAACTACCAG
GGAATCTAATCCGGTTGCTCTCCCCACGCTTTCACACCTCACGGTCATTATCAGTCCAGGAGCCCGCCT
CTCGCACACGGTGTGTTCCTTCAATATCTCTACACATTTCACTCGCTACTCGGAAATTCACACCACCTC
TCTACGGTACTCAACGATGCCATCTTTAGAATGAAGTTTCCAGGTTAGACTCCGGGGGTTTTCCCTCTT
AACTTTAAAAAAACCCCCTACATGCGCCCTTTAGCCCGTAATTTTCAAATAAACGTATCTCCCCCTCGT
GATATACCCCCGGCTGTCTGGCCAGAGAAGTATATCGGAGGCTTAATCCTCGGCGGGAAAGGTCATTAT
CATTCCCCGTA

>Culture_D5_1492R.ab1
CCGTAGCTGTCTACCATTCGGCGGCTGGCTCCATAAAGGTTACCCTACCGACTTCGGGTGTTACAAACT
CTCGTGGTGTGACGGGCGGTGTGTACAAGGCCCGGGAACGTATTCACCGTGGCATGCTGATCCACGATT
ACTAGCGATTCCGGCTTCATGTAGGCGAGTTGCAGCCTACAATCCGAACTGAGAATAGTTTTATGGGAT
TAGCTCCACCTCGCGGCTTCGCGACCCTTTGTACTATCCATTGTAGCACGTGTGTAGCCCAGGTCATAA
GGGGCATGATGATTTGACGTCATCCCCACCTTCCTCCGGCTTGCACCGGCAGTCACTTTAGAGTGCCCA
ACTAAATGCTGGCAACTAAAATCAAGGGTTGCGCTCGTTGCGGGACTTAACCCAACATCTCACGACACG
AGCTGACGACAACCATGCACCACCTGTCACTTTGTCCCCGAAGGGAAAGCTCTGTCTCCAGAGTGGTCA
AAGGATGTCAAGACCTGGTAAGGTTCTTCGCGTTGCTTCGAATTAAACCACATGCTCCACCGCTTGTGC
GGGCCCCC
GTCAATTCCTTTGAGTTTCAACCTTGCGGTCGTACTCCCCAGGCGGAGTGCTTAATGCGTTAGCTGCAG
CACTAAGGGGCGGAAACCCCCTAACACTTAGCACTCATCGTTTACGGCGTGGACTACCAGGGTATCTAA
TCCTGTTTGCTCCCCACGCTTTCGCGCCTCAGCGTCAGTTACAGACCAGAGAGTCGCCTTCGCCACTGG
TGTTCCTCCACATATCTACGCATTTCACCGCTACACGTGGAATTCCACTCTCCTCTTCTGCACTCCAGT
CTTCCAGTTTCCAATGACCCTCCCCGGTTAAGCCGGGGGCTTTCACATCAGACTTAAAAGACCGCCTGC

GCGCGCTTTACGCCCAATAATCCGGACAACGCTTGCCACCTACGTATTACCGCGGCTGCTGGCACGTAG
TTAGCCGTGGCTTTCTGGTTAGATACCGTCAGGGAACAAGCAGTTACCTCTAAT

>Culture_H1_1492R.ab1
CAGAAGATAACCGTGGTACCGTCCTCCCGAAGGTTAGACTAGCTACTTCTGGTGCAACCCACTCCCATG
GTGTGACGGGCGGTGTGTACAAGGCCCGGGAACGTATTCACCGTGACATTCTGATTCACGATTACTAGC
GATTCCGACTTCACGCAGTCGAGTTGCAGACTGCGATCCGGACTACGATCGGTTTTATGGGATTAGCTC
CACCTCGCGGCTTGGCAACCCTTTGTACCGACCATTGTAGCACGTGTGTAGCCCAGGCCGTAAGGGCCA
TGATGACTTGACGTCATCCCCACCTTCCTCCGGTTTGTCACCGGCAGTCTCCTTAGAGTGCCCACCATT
ACGTGCTGGTAACTAAGGACAAGGGTTGCGCTCGTTACGGGACTTAACCCAACATCTCACGACACGAGC
TGACGACAGCCATGCAGCACCTGTCTCAATGTTCCCGAAGGCACCAATCCATCTCTGGAAAGTTCATTG
GATGTCAAGGCCTGGTAAGGTTCTTCGCGTTGCTTCGAATTAAACCACATGCTCCACCGCTTGTGCGGG
CCCCCGTC
AATTCATTTGAGTTTTAACCTTGCGGCCGTACTCCCCAGGCGGTCAACTTAATGCGTTAGCTGCGCCAC
TAAGAGCTCAAGGCTCCCAACGGCTAGTTGACATCGTTTACGGCGTGGACTACCAGGGTATCTAATCCT
GTTTGCTCCCCACGCTTTCGCACCTCAGTGTCAGTATCAGTCCAGGTGGTCGCCTTCGCCACTGGTGTT
CCTTCCTATATCTACGCATTTCACCGCTACACAGGAAATTCCACCACCCTCTACCATACTCTAGCTCGA
CAGTTTTGAATGCAGTTCCCAGTTGAGCCCGGGGATTTCACATCCAACTTAACGAACCACCTACGCGCG
CTTTACGCCCAGTAATTCCGATTAACGCTTGCACCCTCTGTATTACCGCGGCTGCTGGCACAGAAGTTA
GCCGGTGCTTATTCCTGTCGGTAACGTCAAAATTTGCAGAAGTTATTAATCTA

>Culture_H3_1492R.ab1
CAGTGATCAACCGTGGTACCGTCCTCCGAAGGTTAGACTAGCTACTTCTGTGTGCAACCCACTCCCATG
GTGTGACGGGCGGTGTGTACAAGGCCCGGGAACGTATTCACCGCGACATTCTGATTCGCGATTACTAGC
GATTCCGACTTCACGCAGTCGAGTTGCAGACTGCGATCCGGACTACGATCGGTTTTCTGGGATTAGCTC
CACCTCGCGGCTTGGCAACCCTCTGTACCGACCATTGTAGCACGTGTGTAGCCCAGGCCGTAAGGGCCA
TGATGACTTGACGTCATCCCCACCTTCCTCCGGTTTGTCACCGGCAGTCTCCTTAGAGTGCCCACCATT
ACGTGCTGGTAACTAAGGACAAGGGTTGCGCTCGTTACGGGACTTAACCCAACATCTCACGACACGAGC
TGACGACAGCCATGCAGCACCTGTCTCAATGTTCCCGAAGGCACCAATCTATCTCTAGAAAGTTCATTG
GATGTCAAGGCCTGGTAAGGTTCTTCGCGTTGCTTCGAATTAAACCACATGCTCCACCGCTTGTGCGGG
CCCCCGTC
AATTCATTTGAGTTTTAACCTTGCGGCCGTACTCCCCAGGCGGTCAACTTAATGCGTTAGCTGCGCCAC
TAAGAGCTCAAGGCTCCCAACGGCTAGTTGACATCGTTTACGGCGTGGACTACCAGGGTATCTAATCCT
GTTTGCTCCCCACGCTTTCGCACCTCAGTGTCAGTATCAGTCCAGGTGGTCGCCTTCGCCACTGGTGTT
CCTTCCTATATCTACGCATTTCACCGCTACACAGGAAATTCCACCACCCTCTACCATACTCTAGCTCGT
CAGTTTTGAATGCAGTTCCCAGTTGAGCCCGGGGATTTCACATCCAACTTAACGAACCACCTACGCGCG
CTTTACGCCCAGTAATTCCGATTAACGCTTGCACCCCTCTGTATTACCGCGGCTGCTGGCACAGAGTTA
GCCGGTGCTTATTCTTGTCGGTAACGTCAAACAGCAAAGTATTAATTTACTGCCC

APPENDIX B

Measurement of total protein concentration by Bradford assay

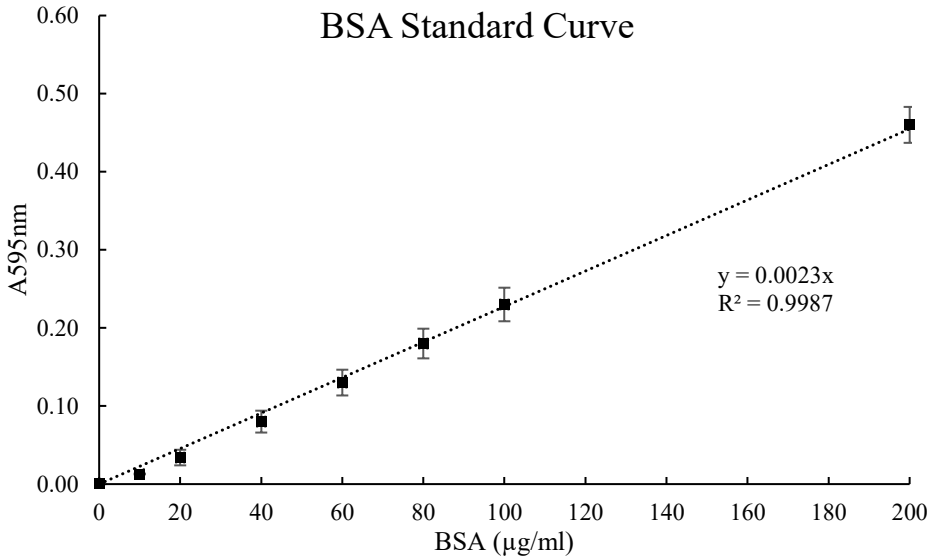

Figure B: Standard Curve of BSA (Bovine Serum Albumin) for the estimation of protein concentration in unknown protein samples.

Total protein concentration in a sample was calculated as

$$\text{Concentration } (\mu g/mL) = (A595nm)/0.0023$$

APPENDIX C

Units of lipase activity, calculated as per spectrophotometry

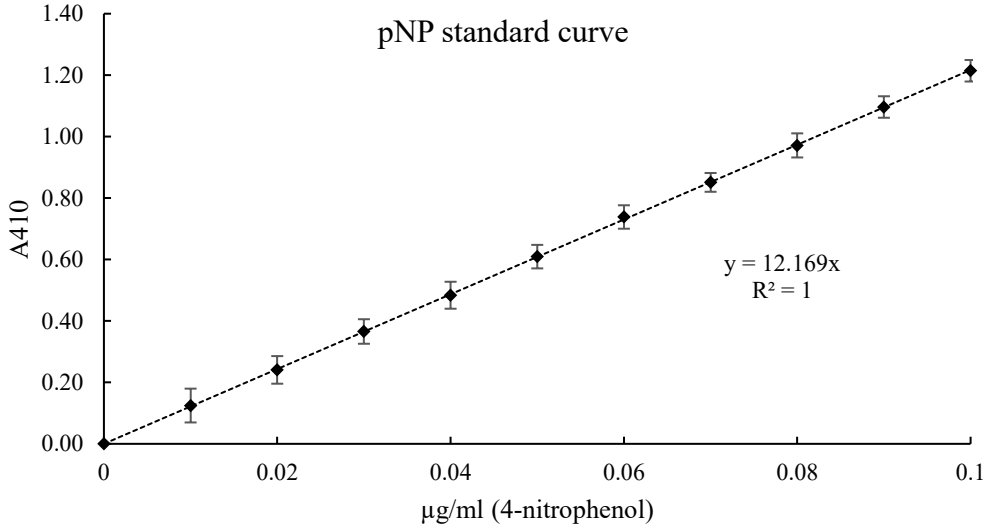

Figure C: Standard Curve of p-NP for the estimation of lipase activity in protein samples.

0.1µM of 4-nitrophenol was prepared in 50mM Tris-HCl buffer pH 7.5 and was further diluted to various concentrations. Absorbance at 410nm was measured to plot the standard curve. The graph represented here is the mean of three independent determinations and error bars represents standard deviation. One International Unit (IU) of lipase activity was defined as the amount of enzyme needed to liberate 1µmol of *p*-NP per minute, under the conditions described for each assay system.

APPENDIX D

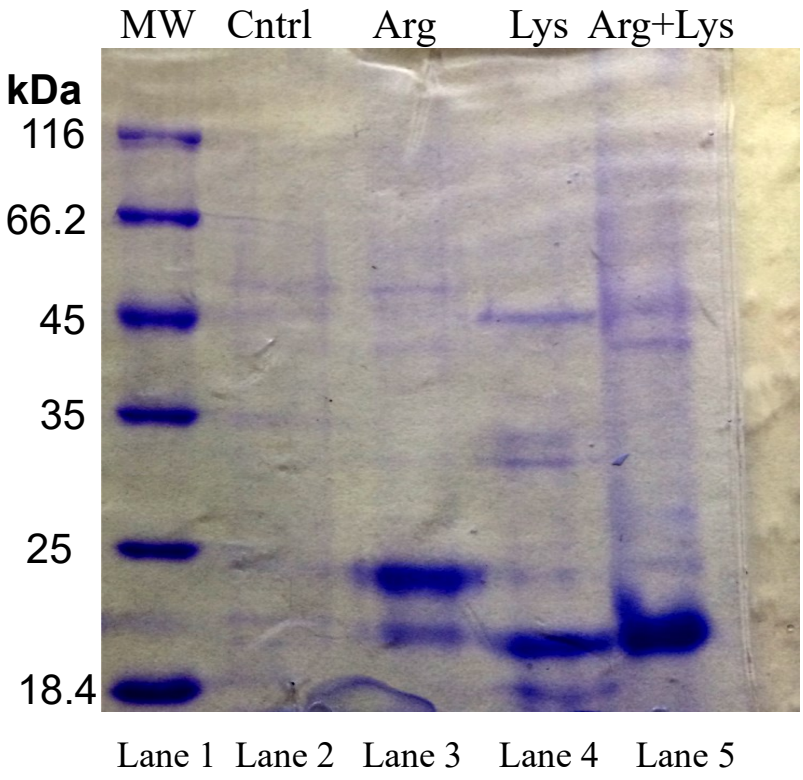

Figure D: 12% (v/v) reducing SDS PAGE of cell free supernatant fermented at 28°C for 6 days with 15% (v/v) inoculum from: Lane 2: Control: Basal lipase media (containing 1% w/v bacteriological peptone); Lane 3: Arg: 1% (w/v) *L*-Arginine in basal lipase producing media; Lane 4: Lys: 1% (w/v) *L*-Lysine in basal lipase producing media; Lane 5: Arg+Lys: 1%(w/v) *L*-Arginine+1%(w/v) *L*-Lysine in basal lipase producing media; While Lane 1: MW: Molecular weight marker

APPENDIX E

Tables below detail the results of lipase purification trials performed on cell free supernatants of H1 (*P. reinekei*) and H3 (*P. brenneri*).

Table E.1a: Data represented here are the amount of lipase (IU) precipitated from the cell free supernatant of H1 (*P. reinekei*) when different precipitants were used in their saturated concentrations. No lipase activity was observed in precipitated protein when acetone and PEG 10,000 were used as precipitants. The yield for 28% (w/v) was obtained when 60%(w/v) ammonium sulfate was used as precipitant in 4°C.

Precipitant	Concentration	Condition	CFS (IU)	Pellet (IU)
Ammonium Sulfate	60% (w/v)	ambient temp	96.44	0.00
Ammonium Sulfate	60% (w/v)	4°C	96.44	27.50
Acetone	50% (v/v)	4°C	96.44	0.00
PEG 10,000	50% (w/v)	ambient temp	96.44	0.64

Table E.1b: Data represented here are the amount of lipase (IU) precipitated from the cell free supernatant of H3 (*P. brenneri*) when different precipitants were used in their saturated concentrations. No lipase activity was observed in precipitated protein when acetone and PEG 10,000 were used respectively as precipitants. The yield for 19.67% (w/v) was obtained when 60% (w/v) ammonium sulfate was used as precipitant in 4°C.

Precipitant	Concentration	Condition	CFS (IU)	Pellet (IU)
Ammonium Sulfate	60% (w/v)	ambient temp	120.9	0.00
Ammonium Sulfate	60% (w/v)	4°C	120.9	19.67
Acetone	50% (v/v)	4°C	120.9	0.00
PEG 10,000	50% (w/v)	ambient temp	120.9	1.29

Table E.2a: Data represented here are the binding conditions used during the initial purification trials of lipase using dialysed cell free supernatant of H1 (*P. reinekei*). A 34% yield obtained from anion exchange chromatography favoured its usage for further optimisation over cation and HIC.

Chromatography mode	Condition	Lipase in Load (IU)	Lipase in Flow through (IU)	Lipase in Elution (IU)	% Yield
Cation	Dialysate with 10mM sodium acetate pH 5.0	140.9	130.58	8.67	6.15
Anion	Dialysate with 10mM Tris-HCl pH 9.0	141.5	82.58	48.67	34.40
HIC	Dialysate with 10mM Tris-HCl and 1M ammonium sulfate at pH 7.5	145.3	129.11	6.89	4.74

APPENDIX E

Tables below detail the results of lipase purification trials performed on cell free supernatants of H1 (*P. reinekei*) and H3 (*P. brenneri*).

Table E.2b: Data represented here are the binding conditions used during the initial purification trials of lipase using dialysed cell free supernatant of H3 (*P. brenneri*). A 36% yield obtained from anion exchange chromatography favoured its usage for further optimisation over cation and HIC.

Chromatography mode	Condition	Lipase in Load (IU)	Lipase in Flow through (IU)	Lipase in Elution (IU)	% Yield
Cation	Dialysate with 10mM sodium acetate pH 5.0	120.9	117.2	0.00	0
Anion	Dialysate with 10mM Tris-HCl pH 8.5	120.9	18.45	43.1	35.91
HIC	Dialysate with 25mM Tris-Acetate and 0.9M ammonium sulfate at pH 6.5	120.9	78.4	19.3	24.7

Table E.3: Data represented here are the binding conditions used during the initial purification trials of lipase using dialysed cell free supernatant of H1 (*P. reinekei*).Maximum yield of 48.31% at pH 8.5 favoured using this pH for purification of lipase from H1 (*P. reinekei*).

Anion Exchange pH	Lipase in Load (IU)	Lipase in Flow though (IU)	% Lipase Yield in elution
8.5	526.78	254.51	48.31
9.0	493.99	233.78	47.33
9.5	790.64	350.07	44.28

Table E.4: Data represented here are the binding conditions used during the initial purification trials of lipase using dialysed cell free supernatant of H3 (*P. brenneri*) on Toyopeal® Phenyl resin for hydrophobic interaction chromatography. A yield of less than 10% from HIC did not favour its usage for further purification optimisation.

Condition on HIC	Lipase in Dialysate (IU)	Lipase in Load after ammonium sulfate addition (IU)	Lipase in Flow though (IU)	% Lipase Yield in elution
25mM Tris Acetate +0.9M Amm. Sulp., pH 6.5	120.9	48.36	20.45	7.5%
25mM Tris Acetate+0.75M Amm. Sulp. pH 5.5	120.9	76.04	30.9	5.8%

APPENDIX F

12% (v/v) SDS gel, representing purification trial of lipase from cell free supernatant of H1 (*P. reinekei*)

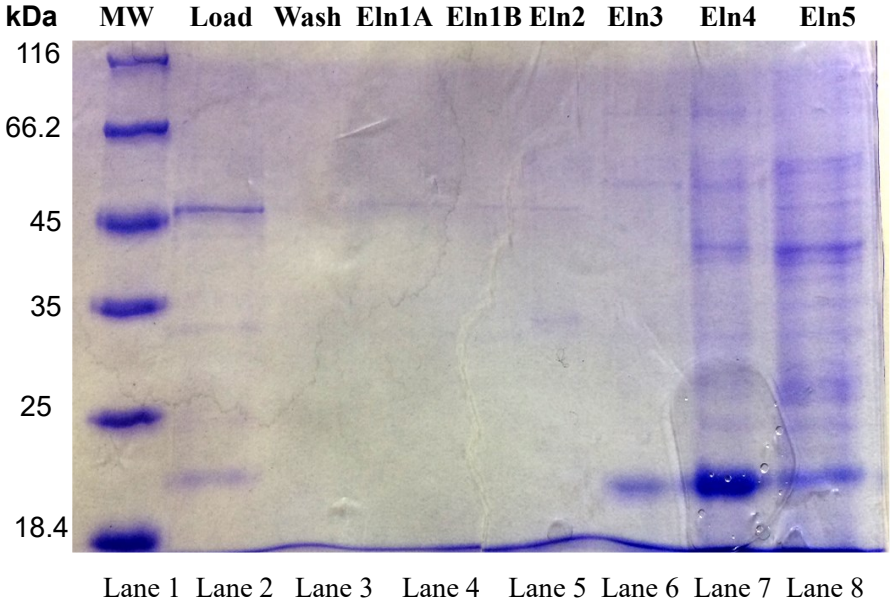

Figure F.1: 12% (v/v) reducing SDS PAGE: representing Lane 1: MW: molecular weight marker; Lane 2: Load: H1 cell free supernetanat dialyzed in 10mM Tris-HCl pH 9.0; Lane 3:Wash: 10mM Tris-HCl pH 9.0 buffer wash after protein load; Lane 4,5: Elu1A and Elu 1B: 10mM Tris-HCl pH 9.0+100mM NaCl; Lane 6: Elu2: 10mM Tris-HCl pH 9.0+250mM NaCl; Lane 7: Elu 3: 10mM Tris-HCl pH 9.0+500mM NaCl; Lane 8:Elu 4: 10mM Tris-HCl pH 9.0+750mM NaCl; Lane 9: Elu5: 10mM Tris-HCl pH 9.0+1M NaCl (eluted lipase)

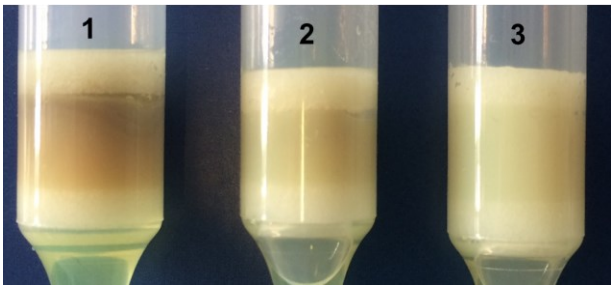

Figure F.2: Change in Q-Sepharose resin colour after addition of salt in Protein load (left to right): Column 1: Protein load with no salt; Column 2: protein load with 0.1M NaCl; Column 3: protein load with 0.25M NaCl

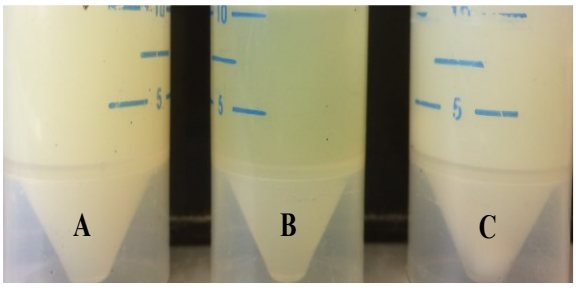

Figure F.3: (A) Cell free supernatant of H3 (*P. brenneri*); (B): dialysate at pH 9.0 (during alkaline precipitation); (C): after alkaline precipitation at pH 8.5

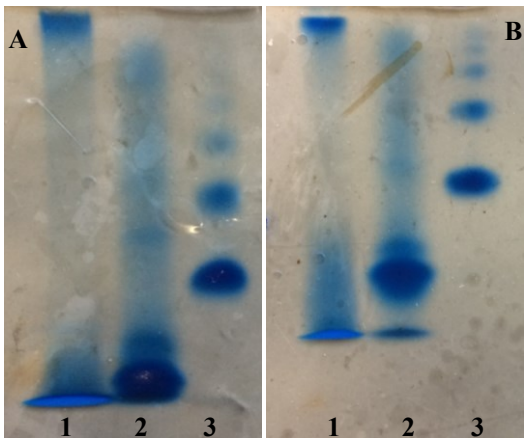

Figure F.4: (A), (B) represent 6% (v/v) and 8% (v/v) native agarose gel. Lane 1: partially purified lipase from H3 (*P. brenneri*), Lane 2: Std. (porcine pancreas lipase) and Lane 3: BSA.

APPENDIX G:

Calculations for estimation of molecular weight of purified protein using migration of molecular weight markers

Table G: Distance travelled by molecular weight markers in gel and their respective retention factors

Molecular weight of marker	MW migration (cm)	Dye front migration (cm)	Molecular Weight Estimation (Rf)*	Log 10 of Molecular weight marker size (log 10 kDa)
116	0.6	6.2	0.097	2.06
66.2	1.5		0.242	1.82
45	2.3		0.371	1.65
35	3.1		0.500	1.54
25	3.9		0.629	1.40
18.4	4.9		0.790	1.26
14.4	5.1		0.823	1.16

*Molecular Weight Estimation = Dye front migration/MW migration

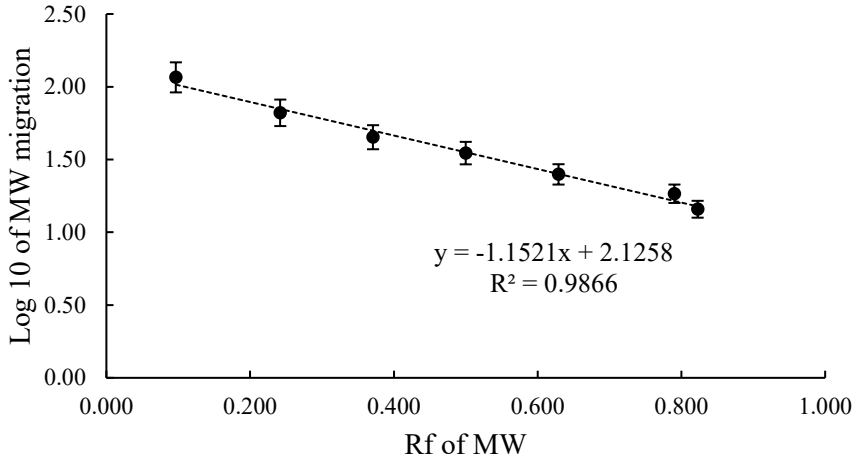

Figure G: Graph representing migration of molecular weight marker on the SDS gel.

Migration of lipase on gel = 2.1cm

Rf= 2.1/6.2 (migration of protein/migration of dye front) = 0.34

Molecular weight= antilog {(-1.1521*Rf) +2.1258} = 54.4kDa = ~55kDa

APPENDIX H:

Standard curve of gold nanoparticles using AAS for the concentration estimation of gold nanoparticles

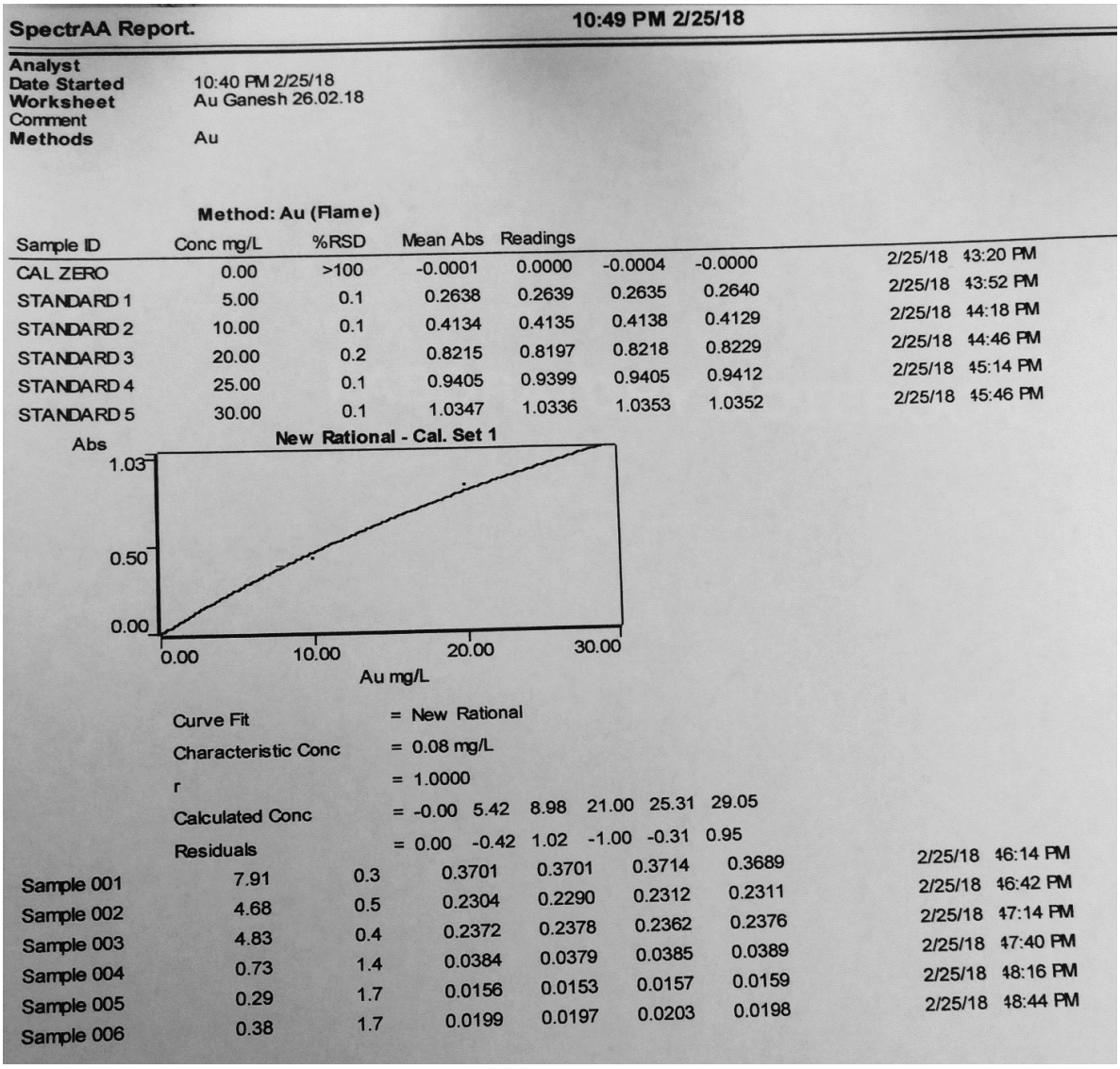

SpectrAA Report. 10:49 PM 2/25/18

Analyst
Date Started 10:40 PM 2/25/18
Worksheet Au Ganesh 26.02.18
Comment
Methods Au

Method: Au (Flame)

Sample ID	Conc mg/L	%RSD	Mean Abs	Readings			
CAL ZERO	0.00	>100	-0.0001	0.0000	-0.0004	-0.0000	2/25/18 13:20 PM
STANDARD 1	5.00	0.1	0.2638	0.2639	0.2635	0.2640	2/25/18 13:52 PM
STANDARD 2	10.00	0.1	0.4134	0.4135	0.4138	0.4129	2/25/18 14:18 PM
STANDARD 3	20.00	0.2	0.8215	0.8197	0.8218	0.8229	2/25/18 14:46 PM
STANDARD 4	25.00	0.1	0.9405	0.9399	0.9405	0.9412	2/25/18 15:14 PM
STANDARD 5	30.00	0.1	1.0347	1.0336	1.0353	1.0352	2/25/18 15:46 PM

Curve Fit = New Rational
Characteristic Conc = 0.08 mg/L
r = 1.0000
Calculated Conc = -0.00 5.42 8.98 21.00 25.31 29.05
Residuals = 0.00 -0.42 1.02 -1.00 -0.31 0.95

Sample 001	7.91	0.3	0.3701	0.3701	0.3714	0.3689	2/25/18 16:14 PM
Sample 002	4.68	0.5	0.2304	0.2290	0.2312	0.2311	2/25/18 16:42 PM
Sample 003	4.83	0.4	0.2372	0.2378	0.2362	0.2376	2/25/18 17:14 PM
Sample 004	0.73	1.4	0.0384	0.0379	0.0385	0.0389	2/25/18 17:40 PM
Sample 005	0.29	1.7	0.0156	0.0153	0.0157	0.0159	2/25/18 18:16 PM
Sample 006	0.38	1.7	0.0199	0.0197	0.0203	0.0198	2/25/18 18:44 PM

Figure H: Standard curve of AAS for the estimation of AuNPs concentration. Sample 001: AuNPs with 1:30 dilution in distilled water=7.91mg/L. Sample 002: AuNPs with 1:50 dilution in distilled water=4.68mg/L. Sample 003-006: irrelevant. Based on the values from sample 001 and sample 002, conc. of AuNPs was calculated as (237.3+234)/2= 235mg/L

APPENDIX I:

Size distribution of AuNPs as estimated by Nanoseries zeta sizer

Z-Average (nm):	24.48688	**Derived Count Rate (kcps):**	93623.3860407...
Standard Deviation:	0	**Standard Deviation:**	573.569351515...
%Std Deviation:	0	**%Std Deviation:**	0.61263470140...
Variance:	0	**Variance:**	328981.800997...

Size d.nm	Mean Intensity Percent	Std Dev Intensity Percent	Size d.nm	Mean Intensity Percent	Std Dev Intensity Percent	Size d.nm	Mean Intensity Percent	Std Dev Intensity Percent	Size d.nm	Mean Intensity Percent	Std Dev Intensity Percent
0.4000	0.0	0.0	5.615	0.0	0.0	78.82	0.3	0.2	1106	0.0	0.0
0.4632	0.0	0.0	6.503	0.0	0.0	91.28	0.0	0.0	1281	0.0	0.0
0.5365	0.0	0.0	7.531	0.0	0.0	105.7	0.0	0.0	1484	0.0	0.0
0.6213	0.1	0.2	8.721	0.0	0.0	122.4	0.0	0.0	1718	0.0	0.0
0.7195	0.3	0.5	10.10	0.0	0.0	141.8	0.0	0.0	1990	0.0	0.0
0.8332	0.5	0.8	11.70	0.4	0.2	164.2	0.0	0.0	2305	0.0	0.0
0.9649	0.5	0.8	13.54	2.0	0.3	190.1	0.0	0.0	2669	0.0	0.0
1.117	0.3	0.6	15.69	4.8	0.3	220.2	0.0	0.0	3091	0.0	0.0
1.294	0.1	0.2	18.17	8.1	0.4	255.0	0.0	0.0	3580	0.0	0.0
1.499	0.0	0.0	21.04	11.1	0.6	295.3	0.0	0.0	4145	0.0	0.0
1.736	0.0	0.0	24.36	13.2	0.9	342.0	0.0	0.0	4801	0.0	0.0
2.010	0.0	0.0	28.21	14.0	0.9	396.1	0.0	0.0	5560	0.0	0.0
2.328	0.0	0.0	32.67	13.3	0.8	458.7	0.0	0.0	6439	0.0	0.0
2.696	0.0	0.0	37.84	11.5	0.5	531.2	0.0	0.0	7456	0.0	0.0
3.122	0.0	0.0	43.82	8.9	0.2	615.1	0.0	0.0	8635	0.0	0.0
3.615	0.0	0.0	50.75	6.0	0.1	712.4	0.0	0.0	1.000e4	0.0	0.0
4.187	0.0	0.0	58.77	3.3	0.3	825.0	0.0	0.0			
4.849	0.0	0.0	68.06	1.3	0.3	955.4	0.0	0.0			

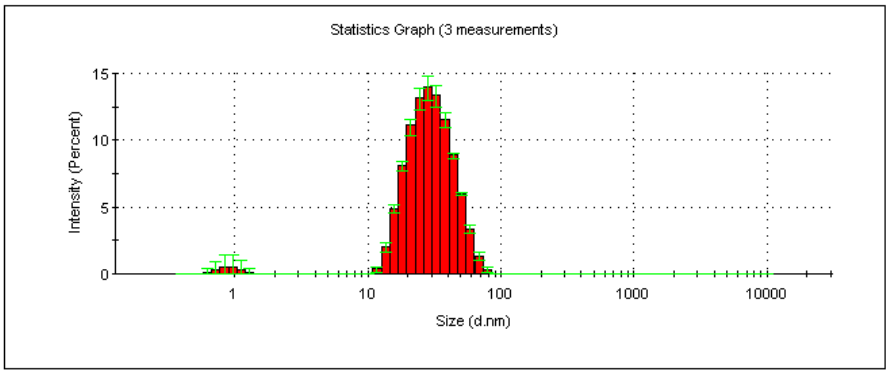

Figure I: Size distribution profile of AuNPs, as estimated by *Nanoseries Zeta-sizer.*

APPENDIX J:

Standard curve of triolein prepared using Nile red fluorescence spectrophotometer assay for the estimation of neutral lipids in microalgae

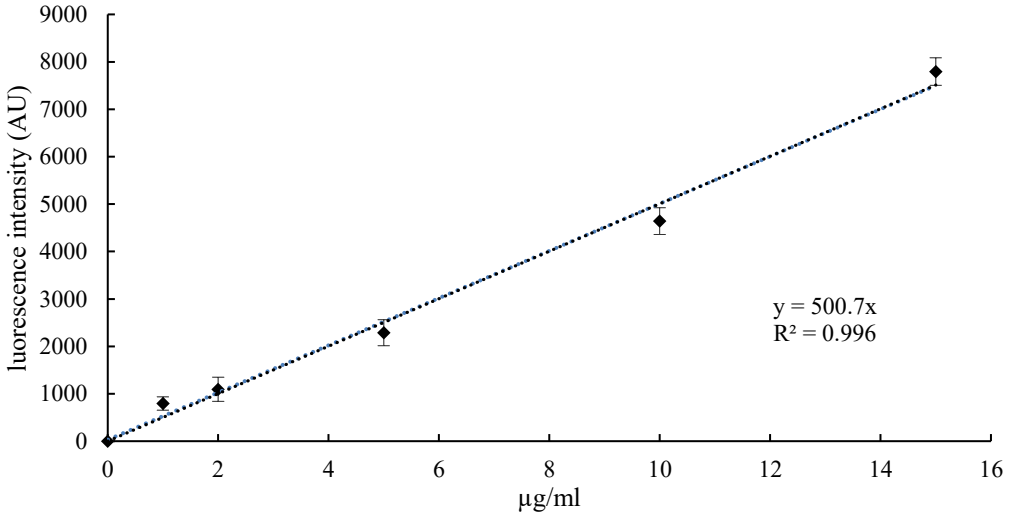

Figure J: Standard curve for the quantification of neutral lipids in microalgae cells using triolein as standard.

APPENDIX K:

GC chromatogram of Biodiesel Standard, as per Section 3.2.7.3

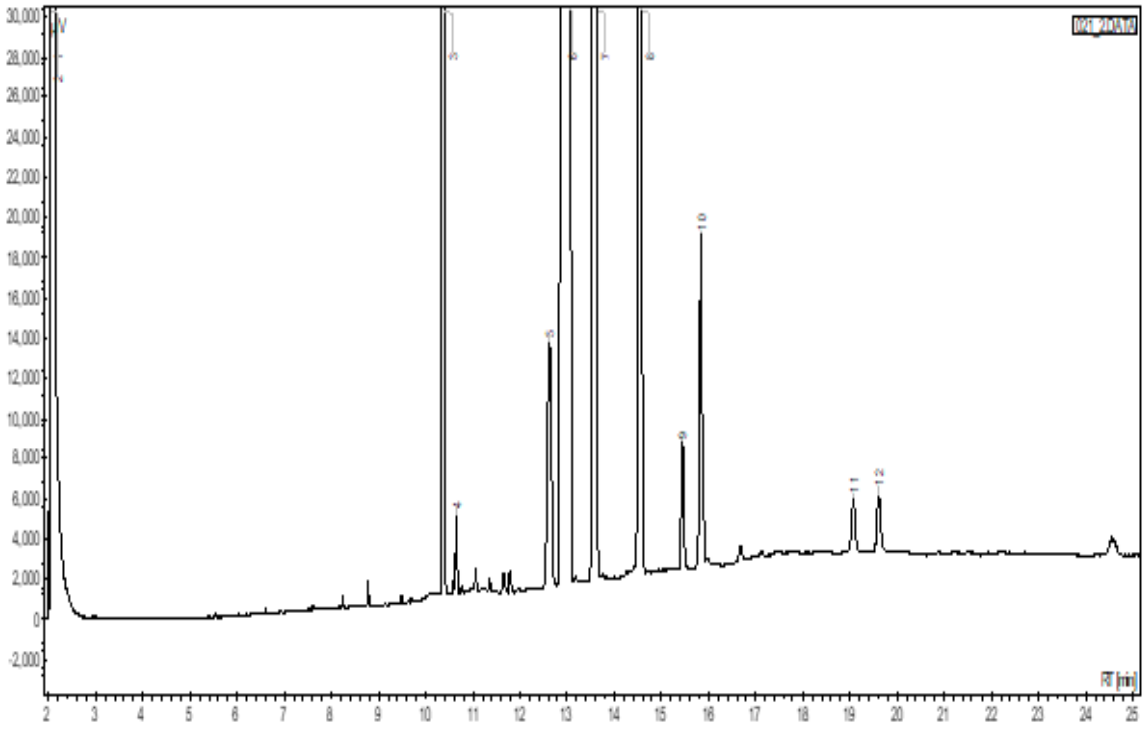

Figure K: GC chromatogram of FAME standard 1: Solvent; 2: caproic acid (C6:0); 3: stearic acid (C18:0); 4: elaidic acid (C18:1n9t); 5: γ-linolenic acid (C18:3n6); 6: α-linolenic acid (C18:3n3); 7: arachidic acid (C20:0); 8: cis-11,14-eicosadienoic acid (C20:2); 9: cis-8,11,14-eicosatienoic acid (C12:3n6); 10: heneicosanoic acid (C21:0); 11: erucic acid (C22:1n9); 12: cis-13,16-docosadienoic acid (C22:2). GC and peak identification were done as per section 3.2.7.3

APPENDIX L:

GC chromatogram of 37 component FAMEs Mix, as per Section 3.2.7.3

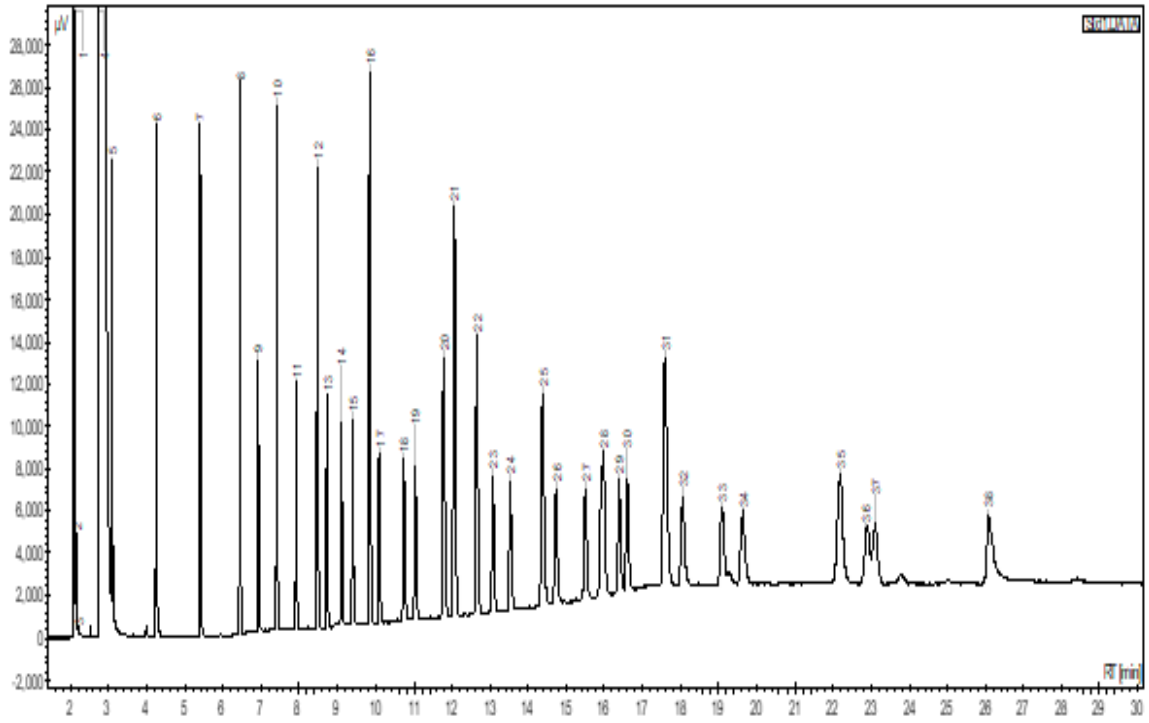

Figure L: GC chromatogram of FAME Mix. 1: Butyric acid+ solvent (C4:0); 2: caproic acid (C6:0); 3: caprylic acid (C8:0); 4: Solvent peak; 5: Capric acid (C10:0); 6: undecanoic acid (C11:0); 7: lauric acid (C12:0); 8: Tridecanoic acid (C13:0); 9: myristic acid (C14:0); 10: myristoleic acid (C14:1); 11: pentadecanoic acid (C15:0); 12: cis-10-pentadecenoic acid (C15:1); 13: palmitic acid (C16:0); 14: palmitoleic acid (C16:1); 15: hepradecanoic acid (C17:0); 16: cis-10-heptadedenoic acid (C17:1); 17: stearic acid (C18:0); 18: elaidic acid (C18:1n9t); 19: oleic acid (C18:1n9c); 20: linolelaidic acid (C18:2n6t); 21: linoleic acid (C18:2n6c); 22: γ-linolenic acid (C18:3n6); 23: α-linolenic acid (C18:3n3); 24: arachidic acid (C20:0); 25: cis-11-eicosenoic acid (C10:1n9); 26: cis-11,14-eicosadienoic acid (C20:2); 27: cis-8,11,14-eicosatienoic acid (C12:3n6); 28: heneicosanoic acid (C21:0); 29: cis-11,14,17-eicosatienoic acid (C20:3n6); 30: arachidonic acid (C20:4n6); 31: cis-5,8,11,14,17-eicosapentaenoic acid (C20:5n3); 32: behenic acid (C22:0); 33: erucic acid (C22:1n9); 34: cis-13,16-docosadienoic acid (C22:2); 35: tricosanoic acid (C23:0); 36: lignoceric acid (C24:0); 37: cis-4,7,10,13,16,19-docosahaenoic acid (C22:6n3); nervonic acid (C24:1n9). GC and peak identification were done as per 3.2.7.3